ABSTRACT

RORIE, DENNIS. **Investigation of Soil Suction in a Compacted Low-Plasticity Clay.** (Under the direction of Roy H. Borden).

The purpose of this research is to investigate soil suction in low density silty sands. Research has been performed to develop the Soil Water Characteristic Curves for both the drying and wetting phases. The research attempts to mimic the behavior of partially saturated soil compacted at various degrees of as-compacted water contents and with varying compactive efforts.

Pressure plate tests (ASTM D 6836-02) were conducted on compacted specimens (brown silty-soil classified as a low plasticity clay,CL according to USCS) with as-compacted water contents of 4.8% and 11.6%, and as-compacted dry densities of 1.60 Mg/m^3 and 1.78 Mg/m^3. Specimens were tested under 0 and 100 kPa overburden pressure. Results showed that the air-entry value increased with increasing as-compacted water content and overburden pressure, respectively.

Filter paper tests (ASTM 5298-03) for determining the matric suction were performed on compacted specimens ranging in as-compacted water content and dry density from 4.7% to 22%, and 1.53 Mg/m^3 to 1.90 Mg/m^3, respectively. Results showed that the matric suction was influenced more by the as-compacted water content then the as-compacted dry density.

Collapse potential (ASTM D 5333-03) tests were conducted on specimens prepared to the same water contents and dry densities as the filter paper tests. Data showed that the collapse potential increases with decreasing as-compacted water content, and relative compaction due the change in structure that occurs from change in compaction conditions.

Investigation of Soil Suction in a Compacted Low-Plasticity Clay

by

Dennis E. Rorie

A thesis submitted to the Graduate Faculty of
North Carolina State University
In partial fulfillment of the
Requirements for the degree of
Masters of Science

Civil Engineering

Raleigh, NC

2006

Approved by:

Mohammed A. Gabr, Ph.D.	**M. Shamimur Rahman, Ph.D.**
Committee Member	**Committee Member**

Roy H. Borden, Ph.D.
Chair of Advisory Committee

DEDICATION

This thesis is dedicated to my parents Delane and Linda Rorie. They have supported me through all the dreams that I have pursued. I will forever be thankful for being blessed with two loving parents who've selflessly given of themselves to the success of their children. I am thankful to them for being positive influences and role models on my life.

BIOGRAPHY

Dennis Ervin Rorie was born in Greenville, South Carolina. He is the son of Delane (Father) and Linda (Mother) Rorie whom hail from Peachland and Polkton, NC, respectively, and the brother of Kevin Rorie. He is a product of the Greenville County Public School System where he attended Mitchell Road Elementary, Greenville Middle, and is a graduate of the 2000 class at Eastside High School. While at Eastside High School he was a member of the Football, Wrestling and Baseball teams. He is also of an Alumnus of the University of South Carolina where he obtained a Bachelor of Science Degree in Civil Engineering in May of 2004. While at the University of South Carolina, he served in numerous capacities. He served as a Resident Advisor for two consecutive years, counselor three consecutive summers for the S.C.A.M.P. (South Carolina Alliance for Minority Participation) Summer Bridge program, undergraduate lab assistant, and mentor for freshmen engineering students. While at NC State University he continued his active community involvement through several service organizations.

ACKNOWLEDGMENTS

I would first and foremost like to thank my Lord and Savior Jesus Christ, who has made this dream and all other realities possible.

I also would like to thank Dr. Roy H. Borden for his guidance throughout my academic career at North Carolina State. Dr. Borden served not only as an academic advisor, but also as a mentor who encouraged me through some of the trials and tribulations of my graduate career. Dr. Borden has encouraged me to strive for a higher pursuit of excellence throughout engineering career and life in general. I would also like to thank Dr. Mohammed Gabr for his support. Dr. Gabr's responsiveness to me inside and outside of the classroom does not go unnoticed and is most definitely appreciated. A thanks also goes to Dr. Shamimur Rahman for his assistance during my stay at North Carolina State.

I would like to acknowledge Professor Craig Benson, University of Wisconsin for information on their design of the test devices and Rick Lamy of the NCSU Precision Machine Shop for constructing each device. I would like to thank Wan Soo Kim for his guidance and efforts through out the duration of this project. I would also like to thank the NC State Department of Civil, Construction, and Environmental Engineering for their financial support throughout my stay in Raleigh.

Lastly I would like to personally thank the following individuals who supported me throughout the duration of my graduate experience. Among those I would like to thank are my parents, friends and my entire church family in South Carolina for all that they have done. Their continued support and prayers kept me motivated as I marched onward in the pursuit of my dream.

TABLE OF CONTENTS

LIST OF FIGURES

LIST OF TABLES

1 INTRODUCTION

1.1 Unsaturated Soil Mechanics

Unsaturated Soil Mechanics is a branch of traditional soil mechanics that takes into account the affects of the pore air phase when quantifying values such as shear strength, permeability and volume change. Unlike tests in traditional soil mechanics, tests that directly measure unsaturated soil properties are not as easily accessible and are often extremely labor intensive. One tool that has made the analysis of unsaturated soil data simpler and more practical is the soil water characteristic curve. This plot of gravimetric water content, volumetric water content, or degree of saturation versus suction (matric or total) indirectly allows for the determination of unsaturated soil properties that can be used to determine the shear strength, permeability, and volume change of material. There are several methods available to determine the unsaturated soil properties of material. Methods include the direct determination of soil properties through experimental procedures, matching material properties to those available in databases, and through the use of the soil water characteristic curve. Figure 1.1.1 depicts a comprehensive list of methods and techniques available to determine these properties.

The soil water characteristic curve, originally developed in the agriculture science field, is a plot that represents the water storage capacity of a specific material (Fredlund 1993). The majority of soil water characteristic curve data generated using volumetric pressure plate extractors has been developed for material in its natural state, or compacted near the optimum moisture content. There has been very limited data generated that takes into account the affects of overburden pressure on the shape and air entry value (suction

required to cause the largest pores to desaturate) of the soil water characteristic curve. Additionally, an assumption of zero volume change during pressure plate testing has been generally assumed, as there has been limited research that has collected volume change data during suction testing (Ng and Pang, 2000).

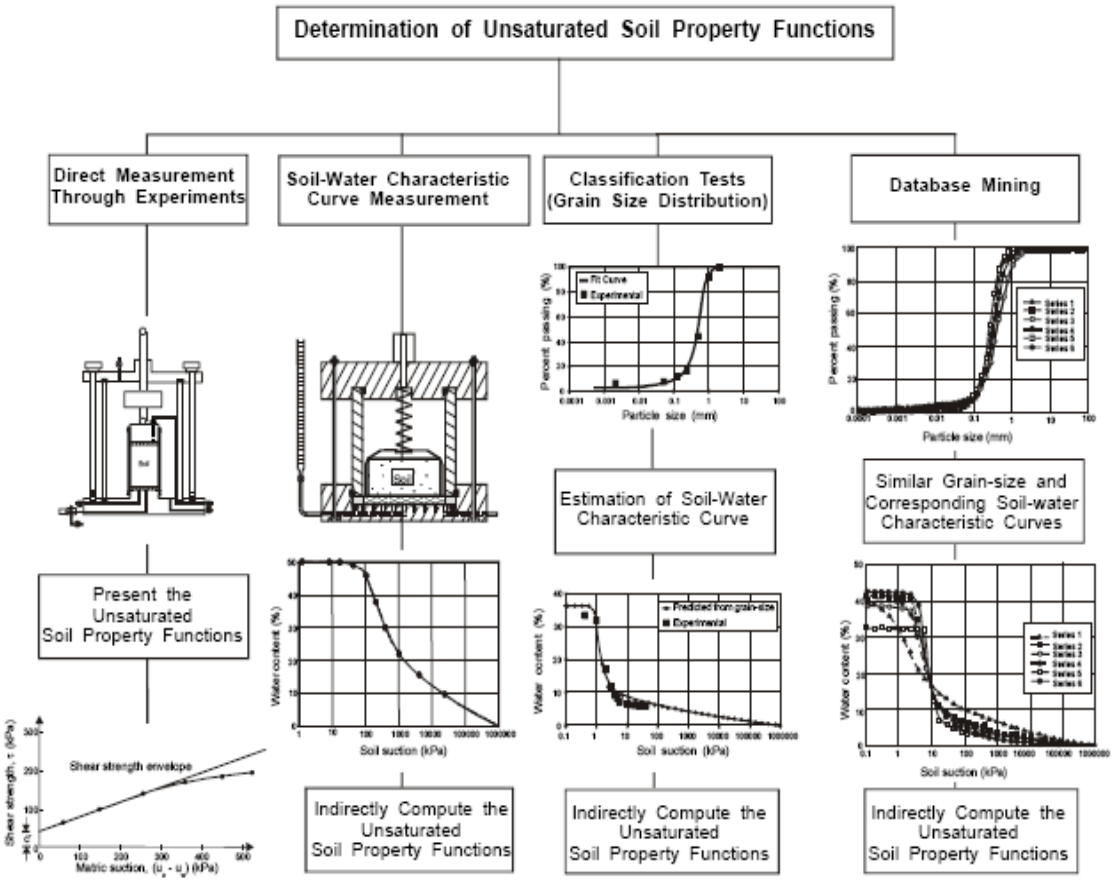

Figure 1.1.1: Methods for Determining Unsaturated soil properties (Fredlund)

1.2 Soil Structure and Compaction

Soil Structure as it relates to geotechnical engineering is defined as the geometric

arrangement of soil particles and the interparticle forces that exist between the particles, while soil fabric neglects the interparticle forces and focuses solely on the geometric arrangement of the particles (Holtz and Kovacs, 1981). Due to the small interparticle forces that exist in cohesionless soils, both fabric and soil structure are synonymous. This definition is consistent with that given by Lambe and Whitman (1969) that defined structure and fabric as "the orientation and distribution of particles in a soil mass and the forces between adjacent soil particles". An understanding of the affects of compaction on soil fabric and structure is key when analyzing compacted fine-grained material. The structure of fine-grained materials is very dependant on the compaction conditions (i.e. as-compacted water content and compactive effort) that directly affect the engineering properties of the compacted material.

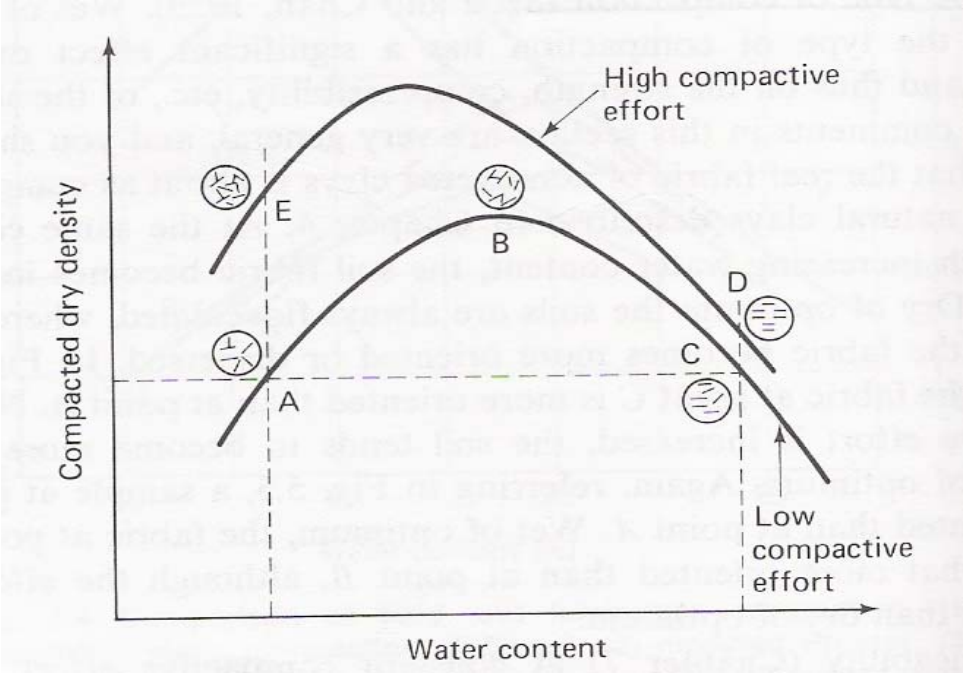

Figure 1.2.1: Effect of compaction on structure (Holtz and Kovacs 1981)

Materials compacted dry of optimum exhibit flocculated structures while materials compacted wet of optimum posses dispersed structures (Holtz and Kovacs, 1981). The two differing soil structures cause the same material (identical mineralogy) to behave differently in terms of their strength parameters, volume change (for the purpose of this study volume change will refer to the collapse potential which is the volumetric strain difference between an as-compacted specimen and an inundated specimen that has been loaded to the same magnitude of overburden pressure), permeability and moisture retention/release (soil water characteristic behavior). Materials compacted dry of optimum tend to exhibit higher magnitudes of volume change due to the more aggregated structure. Also, the permeability of material compacted on the dry side of optimum is higher than material compacted wet of optimum due the large pore voids between the aggregated soil peds (Mitchell et al., 1965). The soil water characteristic behavior of compacted fine-grained material is also largely dependant on the soil structure. The more aggregated structure of material compacted dry of optimum results in soil water characteristic curves with lower air entry values (magnitude of suction that causes the largest pores to drain) and steeper slopes past the air entry value in comparison to material compacted wet of optimum (Vanapalli et al., 1999). It should be noted that the materials compacted at optimum conditions exhibit structures and resulting engineering behavior intermediate between the structure and engineering behavior of materials compacted dry and wet of optimum.

1.3 Gravimetric Water Content vs. Volumetric Water Content

Soil water characteristic curves are commonly reported as matric suction vs. degree of saturation, gravimetric water content and/or volumetric water content. There has recently

been a comparison of the way in which the curve should be represented and the associated benefits and detractions of each (Fredlund, 2006).

One explanation of the popularity of the use of the gravimetric water content when representing the soil water characteristic is due to its common usage in traditional soil mechanics. Its measurement requires the knowledge of the mass of the soil solids, which remains constant through out the duration of the test. A major problem associated with the use of the gravimetric water content is that it does not give the correct air entry value of the soil when the soil undergoes volume change during the drying phase (Fredlund, 2006).

Use of the volumetric water content to show the relationship between the matric suction and the water storage capacity of a material has been the most popular means by which to display the curve within the soil science discipline. The volumetric water content is the most common water content used in soil databases, that derive their results from studies conducted in the soil science discipline. From an analysis view, it allows for a quick interpretation of the change in volume of a material during testing. Use of the volumetric water content eliminates the need for taking continual mass readings to determine the gravimetric water content. It does however require some form of an outflow measurement device in order for the volumetric outflow to be determined.

1.4 Thesis Objectives

The objective of this thesis is to design, perform and present the findings of an experimental program used to generate the soil water characteristic curves (desorption and sorption) using pressure plate testing apparatus. This study shows the soil water characteristic curves for both the drying and wetting conditions. Also, this thesis examines

the effects of the as-compacted water content and compactive effort on the shape of the soil water characteristic curve. Finally the effects of the overburden pressure on the soil water characteristic curve will be examined.

In addition to the soil water characteristic curves presented in this body of work, an experimental program that evaluates the collapse potential of as-compacted material has been presented. The filter paper method (ASTM D 5298-03) was used to determine the matric suction of the material used for this portion of the experimental program. The affects of the as-compacted water content, dry density, relative compaction, and matric suction on the collapse potential have been examined.

Finally, the results of falling head permeability tests are presented in this study. Three separate overburden pressures (0 kPa, 50 kPa, and 100 kPa) were selected to examine the effects of the void ratio on the permeability of the compacted material.

1.5 Thesis Outline

- **Previous Work**

This section is intended to serve as a summary of the prior work that has been performed in the area of unsaturated soil mechanics. More specifically, this section will present the historical background of the results of soil suction test methods, and prediction methods used to determine the soil water characteristic curve. It additionally addresses the research that has been performed regarding the collapse potential of compacted material.

- **Experimental Program**

The experimental program section provides a detailed discussion of the testing procedure performed. This section discusses in detail the material and methods used

throughout this study. Included in this section are complete explanations of each component of the experimental program. Components include pressure plate testing, collapse potential testing, filter paper tests (contact method), and falling head permeability within a consolidometer. In addition, the vendor names and locations where the materials used for the pressure plate tests were obtained are included in this section of the study.

- **Results & Analysis**

Results from the experimental program are presented in this section. The results are included in both graphical and tabular forms. In addition, a comparison between test data and data found within the literature has been made. The organizational structure follows that of the experimental program with the following order: pressure plate, collapse potential, filter paper, and falling head permeability using a consolidometer.

- **Future Outlook**

The final section of this study proposes how to further this particular field of study. This section speaks on how the materials and methods may be improved for future studies.

2 PREVIOUS WORK

This section presents a detailed description of soil suction, suction measurement techniques, and prediction methods based on mathematical models. Various test methods exist to determine the soil water characteristic curve. Such methods include; Tensiometers, Conductivity Sensors, Pressure-Plate extractors, Pyschrometers, and the Filter Paper Method. Each method applies to specific applications and has the ability to be used for varying suction ranges.

2.1 Soil Suction

Soil suction (which will be used interchangeably with total suction), commonly expressed in terms of relative humidity, is defined as the free energy of the soil water (Fredlund 1993). It represents the thermodynamic potential of pore water relative to free water, where free water is defined as water with no dissolved solutes (Lu 2004).

The total suction (free energy) of soil is divided into two components. First the osmotic component, that represents the suction that originates from dissolved solutes in the pore water (Lu, 2004). "In suction terms, it is the equivalent suction derived from the measurement of the partial pressure of the water vapor in equilibrium with a solution identical in composition with the soil water, relative to the partial pressure of water vapor in equilibrium with free pure water" (Fredlund, 1993). Stated differently, the osmotic component of soil suction arises from the chemical interactions between dissolved salts and free water (defined as water containing no dissolved solutes).

The second component of soil suction is the matric suction (sometimes referred to as matrix suction). The matric suction component of soil suction results from the combined

effects of capillary tension (explanation below) and short-range adsorption forces (Lu, 2004). "In suction terms, it is the equivalent suction derived from the measurement of the partial pressure of the water vapor in equilibrium with the soil water, relative to the partial pressure of the water vapor in equilibrium with a solution identical in composition with the soil water" (Fredlund 1993). In unsaturated soil mechanics it is most notably defined as the difference between the pore air pressure and pore water pressure (u_a-u_w). Osmotic suction will not be discussed further as matric suction is the parameter of primary interest for this particular study (a more detailed discussion on osmotic suction can be found in McDowell 2004). In engineering applications, soil suction is most commonly measured in the conventional pressure/stress units (kPa & psi). However, in the areas of soil science and agriculture the units are often considered in terms of cm of head and bar, respectively.

As stated previously, matric suction results from a combination of short-term adsorption forces and capillary tension that exists between individual particles. Capillary tension (suction) is a parameter that has been commonly documented and understood in the geotechnical community (Lambe and Whitman, 1969; Mitchell, 1976; Holtz and Kovacs, 1981). It can be best understood in terms of a brief discussion on capillarity.

Capillarity is a phenomenon that results from the surface tension that exists between water molecules and additional molecules of liquid or gas at a given temperature (Lambe and Whitman 1969). It is best understood through the classic example of water rising and remaining above the line of atmospheric pressure within a small diameter tube, Figure 2.1.1 shows that the height of capillary rise is a function of the tube diameter, contact angle between the tube and wetting liquid. The mathematical relationship is shown below;

$$h_c = \frac{2T}{r\gamma}\cos\alpha \qquad (2.1)$$

where T is the surface tension of the fluid (water for this discussion), r is the radius of the capillary tube, γ is the unit weight of water, and α is the contact angle between the water and capillary tube. Assuming a clean glass tube and pure water (contact angle α becomes 0, therefore $\cos(\alpha)=1$), equation 2.1 reduces to the following:

$$h_c = \frac{-4T}{\gamma d} \qquad (2.2)$$

where T is the surface tension of the fluid, d is the diameter of the capillary tube, and γ is the unit weight of water. Since water pressures are measured from a reference pressure of atmospheric (zero), values above the atmospheric line are considered negative and positive pore pressure are those below the atmospheric line.

The previous explanation of capillarity allows for the understanding of non-chemical particle-to-particle attraction. It can be seen from examining Figure 2.1.2 that the soil particles are similar to the walls of the capillary tube and the surface tension contractile skin (air-water interface) holds both the water intact and the two soil particles together. It is these forces that are of most importance to this study as they are the basis for which the matric suction is described.

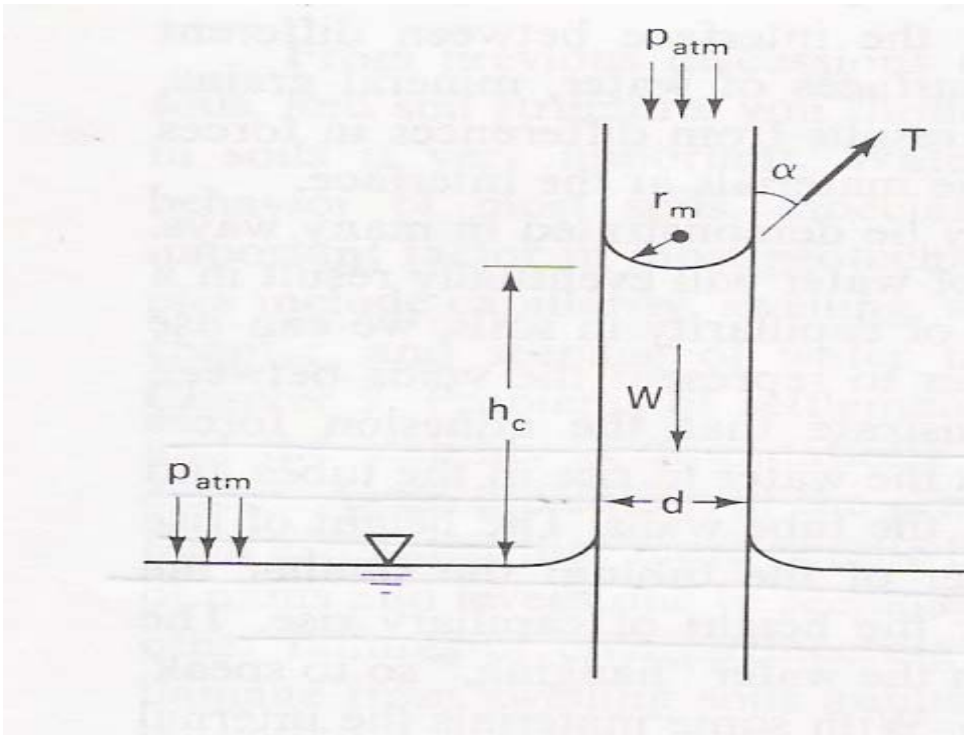

Figure 2.1.1: Capillary tube schematic (Holtz and Kovacs 1981)

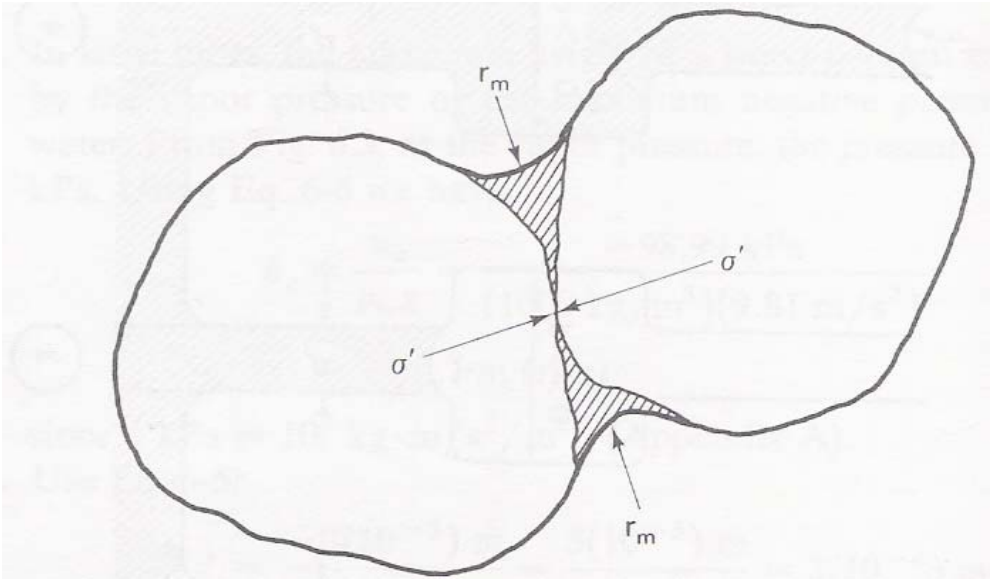

Figure 2.1.2: Particles held together by capillary forces (Holtz and Kovacs 1981)

2.2 Suction Measurement Techniques

Several measurement techniques are available to measure the suction of a soil sample. The method selected should depend upon the suction desired. Different methods are used to determine the total suction and matric suction respectively. The following measurement techniques, and their applicable range of suction measurements will be described: Tensiometers, Conductivity Sensors, Pressure Plate Extractors, Pyschrometers, and Filter Paper Method.

The following tests described are applicable when determining the matric suction of the soil. Matric suction can be measured direct or indirectly. In the direct measurement method, the negative pore water pressure is measured, however, for indirect methods, thermal or electrical properties of a ceramic are indicators of the matric suction of the soil (Fredlund, 1993).

2.2.1 Tensiometers (0-100 kPa)

Tensiometers provide for direct measurement of the negative pore water pressures in soil within the range of 0-100 kPa. The device usually consists of a tube filled with water containing a high air entry ceramic tip at one end, and a sensor used to measure the negative pore water pressure at the other end (Lu, 2004). Tensiometers are equipped with gauges to read the values of negative pore water pressure. These gauges are typically Bourdon gauges. Figure 2.2.1 shows a standard Tensiometer. The tensiometer is inserted into a soil sample. Negative pressure within the soil causes water within the tensiometer to be pulled through the high air entry ceramic tip until an equilibrium condition is reached between the inside of the

tensiometer and the surrounding soil. The sensor tip is permeable to dissolved solutes; therefore the osmotic component of suction does not affect the gauge readings (Lu, 2004).

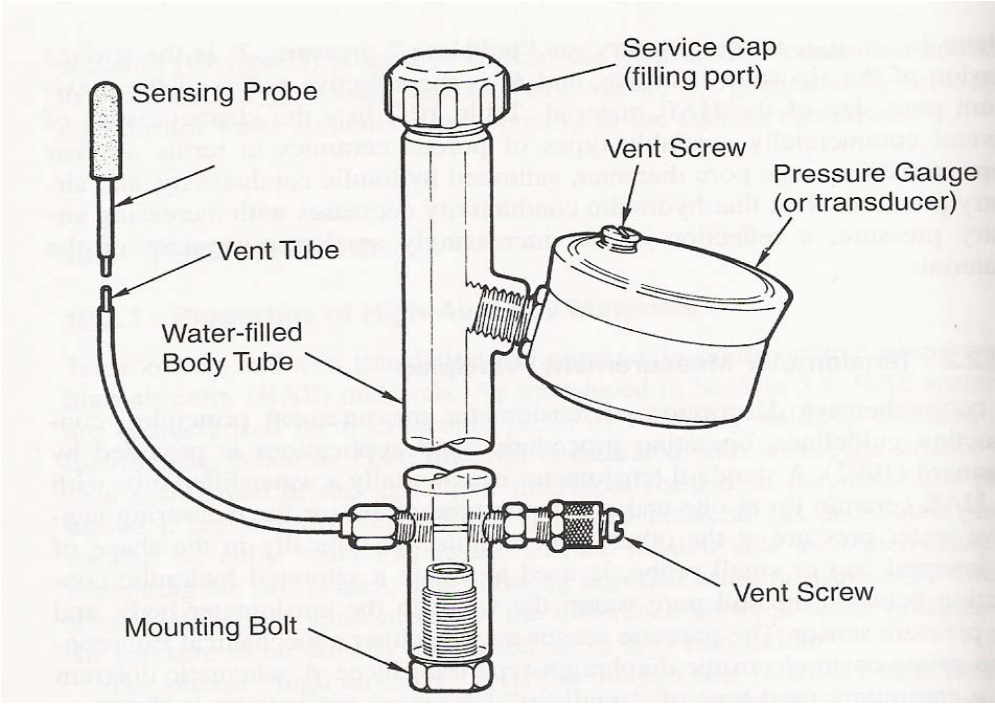

Figure 2.2.1: Tensiometer Schematic (Lu 2004)

2.2.2 Electrical & Thermal Conductivity Sensors (0-400 kPa)

Studies have shown that the thermal properties of a soil are a function of the water content of the material being examined (Fredlund, 1993). The thermal conductivity of a soil increases with increasing water content. The device, originally developed by Shaw and Beaver (1939), consists of a sensor and small heater that is inserted into the soil. Modern sensors referred to generally as “gypsum blocks” (Lu, 2004) measure the rate of internal heat dissipation following an applied heat source. The results of the heat dissipation are directly

related to the moisture content within the porous medium. Heat that has not dissipated will cause the temperature to rise within the gypsum block. The rise in temperature is measured in terms of voltage output that is correlated to a unique calibration curve for the sensor. Values of matric suction are determined from the measured results with the use of the calibration curve.

2.2.3 Pressure Plates Extractors (0-1500 kPa)

The axis translation technique (Hilf, 1956), involves using some variation of a pressurized chamber to apply air pressure to a material while keeping the water pressure at a constant value (usually zero). A soil sample is placed within the chamber onto a saturated high air entry disk that will only allow for the flow of water through the saturated pore spaces but prevents air up to a rated value (air entry value) of matric suction. The air pressure inside of the chamber is elevated to a desired value while keeping the pore water pressure at a constant value (normally atmospheric pressure). The difference between the applied air pressure and the constant pore water pressure is the matric suction (u_a-u_w) at the existing water content or degree of Saturation. As the pore air pressure is elevated, water is expelled from the soil sample through the saturated high air entry disk, and volume outflow measurements are able to be determined.

A typical pressure plate device is shown in Figure 2.2.2. The pressure plate devices, initially used in the agricultural discipline, normally measure matric suction to a maximum value of 1500 kPa (15 bar). This value is defined as the wilting point for plants, or the water content at which roots can no longer draw water from the soil.

Figure 2.2.2: Conventional 15 Bar Pressure Plate Extractor (Leong et al 2004)

2.2.4 Thermocouple Psychrometers (0-8000 kPa)

Thermocouple Psychrometers are used to determine the total suction of the soil by measuring the relative humidity in the air space within the soil (Fredlund, 1993). These devices use a change in temperature between a non-evaporation reference location and an evaporating measurement location to determine changes in relative humidity through the use of a metal sensor (Lu, 2004). Pyscrometers must be calibrated before testing can commence. The calibration allows for a relationship between the sensor output (at the dew point temperature), and previously established values of relative humidity. Salt solutions at specific temperatures can be used to dictate the relative humidity (total suction). The relative humidity (total suction) of the material can be determined from the sensor output and the calibration data.

2.2.5 Filter Paper Method (Entire Suction Range)

One of the most common and cost efficient methods for measuring soil suction is through the use of the filter paper method. The filter paper method, originally developed within the soil science discipline, operates on the premise of determining the amount of water transferred from an unsaturated soil specimen to an initially dry piece of filter paper. Two filter paper methods exist depending upon if the total or matric suction is to be determined. If total soil suction is desired the non-contact option should be explored, however, the contact method is applicable when the matric suction is desired. The water content measure is correlated to a calibration curve unique for the filter paper used, and the suction, matric or total, is able to be determined depending upon the calibration curve selected.

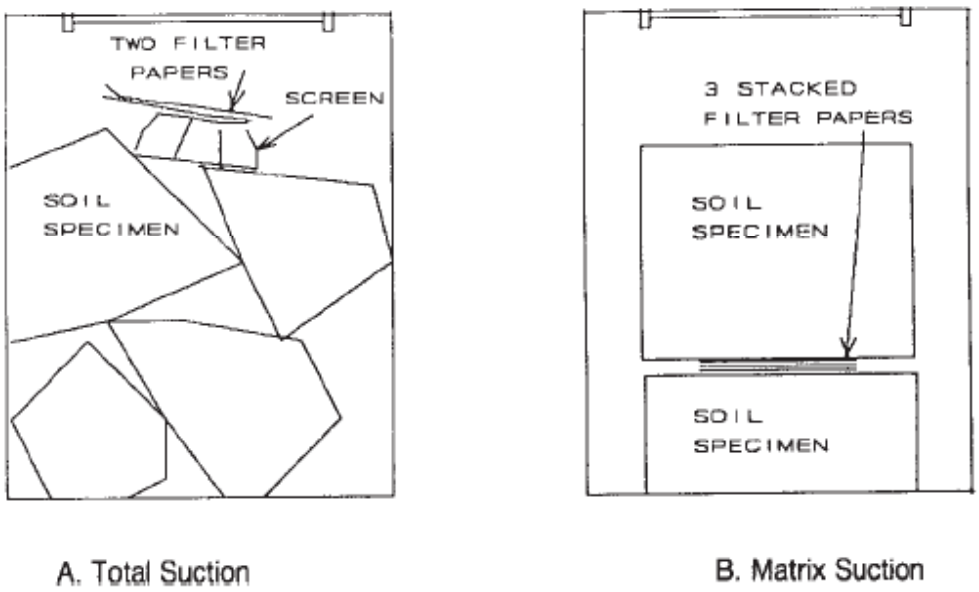

Figure 2.2.3: Filter Paper Testing Apparatus (ASTM D 5298-03)

2.3 Soil Water Characteristic Curve

The soil water characteristic curve is a graphical representation of the mathematical relationship between the matric suction of a soil (defined as the difference between the pore air pressure (u_a) and the pore water pressure (u_w)) and either its water content (gravimetric or volumetric) or degree of saturation (S) (Fredlund and Rahardjo 1993). Originally developed by soil and agricultural science (commonly referred to as moisture characteristic curve), it has gained popularly within the geotechnical engineering community through the research of Fredlund, Vanapalli and others. It represents the water storage (capacity) ability of a given material and allows for the determination of changes in matric suction with represect to changes in water content or degree of saturation. The soil water characteristic curve can be used to describe both the air pressure increase necessary to cause water to be expelled from the sample (desorption), and the pressure reduction needed for water to be imbibed into the soil (sorption).

Figure 2.3.2 shows a typical soil water characteristic curve for both the desorption and sorption phases. The figure shown is often represented with the degree of saturation versus the matric suction. Several points of emphasis will be made about the figure. First, it is a hysteretic plot, as there generally exists two different values of suction for each value of suction in the both the wetting and drying phases. The hysteric nature of the curve can be attributed to the "ink bottle effect" (Figure 2.3.1), which is the size differences between the pore spaces and the interconnecting pore throats, and air entrapment that occurs when transiting from the drying to the wetting phase (Tinjum et al., 1997).

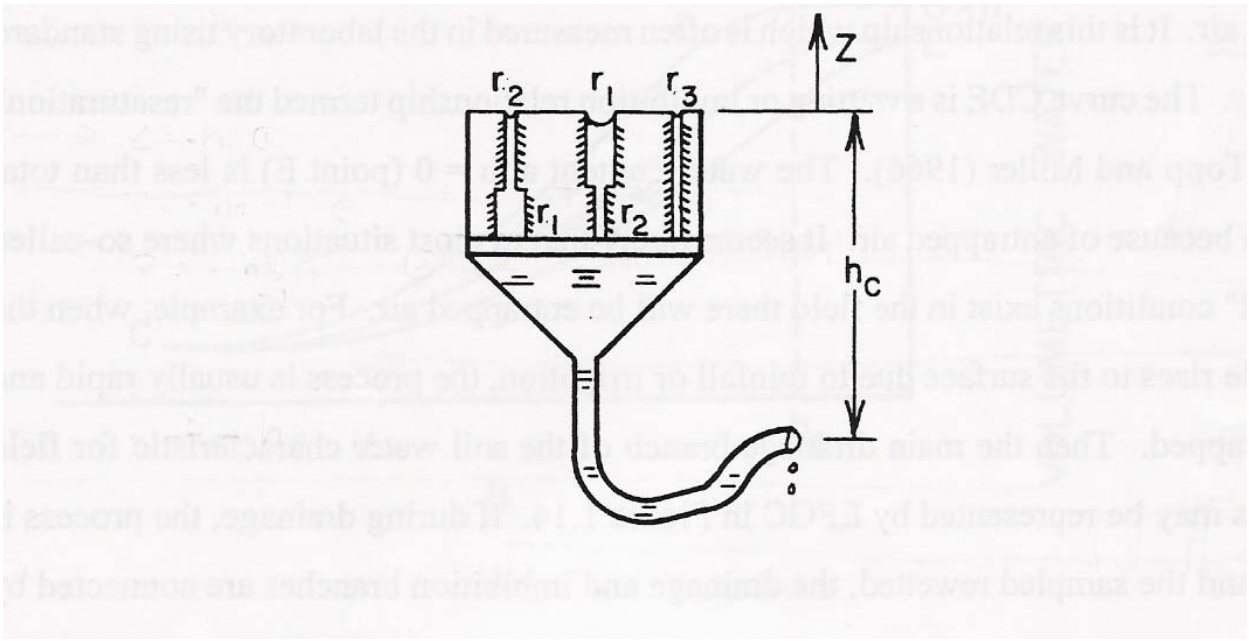

Figure 2.3.1: Nonuniform capillary tubes (Skaggs)

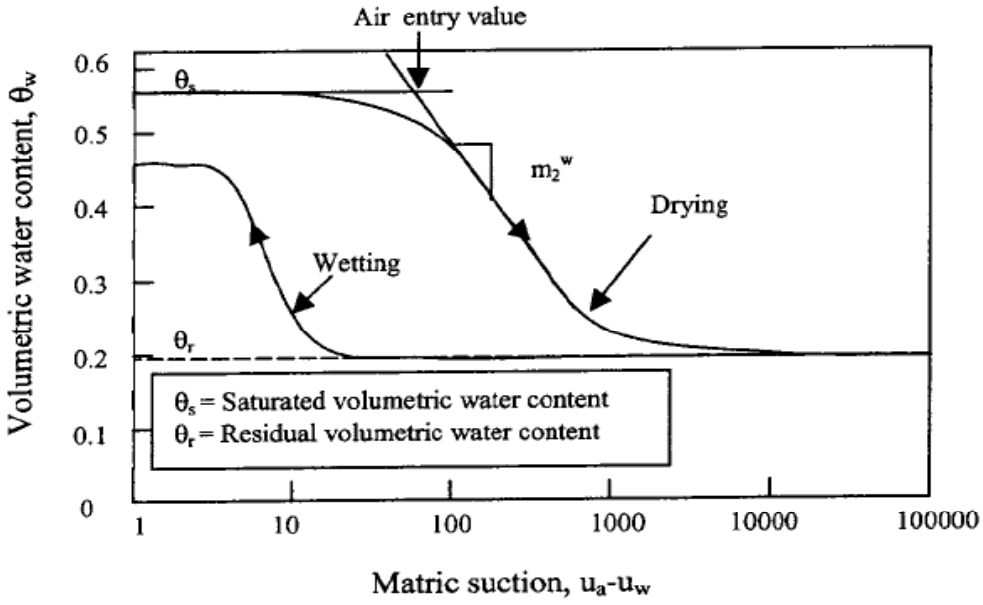

Figure 2.3.2: Typical Soil Water Characteristic Curve (Aung and Rahardjo 2001)

One parameter of interest on the SWCC is the air entry value. The air entry value represents the matric suction value needed to cause water to be drawn from the largest pore space within the soil (Brooks and Corey, 1966). In addition to the air entry value both the saturated volumetric water content and residual water content will be defined. The saturated volumetric water content is defined as the water content measured when the applied matric suction value is equal to zero, while the residual water content corresponds to highest value of matric suction that produces no additional water expulsion.

2.4 Soil Water Characteristic Measurement Techniques

This section describes commons methods used to determine the soil water characteristic curve. It is separated into several different subsections, each of which addresses different available methods. A summary of two of the most common mathematical models (van Genuchten, 1980; Fredlund and Xing, 1994) used to model the soil water characteristic curve is initially presented. The next subsection describes techniques available to estimate the soil water characteristic curve. Techniques include estimations from the grain size distribution curve and the pore size distribution for a specific material. Finally, a synthesis of the experimental methods available for determining the soil water characteristic curve is provided.

2.4.1 Mathematical Models

This section describes the mathematical models used to describe the soil water characteristic curve. It attempts to give an overview of some of the most common models used to estimate the soil water characteristic curve. There are several papers from the literature that have not been presented in this section, as Leong and Rahardjo (1997) have

presented an excellent review of the soil water characteristic models presented in the literature.

2.4.1.1 van Genuchten (1980)

Based on Mualem's theory (Muealem, 1976), van Genuchten developed an equation for the soil water content-pressure head curve that when fit to experimental data resulted in three independent parameters that could be used to determine the hydraulic conductivity based on models proposed by Burdine and Mualem. Mualem's model, given below, showed that the permeability could be determined based on information obtained from the soil water characteristic curve.

$$K_r = \Theta^{1/2}\left[\int_0^{\Theta}\frac{1}{h(x)}dx \Big/ \int_0^{1}\frac{1}{h(x)}dx\right]^2 \tag{2.3}$$

where h is the pressure head, that's a function of the dimensionless water content, Θ.

$$\Theta = \frac{\theta - \theta_r}{\theta_s - \theta_r} \tag{2.4}$$

r and s represent the residual and saturated water contents, respectively.

Van Genucten used the following relationship to relate the dimensionless water content to the soil water retention curve.

$$\Theta = \left[\frac{1}{1+(\alpha h)^n}\right]^m \tag{2.5}$$

where α, m, and n are parameters determined from the soil water retention curve. Combining equations (2.4) and (2.5), the following model was proposed.

$$\theta = \theta_r + \frac{(\theta_s - \theta_r)}{\left[1 + (\alpha h)^n\right]^m} \quad (2.6)$$

Four independent parameters (α, n, θ_s, and θ_r) were estimated from the soil water retention curve. Values of saturated water content (θ_s) were obtained by determining the water content of soil specimens in their saturated conditions. Residual water contents (θ_r) were either determined from the soil water retention curve or determined by measuring the water content of dry soil samples (no distinction between air or oven dry was provided by the author). A parameter S that was evaluated at the midway point of the curve (Θ = ½) was selected and used to describe the slope of the moisture retention curve. The subscript P, in Equation 2.7 was used to denote the halfway location on moisture retention curve and the location in which each equation was evaluated. The parameter m was determined from evaluating S_p using the following.

$$m = 1 - e^{(-.8S_p)} \qquad (0<S_p \leq 1) \quad (2.7)$$

$$m = 1 - \frac{.5755}{S_P} + \frac{.1}{S_P^2} + \frac{.025}{S_P^3} \qquad (S_p>1) \quad (2.8)$$

The parameters n and α were determined from the following two relationships.

$$m = 1 - \frac{1}{n} \quad (2.9)$$

and,

$$\alpha = \frac{1}{h}(\Theta^{-1/m} - 1)^{1/n} \quad (2.10)$$

2.4.1.2 Fredlund and Xing (1994)

Fredlund and Xing proposed a new model for estimating the soil water characteristic

curve based on the shape of the soil water characteristic curve being a function of the material's pore size distribution. They initially started with an integrated form a frequency distribution (Equation 2.11) with the ability of modeling the soil water characteristic curve over the entire suction range (0 to 10^6 kPa).

$$\theta(\psi) = \int_{\psi}^{\infty} f(h)dh \tag{2.11}$$

where f(h) represents the pore size distribution of the material as a function of suction. The researchers determined that this particular form of the model produced non-symmetrical S-shaped curves. Several different frequency distributions (Normal, Gamma, Beta) were selected to test the accuracy of the previous mentioned model.

Fredlund and Xing modified the van Genuchten 1980 (Equation 2.5) model to account for the pore size distribution of the material (Equation 2.12).

$$f(\psi) = \frac{mnp(p\psi)^{n-1}}{\left[1+(p\psi)^n\right]^{m+1}} \tag{2.12}$$

where m, n, and p are independent curve fitting parameters.

The researchers determined that the modified model decreased to zero over a small range of suction and deemed it inappropriate for use over the entire suction range.

A new model was proposed that could be used to fit experimental data over the entire suction range (Equation 2.13).

$$f(\psi) = \frac{mnp(\psi/a)^{n-1}}{a\left[e+(\psi/a)^n\right]\left\{\log\left[e+(\psi/a)^n\right]\right\}^{m+1}} \tag{2.13}$$

where a=1/p,n, m are independent parameters

The researchers fit the previous equation to several experimental curves and determined that there existed a good relationship between experimental and estimated data.

2.4.2 Estimations from Grain Size Distribution (GSD)

Due to the intensive laboratory work and high associated costs, it has become increasingly important to predict the soil water characteristic curve from easily measured material properties. One prediction method involves estimating a materials soil water characteristic curve from its grain size distribution curve. The following subsections provide a review of the prior research conducted to estimate the soil water characteristic curve from the Grain Size Distribution.

Fredlund et al (1997) used the grain size distribution curves, dry density and specific gravity of a material to estimate the soil water characteristic curve. Swanson et al (1999) used a similar analysis method along with the SOILVISION database to compare estimated curves to experimental data. They determined that there existed a good fit for material with a more uniform particle size distribution. Fredlund et al (2002) conducted further research that used a physio-empirical model to estimate the soil water characteristic curve from its particle size distribution.

2.4.2.1 Fredlund et al (1997)

Fredlund et al (1997) proposed a modified Fredlund and Xing (1994) model to predict the soil water characteristic curve based on the grain size distribution curve, dry density, void ratio and specific gravity of the soils. Grain size distribution curves were analyzed as small increments of uniform particles

Prior research (Wagner 1994) used lognormal distributions to model experimental grain size distribution data. Fredlund et al noted that lognormal distributions did not provide the best fit in the extremes of grain size distribution curves. As a result, the researchers used the following modification to the Fredlund and Xing (1994) to fit experimental data.

$$P_p(d) = \frac{1}{\ln\left[\exp(1) + \left(\frac{g_a}{d}\right)^{g_m}\right]}\left[1 - \left[\frac{\ln\left(1 + \frac{d_r}{d}\right)}{\ln\left(1 + \frac{d_r}{d_m}\right)}\right]^7\right] \qquad (2.14)$$

where: $P_p(d)$ is the percent passing a certain particle size, g_a is a fitting parameter associated with the initial curve in the grain size distribution curve, g_n corresponds to the maximum slope of the grain size distribution curve, gm relates the curvature of the curve, d is the particle diameter (mm), d_r and d_m are the residual particle diameter and minimum particle diameter, respectively.

Fredlund et al used the mathematical model (Equation 2.14) to predict the soil water characteristic curve. Three separate approaches were used. One approach used statistical estimations of properties that described the soil water characteristic curve. Based on poor accuracy, this option was not further explored. The second method converted grain size distribution curves to pore size distribution curves, which were then used to develop the SWCC. Predicted curves contained unexpected “humps”, and terminated to zero volumetric water content much earlier than experimental data.

The third method (proposed method) treated the grain size distribution curve as segments of small uniform soil particles. Beginning with the smallest diameter size, a packing porosity term was selected for each segment. A unique soil water characteristic

curve was assigned to each segment and summed to develop the entire predicted soil water characteristic curve (Figure 2.4.1).

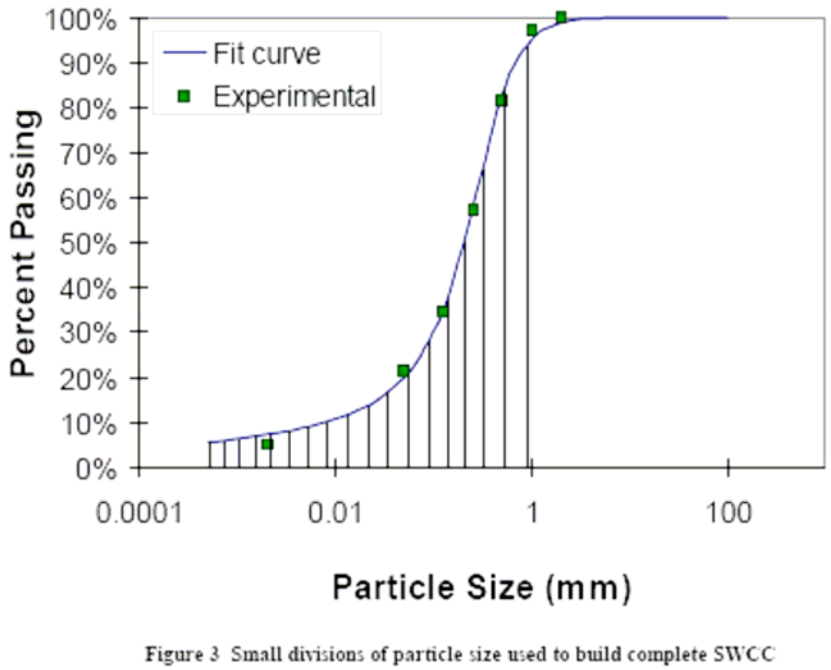

Figure 3 Small divisions of particle size used to build complete SWCC

Figure 2.4.1: Segments used to determine SWCC (Fredlund et al., 1997)

2.4.2.2 Swanson et al (1999)

Swanson et al used grain size distribution curves to predict the soil water characteristic curves for unsaturated mine soils as a means of preliminary engineering analysis and design. Swanson et al separated the grain size distribution curve into several uniform particle sizes, and estimated a SWCC from each uniform particle size. A complete SWCC was determined by summing each estimated individual curve. The researchers used the SOILVISION® computer program developed by Fredlund (1996) that combined a theoretical model with a knowledge-based system.

Grain size distribution curves for each soil sample were fit to the aforementioned model. Results showed that the model fit the curves for tailings with good accuracy, but underpredicted the soil water characteristic curves for the waste rock. It was concluded that curves were better predicted for soils with more uniform grain size distribution curves and least accurate for specimens with well-graded distributions.

2.4.2.3 Fredlund et al (2002)

Fredlund et al used parameters obtained from grain size distribution curves to predict the soil water characteristic curve (drying curve) for materials classified from sands to silty clay loam that had been prepared near the liquid limit. It is important to note that the model used by the researchers did not address the effects of the soil structure, stress history, effective confining pressure, and hysteresis on the soil water characteristic curve.

The researchers used a physio-empirical model (Arya and Paris, 1981) to estimate the soil water characteristic curve. The model uses a combination of physical material properties and empirical relationships to model the soil water characteristic behavior. The model mimicked the soil porosity through the use of a packing arrangement factor (n) that was a function of individual grain sizes. Three theorems were developed to describe the proposed model:

i. Soil with all uniform, homogenous particles has a unique drying curve;
ii. The capillary model was adequate in estimating the air-entry value for each homogenous particle size; and
iii. The entire SWCC for soil composed of more than one particle size can be represented as the sum of the SWCCs for each individual grain size.

The model performs on the same basis as the model used by Fredlund et al. (1997) whereby grain size distribution curves were sectioned into uniform particle sizes, assigned an individual SWCC and summed to develop the entire curve. In addition, the new model contained a capillary model that allowed for the estimation of the air entry value based on the assumption of the soil being composed of several homogeneous particle sizes (Equation 2.15).

$$\psi = 2T_s \frac{\cos\alpha}{\rho_w g r} \tag{2.15}$$

where T_s is the surface tension of water, α is the contact angle, ρ_w is the density of water, g is the gravitational acceleration constant, r is the pore radius, and ψ is the soil suction.

Using Equation 2.16, Fredlund et al. determined an effective grain diameter, d_e, for each grain distribution curve obtained from a combined data set (Rawls and Brakensiek, 1985; Sillers, 1996, CECIL soil survey (Bruce et al. 1983)).

$$\frac{1}{d_e} = \frac{3}{2}\frac{\Delta g_1}{d_1} + \sum_{i=2}^{i=m}\frac{\Delta g_i}{d_i} \tag{2.16}$$

where d_1 is the largest diameter of the most coarse fraction of the material, and Δg_1 is the weight of the material of the last fraction in terms of total weight.

Effective grain diameters obtained from Equation 2.16 were plotted against the n_f and m_f parameters, and Equation 2.17 was used to fit the previously mentioned data to obtain an estimate of the n_f and m_f parameters.

$$p(\phi) = p_1 \left[\frac{1}{\ln\left\{ \exp(1) + \left[\frac{10^{-\log(d_e)-1}}{p_2} \right]^{p_3} \right\}} \right]^{p_4} + p_5 \qquad (2.17)$$

where p_1 through p_5 are curve-fitting parameters, d_e is the effective grain-size diameter, and $p(\phi)$ is the value of either n_f or m_f.

Results showed that the proposed model provided good estimates of the soil water characteristic curves for sands and silts, however, there appeared to be difficulty in estimating the soil water characteristic curves for clays, tills, and loams. It was determined that while there existed more difficulty for estimating the SWCCs for the previously mentioned soils, the estimations appeared reasonable.

2.4.3 Estimations from Pore Size Distribution (PSD)

Similar in nature to predictions from the grain size distribution, it has been noted that the shape and behavior of the soil water characteristic curve is closely related to the pore size distribution of the material in question (Fredlund and Xing, 1994). Knowledge of the pore size distribution of materials allows for the estimation of the soil water characteristic curve through the use of the mathematical modeling techniques that will be described in the following sections.

2.4.3.1 Simms and Yanful (2004)

Simms and Yanful used data obtained from Pore Size distribution analyses to predict the drying portion of the soil water characteristic curve. Laboratory samples were compacted

using the Standard Proctor mold at various as-compacted water contents. The saturated permeability of the specimens was then determined using a flexible wall hydraulic conductivity device. Immediately following permeability tests, pore-size distribution tests were conducted on trimmed 1 g soil samples.

Pore size distribution results showed that the curves were bimodal with larger modes peaking between pore diameters of 1 and 10μm, and smaller modes peaking between 1 and 0.1μm. It was also determined that the pore mode size changes with changing water content, however, the size and shape of pore modes less than 0.1mm were a function of the soil mineralogy and not changes in test conditions.

Simms and Yanful used the pore size distribution data to predict the gravimetric soil water characteristic curve. The process was generated by the assumption that a change in specimen water content corresponded to a change in the volume of pores drained. It was also assumed that the water remained at a constant density of 1 cm^3, therefore, a gravimetric change of 1g corresponded to a volumetric change of 1 cm^3 of water. The researchers used the following model to predict the soil water characteristic curve from the pore size distribution.

$$X(\psi) = X(0) - \sum_{0}^{\psi} \upsilon f(\psi) \tag{2.18}$$

where, X = gravimetric water content, and $\upsilon f(\psi)$ = pore size distribution function based on porosimetry data.

Assumptions for the above relationship were used to account for the functions underprediction of gravimetric water contents when predicted directly from pore size

distribution curves. It was believed that the discrepancy was due to smaller pores entrapping large pores, thus preventing proper desaturation. Simms and Yanful also assumed that pore cylinders shrank elastically as the pore volumes drained.

2.4.3.2 Zhang and Chen (2005)

Using the capillary law for the basis of their model, Zhang and Chen (2005) predicted the soil water characteristic curve for gap graded soils. The researchers used the model proposed by Fredlund and Xing (1994) as a means of predicting the soil water characteristic curve. The model used worked under the premise that the soil pore spaces are different sized cylindrical tubes and that the capillary law, which states that water will fill the smallest pores first, is valid. The researchers addressed soils with both bimodal and multimodal pore size distribution functions (Figure 2.4.2).

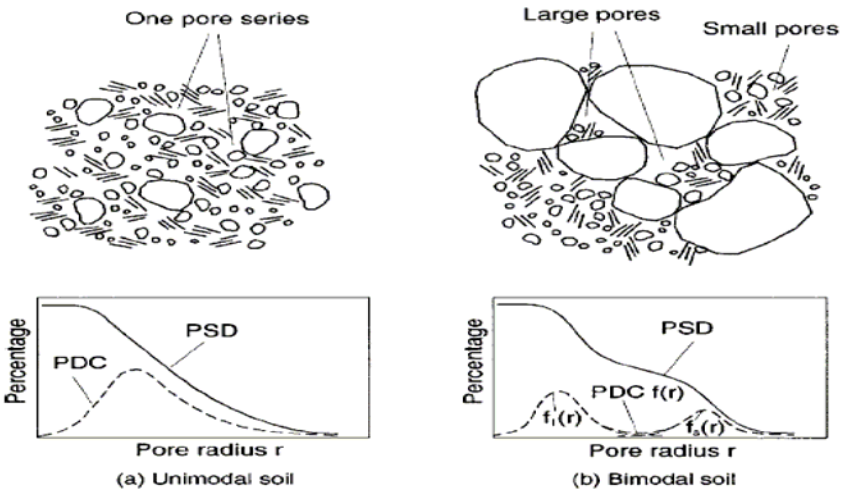

Figure 2.4.2: Soil Structure and pore-size distribution (Zhang and Chen 2004)

Zang and Chen used the preexisting van Genucten (1980) and Fredlund and Xing (1994) models to predict the soil water characteristic curves for materials with bimodal pore

size distributions. They suggested that material with a multimodal grain size distribution could have a multimodal pore size distribution and needed to be fit by a modified model to accomadate for the multimodal distribution. They used the following model (extension of Fredlund and Xing, 1994) to fit experimental data that contained multimodal grain size distributions:

$$\theta(\psi) = \sum_{i=1}^{N} p_i \theta_i(\psi) \tag{2.19}$$

where *N*= number of pore series: p_i=polumetric percentage of the soil component with the ith series; and $\theta_i(\psi)$= soil water characteristic curve associated with ith pore series. Results showed that there existed good correlation between the experimental and predicted soil water characteristic curves.

2.4.4 Experimental Methods

There are several different experimental techniques available for determining the soil water characteristic curve. Some of the methods include the Filter Paper Method, Hanging Column, and Chilled Mirror Hygrometer methods, among others. Another method that has gained popularity within the geotechnical engineering community involves the use of pressure plate testing devices. Pressure plate devices operate on the basis of the axis translation technique originally proposed by Bishop (1960) that allows for the independent measurements of the pore-air pressure and pore-water pressure by keeping the pore-water pressure at a constant value (usually zero) through the use of a high air entry ceramic disc. The following discussion serves as a review of the research that has been conducted using the volumetric pressure plate extractors.

2.4.4.1 Tanner and Elrick (1958)

Tanner and Elrick (1958) addressed two concerns with the use of volumetric pressure plate extractors originally proposed by Richards and Fireman (1943). The researchers new modified pressure plate device addressed the volume measurement inconsistencies that arose from condensation that developed within the interior walls of the pressure plate apparatus. These individuals also addressed issues of accumulated gas that was collected beneath the porous plate.

Tanner and Elrick measured the quantity of water release and intake on a volumetric basis in addition to the gravimetric method that had been used by previous researchers. Volumetric outflow was measured through the use of a horizontal ballast tube. The horizontal elevations of the ballast tube and the porous plate were set to an equivalent value in order to prevent a head difference within the test set-up.

A 3-watt heater was placed on top of the pressure plate apparatus to counteract the effects of the condensation that developed on the interior walls of the device. The heater provided a low temperature gradient that was assumed to have negligible effects on the soil sample. Gas accumulation beneath the porous plate resulted in inaccurate volume measurements and prevented water from being imbibed into the soil sample when the suction was decreased. A glass air collection device was placed below the porous plate so that liquids could be continuously cycled below the porous plate while allowing the air to be collected in the collection device.

2.4.4.2 Tinjum et al. (1997)

Tinjum et al. (1997) measured the soil water characteristic curve for four soil samples using the volumetric pressure plate extractors. Specimens were compacted dry, optimum, and wet of optimum moisture content. In addition, both the Standard and Modified Proctor energies were used. The researchers studied the affects of the as-compacted water content on the shape of the soil water characteristic curve. Results showed that the air entry value increased as the as-compacted water content increased (Figure 2.4.3). These findings were consistent with prior research (Vanapalli 1996). Experimental curves were fit using the van Genuchten model and results were presented in terms of the van Genucthten α and n parameters (note that α and Ψ_a are inversely related).

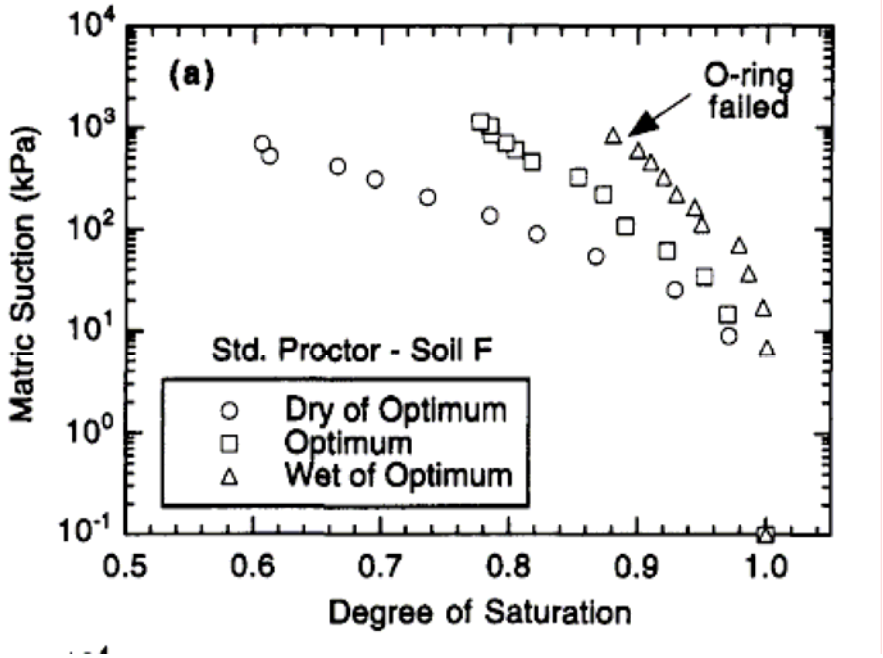

Figure 2.4.3: Soil Water Characteristic Curve-Standard Proctor (Tinjum et al 1997)

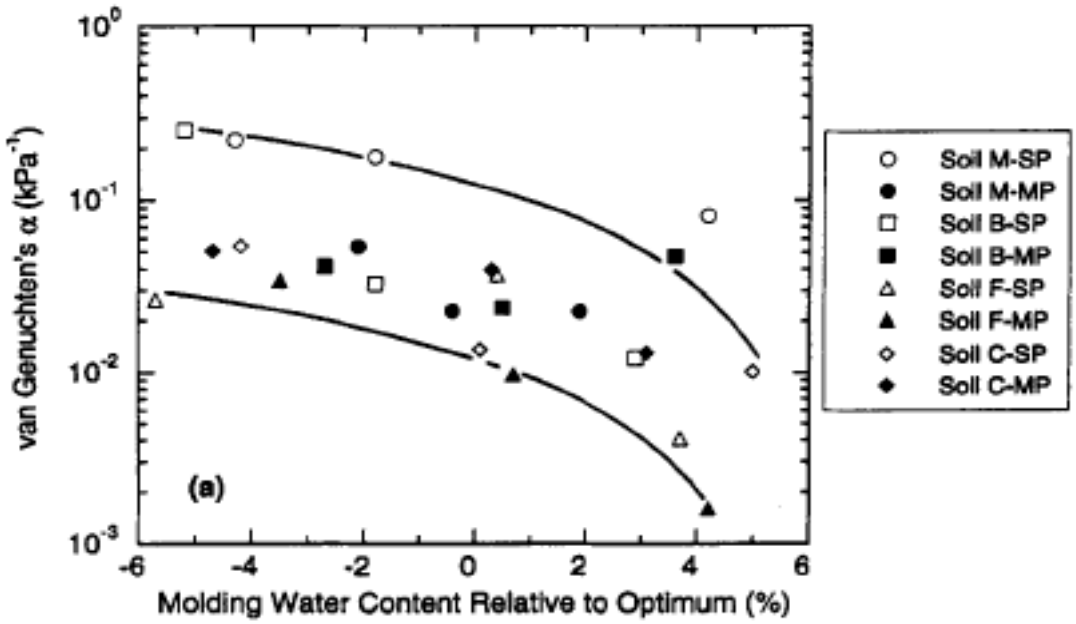

Figure 2.4.4: van Genuchten's α vs. as-compacted water content (Tinjum et al 1997)

Tinjum et. al used the curve fit to confirm the effects of the as-compacted water content on the air entry value of the material tested. They showed that as the as-compacted water content increased (Figure 2.4.4), the van Genuchten α parameter decreased (by model definition, the α parameter is inversely related to Ψ_a, the air-entry value (Equation 2.6)). It was also shown that no relationship between the dry density and the α parameter could be achieved (Figure 2.4.5) for material compacted using the Standard Proctor energy. This suggested that the as-compacted dry density (unit weight) has little affect on the air entry value at the Standard energy, and it is the as-compacted water content that is the controlling parameter.

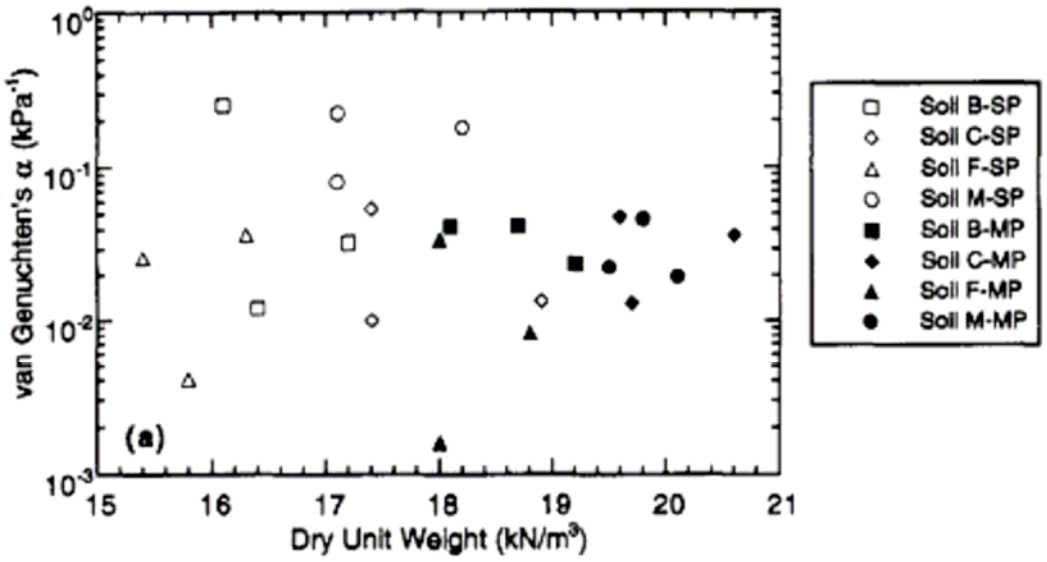

Figure 2.4.5: van Genuchten's α vs. dry unit weight (kN/m^3) (Tinjum et al 1997)

2.4.4.3 Vanapalli et al (1999a)

Vanapalli et al presented the results of an experimental program that showed the soil structure of clay till obtained from Indian Head, Saskatchewan, Canada, was influenced by the as-compacted water content. In addition to the as-compacted water content, the researchers examined the effects of stress history on the soil water characteristic curve. Based on the shape of the curves, they indirectly confirmed that the macrostructure of the same soil compacted at a different as-compacted water contents is different even though they share the same mineralogy and compaction method.

Material was compacted to the desired density and as-compacted water content and saturated under a 3.5 kPa overburden pressure. Material was then consolidated under the desired overburden pressure (Figure 2.4.7 Point A). Samples were then allowed to swell

under a 3.5 kPa overburden pressure. The void ratio obtained during the unloading procedure was paired with an overburden pressure on the virgin compression curve to achieve an "equivalent pressure". Figure 2.4.6 shows the material matrix used for the experimental program, and Figure 2.4.7 shows the procedure used to obtain the equivalent pressure for the material tested for the soil water characteristic curve.

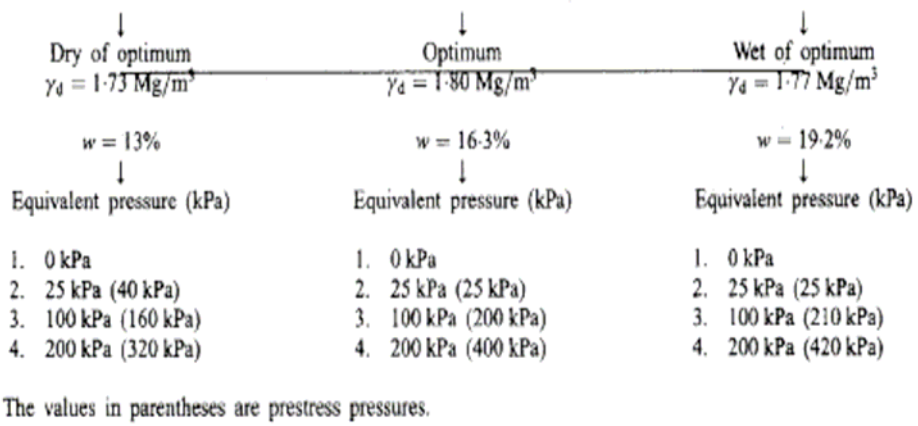

Figure 2.4.6: Soil matrix used for experimental program (Vanapalli 1999a)

Materials compacted dry of optimum were shown to have a lower resistance to water flow (lower air entry value) due to the large pore spaces located between clods of soil. Vanapalli et al also showed that the shape of the soil water characteristic curve is influenced by the structure of the soil. Specimens compacted dry of optimum exhibited a lower air entry value, and a steeper slope past the air entry value in the desaturation stage. Wet of optimum specimens, in comparison to those compacted dry of optimum, produce a flatter SWCC slope past their higher air entry value as the resistance to water flow is higher for a given suction (due to the microstructure controlling desaturation) that results in a smaller water release for a given incremental change in matric suction than dry of optimum material.

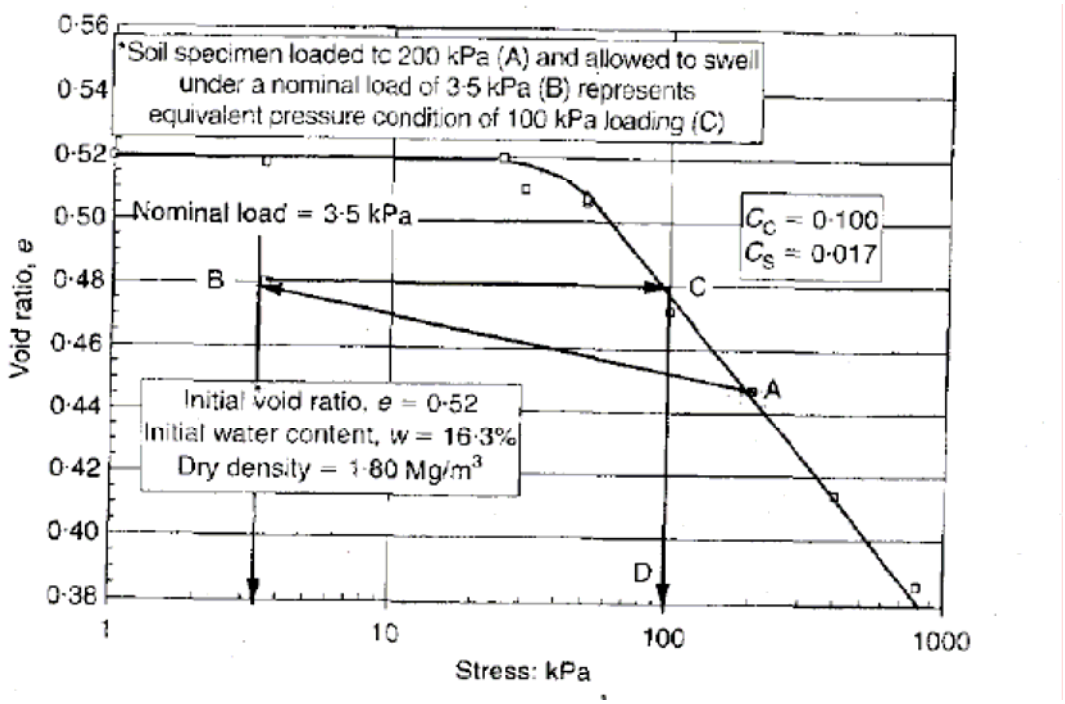

Figure 2.4.7: Procedure used to obtain equivalent pressure (Vanapalli (1999a)

In addition to the investigation of soil structure on the behavior of the soil water characteristic curve, the researchers also examined the effects of the as-compacted water content and overburden pressure (equivalent pressure). Figure 2.4.8 through Figure 2.4.10 show the soil water characteristic curves for material compacted dry, at optimum, and wet of optimum, respectively. It can be seen from these three figures that the air entry value of the material tested is more affected by overburden pressure when compacted dry of optimum (Figure 2.4.8), and becomes less influenced as the as-compacted water content transitioned (Figure 2.4.9) to more wet of optimum conditions. At wet of optimum conditions (Figure 2.4.10), the influence of the overburden pressure resulted in minimal changes in the air entry value (20 kPa difference in air entry value for equivalent pressures ranging from 0 to 200 kPa).

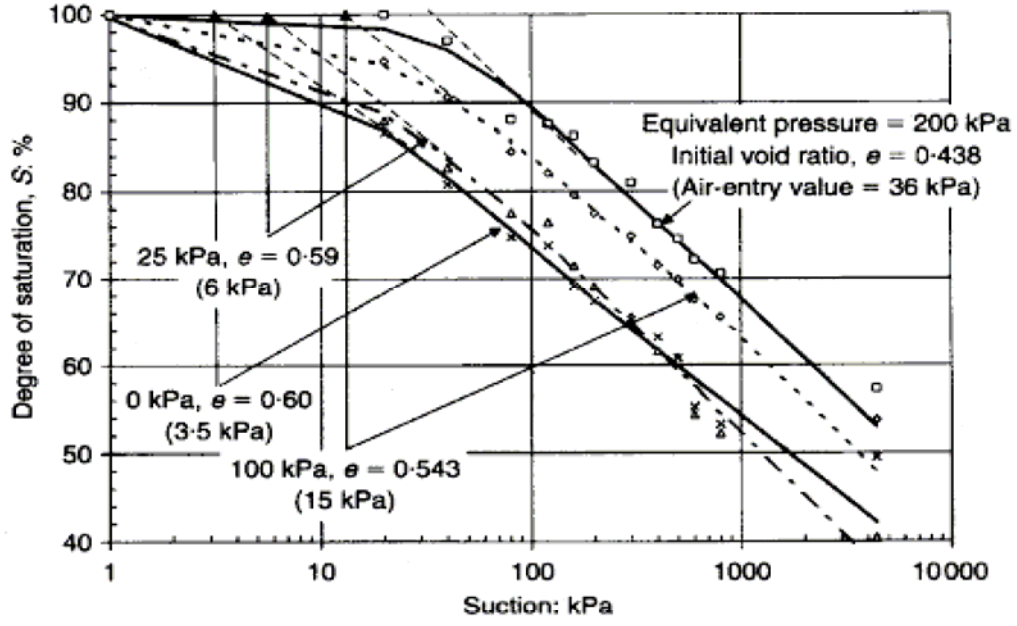

Figure 2.4.8: SWCCs for material compacted dry of optimum (Vanapalli 1999a)

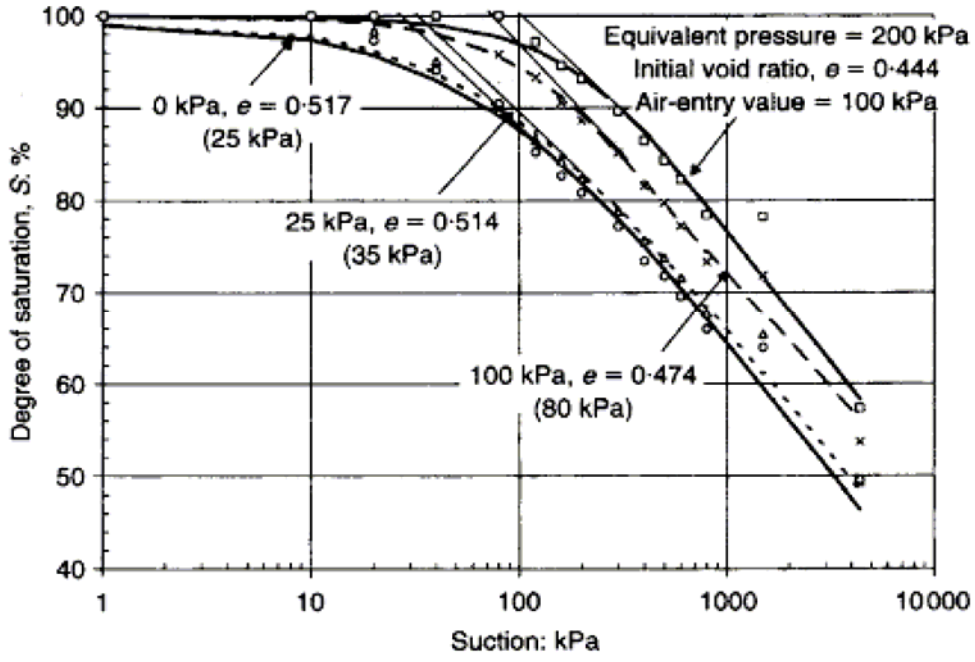

Figure 2.4.9: SWCCs for material compacted at optimum moisture (Vanapalli 1999a)

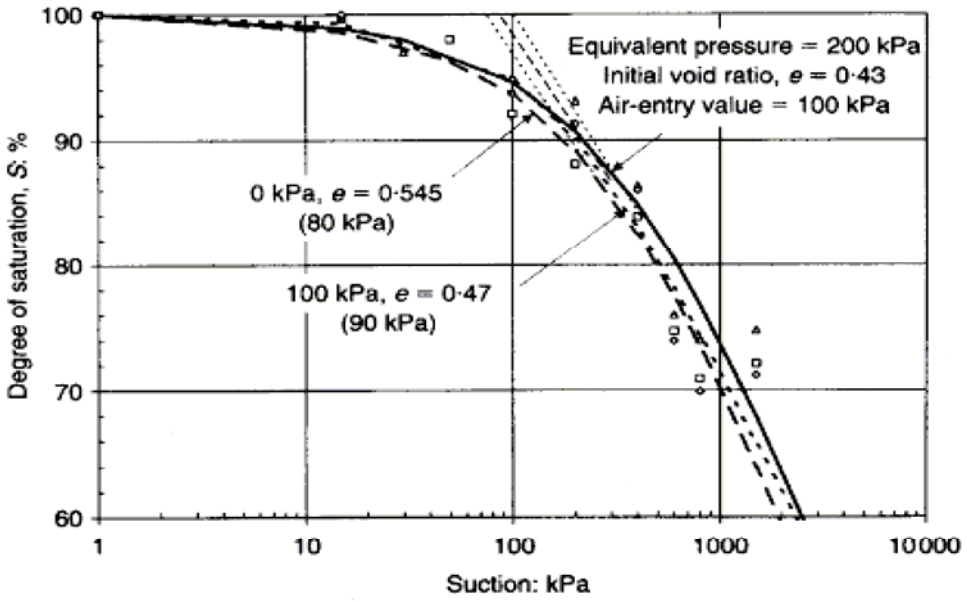

Figure 2.4.10: SWCCs for material compacted wet of optimum (Vanapalli 1999a)

Figure 2.4.11 shows the influence of the initial void ratio (void ratio corresponding to the respective equivalent pressure [i.e. 0, 25, 100, and 200 kPa]) on the air entry value. It also shows the influence of the as-compacted water content on the air entry value. It is key to note that based on these findings the air entry value increases with increasing density (obtained from equivalent density technique). The results also showed that for the material tested, the effects of the initial density on the air entry value were more pronounced on material compacted at optimum moisture content than for material compacted either dry or wet of optimum moisture content.

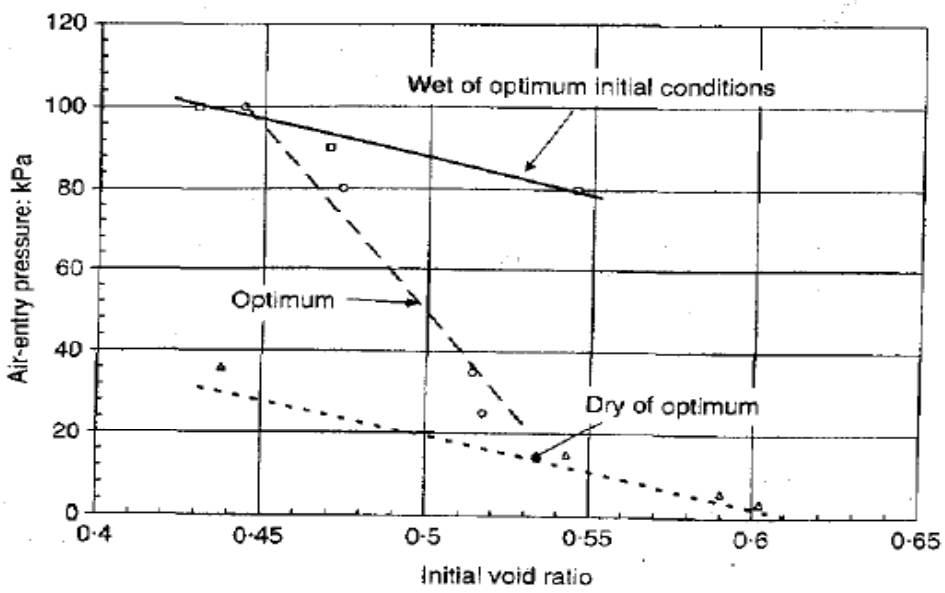

Figure 2.4.11: Air entry value vs. Initial void ratio (Vanapalli 1999a)

2.4.4.4 Vanapalli et al (1999b)

Based on an experimental program (explained in detail in previous section Vanapalli et al 1999a) that included testing compacted material, statically and conventionally (using the Standard Proctor), Vanapalli et al concluded that the soil water characteristic curve is largely dependant on the structure of the soil. By comparing the soil water characteristic curves obtained from specimens tested in a pressure plate apparatus to individual compacted specimens tested in a null type device, they concluded that the as-compacted water content governs the structure of the soil.

The researchers showed that specimens compacted dry of optimum contained lower air entry values than their wet of optimum counterparts (Figure 2.4.12). This finding is due to the large pore spaces between the soil flocs that allow for easier removal of water under a given matric suction.

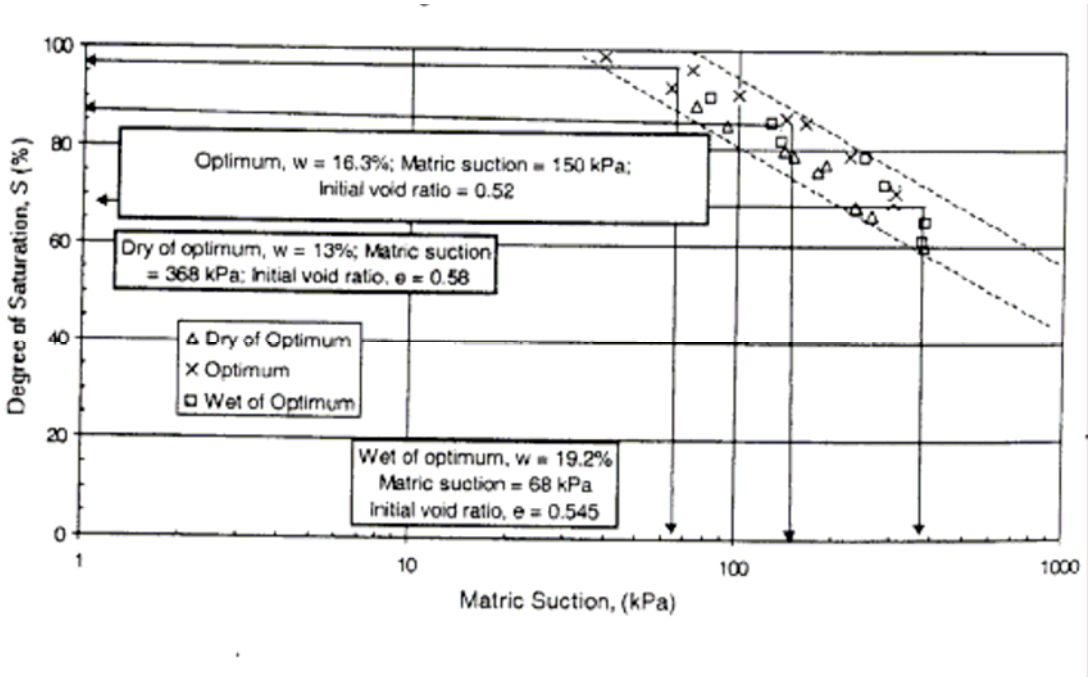

Figure 2.4.12: SWCCs for individually compacted specimens (Vanapalli 1999b)

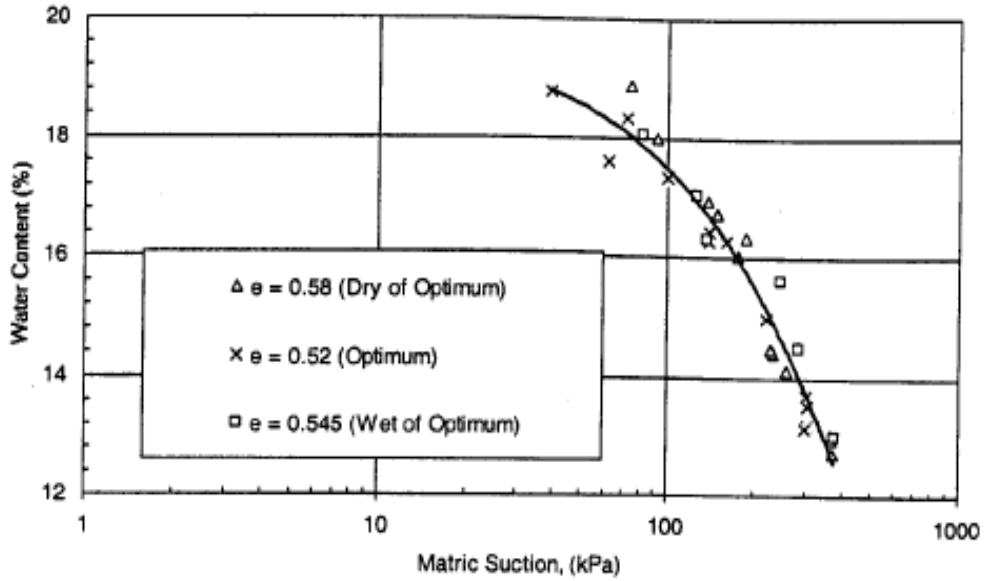

Figure 2.4.13: Gravimetric water content vs. Matric Suction (Vanapalli et al 1999b)

The air entry value increases for specimens compacted wet of optimum due the water being trapped within smaller pore spaces between individual soil particles in the flocs.

Based on comparisons of individually compacted specimens (prepared at same dry density and different as-compacted water contents), Vanapalli et al. determined that the initial density of the specimens tested had little influence on the air entry value and the shape of the curve (Figure 2.4.13). They showed that the variation in curve shape and air entry values of the material tested resulted from the varying as-compacted water content, as Figure 2.4.13 presents data from test specimens prepared at similar dry densities and different as-compacted water contents.

2.4.4.5 Wang and Benson (2004)

Due to air leakage experienced in previous designs of pressure plate extractors, Wang and Benson (2004) developed the Leak Free Pressure Plate Extractor. Not only did the new design prevent air leakage from the bottom edge of the chamber, it also allowed for the installation of an overburden piston.

The pressure plate design was intended to remain leak-free up to an air pressure of 1500 kPa. The device was machined from brass bar stock to have a circular top plate that contained a cylindrical body that rests into a recessed groove located on the circular bottom plate. The bottom plate included a 79 mm circular recessed region where a 15 bar ceramic high air entry disc could be situated. A 9.5 mm square Buna-N cord gasket (chamfered at 45^{o}) was placed around the 79 mm diameter and 7 mm tall ceramic high air entry disc. Once the top chamber was lowered into the recessed area on the bottom plate and the bolts

tightened, the Buna-N cord was sealed at the 45^{o} chamfer, thus preventing the escape of air from the chamber.

Trapped gas beneath the ceramic disc was removed through the use of 0.8 mm deep grooves that were machined in the bottom plate beneath the location where the ceramic rested and through the application of a flushing fitting that was attached onto the exterior of the bottom plate. Any trapped air can be flushed from beneath the ceramic disc by circulating water through the outflow tubing.

The researchers also adapted a new procedure to determine the soil water characteristic curve using the Leak Free Pressure Plate Extractor. The procedure used by the researchers has been adopted as Method B in the ASTM D 6836 – 02 standard. Unlike other pressure plate extractors that were able to test multiple samples at one time, the new device tested only one sample per chamber. Based on the outflow volume of water (determined by measuring the air water interface movement in a capillary tube using a scale with a $\pm 0.5mm$ precision) , the water content of the soil was determined on a volumetric basis as opposed to the more common gravimetric basis. The following equation was used to determine the volumetric water content. The volumetric water content (θ_i) for a given matric suction value is determined by taking the difference

$$\theta_i = \theta_{i-1} - \frac{\Delta L A_c}{V} \tag{2.20}$$

between the volumetric water content at a previous value of suction (θ_{i-1}) and the quantity representing the combined effects of the change in position of the air-water interface (ΔL) under a given suction, the cross-sectional area of the capillary tube (A_c), and the volume of

the specimen (V).

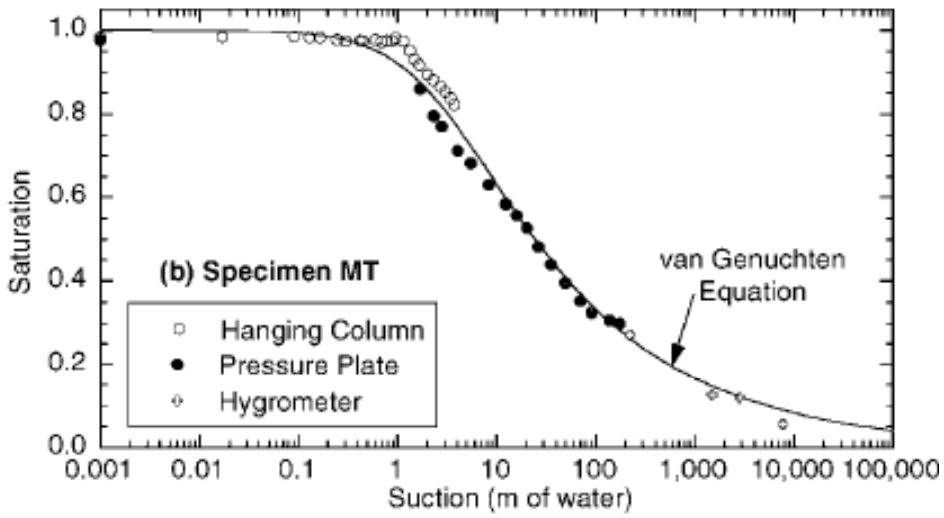

Figure 2.4.14: SWCC for entire suction range (Wang and Benson 2004)

Soil Water Characteristic Curves obtained by the experimental work were fit to the van Genuchten 1980 function shown below.

$$\frac{S - S_r}{1 - S_r} = \left\{ \frac{1}{1 + (\alpha\psi)^n} \right\}^{1-1/n} \tag{2.21}$$

where the degree of saturation is denoted by S, the residual degree of saturation is represented by S_r, and α and n represent empirical curve fitting parameters. Results (Figure 2.4.14) showed that there existed a good fit between the experimental data and the fit of the van Genuchten function.

2.4.5 Soil Water Characteristic Curve Measurement Techniques Summary

The soil water characteristic curve is one, if not the single most important, parameter needed to analyze unsaturated soils. The previous sections have served as a synthesis of the

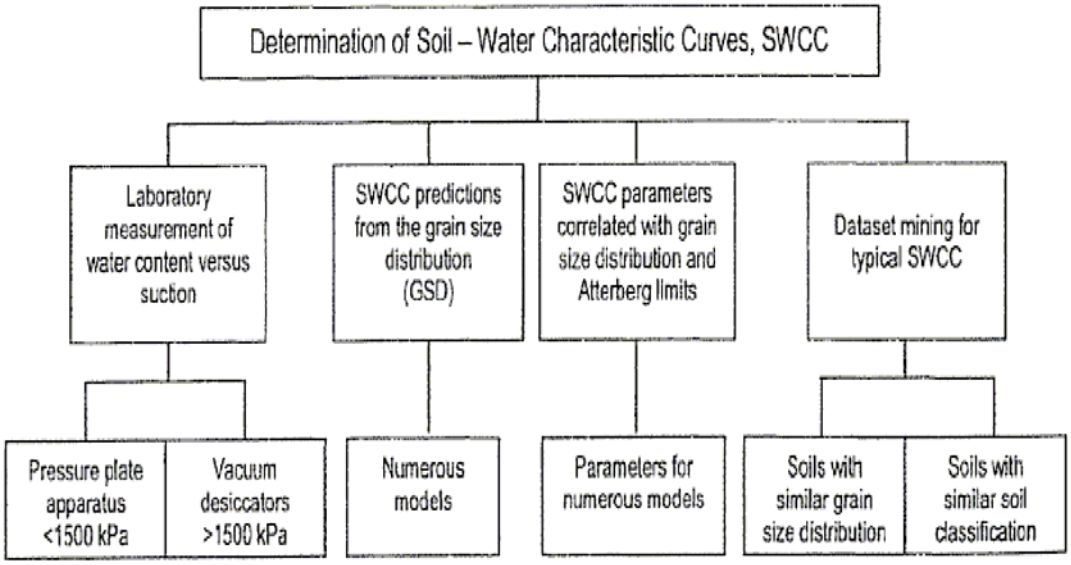

Figure 2.4.15: Soil Water Characteristic Determination Methods (Fredlund 2006)

literature involving the estimation, prediction and experimental methods available for obtaining the soil water characteristic curve. Figure 2.4.15 provides a comprehensive list of available methods for determining the soil water characteristic curves. This following discussion summarizes the literature presented in the previous section. It primarily focuses on the experimental methods, as the primary goal of the current study is to experimentally determine the soil water characteristic curve of fine-grained compacted material.

Results from pressure plate tests conducted on compacted material by Tinjum et al. (1997) concluded that for the range of void ratios tested, the as-compacted water content governed the air entry value and shape of the soil water characteristic curves. No relationship between the density and the air entry value could be established for material compacted with the Standard Proctor energy. Vanapalli et al. (1999a) examined the influence of the soil structure as stress history on a compacted fine-grained material. They

determined that for the material tested, specimens with higher magnitudes of prestress exhibited soil water characteristic curves with higher air entry values, for a given as-compacted water content. The researchers also showed that the air entry value increased with increasing as-compacted water contents. Results presented by Vanapalli et al (1999a) agreed with the findings of Tinjum et al (1997), as they showed that material compacted at different initial densities exhibited similar air entry values. Their results showed that the air entry value exhibited a strong dependence on the as-compacted water content. Material compacted dry of optimum exhibited lower air entry values than material compacted wet of optimum due to the macrostructure controlling desaturation in the dry of optimum conditions.

2.5 Collapse Potential

Collapse potential, which is defined as the volumetric strain difference between an as-compacted specimen and a separate "identical" sample that has been inundated (double oedometer method), is an important parameter to consider when examining the volume change characteristics of partially saturated compacted material. This section provides information regarding the previous research that has been conducted on the collapse potential of compacted unsaturated material. This section provides the four mechanisms (open structure, partially saturated structure, presence of bonding agent in unsaturated state, and infiltration that reduces bonding agent) necessary for collapse to occur in unsaturated soils. It is intended to serve as a guide to illustrate how the as-compacted water content and relative compaction affect the structure (micro and macro) that directly control the collapse potential of a compacted soil specimen. This section also presents information regarding the influence of matric suction on collapse potential.

2.5.1 Barden et al (1973)

Using scanning electron microscope (SEM) technology, Barden et al (1973) examined the structure of collapsible soils from various locations around the world. The researchers proposed three mechanisms necessary for soil collapse to occur:

i. Open unstable partially saturated soil structure;
ii. Normal stress large enough to cause structural instability; and,
iii. Bonding agent (suction) that is present in partially saturated case that is mitigated upon water infiltration.

An explanation of how an open structure could be created was proposed. The researchers stated that sand grain-size particles could be cemented together by capillary action that exists between the silt particles that were present between the individual sand particles. Barden et al stated that the majority of collapsible soil structures are a result of clay platelets that serve as a bonding agent between larger sand and silt particles. Upon infiltration, pore water pressure become positive and the negative suction is mitigated thus causing volume change to occur.

2.5.2 Lawton et. al (1989)

Research by Lawton et. al showed the affects of the as-compacted water content and relative compaction on the collapse potential of a partially saturated compacted SC (clayey sand) material. The study included material compacted to the Modified Proctor energy, and a reduced Proctor energy. The researchers showed that there existed an inverse relationship between the collapse potential and the degree of relative compaction. It was also shown that

there existed an inverse relationship between the as-compacted water content and collapse potential (Figure 2.5.1)

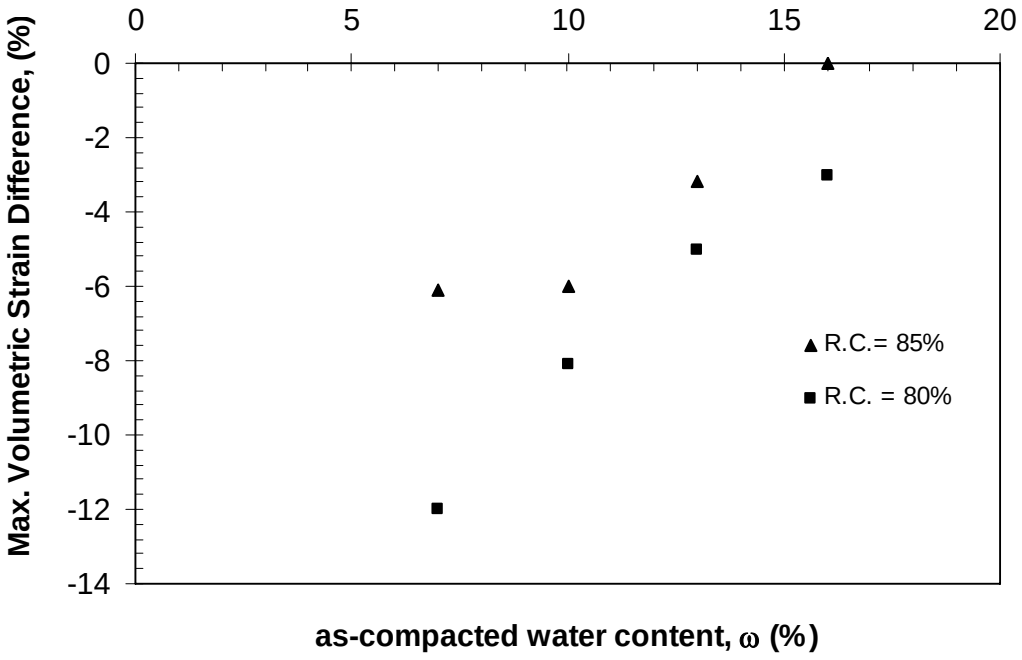

Figure 2.5.1: Collapse vs. as-compacted ω (after Lawton et al 1989)

Results showed that collapse increased with increasing as-compacted water contents for all degrees of relative compaction examined. Lawton et al showed that there also existed a critical as-cmpacted water content (water content that corresponds to a degree of saturation along the line of optimums) where collapse potential could be mitigated. Compaction at water contents higher than this critical value produced specimens that exhibited swelling behavior.

2.5.3 Lawton et. al (1992)

Lawton et al presented a detailed review of the parameters affecting the collapse of compacted soils. The researchers provided a detailed review of the research that has been conducted on the wetting induced collapse potential of compacted material. They provided their knowledge base on susceptible soil types, and the parameters affecting collapse potential.

Based on their literature review, it was shown that nearly all soils are prone to collapse. Single oedometer results showed that the collapse potential for a sand-clay mixture reaches a maximum value with a clay content ranging from 30-40%, and 10-20% for silt-clay mixes (Figure 2.5.2). It was shown that at low clay contents, the silt specimens exhibited higher collapse potential than their sand counterparts. Conversely, at higher silt contents, specimens experienced collapse potential smaller than the sand specimens. It was hypothesized that at low clay contents, macropeds (large soil flocs) were able to develop and the clay served as a bonding agent that held the larger silt and/or sand particles intact. Upon wetting, the bonging agent was lessened and volume densification (collapse) was allowed to commence. Lawton et al stated that at a higher clay content, the collapse potential is offset by the soils tendency to swell.

Lawton et al stated that the most important parameters that control collapse potential are the prewetted moisture content, dry density, and stress state. They showed that the pre-wetted moisture content governed the collapse potential, and not the as- compacted water content as had been previously reported. It was concluded that collapse potential increases as the water content and density decrease, and the vertical stress increases. It is to be noted that

there existed a vertical stress at which collapse potential was maximum; past this critical value soil samples experience minimal volume change. Finally, they stated that there existed a critical degree of saturation above which collapse potential becomes negligible.

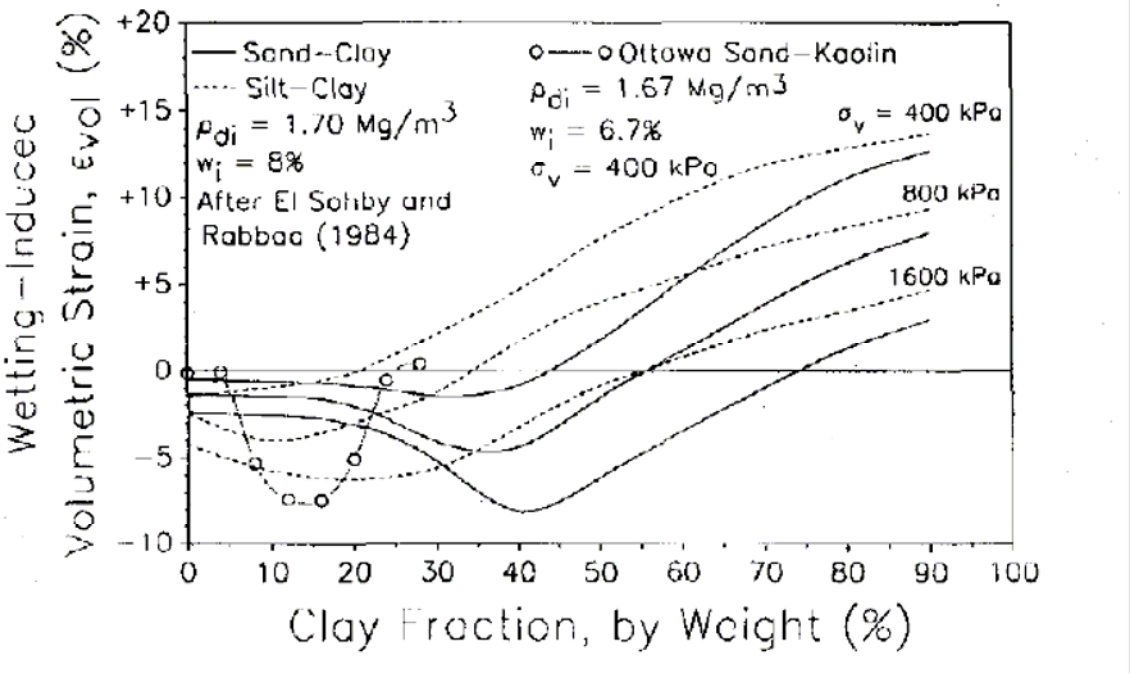

Figure 2.5.2: Influence of Clay % on collapse potential (Lawton et al 1992)

2.5.4 Rao and Revanasiddappa (2000)

Rao and Revanasiddappa studied the effects of the matric suction on the collapse behavior of compacted Bangalore clay soil specimens. In addition, they examined the effects of the compaction parameters (as-compacted water content and relative compaction) on the matric suction and collapse potential of the compacted clay specimens.

Specimens were statically compacted into consolidometer rings (76 mm diameter, 25 mm height) to obtain the desired density. The filter paper method (ASTM D5928-94) was

used to determine the matric suction of the compacted specimens in their as-compacted state for the range of relative compaction studied (Figure 2.5.3).

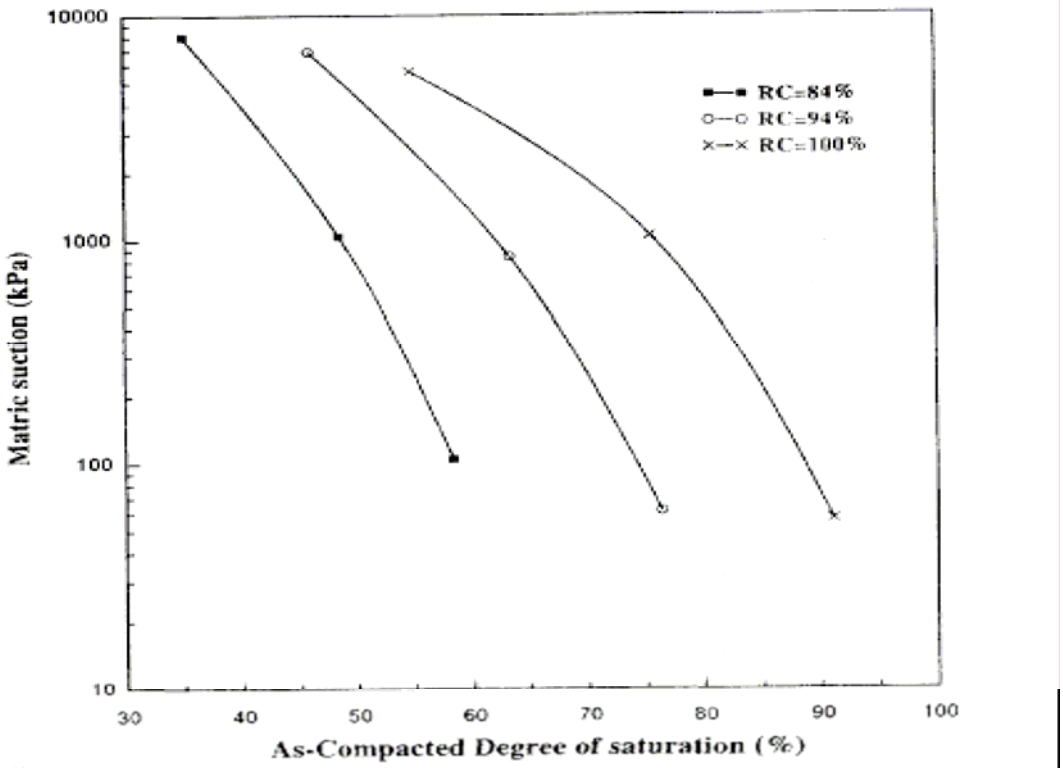

Figure 2.5.3: Matric Suction vs. As-Compacted S (%) (Rao and Revanasiddappa 2000)

The researchers used the soaked after loading technique proposed by Lawton et al (1989) to determine the collapse potential. Specimens were initially loaded in their as-compacted state to a desired normal stress. After equilibrium had been reached, the specimens were inundated and deformation readings were recorded. It was determined that the majority of collapse occurred within the initial five minutes of loading after the specimens had been inundated. Collapse potential was determined based on deformation values that had occurred over a 24-hour period.

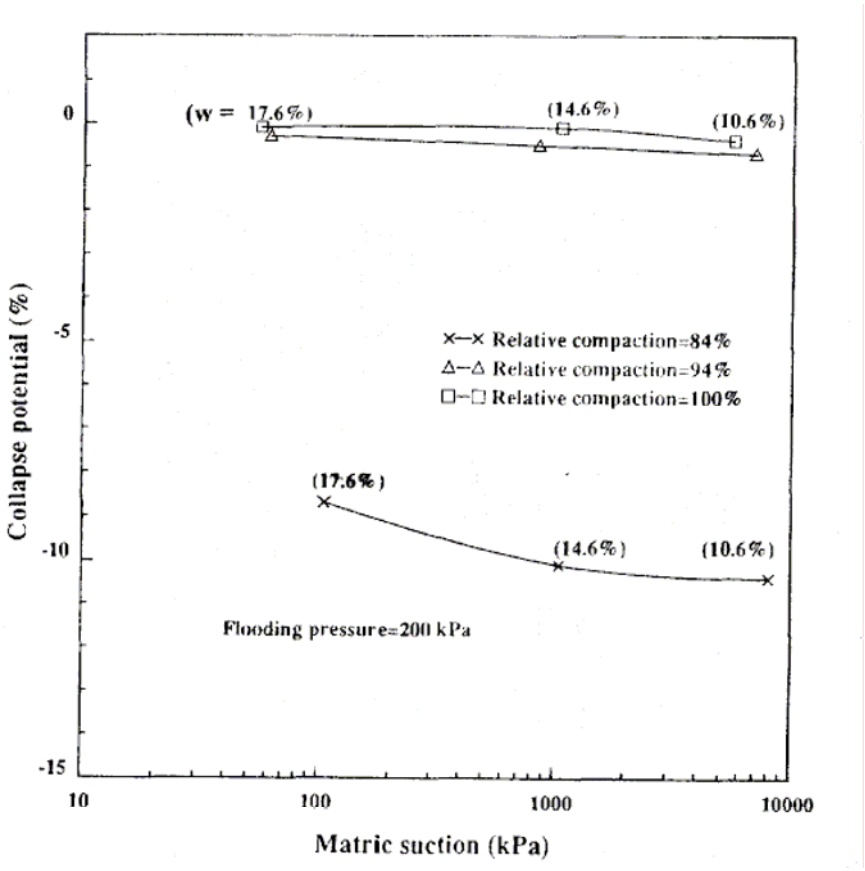

Figure 2.5.4: Effects of R.C. on Collapse Potential (Rao and Revanasiddappa 2000)

The researchers concluded that regardless of relative compaction, material compacted at 7% dry of optimum moisture content exhibited matric suctions 75 to 100 times higher than material compacted at optimum moisture content (Table 2.5.1).

Results also showed that material compacted at 100% relative compaction exhibited collapse potential less that 1%, regardless of as-compacted water content and initial matric suction (Figure 2.5.4). The researchers concluded that the effect of the matric suction on collapse potential of a specimen is governed by the relative compaction used in its preparation and normal stress under which it was inundated.

Table 2.5.1: Soil Test Matrix (Rao and Revanasiddappa 2000)

Relative compaction (%) (1)	As-compacted water content (%) (2)	Average matric suction (kPa) (3)	As-compacted degree of saturation (%) (4)
84 (1.49 mg/m^3)	7% dry of OMC (10.6%)	8,042 ± 19%	35
84	3% dry of OMC (14.6%)	1,044 ± 11%	48
84	OMC (17.6%)	105 ± 9%	58
94 (1.66 mg/m^3)	7% dry of OMC	6,893 ± 8%	46
94	3% dry of OMC	839 ± 14%	63
94	OMC	61 ± 2%	76
100 (1.77 mg/m^3)	7% dry of OMC	5,619 ± 18%	54
100	3% dry of OMC	1,042 ± 10%	75
100	OMC	56 ± 0	91

2.5.5 Rao and Revanasiddappa (2002)

Rao and Revanasiddappa examined the influences of the microstructure and matric suction on the collapse behavior of compacted Bangalore clay specimens (termed "representative samples"). Clay specimens were tested at three different compaction conditions: 100% and 84% relative compaction (7% dry of optimum), and 84% relative compaction (8.8% wet of optimum). The soaked after loading technique was used to determine the collapse potential of each soil specimen. Mercury intrusion porosimetry (MIP) tests were conducted on each specimen in order to determine its microstructure. In addition to the compacted Bangalore clay, artificial samples were prepared by adjusting the both the clay content from 12 – 26% and the quantity of organic matter from 0.4 to 0.7%. Artificial samples were statically compacted at 10.6% water content to a dry density of 1.49 g/cm^3.

The researchers showed that the relative compaction strongly influenced the collapse

potential of the material tested (Figure 2.5.5). Material compacted with 100% R.C. experienced a 14.5 % smaller collapse potential than the material compacted at 84% R.C. In addition, it was concluded that the as-compacted water content did have a significant affect on the collapse potential of the soils tested. Soils compacted dry of optimum experienced considerable collapse, while specimens compacted 8.8 % wet of optimum experienced a less significant magnitude of collapse. The higher magnitude of collapse was believed to be due to the more aggregated soil structure of the material compacted dry of optimum.

Results showed that there existed a critical clay content (10-40%) where collapse potential was maximum, and clay contents higher than that caused the material to swell (Figure 2.5.6). It was determined that the range of critical clay content was influenced by the magnitude of the flooding pressure (pressure at which specimens were inundated). They also noted that adjusting the clay content in artificial materials influenced both the matric suction and collapse potential.

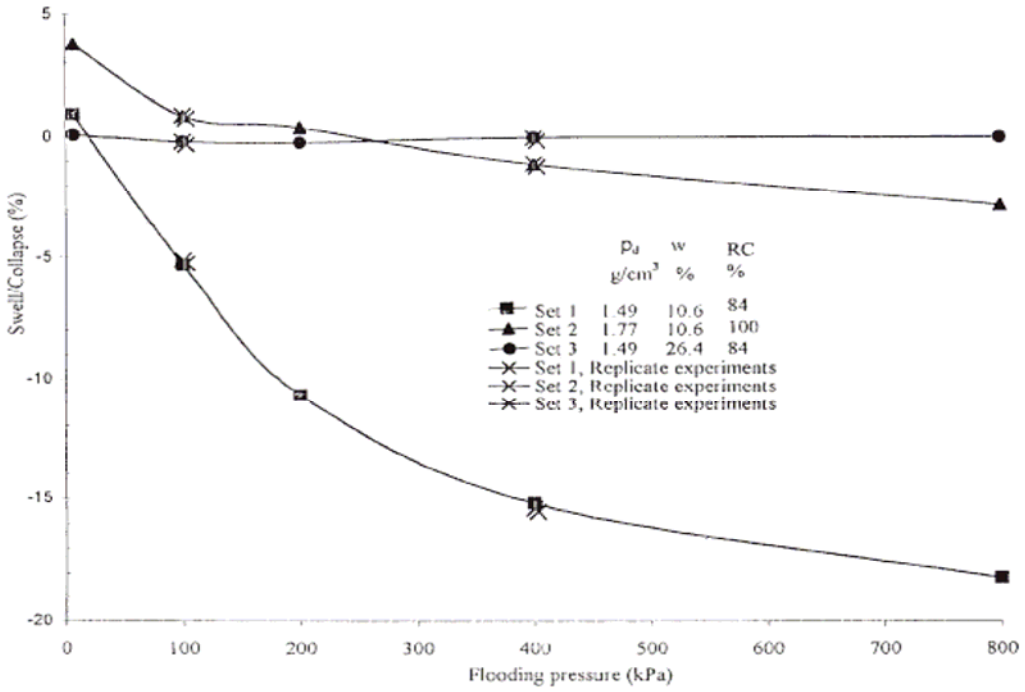

FIG. 1—*Effect of relative compaction and compaction water content on collapse potentials of specimens from Sets 1, 2, and 3.*

Figure 2.5.5: Collapse vs. Flooding Pressure (Rao and Revanasiddappa 2002)

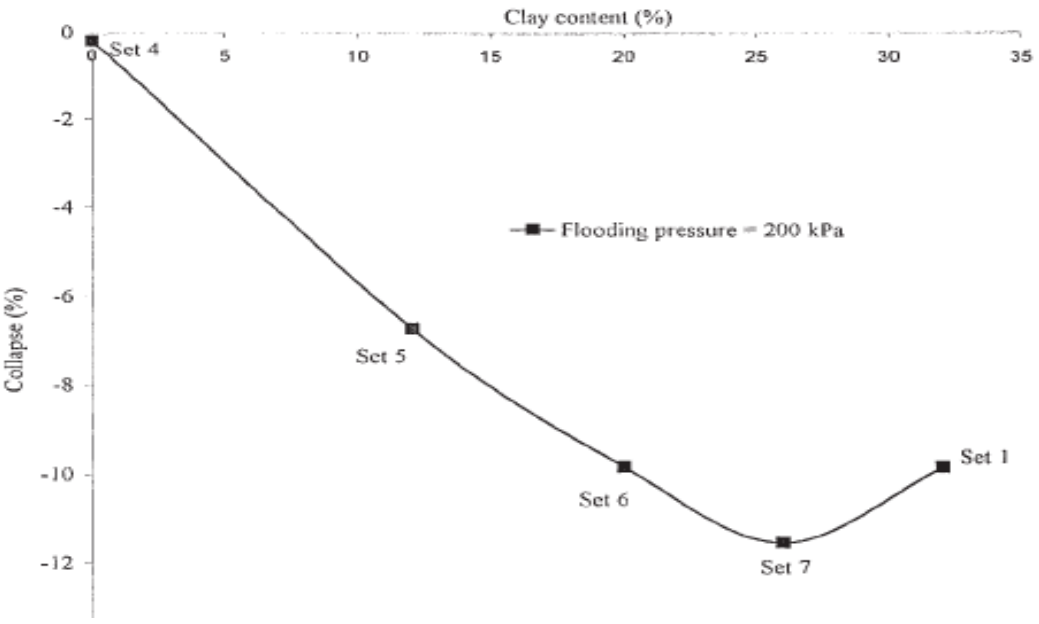

Figure 2.5.6: Collapse vs. Clay Percentage (Rao and Revanasiddappa 2002)

2.5.6 Lim and Miller (2004)

Lim and Miller used the single oedometer test to determine the collapse potential of twenty-two Oklahoma soils that were deemed suitable for use in compacted fills based on compaction specifications by the Oklahoma Department of Transportation (ODOT). Previous research had been conducted on specimens that would not qualify for field compaction applications. Collapse potential tests were performed on material that included clays (low and high plasticity), low plasticity silts, weathered sandstone, non-plastic sands, and weathered shale. Double oedometer tests were conducted on various samples to gain a larger coverage of overburden stresses.

Lim and Miller showed through correlation that the collapse index increases with increasing Plasticity Index (PI), Liquid Limit (LL), clay size fraction, and Activity (A) for a given as-compacted water content and compactive effort, where collapse index is defined by the following:

$$I_e\,(\%) = 9.805 - 0.261w(\%) - .424\gamma_d(\mathrm{kN/m^3}) + 0.0580\mathrm{PI}(\%) + 0.0697\mathrm{C}(\%) \qquad (2.22)$$

Where w is the as compacted water content, γ_d is the dry unit weight, PI is the plasticity index, and C is the clay-size fraction. The researchers noted that there existed significant scatter when correlating the collapse index to a single parameter such as the PI. The scatter is attributed to the collapse index being a function of several additional factors such as environmental interactions (water content and overburden stress), clay mineralogy, and pore fluid chemistry.

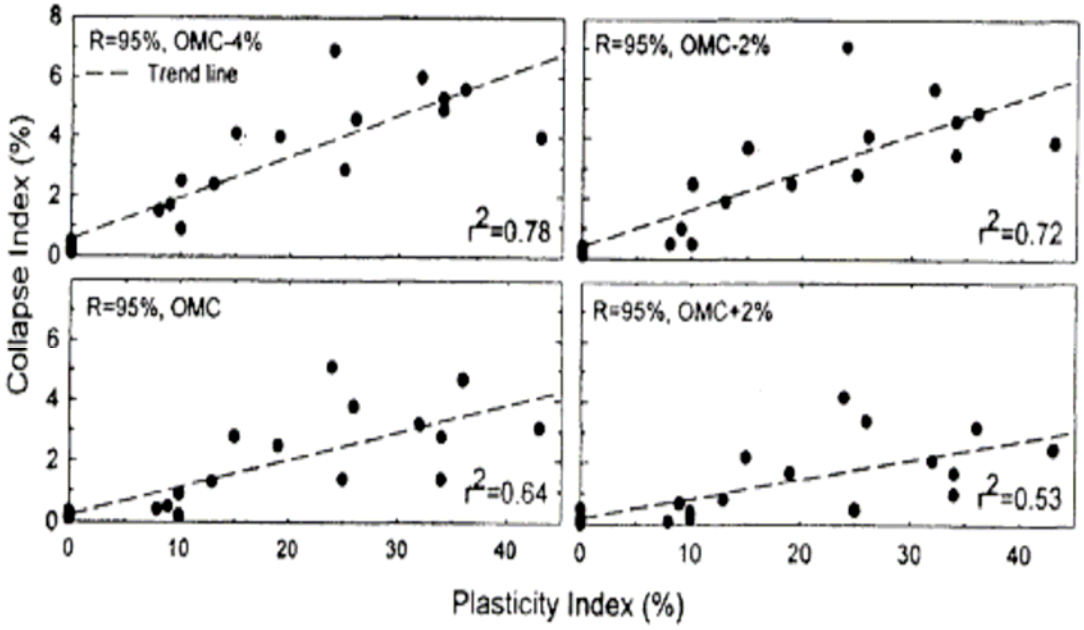

Figure 2.5.7: Collapse potential correlation to PI (Rao and Revanasiddappa 2002)

In addition, the researchers proposed an alternate method to ASTM D 5333 for assessing collapse settlement in compacted fills. The researchers showed that the severity of collapse guideline suggested by the ASTM Standard should also be based on the on height of the compacted fill, and not only the collapse potential of the soil, in order not to underestimate possible compacted fill settlements.

Lim and Miller concluded that cohesionless sandy soils compacted to Oklahoma Department of Transportation (ODOT) specifications for embankments experienced negligible collapse potential. It was determined that collapse potential decreased approximately linearly with as compacted water content for 95% relative compaction. Based on single oedometer testing, a model was developed to predict the collapse index. Finally,

the researchers showed that one-dimensional oedometer tests underpredicted embankment settlement beneath the center by 1.5 to 2.5 times the measured settlements

2.6 Literature Review Summary

A synthesis of the literature involving methods (mathematical and experimental) available for determining the soil water characteristic curve, collapse potential, and the filter paper method for determining the matric suction of compacted material has been presented. Based on the review of the literature presented in the previous sections, the follow general conclusions can be stated:

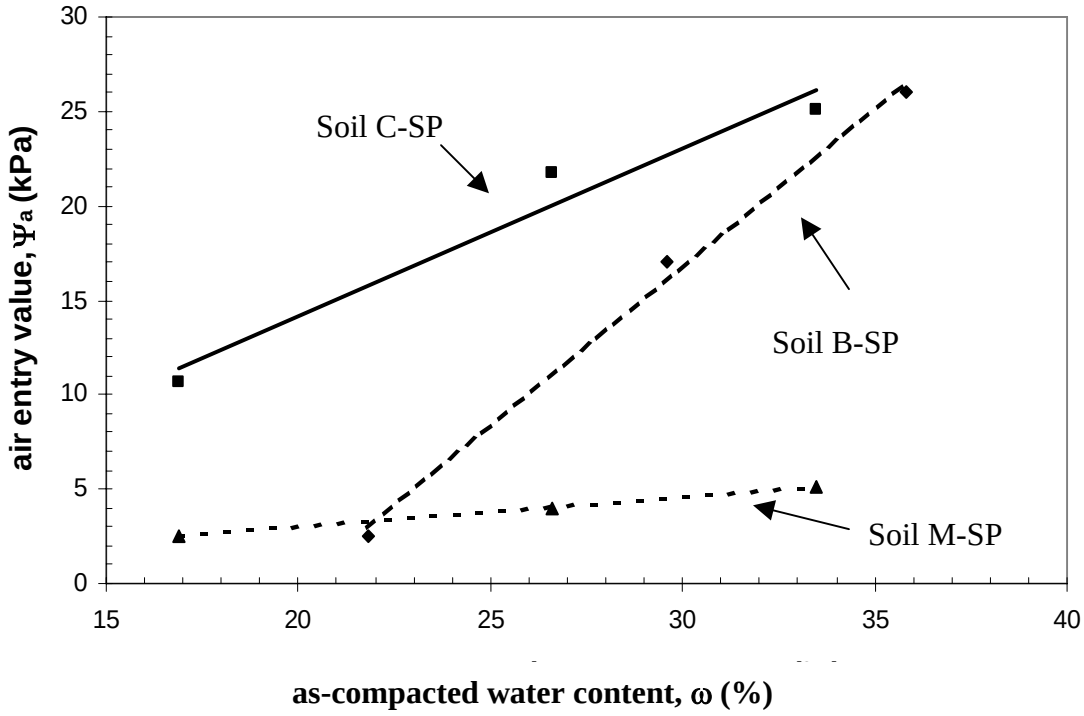

Figure 2.6.1: Air Entry Value vs. As-Compacted Water Content (after Tinjum et al 1997)

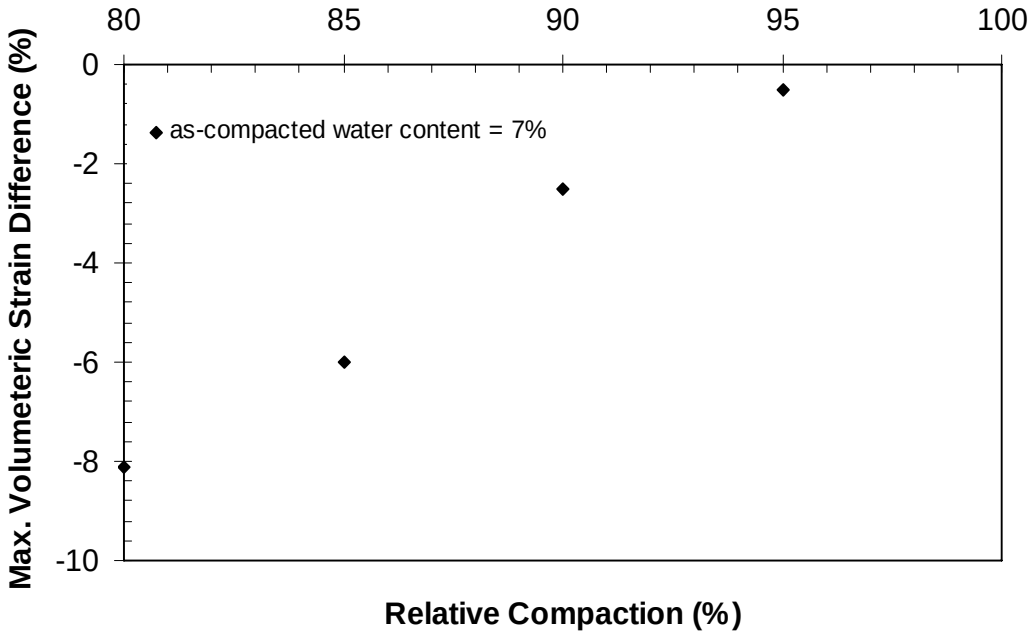

Figure 2.6.2: Influence of relative compaction on collapse (after Lawton et al 1989)

- **Soil Water Characteristic Curve**

  - The shape of the soil water characteristic curve and the air entry value for compacted fine-grained materials are a function of the as-compacted water and not the initial density (Vanapalli et al 1996, Vanapalli et al 1999a, Vanapalli 1999b, Tinjum et al 1997). Materials compacted dry of optimum contain lower air entry values and steeper slopes past the air entry value than materials compacted wet of optimum (with material compacted at optimum conditions lying in between). Data from the literature states that the as-compacted water content influences the structure (macro and micro) that in turn controls the rate of desaturation. It has been concluded that the air entry value increases with increasing as-compacted water content (Figure 2.6.1).

- **Collapse Potential**

  - Data within the literature has suggested that given the proper conditions (compaction conditions, clay content) all soils are susceptible to collapse (Lawton et al 1989, Lawton et al 1991, Lawton et al 1992)
  - Based on the review of the literature involving collapse potential, four parameters needed for collapse to occur have been generally accepted as being: an open soil structure, a bonding agent holding material intact in unsaturated state, the presence of

overburden pressure, and finally, infiltration resulting in the weakening of bonding agent) (Barden et al 1973, Mitchell 1976, Lawton et al 1989, Lawton et al 1992).

- The collapse of partially saturated soils is a function of the as-compacted water content, with the magnitude of collapse increasing with decreasing as-compacted water content (Lawton et al 1989, Lawton et al 1992, Rao and Revanasiddappa 2000, Rao and Revanasiddappa 2002, Lim and Miller 2004).
- Collapse potential is directly related to the matric suction of compacted material. Materials compacted dry of optimum contain higher matric suction and collapse potential values than materials compacted wet of optimum for degrees of relative compaction less than 100% (Rao and Revanasiddappa 2000). The effects of matric suction and soil structure are greatly reduced (Figure 2.5.4) by compacting material to a degree of relative compaction of 100% (Rao and Revanasiddappa 2000, Rao and Revanasiddappa 2002).

3 EXPERIMENTAL PROGRAM

3.1 Introduction

The primary objective of the experimental program was to determine soil water characteristic curve (drying and wetting) of compacted material (classified as CL according to the USCS soil classification) using a volumetric pressure plate apparatus. In addition to pressure plate testing, several auxiliary tests were conducted to gain a better understanding of the unsaturated compacted material used throughout the experimental program. Another objective of the experimental program was to examine the effects of the soil structure on the volume change behavior of the material. Double Oedometer tests were conducted on material with as-compacted water contents ranging from 4.7% to 22%, and dry densities ranging from 1.53 Mg/m^3 to 1.90 Mg/m^3. Auxiliary tests included filter paper tests (contact method) for determining matric suction, and falling head permeability (using a consolidometer).

Finally, this section presents the materials and methods used to execute the experimental program. A detailed description of the pressure-plate testing set-up is presented.

3.2 Overview

In order to achieve the stated objectives of the experimental program, three volumetric pressure plate extractors were built to produce the soil water characteristic curves for this study. The following section provides a detailed outline of the materials used through out the experimental program along with detailed information (vendor name and product numbers) regarding how the material was obtained.

3.3 Materials Tested

The material investigated in this thesis was obtained from an MSE wall, located adjacent to US 54, in the Research Triangle Park (RTP) of North Carolina. Commencement of the experimental program included index testing to determine the material properties of the soil used throughout the experimental process. Tests included Specific Gravity (ASTM D 792), Particle Size Distribution and Hydrometer Analysis (ASTM D 421-02), Atterberg Limit testing (ASTM D 4318-00), and Compaction (ASTM D 698-00). Material classification (low plasticity clay, CL) was made in accordance to the Unified Soils Classification System (USCS).

A particle size distribution analysis was conducted as an initial means of determining the distribution of particles and gradation of the material, with the results shown in Figure 3.3.1.

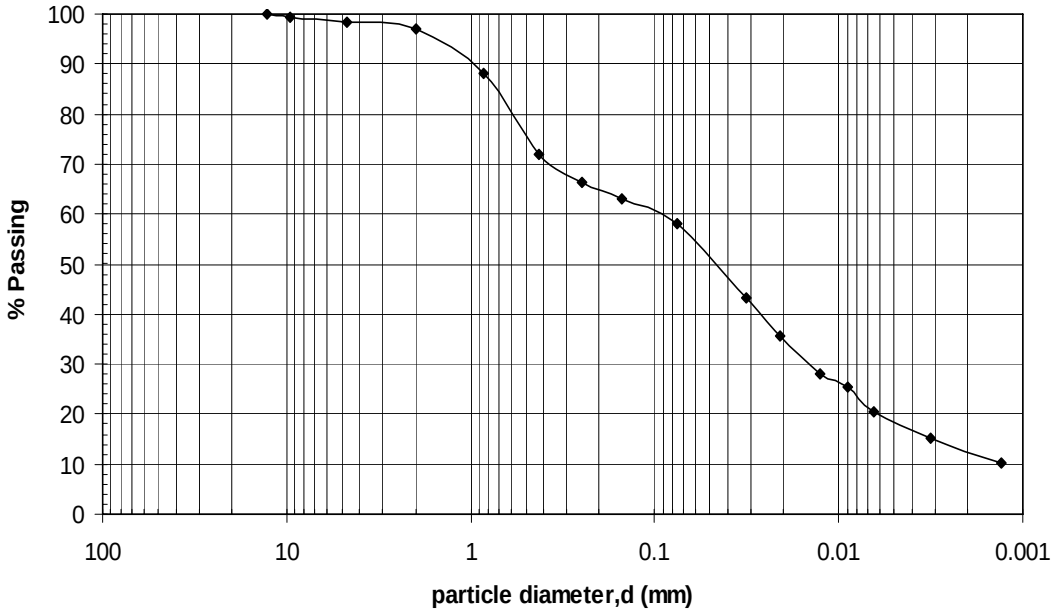

Figure 3.3.1: Grain Size Distribution Curve

Based on the grain size distribution, the soil was determined to be a fine-grained material as 58% of the material was finer than 0.075 mm (No. 200 sieve). There was a minimal percentage (1.5%) of gravel-sized particles (coarser than No. 4), and a significant percentage of sand (39%). Table 3.3.1 summarizes the results of the grain size analysis.

A hydrometer analysis was conducted to determine the soil's distribution of finer grained material. Results showed that the soil contained a clay fraction of 10.2%, with the remaining 47.8% determined to be silt-sized particles (0.075 mm-0.002mm). A specific gravity (Gs) of 2.64 Mg/m^3 was determined in accordance to ASTM D 854-02. While no specific tests (x-ray diffraction) were conducted to determine soil mineralogy, comparisons with published data (Lambe and Whitman 1969, Holtz and Kovacs 1981, Coduto 1999) were made to estimate the mineral composition of the material. Using the specific gravity (Gs) and clay fraction of 10.2 %, an Activity (A) of 0.98 was determined. The combined comparison of specific gravity (Gs) and Activity values yielded a predominant Illite mineral composition.

Table 3.3.1: Particle Size Distribution Summary

Sieve No.	% Finer	% Retained
4	98.5	1.5
10	97.1	2.9
40	71.8	28.2
200	58	42

Atterberg Limit (ASTM D4318-00) testing was conducted to determine the material's Liquid Limit and Plastic Limit. Plastic Limit (PL) testing (thread method) yielded a plastic limit of 19 based on the average of three determinations, and a Liquid Limit (LL) value of 29 was determined using the Casagrande method. Figure 3.3.2 shows the Flow Curve used to determine the index properties of the soil. In addition, Table 3.3.2 shows comprehensive results for specific gravity and Atterberg Limits.

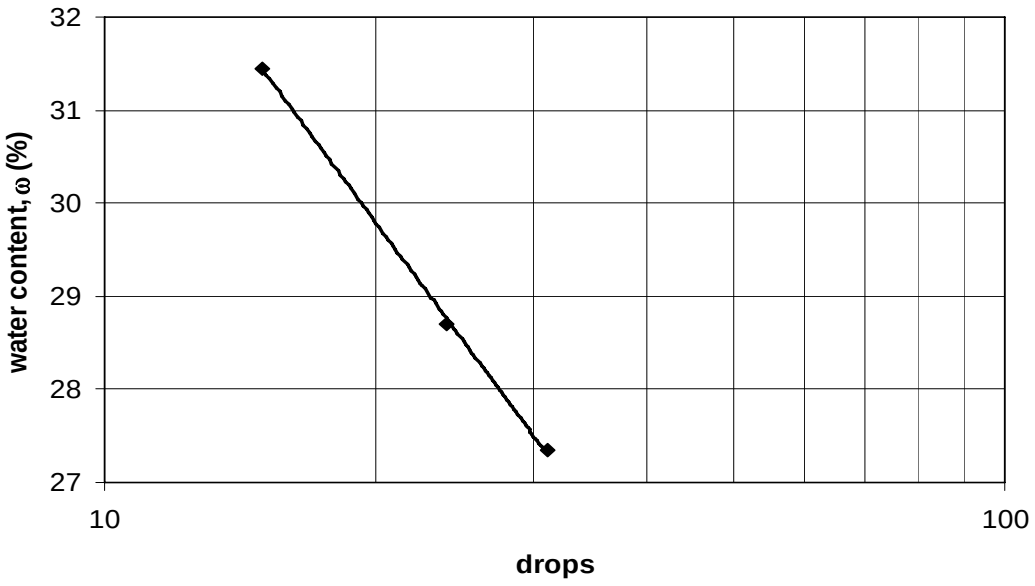

Figure 3.3.2: Flow Curve

Table 3.3.2: Material Index Properties

Specific Gravity, Gs	Liquid Limit, LL (%)	Plastic Limit, PL (%)	Plasticity Index, PI (%)
2.64	29	19	10

3.4 Materials and Methods

The following section provides a thorough explanation of the materials (pressure plate extractor, falling head permeability apparatus) and methods (testing procedures) used throughout each phase of the experimental program. It provides vendor names and product codes for each item associated with the pressure plate testing apparatus. Machine drawings, pictures and schematics are contained within this section to provide the reader with a clear understanding of the items used to generate the Soil Water Characteristic Curves.

3.4.1 Pressure Supply

A 300 cubic foot compressed air cylinder (Product Code CA300) was obtained through National Welders online supply order program. The cylinder, with a CGA 590 adaptor, served as the air source used to apply the matric suction to each individual soil sample. As an added safety measure, a metal cylinder harness was obtained from McMaster-Carr (Part No. 2283 T3). The harness included a chain with the ability of adjusting to cylinders from 9" to 16" in diameter.

A single stage regulator (Model ASG-SSD-250-590 obtained from National Welders) with the ability of producing delivery pressures from 0-250 psi was used to regulate the pressure from the pressure source. The regulator included dial gauges with 0-400 psi, and 0-4000 psi ranges on the outlet and inlet locations respectively. A ¼" NPT male outlet connection was used to connect the regulator to a ¼" inner diameter (1/16" wall thickness) Nalgene 489 polyethylene tubing (Fisher Scientific Product No. 14-126-123). Sections of the plastic tubing were used to connect the pressure source to a quick-connect (Swagelok part no. B-QC4-B-400 & B-QC-D-400) inlet connection.

A 24” x 24” x 6” wooden control box was built to house two line regulators (McMaster part no. 6763 K821 and 4959 K21), two dial gauges (McMaster part no. 4007K91 & 4007K95), four quick connections (Swagelok part no. B-QC4-B-400 & B-QC4-D-400.), and centralize the various tubing and connections that were required to unify the low pressure and high-pressure systems. A schematic and two photographs of the control box are shown in Figure 3.4.1 and Figure 3.4.2 respectively. One regulator (McMaster-Carr part no. 4007K91) was used to regulate pressures from 0 to 100 kPa and the second regulator (McMaster-Carr part no. 4007K95) was used to apply pressures from 300 kPa to 1000 kPa.

All fittings obtained for the laboratory apparatus were Swagelok products obtained at the Raleigh Value & Fitting Co. in Raleigh, NC. Three (3) quarter-turn instrument ¼” plug valves (Swagelok Part No. B-4P4T) were purchased and used to transfer the airflow from both the high and low-pressure regulators to each of the pressure plate devices. The airflow could be directed to a single chamber while maintaining a no flow condition to the other two, or airflow could be allowed to flow simultaneously to all three chambers. The system was designed with a redundancy feature that allowed for the pressure to bypass both line regulators and be applied directly from the compressed air cylinder to each volumetric pressure plate extractor.

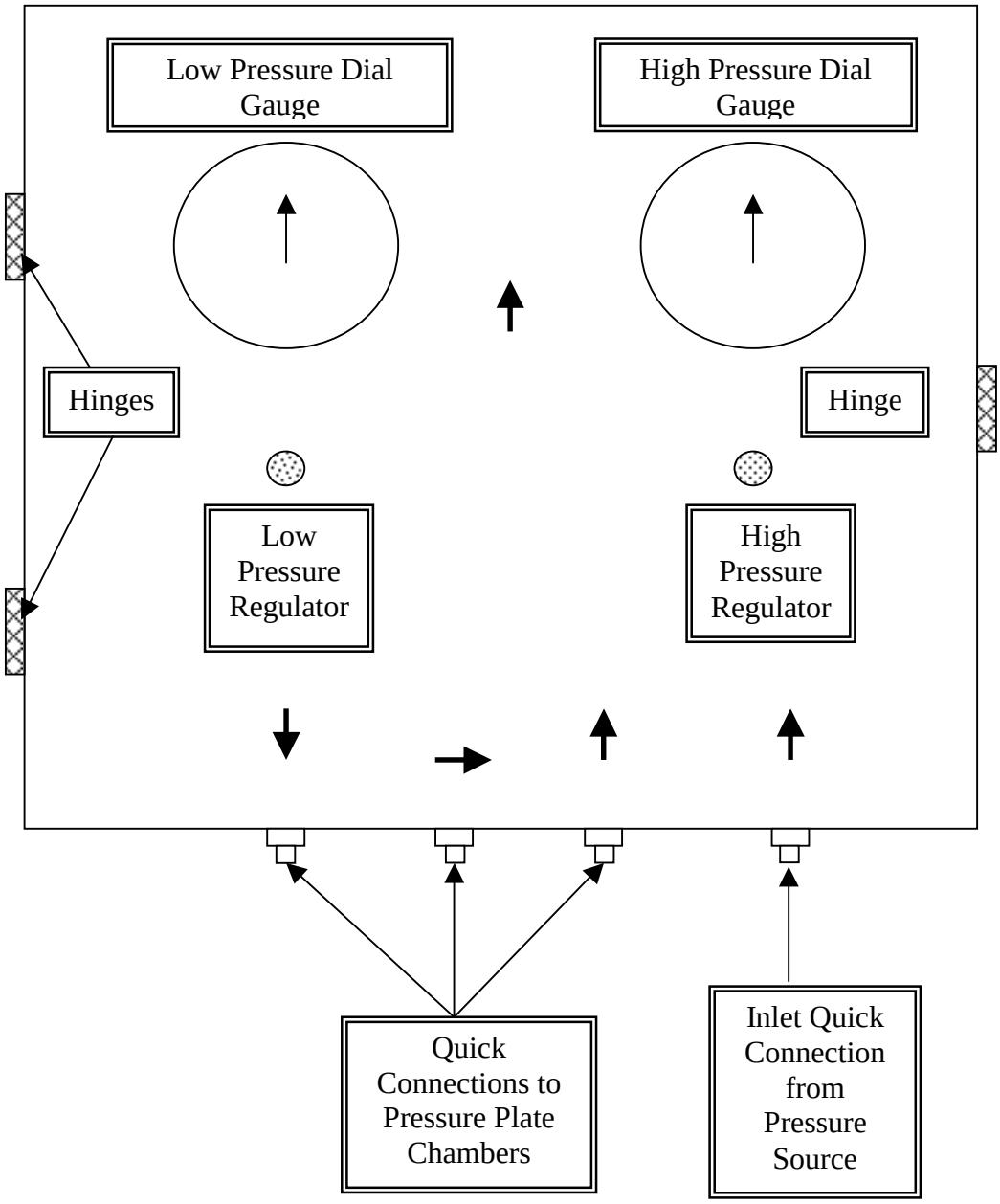

Figure 3.4.1: Control Box Schematic

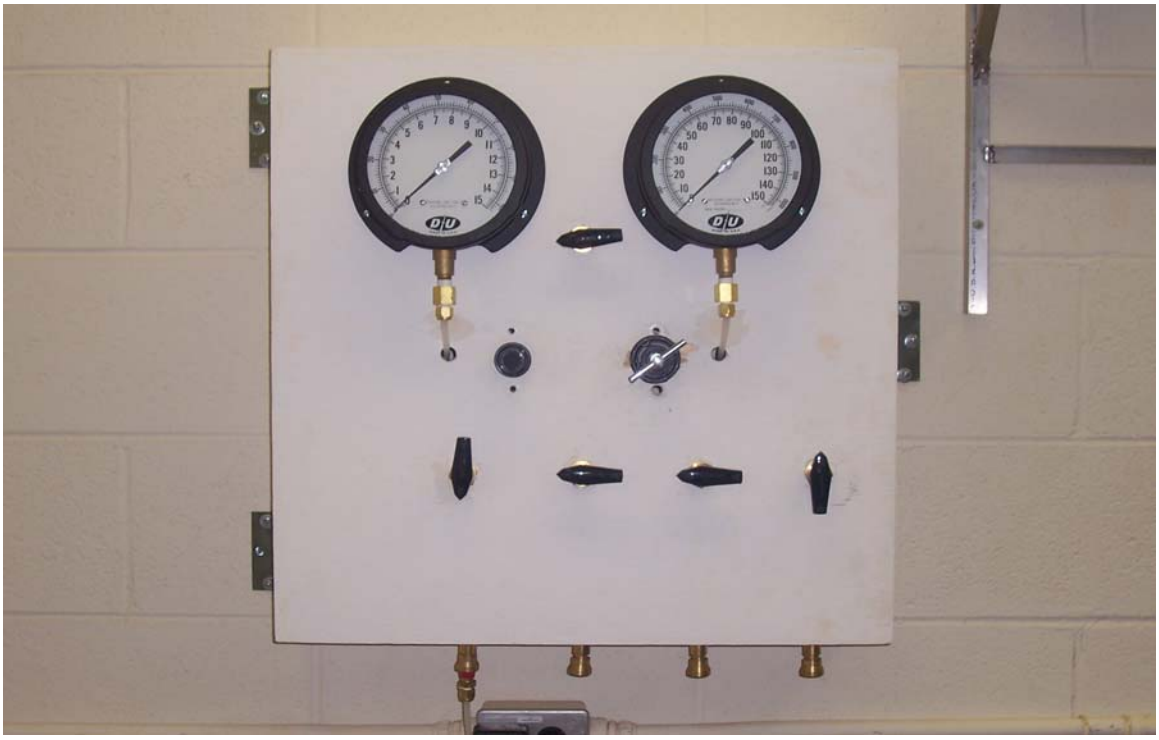

Figure 3.4.2: Control Box (Front View)

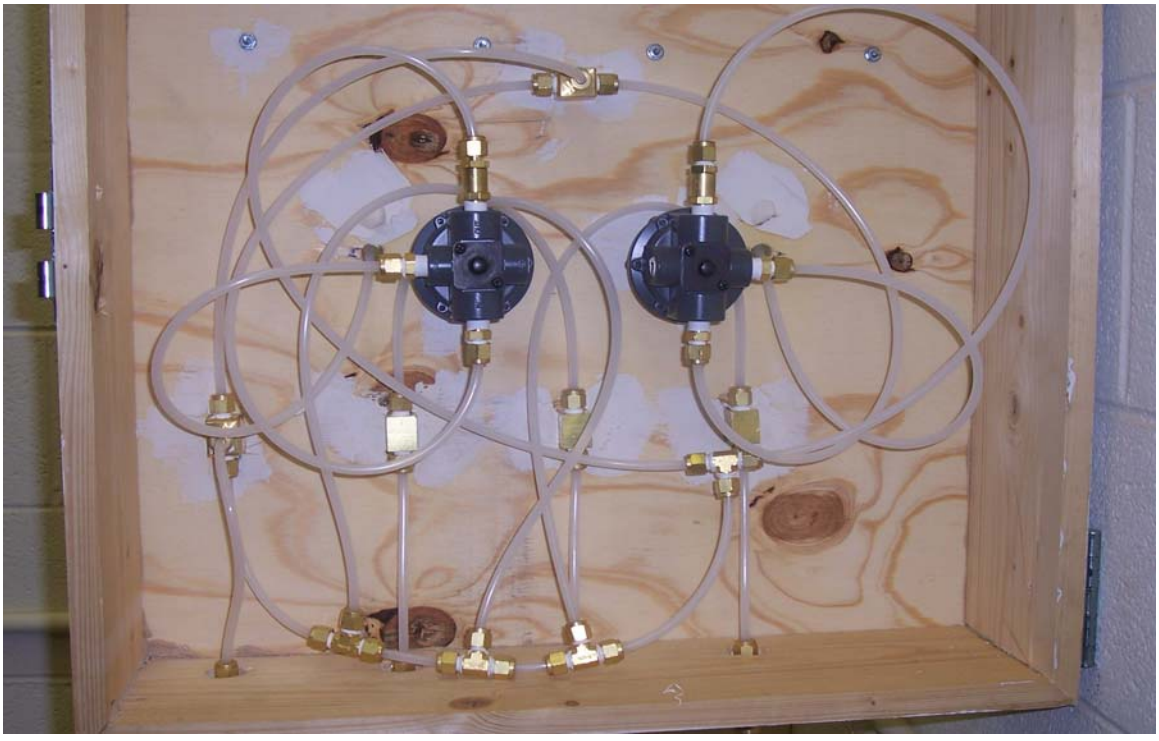

Figure 3.4.3: Control Box (Rear View)

3.4.2 Pressure Plate Extractors

Three pressure plate extractors, designed to handle air pressure up to 1500 kPa (217 psi), were constructed from plans provided by Wang and Benson, 2004 out of sheets of brass bar stock machined to the dimensions shown in Figure 3.4.4 through Figure 3.4.6. Two devices were machined to allow a piston assembly (steel rod and chrome housing) obtained from Trautwein Geotac (Part No. 100020) to be attached. The piston assembly allowed for an overburden pressure of 100 kPa to be applied to individual samples during each application of suction. The steel piston rod was cut to a length of 6 ¾" inches in order to properly fit within the pressure plate device. One of the two devices is shown in Figure 3.4.7.

For each of the two chambers equipped with overburden pistons, three (3) inch diameter support ring (Fisher Part no. 14 050B) was attached to the piston to serve as a contact surface for a digital dial gauge (Humboldt Part No. HM-4469.02) with the ability of measuring vertical deformation to a resolution of .0001 in inches or mm. The third chamber is shown in Figure 3.4.8.

Each chamber was machined with a 98.6 mm diameter recessed region that allowed for a 76.2 mm diameter high air entry ceramic stone and 9.5 mm square Buna n-gasket to be snuggly placed. In order to maintain an airtight device, square 9.5 mm (3/8" Fractional Size) Buna N-Cord (McMaster-Carr Model No. 9700 K151) was positioned situated along the circumference of the ceramic. The N-Cord was chamfered at a 45^{o} angle in order to facilitate a proper seal once the high air entry disk was in place and the top chamber fastened to a torque of 4.5 kN-m using a standard torque wrench (CRAFTSMAN® part no. ^{9}44593).

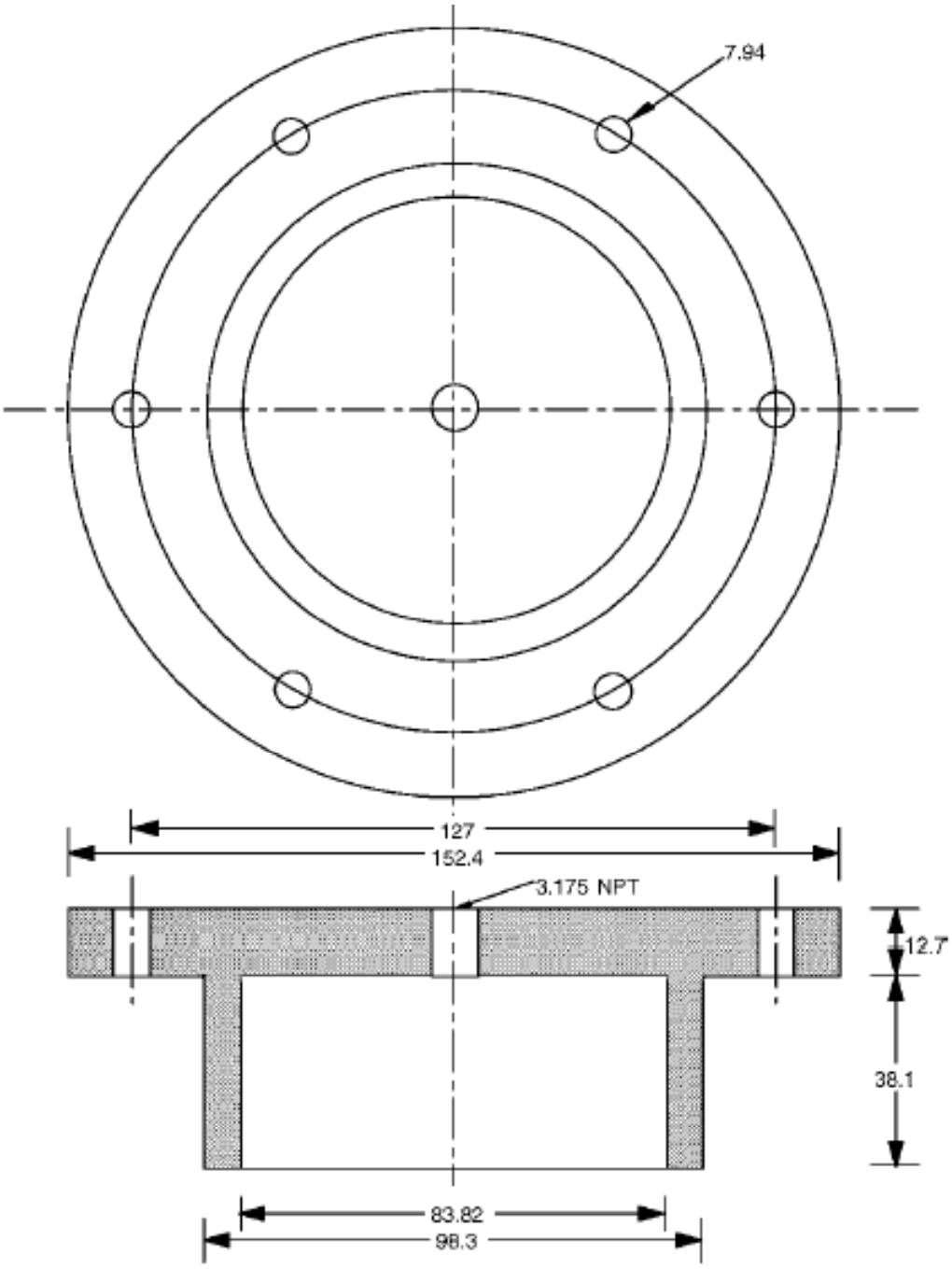

DRAWING A2—*Machine drawing for upper chamber of leak-free pressure plate extractor. All dimensions are in mm.*

Figure 3.4.4: Machine Drawings for Upper Chamber without Overburden (Wang and Benson 2004)

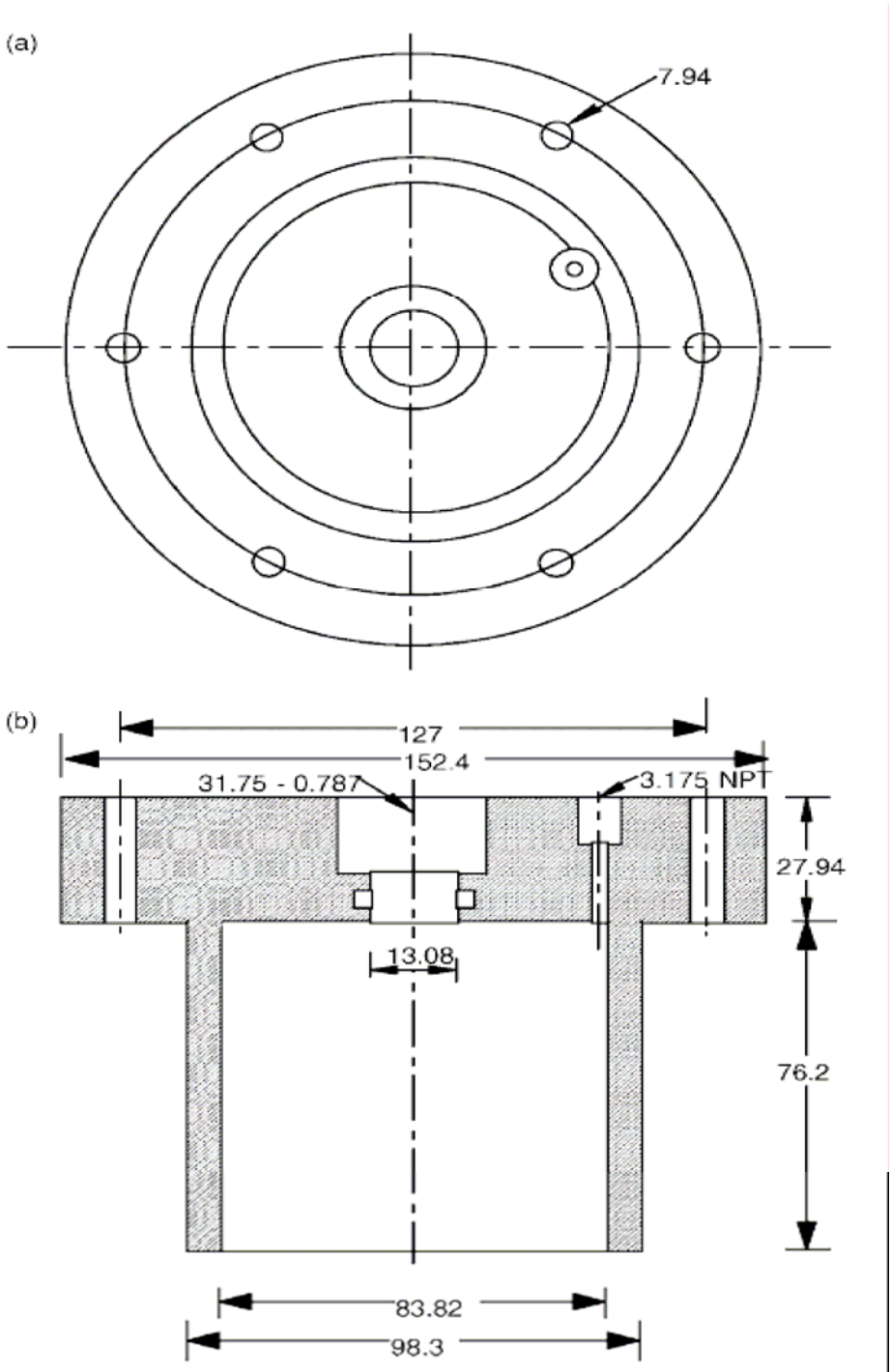

DRAWING A3—*Machine drawing for upper chamber of leak-free pressure plate extractor with overburden piston: (a) plan view and (b) cross section. All dimensions are in mm.*

Figure 3.4.5: Machine Drawings for Upper Chamber with Overburden (Wang and Benson 2004)

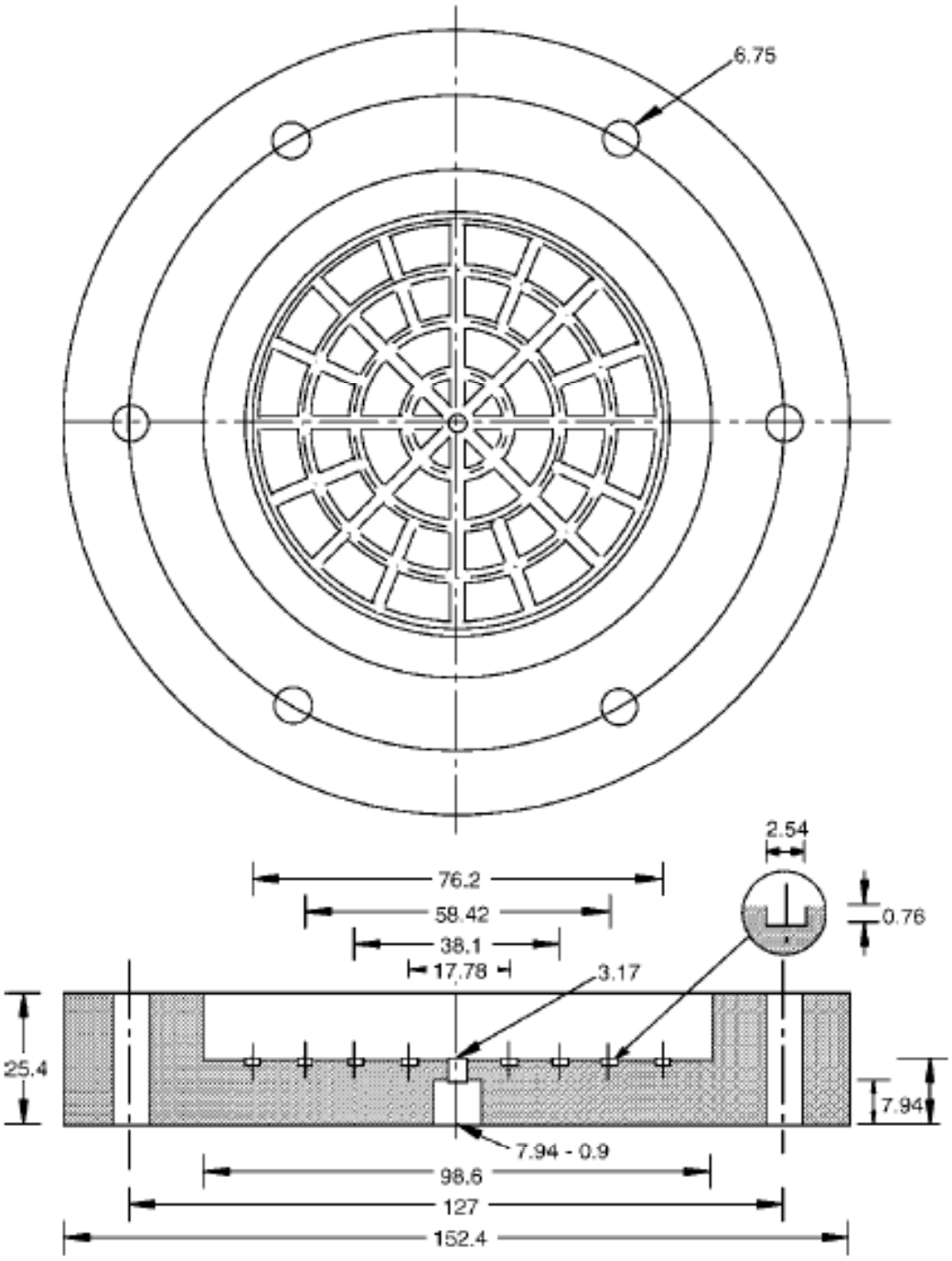

DRAWING A1—*Machine drawing for lower chamber of leak-free pressure plate extractor. All dimensions are in mm.*

Figure 3.4.6: Machine Drawings for Lower Chamber (Wang and Benson 2004)

Figure 3.4.7: Pressure Plate Extractor with Overburden and dial gauge

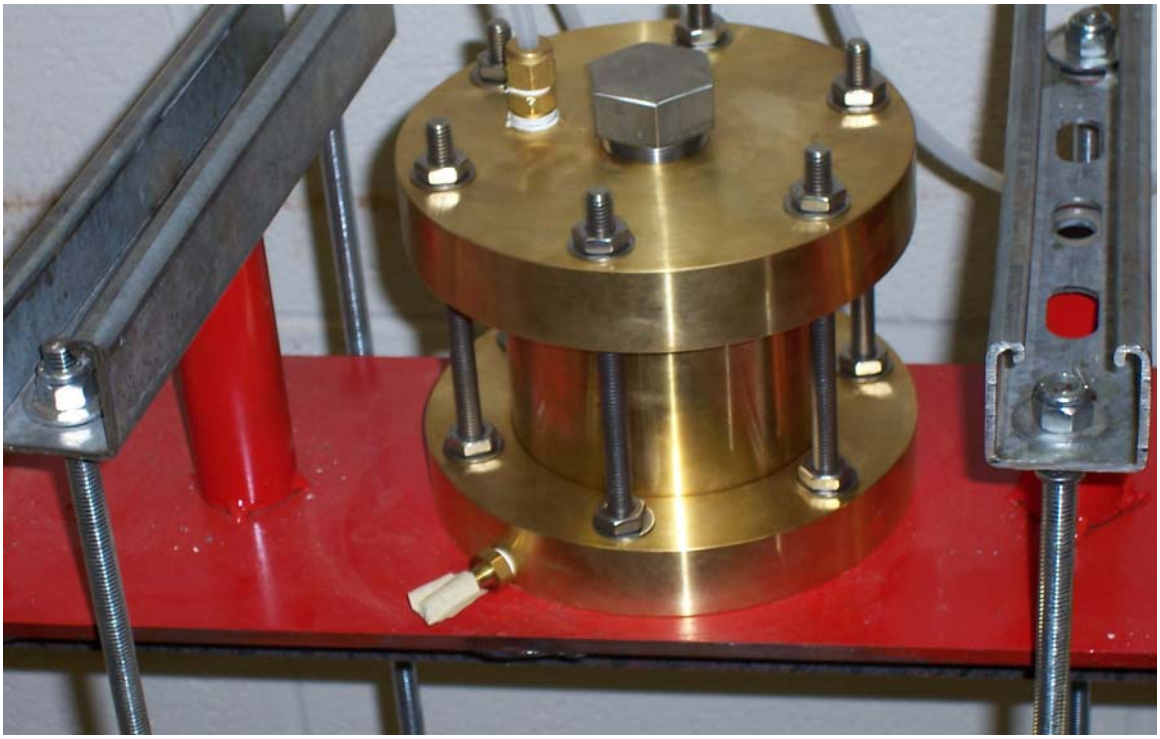

Figure 3.4.8: Pressure Plate Extractor without Overburden Piston

3.4.3 Ceramic Stones

Ceramic stones (Part No. 0604D03-B15M1) were obtained from the Soilmoisture Equipment Corporation. The ceramic stones were three (3) inches in diameter with an air entry value of 1500 kPa (217 psi). The ceramic plates, or high air entry disks, allowed for water to flow through the pore spaces while preventing airflow up to an air pressure of 1500 kPa (air entry value). The ceramics rested in the recessed area machined in the lower half of the chamber, as explained in the previous section (Figure 3.4.6). Prior to placement of compacted test specimens into the chambers, each porous stone was pressure checked in accordance with ASTM D 6836 –02 (Figure 3.4.9).

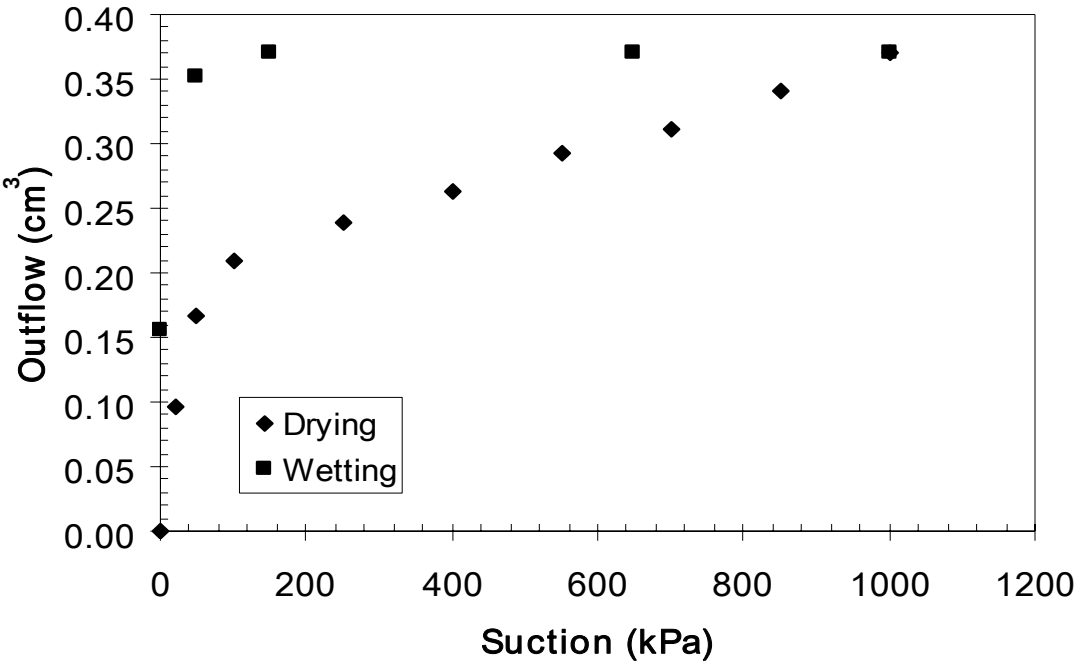

Figure 3.4.9: High Air Entry Disc Pressure Check

3.4.4 Outflow Collection

After the application of suction, outflow was transferred from the volumetric pressure plate extractors through a ¼" inner diameter plastic tubing (Fisher Part No. 14-169-7C) into a 4ft, 0.15" diameter capillary tube (obtained from the NCSU, Chemistry Department glass shop) where the air-water interface was measured. A plastic ¼ " inner diameter Y-shaped connector (Fisher Scientific Part No. 15-320-10C) was inserted in between the chamber and the capillary tube. The Y-tube allowed for air to escape during testing. It also served as the location where water could be added for the sorption test, and to flush any air from below the high air entry disc. Y-connectors were covered with plastic in order to prevent excessive evaporation. In addition to the Y-shaped connector, a ¼" outer diameter t-connector (Fisher Scientific Part No. 15-319C) was placed in between the Y-shaped connector and the capillary tube. The t-connector served as a location where water could be drained from the system to ensure that the air water interface remained within the boundaries of the 500 mm measuring scale (McMaster-Carr Part No.C636-500) used to determine the outflow readings. Pictures of the Y-connectors and capillary tubes are shown in Figure 3.4.10 and Figure 3.4.11, respectively.

A total of six ring stands (Fisher Part No. S47705) were used to support the capillary tube and measuring scale. Two ring stands were needed per chamber. In addition to the ring stands, six two (2) inch inner diameter rings (Fisher Part No. 14-050A) were used to allow the measuring scale and capillary tube to lie horizontal. Rings were adjusted to keep the capillary tube at the same elevation as the water reservoir beneath the ceramic disc.

Figure 3.4.12 presents an overall view of the test setup within the geotechnical laboratory

Figure 3.4.10: Y-Connectors

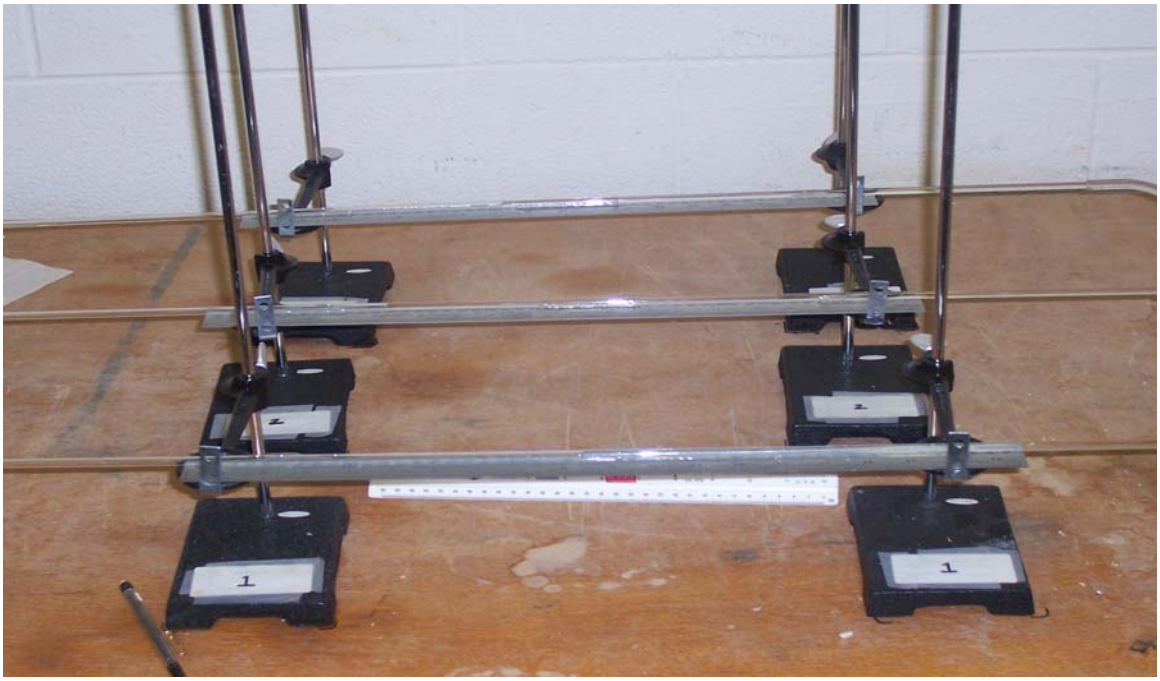

Figure 3.4.11: Outflow Measurement System

Figure 3.4.12: Pressure Plate experimental set-up

3.5 Compaction Methodology

Prior to compacting the material, a method for adjusting the proctor energy was developed so that a condition of mimicking poor field compaction conditions could be developed. Three distinct levels were used to gain a wider range of dry densities for a specific as-compacted water content. It was determined that the three energy levels used would be the conventional Standard Proctor (ASTM D422-02), 30% and 10% of the standard energy (12,375 lbf-ft/ft^3). The energy levels were attained in the following manner. To achieve the 30% energy, three soil lifts were selected with a six-inch hammer drop height (5.5 lb hammer) and 15 blows per lift. The 10% energy level was produced using a three-inch drop height with ten blows on each of the three lifts. Table 3.5.1 presents the combinations and hammer fall height and blows per layer with corresponding Proctor Energy. The adjustment in Proctor energy allowed for comparisons of as-compacted water content and dry densities to be made for material compacted at various energy levels over one log cycle. Figure 3.5.1 shows the three compaction curves developed.

Table 3.5.1: Compaction Methodology

No. of Layers	Hammer wt. (lb)	Drop Height (in)	Blows/Layer	Energy (ft*lb/ft)	%SP
3	5.5	12	25	12.375	100
3	5.5	6	15	3,713	30
3	5.5	3	10	1,238	10

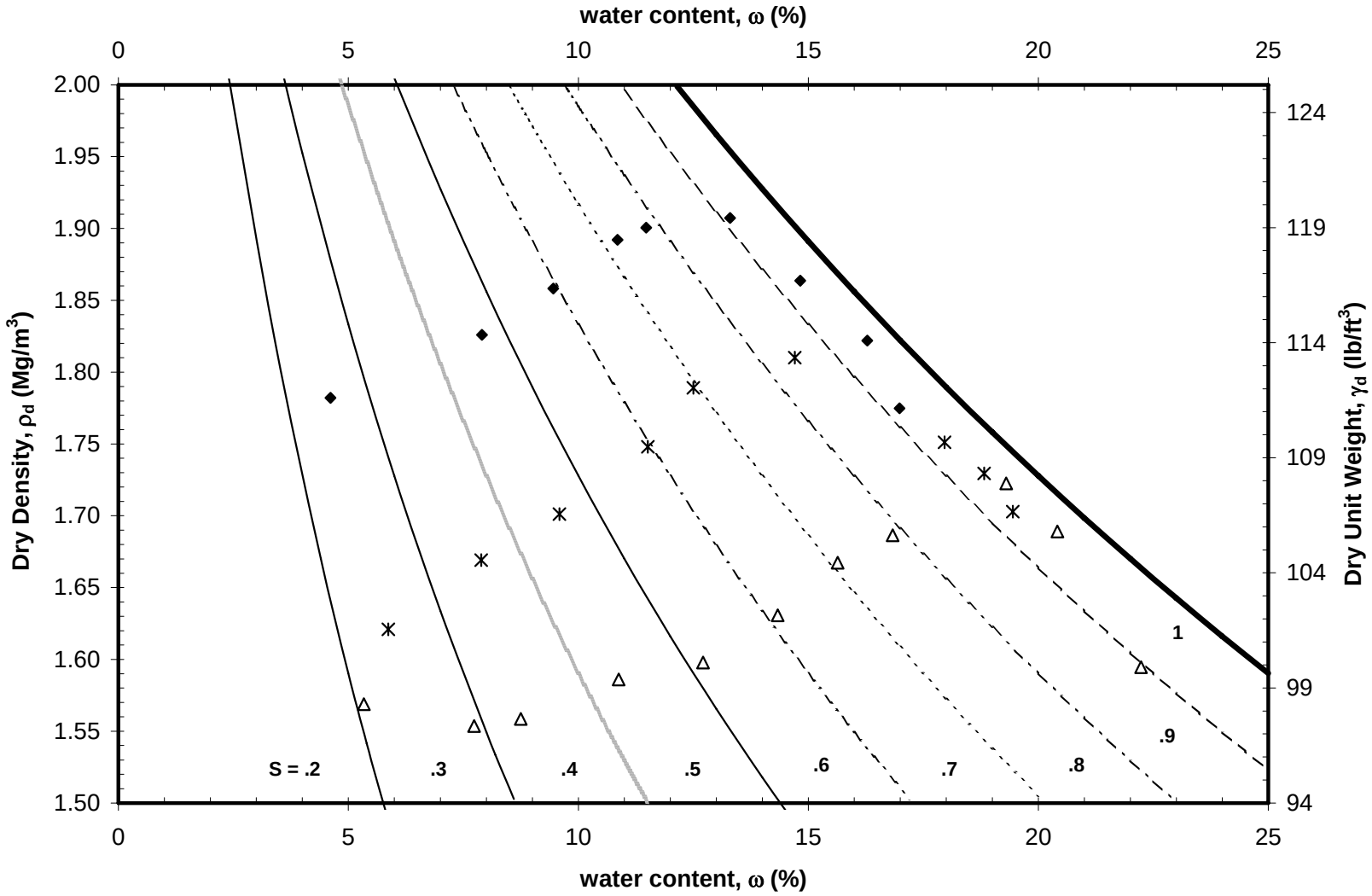

Figure 3.5.1: Compaction Curves for varying energy levels

3.6 Pressure Plate Introduction

Soil water characteristic curves were generated for compacted material using the three volumetric pressure plate extractors discussed in the previous sections. The following sections present the pressure plate testing procedure used to generate the soil water characteristic curves. This section is separated into four subsections that provide detailed explanations of each component necessary to prepare the material for testing. The components included the compaction, saturation, consolidation, and suction measurement processes.

3.6.1 Pressure-Plate Testing Procedure

3.6.2 Compaction:

Approximately 2.5 kg of the test soil (CL according to USCS criteria) was sieved through the No. 10 sieve, moisture conditioned and allowed to equilibrate for 24-hours in a sealed plastic container. Soil was taken from the container and placed into an oven for 24-hours to determine the moisture content. As a secondary check, a microwave moisture content was determined (six minutes on high heat was the time needed to obtain accurate water content values). Comparisons between the two methods showed that an approximately 0.3% maximum difference existed between the two methods (0.1% average difference).

As the result of various trials, it was determined that in order to obtain accurate values of dry density, one ring should be used per mold. The first lift of soil was placed into the mold and compacted to the desired density. One ring (beveled edge in the top position) was placed onto the first compacted layer; the second soil layer was placed into and around the ring and compacted to the desired density.

The final lift of soil was added on top of the second lift and compacted to the desired density.

Compacted material was taken from the Proctor mold, and the material compacted within the rings was separated from the surrounding soil. Each ring sample was trimmed so that the soil was flush with both the top and bottom of the ring. The mass of the compacted material and ring were recorded as the mass of the ring and moist soil.

3.6.3 Saturation

After recording the mass of the compacted material and ring, filter paper (Fisher Scientific Part no. 09-790-2B) was placed on the top and bottom of the compacted material (Note that the mass of each piece of filter paper was determined prior to affixing to the compacted specimen). Due to the loss of soil associated with the low-density specimens during the saturation process, it was decided to place the specimens directly on top of the high air entry ceramic stones, and place a saturated porous stone on the top of the specimen before placing the saturation assembly into the vacuum chamber. Figure 3.6.1 and Figure 3.6.2 show a schematic and photograph, respectively of the soil saturation assembly. Both the soil holder top and bottom were perforated to allow water to freely flow into and out of the test specimen. The soil saturation assembly was then placed into a 6.625” x 9.375” (O.D. x H) vacuum chamber (Fisher Part No. 01-060A), as shown in Figure 3.6.3. The vacuum chamber was large enough to house three saturation assembly devices simultaneously. Material was allowed to remain in the vacuum chamber for 24-hours. After the 24-hour saturation process had been completed, the total

mass of the soil (saturated), ring, filter paper (top and bottom) and high air entry ceramic disc was determined.

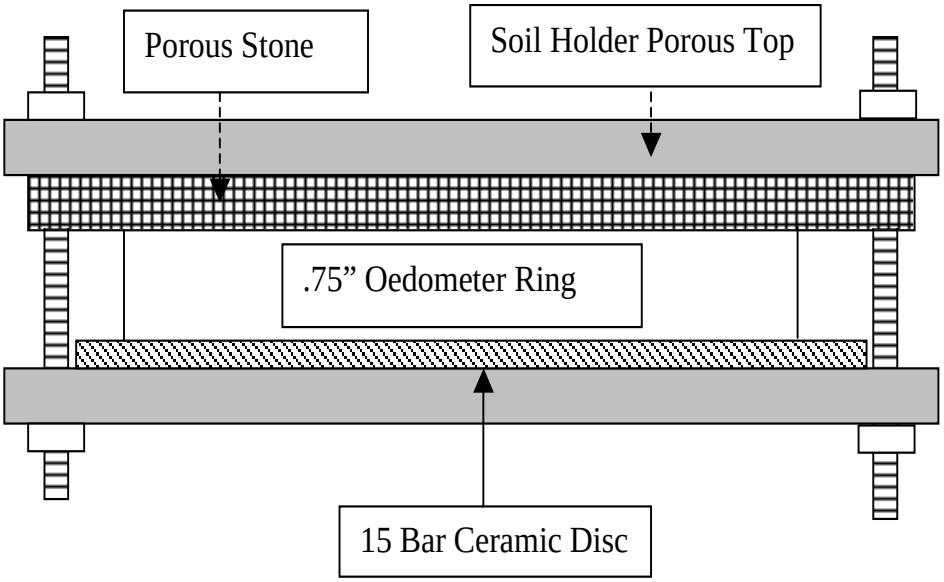

Figure 3.6.1: Saturation Assembly (Schematic)

Figure 3.6.2: Saturation Assembly

Figure 3.6.3: Soil Saturation Apparatus

3.6.4 Consolidation

After completion of the saturation procedure, test specimens were taken and consolidated according to ASTM D2425 under a 100 kPa overburden pressure. 100 kPa was used as it was chosen as the overburden pressure to be applied to the material in the pressure plate chambers. The Taylor Square Root of Time method was used for determining the end of consolidation. Loading was terminated after the samples had reached 100% consolidation. The compacted material was then allowed to unload under 0 kPa overburden pressure in order to determine the void ratio of the compacted material that would be used in the pressure plate test.

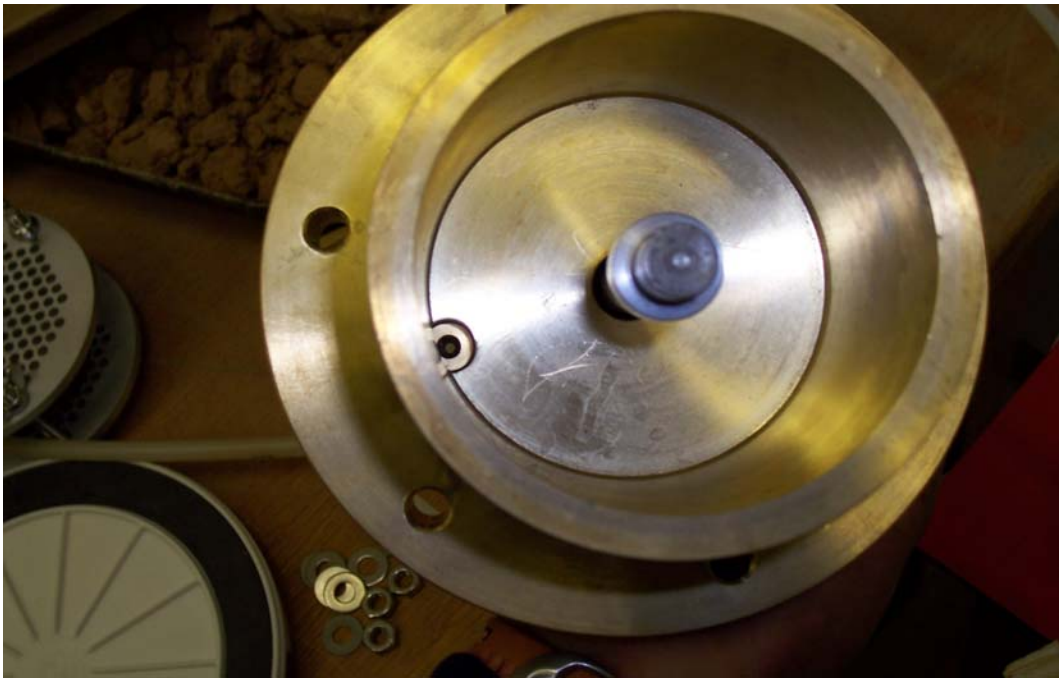

Figure 3.6.4: Pressure Plate Extractor inside top view (w/overburden)

Figure 3.6.5: Pressure Plate Extractor inside bottom view (w/gasket)

Figure 3.6.6: Volumetric Pressure Plate Extractors

3.6.5 Suction Measurement

After consolidation, specimens were taken from the consolidation devices and transferred to the pressure plate chambers, as shown in Figure 3.6.6. Suction application was applied in accordance with ASTM D 6836-02 Method B. Suction values of 10, 50, 100, 300, 500, and 1000 kPa were used for the drying portion of the test. The pressures were lowered in reverse order in the same incremental fashion to generate the wetting curve.

ASTM D 6836-02 Method B was followed for the suction measurements. The soil specimen, ring, and high air entry ceramic were placed into the recessed area in the lower half of the chamber. The Buna-N cord was placed along the circumference of the ceramic. The top chamber was lowered into place and the screws were fastened to a torque of 4.5 kN-m.

Chambers one and three were equipped with pistons to allow for the application of the overburden load. Chamber two was used to test samples under zero overburden pressure. Loading weights were placed onto the loading arm to apply the desired 100 kPa pressure to the soil. Samples were allowed to equilibrate under the 100 kPa loading over a 24-hour period of time. Dial gauges (Humboldt Part No. HM-4469.02) were used to monitor the vertical displacement of the specimens during the equilibrium period and testing. It should be noted that it was assumed that the void ratio of the material after the 24-hour chamber equilibrium period was the same as the void ratio of the material after the 100 kPa loading for consolidation.

Table 3.6.1: Pressure Plate Test Matrix

Sample Identification	As-compacted water content ω (%)	As-compacted dry density ρ_d (Mg/m^3)	Chamber Dry Density ρ_d (Mg/m^3)
HD_SP_DO_4.8_100	4.8	1.78	1.86
HD_SP_DO_4.8_0	4.8	1.79	1.79
HD_SP_DO_11.6_0	11.6	1.83	1.83
MD_.3SP_DO_4.8_100	4.8	1.60	1.81
MD_.3SP_DO_4.8_100	4.8	1.60	1.60
MD_.3SP_DO_11.6_0	11.6	1.78	1.78

3.7 Collapse Potential

Collapse Potential, which is defined as the volumetric strain difference between an as-compacted specimen and an inundated specimen, was determined for soil with as-compacted water contents ranging from 4.7 % to 22 % and dry densities ranging from 1.53 Mg/m^3 to 1.90 Mg/m^3. The following section provides the collapse potential testing procedure along with figures of the apparatus used.

3.7.1 Collapse Potential Testing Procedure

The double oedometer method was used to determine the collapse potential of the compacted material. Material was compacted to approximately the same dry density and as-compacted water content as material tested in the pressure plate chambers. Two specimens were prepared for each test. One specimen was tested in its as-compacted condition and the second sample soaked prior to loading (as proposed by Jennings and Knight 1957).

As-compacted specimens were compacted directly into standard oedometer rings (63.5 mm diameter, 19 mm height) using the desired compactive effort (detailed explanation in compaction procedure). Once the desired density was achieved, the compacted specimens were transferred to standard consolidation loading devices. Both the bottom and top porous stones, which is attached to the loading cap, were wrapped in plastic prior to placing in contact with the as-compacted samples. The plastic seal prevented capillary affects from occurring between the as-compacted specimen and the porous stones. Compacted specimens were then placed in between the porous stones and the entire consolidometer was placed into a plastic bag, which was then sealed in an attempt to minimize the effects of evaporation throughout the duration of the test (Figure 3.7.1).

After assembling the loading devices, various loading increments were selected to develop the relationship between the volumetric strain and overburden pressure. Overburden pressures of 25, 50, 100, 200, 400, and 800 kPa were selected for the study. Each loading increment was allowed to remain for a period of one hour in accordance to the ASTM D533-03 standard. Dial gauge readings were taken at the following time intervals: 0, 0.25, 0.5, 1, 2, 4, 5, 10, 20, 30, 40, 50, and 60 minutes respectively. The as-compacted specimens were immediately loaded using the previously described loading sequence. Additional loading was applied at the end of each 1-hour period until all loading increments had been applied. The second specimen (termed “soaked”) was inundated with water and allowed to come to equilibrium under a 5 kPa seating pressure. After a 24-hour equilibrium period, the soaked specimens were loaded using the same loading sequence used for the as-compacted ones. The Taylor Square Root of Time

method was used to determine when consolidation had been achieved. Based on the knowledge that most of the collapse occurs within the first five

Figure 3.7.1: Collapse Potential Assembly (Unsoaked Test)

minutes (Lawton et al., 1989; Rao and Revanasiddappa, 2000), it was determined that the criteria used was acceptable. The collapse potential was taken as the difference in volumetric strain between the as-compacted and soaked samples.

3.8 Filter Paper Method for Determining Matric Suction

The filter paper method (contact method) was used to determine the matric suction of the as-compacted material tested throughout the duration of this experimental program. This section provides the materials and methods used in the filter paper testing.

3.8.1 Filter Paper Method Testing Procedure

Material finer than the No. 10 sieve was pulverized and moisture conditioned to the appropriate as-compacted water content, covered and sealed, and placed into containers

for a 24-hour moisture equilibrium period. After 24 hours, the material was removed from the containers and compacted to the desired as-compacted water content and dry density using the compaction procedure described, in Section 3.5. Two samples were prepared for one complete test specimen. Whatman No. 42 filter paper was selected for use in this study. This particular material is one of the most common types of filter papers used for studies similar to the current study. In addition, pre-existing calibration curves (Leong et al., 2004) were readily accessible and believed to be accurate for determining the matric suction. Again, the test soil was compacted directly into 63.5 mm diameter oedometer rings, and trimmed flush with the top and bottom of the ring. Initially, two different size filter papers, were used however, due to complications (7 cm diameter filter papers would not fit through the mouth of the glass jars) with the larger sized filter paper; only the 5.5 cm diameter filter paper was used for this study. Three sheets of filter paper were required to determine the matric suction of the compacted material. Two filter paper discs, that served as protection against soil contamination, were placed above and below the one piece of filter paper that was used to determine the matric suction of the material tested.

The three filter papers were sandwiched between the two compacted soil samples (Figure 3.8.1) and taped with electrical tape to ensure good contact between the compacted specimen and the filter paper (Figure 3.8.2). The prepared test specimens were then taken and transferred to twelve (12) glass jars (Fisher Part No. 05 719 65), which were closed and sealed with electrical tape to maintain a constant moisture condition. The glass jars were placed in a styrofoam cooler, shown in Figure 3.8.3, which was closed and sealed with duck tape, and allowed to come to equilibrium over a

seven (7) day period. The temperature was measured prior and post equilibrium period and was determined to be approximately 21^{o}C, with a maximum change in temperature of 0.5^{o}C.

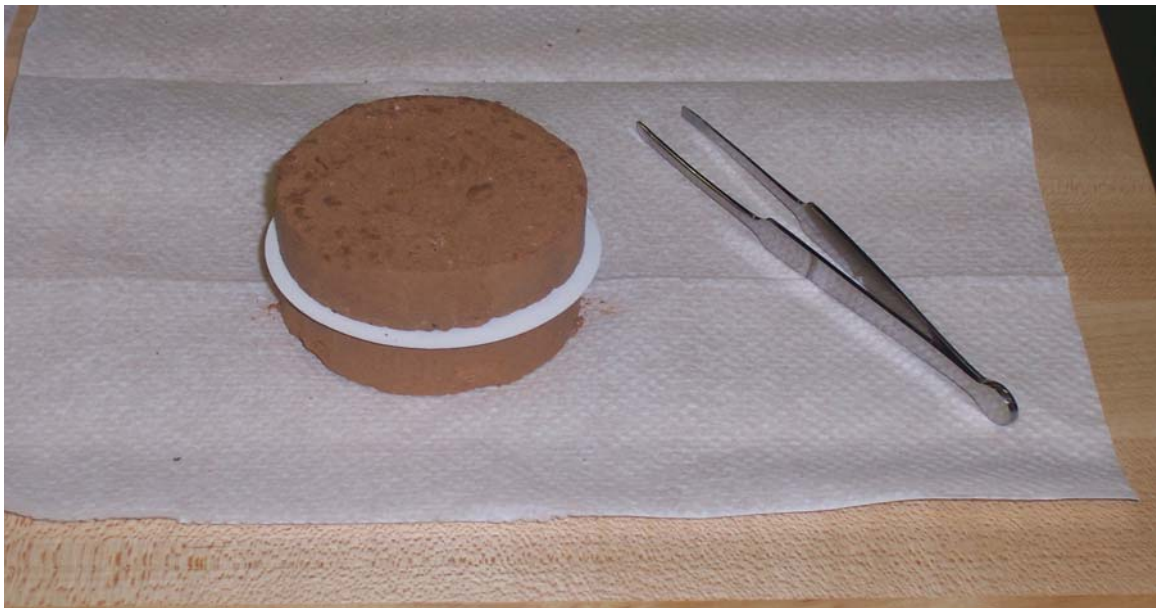

Figure 3.8.1: Compacted material with sandwiched filter paper

Figure 3.8.2: Compacted Material wrapped in electrical tape

Figure 3.8.3: Equilibrium Chamber for Filter Paper Test

After the seven-day equilibrium period, twelve (12) moisture tins (Fisher No. S63629) were labeled, cleaned free of dust, and the mass determined using a balance with 0.0001 g accuracy (Figure 3.8.4). This mass was selected as the cold tare (t_c) mass. The equilibrated specimens were carefully removed from their glass jars, the two halves separated, and the middle filter paper rapidly (within a few seconds) removed using laboratory forceps (Fisher No. 10 280) and placed into the moisture tins. The tops were immediately placed on top of the tins to prevent moisture from escaping the tins. The mass of the wet filter paper and moisture tin was quickly determined and referred to as the cold tare plus wet filter paper (M_1).

The top of each can was removed halfway and the moisture tins placed into an oven for a 48-hour period. After 48 hours, the oven was opened and the lids were placed

back on top of the moisture tins and allowed to come to equilibrium conditions in the oven for approximately five (5) minutes. The moisture tins were removed and placed onto an aluminum block to allow for rapid heat dissipation (The tins were allowed to stay on the aluminum block for approximately forty-five (45) seconds). Each tin was placed onto the scale immediately after the cooling process, and the mass of the hot tare plus dry filter paper (M_2) was determined. Finally, the dry filter paper was removed from the tin and the mass of the empty tin was determined as the hot tare (Th). The water content of the filter paper was obtained and the material's matric suction determined through the use of calibration curves and models provided by Leong et al. (2004).

Figure 3.8.4: Balance used to determine filter paper water content

3.9 Falling Head Permeability

Falling head permeability tests were conducted on compacted specimens using a special oedometer. Three different overburden pressures (5 kPa, 50 kPa, 100 kPa) were

selected to determine the effects of the varying void ratio on the permeability of the material. The following section presents the experimental procedure followed for the falling head permeability tests.

3.9.1 Falling Head Permeability Procedure

Material was compacted to the desired dry density and as-compacted water content in accordance to the same compaction procedure followed throughout the entire experimental program. After compaction, each specimen was placed into the soil saturation assembly and allowed to saturate overnight under a constant vacuum. Specimens were removed from the vacuum chamber and placed into the consolidation device shown in Figure 3.9.1. A load cap was placed onto the top of the compacted specimen, and water was allowed to fill the device prior to testing the permeability. Trapped air was removed by the use of a flushing fitting that was attached to each device at the NCSU precision shop.

Loading increments of 5 kPa, 50 kPa, and 100 kPa were selected to examine the effects of void ratio on the permeability of the compacted specimen. The Taylor Square of Time method was used to determine when 100% consolidation had been achieved under each increment of loading. The same time increments used for consolidation were selected and used for the consolidation portion of the permeability testing. The falling head permeability procedure began once consolidation was completed.

Four separate trials were selected and deemed acceptable for determining the average permeability of the compacted specimen. A head difference of five (5) centimeters was selected as an appropriate fall height needed to determine an accurate value of permeability due to the slow rate at which water moved through the manometer.

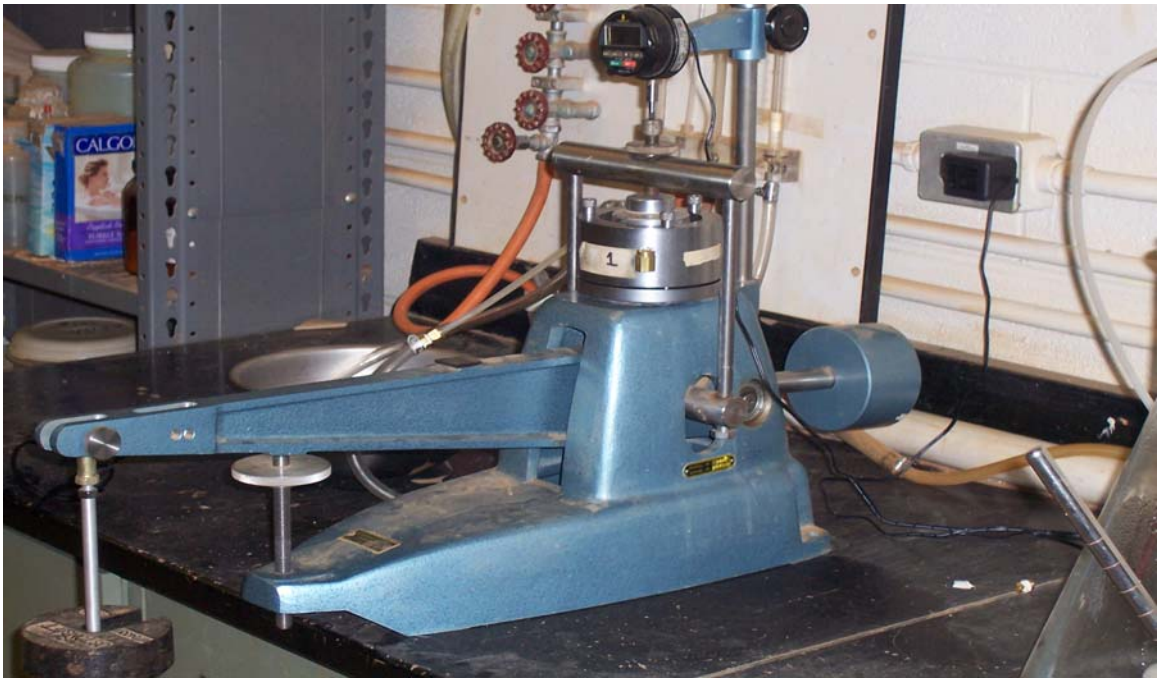

Figure 3.9.1: Falling Head Permeability with Consolidometer Apparatus

3.10 Experimental Program Summary

This chapter described the materials and methods used throughout the entire experimental program. A detailed outline of the materials used and vendor locations for the pressure plate test system has been provided. A detailed experimental procedure for conducting the pressure plate test was presented. The procedure provided a step by step approach to determine the soil water characteristic curve. Among the steps included, were the compaction methodology, specimen saturation, consolidation, and finally pressure plate testing.

Additionally, detailed procedures for each auxiliary tests were presented as well. Procedures for the following tests were included; Collapse Potential, matric suction measurement by the Filter Paper Method (Contact), and Falling Head Permeability.

4 RESULTS

This section presents the results obtained from the experimental program. Among the results included are those obtained from the pressure plate, filter paper, and collapse potential tests. The initial section presents the findings of the pressure plate pilot test, followed by the results of the experimental program in the previously mentioned order and arrangement.

4.1 Pressure Plate Pilot Study

Prior to execution of the pressure plate testing, a pilot test was conducted in order to monitor the volume change of the material during testing, and to address any problems associated with the experimental set-up prior to continuing with the remainder of the experimental program. Specimens prepared for the pilot study were tested using the same procedure mentioned in the experimental program of this document (Chapter 3). One interesting finding of the pilot test dealt with the effects of the porous stone initially used during the application of overburden. Initially a saturated porous stone was used as a partition between the load cap and the compacted specimen. The porous stone allowed for air to flow freely to the specimen (Figure 4.1.1). In addition to the porous stone affects, several issues associated with the system were addressed. Problems included, replacement of the two precision line regulators, replacing a 15-psi spring for the plug valve on the low-pressure side of the system, and the addition of a container that allowed for the application of more precise overburden pressure measurements.

4.1.1 Pilot Test Sample Selection and Preparation

Material was sieved using the No. 10 sieve and moisture conditioned to the desired water content and placed into a plastic bag, sealed, and allowed to come to equilibrium overnight.

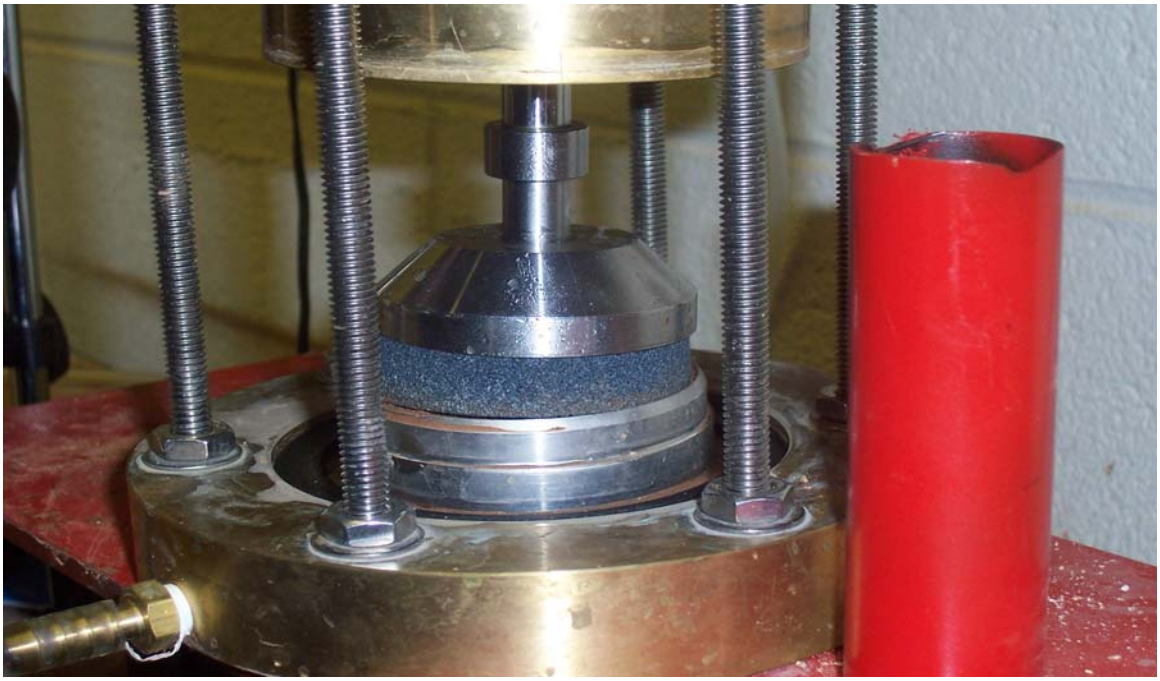

Figure 4.1.1: Compacted specimen with saturated porous stone

The pilot test sample was prepared using ten percent (10%) of the Standard Proctor energy at an as-compacted water content of 5.7%. Ten percent (10%) of the Standard Proctor energy was achieved by compacting material in a conventional proctor mold (944 cm^3) with a reduced quantity of hammer blows along with a reduced hammer fall height (Explained in detail in previous chapter). The low density and dry of optimum conditions were selected due to the fact that these conditions best represented specimens that may be poorly compacted during field applications. Material was compacted directly into a 60.14 cm^3 oedometer ring. The oedometer ring was used to maintain a k_o loading condition

during suction testing. Table 4.1.1 shows the material properties of the soil used for the pilot test.

The compacted specimen was then placed directly on top of a saturated 15 bar high air entry ceramic plate. A porous stone was placed onto the top of the material and placed into the soil saturation assembly so that the saturation procedure could begin. The saturation assembly was placed into a vacuum chamber and allowed to saturate for 24 hours under a constant vacuum. Care was taken when inundating the material in the vacuum chamber to insure that the maximum quantity of air could be removed. The sample was inundated to approximately ¾ of the entire height, allowing a head space above the material that allowed for the evacuation of air as water flowed through the bottom of the sample and out of the top.

Table 4.1.1: Pilot Test Material Properties

ρ_d (g/cm^3)	Void ratio, (e)	Porosity, (n)	ω (%)
1.51	0.73	0.42	5.7

4.1.2 Porous Stone Considerations

Prior to placing the material into the pressure chamber, an initially dry 6.35 cm diameter porous stone (volume = 40.23 cm^3) was placed on top of a saturated soil sample located in a conventional oedometer ring in order to determine if capillary effects existed between the porous stone and the compacted material. An analysis showed that approximately 5-6 grams (5-6 cm^3) of water was imbibed into the porous media during the process. The quantity of water imbibed corresponded to a 24 % possible reduction in volumetric outflow due to the capillary effects. To mitigate the capillary effects, it was

decided to saturate the porous stone prior to suction testing. It was believed that by saturating the stone prior to placing it on top of the compacted specimen, the capillary forces between the stone and material would be eliminated and the volume of sample would be accurately accounted for during suction testing.

4.1.3 Pilot Test Suction Cycle

The pilot test commenced with the application of 10 kPa matric suction followed by suctions of 50 and 100 kPa. The material was allowed to come to equilibrium under each increment of suction. Equilibrium was determined when the change in capillary tube readings were less than or equal to 10% of the cumulative change over a 24-hour time increment. The suction was reduced incrementally back to 0 kPa (10 kPa was not used for the wetting curve due to the minimal change (1 mm) in volumetric outflow from 50 kPa to 10 kPa) for the wetting portion of the test. Figure 4.2.2 through Figure 4.2.4 show the soil water characteristic curves generated during the pilot test.

4.2 Pilot Test Discussion

This section is used to discuss the findings of the pilot study. It addresses problems and concerns encountered through out the pilot study. Several concerns arose upon examining the curves. The concerns included the lack of a clear air entry value, and a large change in outflow volume for the material with a corresponding negligible volume change.

4.2.1 Porous Stone and Air Entry Value

Results showed that the there existed an approximately 23 cm^3 change in outflow during the drying portion of the pilot test. The large change in outflow resulted in a 0.16 % (Δe = .0015) change in void ratio of the material. This condition of large outflow change with minimal volume change of the sample indicated that the majority of the outflow was

attributed to the release of water from the saturated porous stone. Figure 4.2.2 through Figure 4.2.4 shows the soil-water characteristic curve generated from the pilot test. The figure shows both the measured and corrected soil water characteristic curve which takes into account the outflow volume due to the porous stone (10 cm^3).

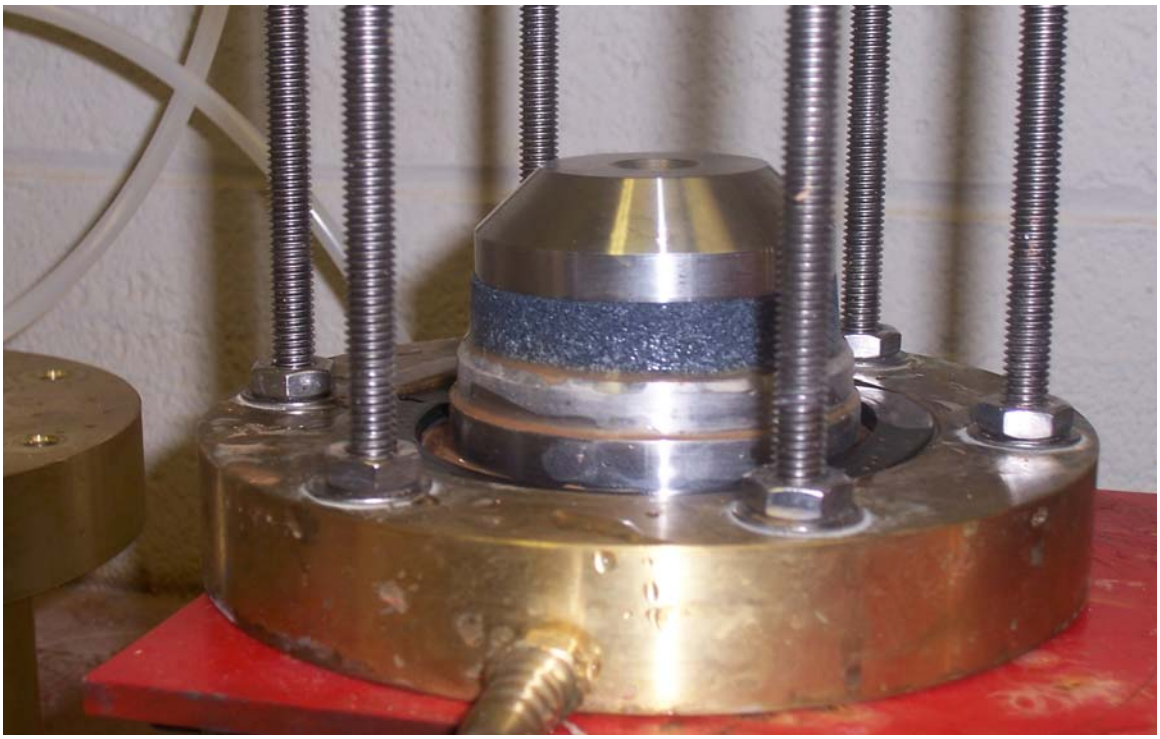

Figure 4.2.1: Original Pressure Plate Soil Assembly with porous stone

The lack of a clear air entry value was attributed to the effects of the saturated porous stone. The quantity of water released resulted in a volumetric water content (gravimetric water content and degree of saturation) rate change large enough to prevent the air entry value from being determined.

4.2.2 Pilot Test Soil Structure

The structure and texture of the compacted material was examined upon termination of the pilot study to gain an understanding of the how the structure of the specimen changed throughout the suction testing.

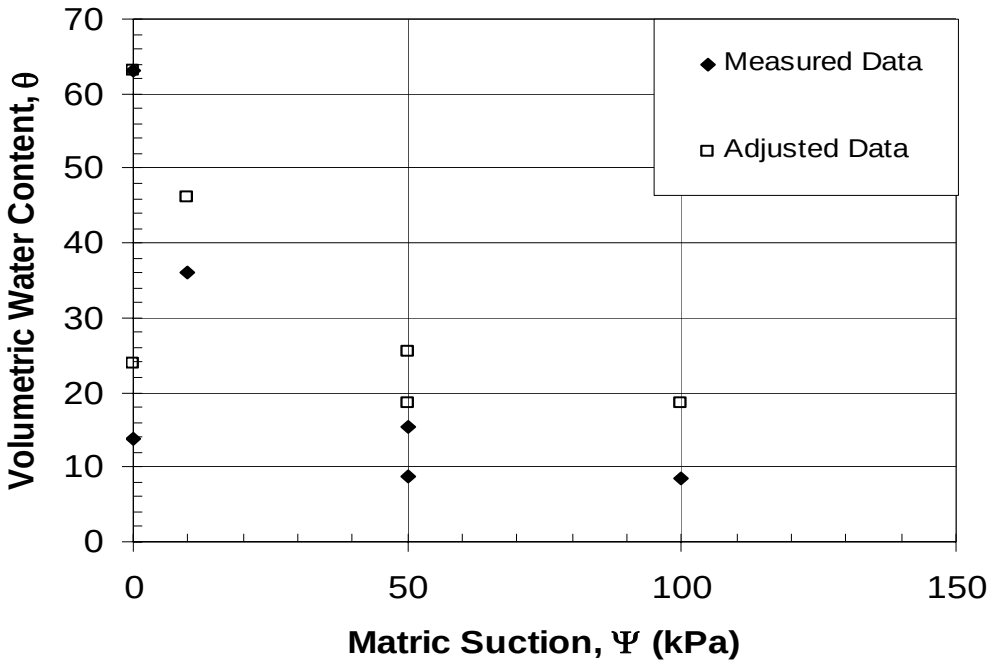

Figure 4.2.2: Pilot Test SWCC (Volumetric Water Content)

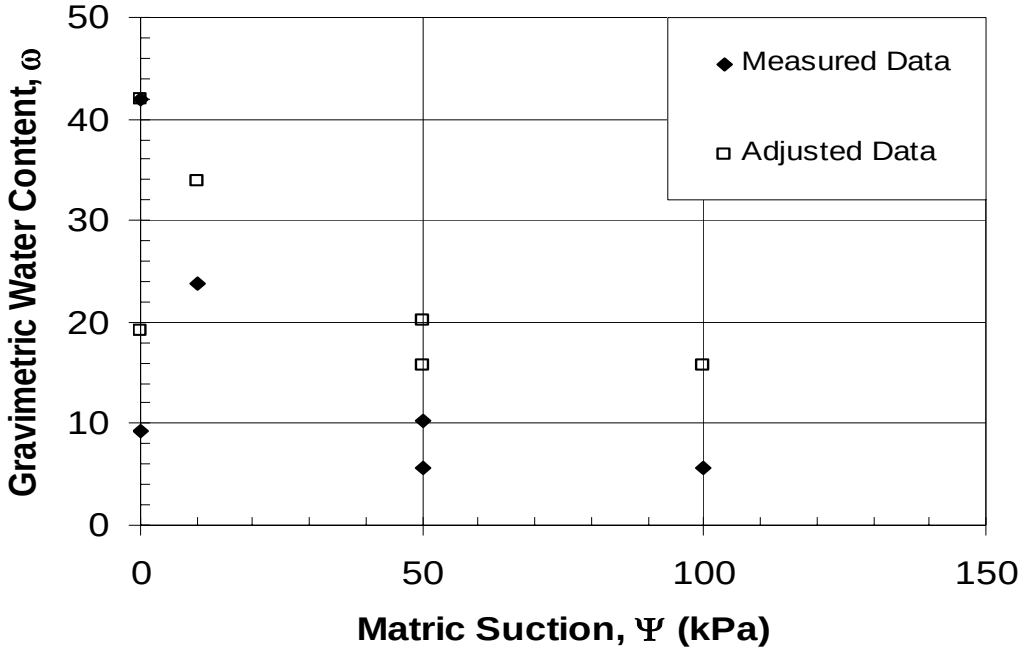

Figure 4.2.3: Pilot Test SWCC (Gravimetric Water Content)

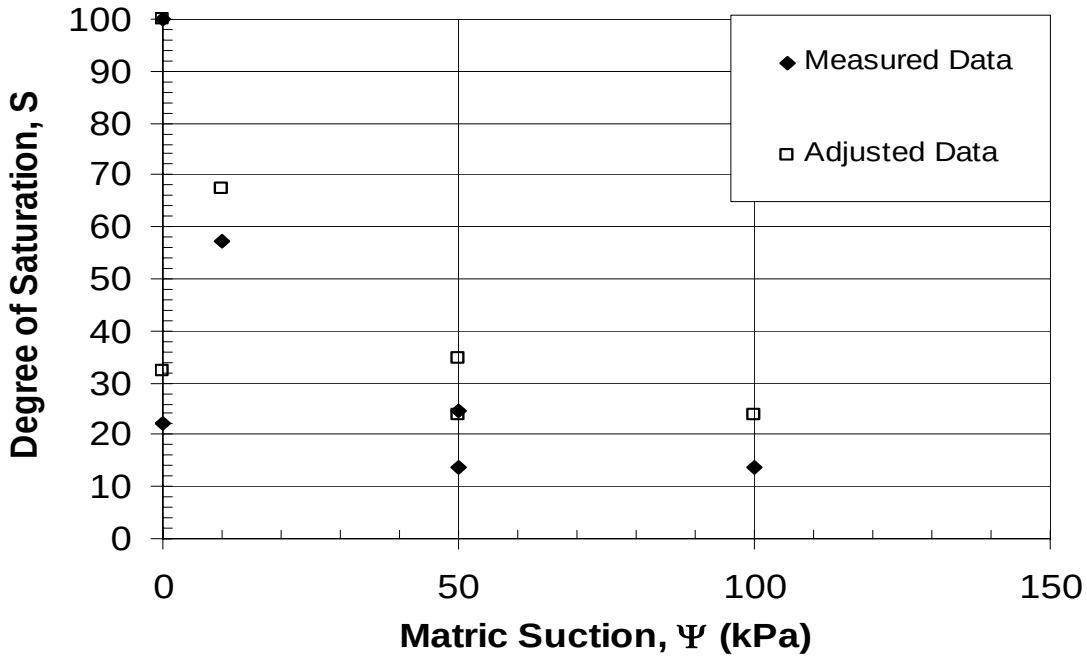

Figure 4.2.4: Pilot Test SWCC (Degree of Saturation)

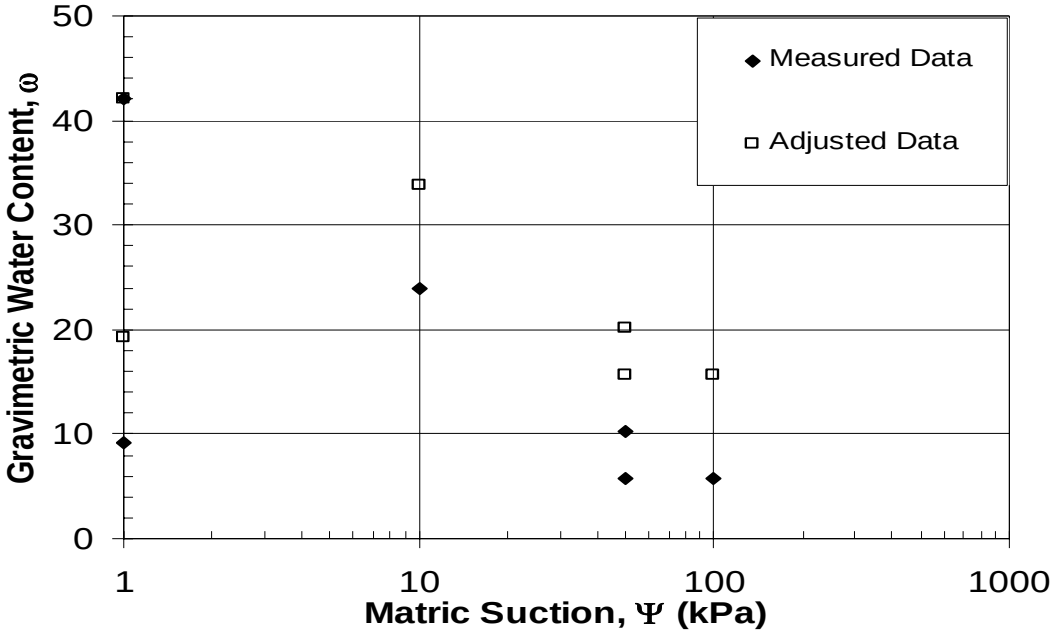

Figure 4.2.5: Pilot Test SWCC (Gravimetric Water Content – Log Scale)

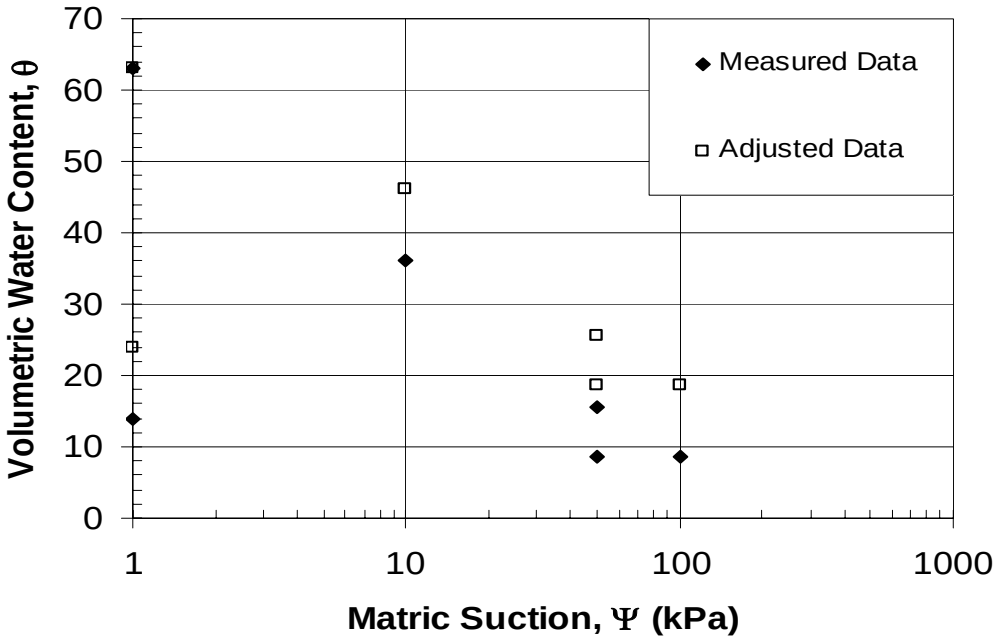

Figure 4.2.6: Pilot Test SWCC (Volumetric Water Content- Log Scale)

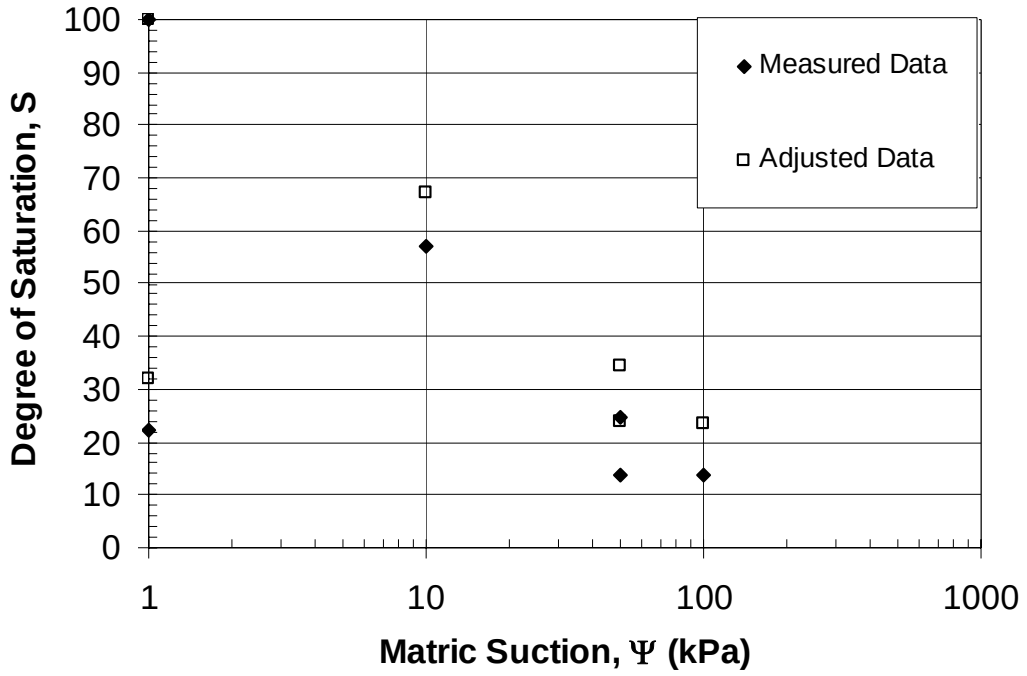

Figure 4.2.7: Pilot Test SWCC (Degree of Saturation-Log Scale)

Figure 4.2.8 and Figure 4.2.9 show the structure of the material used for the pilot study at the termination of the test. From the figures it can be seen that the specimen became brittle and exhibited very noticeable cracks and fractures throughout the entire sample. It was concluded that the combination of the dry of optimum (5.7%) as-compacted water content and low compactive effort (10% of Standard Proctor) resulted in an open structure that could not withstand the combination of the 100 kPa overburden pressure and applied air pressure.

Cracking was experienced on both the top (location where the overburden piston rested) and bottom sides of the compacted material. The open structure is believed to be partly responsible for the continued sharp decrease (between drying suctions of 10 kPa and 50 kPa)

Figure 4.2.8: Pilot test low-density (1.51 Mg/m^3) specimen (Post test-top view)

Figure 4.2.9: Pilot test low-density (1.51 Mg/m^3) specimen (Post test-bottom view)

in water content/degree of saturation after the initial decrease (believed to be a result of the saturated porous stone) prior to the 10 kPa applied air pressure.

4.2.3 Proposed Changes from Pilot Test to Actual Test

Several changes were made due to the findings of the pilot test. The following summary provides the changes made as a result of the findings of the pilot study. In addition, the summary provides an explanation of how each proposed change will be used to benefit the pressure plate test.

- ***CONSOLIDATION***

For the pilot study, compacted material was taken directly from the saturation assembly and vacuum chamber, and placed into the volumetric pressure plate extractors. The combination of low density (1.51 Mg/m^3) and saturated nature of the sample made the material very difficult to handle and preserve the integrity of its structure. Figure 4.2.10 shows one of the trial specimens prepared that was not used due to the slurried state that it was in prior to suction testing. Upon lowering the overburden piston in place, the lack of integrity of the compacted specimen resulted in the sample failing and being lost above and below the consolidometer ring.

Additional trials were attempted until an acceptable specimen had been prepared. After completion of the pilot study, it was determined that the material should be consolidated under a desired normal overburden pressure (100 kPa) prior to being tested in the volumetric pressure plate extractors. Consolidation prior to suction testing was believed to have several benefits for the experimental program. One potential benefit of consolidation would be to make the saturated compacted specimen more structurally intact and easier to physically handle. The increased integrity would aide in preventing

material loss when the sample was being transferred from the saturation assembly to the pressure plate extractors. Allowing the material to be consolidated under 100 kPa also allowed for a more representative specimen to be tested as field conditions were attempted to be mimicked. Testing specimens that had been exposed to a significant overburden pressure would allow f for the analysis and understanding of non-surface soil specimens. Finally, it was believed that consolidating the material prior to suction testing would prevent cracking from occurring as had been displayed in the pilot study.

- ***POROUS STONE***

The most important change to the pressure plate testing procedure involved replacing the saturated porous stone with two non-woven geotextiles. The two geotextiles (Proplex 1198), were hydrophobic and eliminated problems associated with water storage and capillary action between the porous stone and compacted sample. The use of two geotextiles was deemed sufficient as they provided enough separation between the load cap and compacted sample to allow for air to flow undisturbed to the specimen (Figure 4.2.11).

- ***PRESSURE SUPPLY***

The compressed air tank used for the pilot test had to be replaced due to the initial use of high bleed style pressure regulators. Upon termination of the test, two low bleed regulators were selected and used for the remainder of the pressure plate test. The final change to the system dealt with the spring used in the check valve on the high-pressure flow side of the system. The original 15-psi spring was believed to be faulty and caused the pressure source to continually loose air pressure during the pilot study.

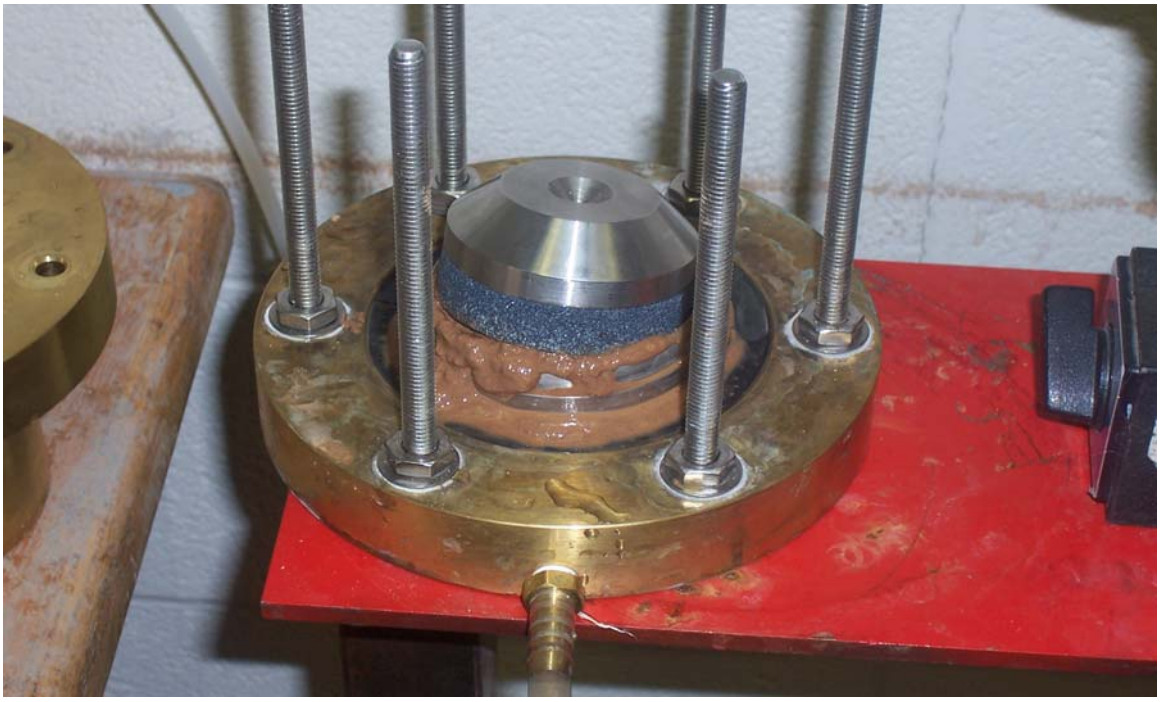

Figure 4.2.10: Pilot test failed specimen

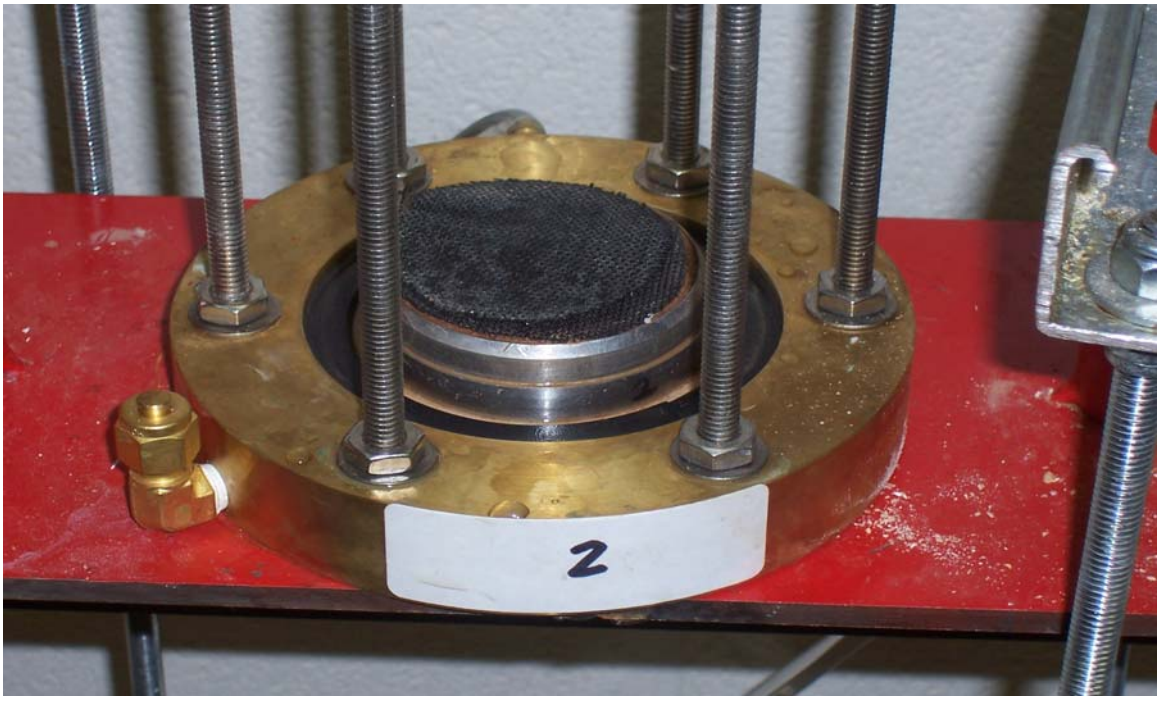

Figure 4.2.11: Compacted Material with two geotextiles

The 15-psi spring was replaced with a stiffer 25-psi spring that kept the plug value in the closed position until the suction on the high-pressure side met and or exceeded the rated spring stiffness.

4.2.4 Pilot Study Summary

A pilot study was conducted in order to gain an initial understanding of the soil water characteristic behavior of as-compacted specimens used through out the experimental program. The previous section has explained the components of the pilot study in detail. An explanation regarding the testing procedure, associated problems with the experimental set-up and corresponding changes from the pilot study to the current study.

4.3 Pressure Plate Test Results

4.3.1 Introduction

Soil water characteristic curves (drying and wetting) were generated for material compacted at varying as-compacted water contents, and dry densities. As-compacted water contents of 4.8 and 11.6 % were selected and as-compacted dry densities ranging from 1.60 to 1.78 Mg/m^3 were used. Additionally, specific samples were exposed to 100 kPa overburden pressure and tested within the volumetric pressure plate devices. This section presents the soil water characteristic curves generated for the material used through out the experimental program. The influence of compaction conditions (as-compacted water content and compactive effort) were examined by comparisons of the air entry values of material compacted using different Proctor energies and varying as-compacted water contents.

4.3.2 Experimental Soil Water Characteristic Curves

This section presents the soil water characteristic curves obtained from the pressure plate testing component of the experimental program. Four (4) curves (Figure 4.3.1 through Figure 4.3.4) were generated and are presented in three different combinations. Curves are plotted as degree of saturation, and volumetric water content (gravimetric water content plots are shown in the appendix) versus the matric suction. The two combinations were selected in order to provide the reader with the option of examining the differences in air entry values obtained when the curves are plotted in varying forms (Fredlund, 2006).

Due to losses in pressure seals, there are three curves that only contain the dry portion

up to an air pressure of 500 kPa. The following three curves contain only drying data up to the specified air pressure: Curves with as-compacted water content of 4.8% and 100 kPa and 0 kPa, and as-compacted water content of 11.6% and 100 kPa overburden. For reasons unknown to the author at this time, nearly all drying experimental curves terminated below zero degree of saturation. It was suggested that water may have been released from the high air entry disc thus causing the degree of saturation to become a negative value. An analysis located in the appendix has shown that negligible (less than 1g) water was released from each high air entry disc. However, a significant amount of capillary change was experienced during the check of each disc. Cumulative capillary reading changes of 26.9 cm, 42.95 cm, and 56 cm were determined for chambers 1, 2, and 3, respectively. Each change in cumulative capillary readings resulted in a change in volumetric water content of 0.0534 cm^3, 0.085 cm^3, and 1.79 cm^3, respectively.

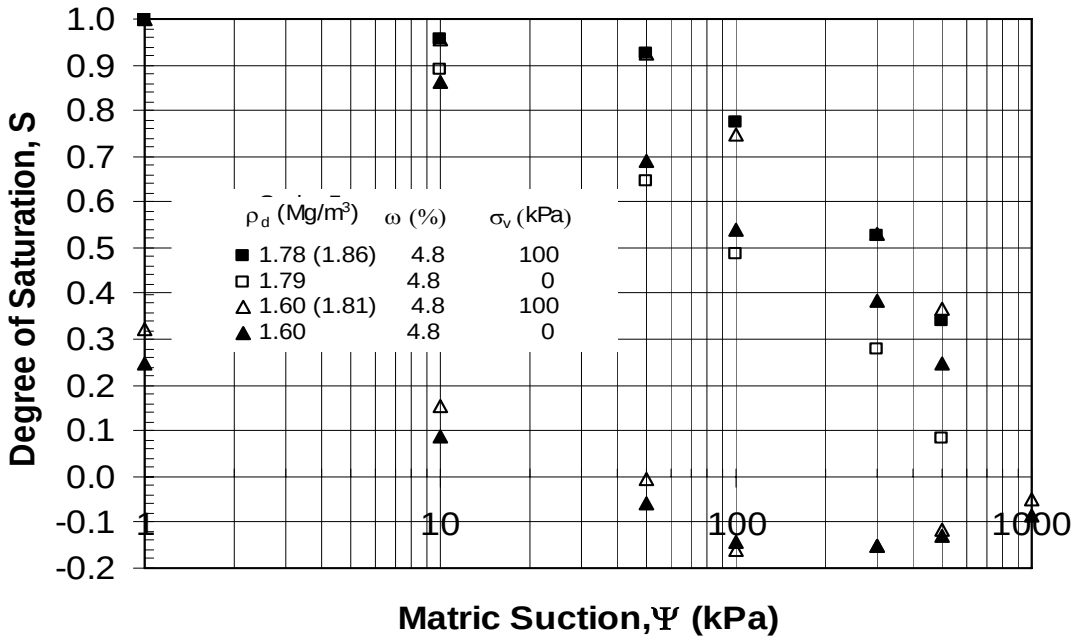

Figure 4.3.1: SWCC in terms of degree of saturation (as-compacted ω = 4.8%)

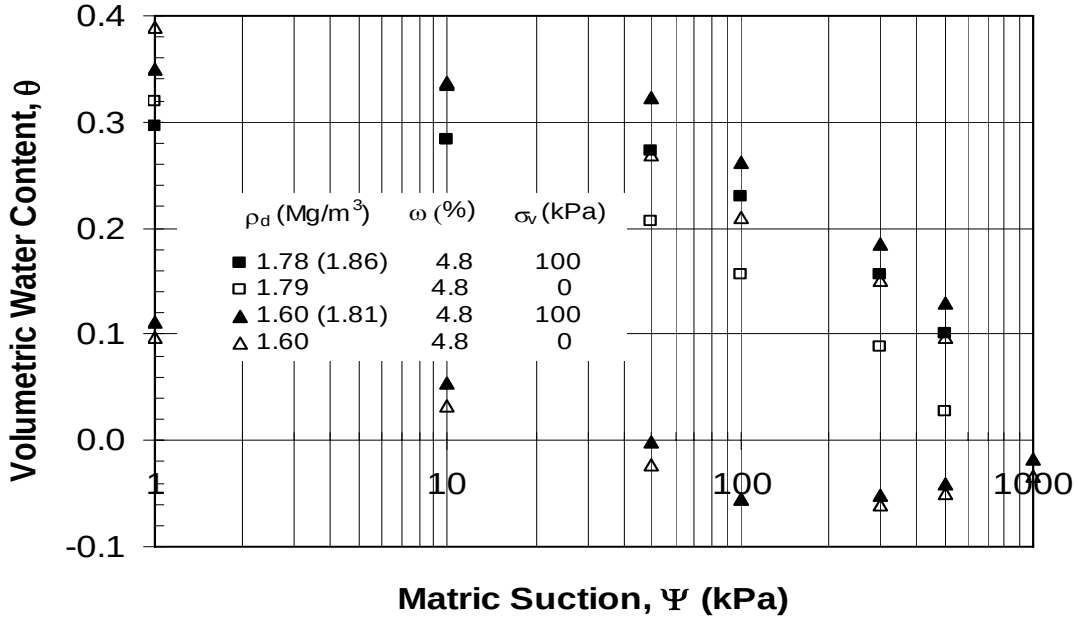

Figure 4.3.2: SWCC in terms of volumetric water content (as-compacted ω = 4.8%)

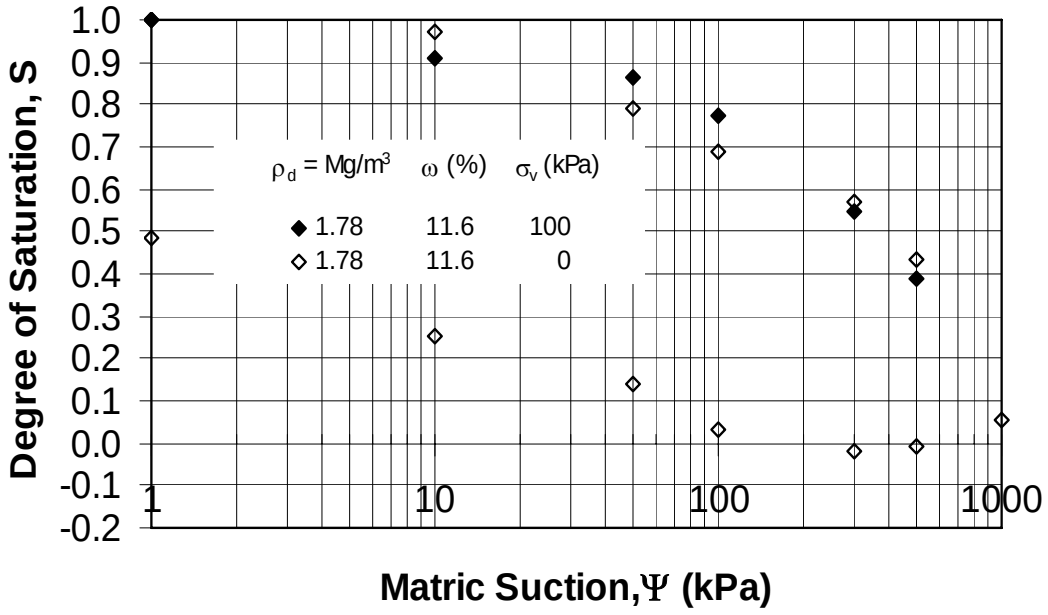

Figure 4.3.3: SWCC in terms of volumetric water content (as-compacted ω = 11.6%)

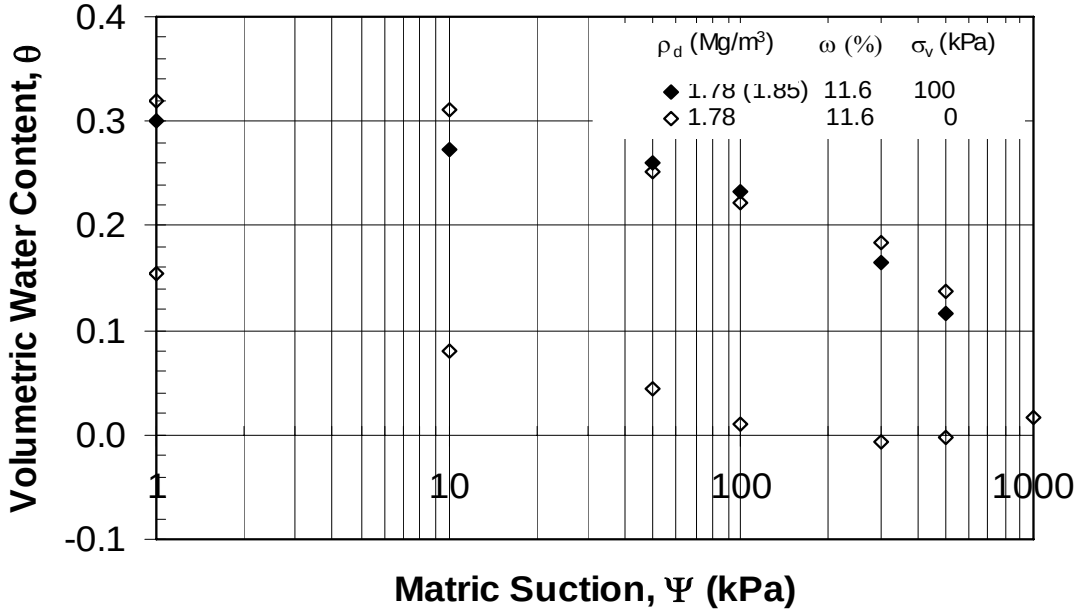

Figure 4.3.4: SWCC in terms of volumetric water content (as-compacted ω = 11.6%)

4.4 Filter Paper Method for Determining Matric Suction (Contact Method)

4.4.1 Introduction

As an additional means of determining the matric suction of the material used throughout the experimental program, filter paper (contact method) tests were conducted. ASTM D 5298-03 was used as the standard. Twelve (12) specimens were prepared at varying as-compacted water contents and as-compacted dry densities. Table 4.5.1 summarizes the test specimens prepared and tested. As-compacted water contents ranged from 4.7 to 22%, and dry densities ranged from 1.53 to 1.90 Mg/m^3. Table 4.5.1 also provides the associated matric suctions obtained for each specimen. Matric suction values were obtained using calibration curves (Figure 4.4.1) generated for Whatman No. 42 filter papers that were found within the literature (Leong et al., 2004).

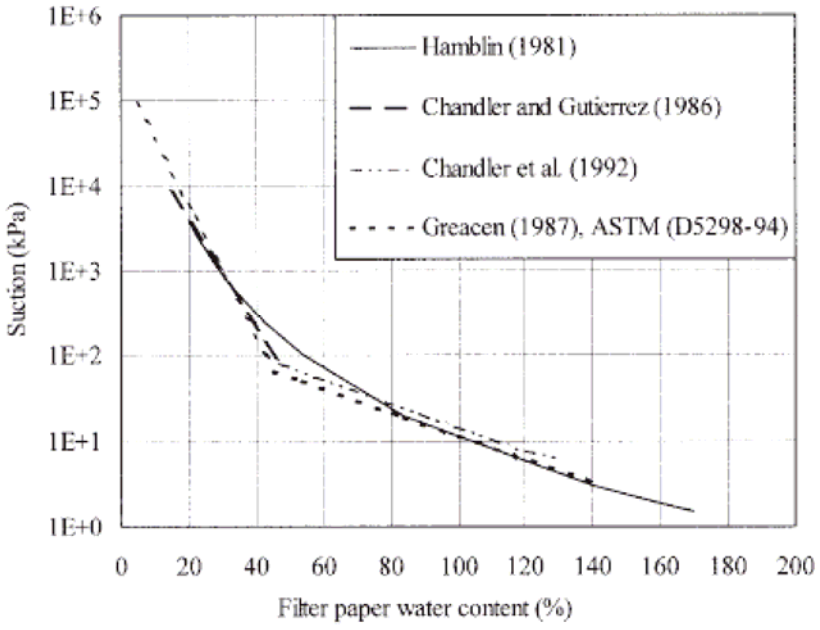

Figure 4.4.1: Whatman No. 42 Filter Paper Calibration Curve (Leong et al., 2002)

4.5 Filter Paper Results

Table 4.5.1: Filter Paper Results Summary

Water content, ω (%)	Dry Density, ρ_d (Mg/m^3)	Matric Suction, Ψ (kPa)
4.7	1.53	833
4.7	1.60	741
4.7	1.78	774
4.7	(un-compacted)	783
9.5	1.85	50
11.7	1.60	40
11.7	1.78	42
11.7	1.90	39
15	1.78	0.76
15	1.85	3
17	1.78	0.28
22	1.60	0.38

Figure 4.5.1 presents the tabular results of Table 4.5.1 in graphical form. A distinct trend exists between the as-compacted water content and matric suction. From the figure it can clearly be seen that the matric suction of the specimens tested decrease with increasing as-compacted water content. For example, specimens compacted at 4.7% as-compacted water content had an average value of 783 kPa matric suction, while specimens compacted at 15% as-compacted water content had an average value of $\approx$ 2 kPa matric suction.

One important finding from the filter paper tests was the relationship between the matric suction and the as-compacted dry density. It can be seen that magnitude of the matric suction appears to be dependant solely on the as-compacted water content, and not the density at which the specimen was compacted. This finding can clearly be seen by examining the specimens compacted at 4.7% and 11.7%.

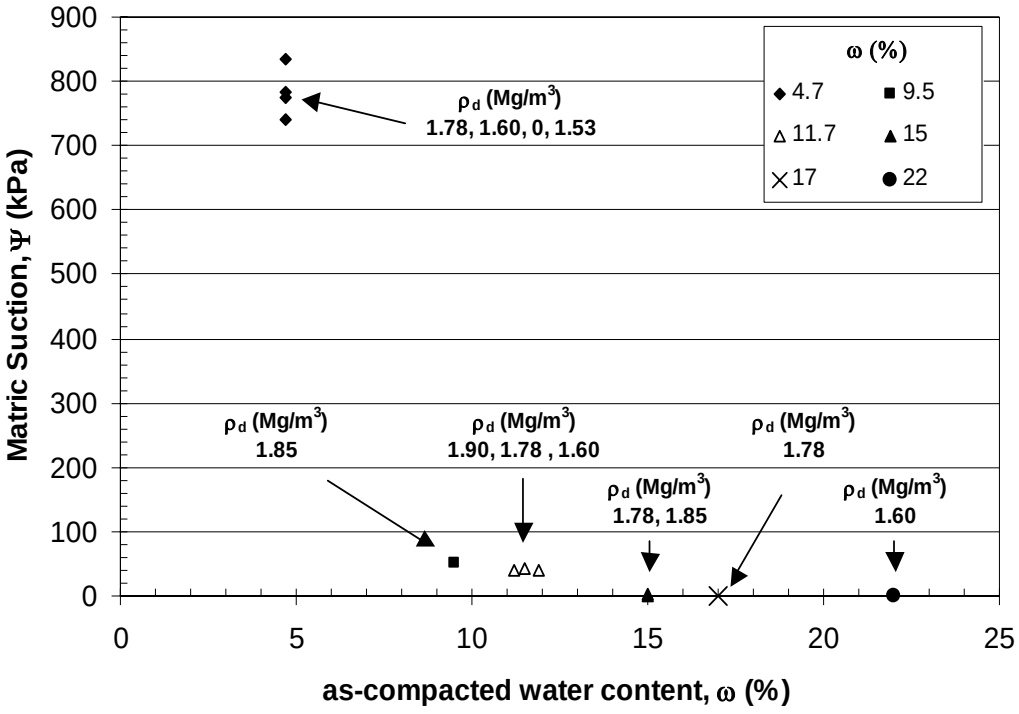

Figure 4.5.1: Filter Paper Results

Three specimens with varying dry densities (1.53 Mg/m^3, 1.60 Mg/m^3, and 1.78 Mg/m^3) were prepared and tested at 4.7%. Additionally, one un-compacted specimen (prepared by placing the soil in its loose condition into sample jar) was tested at 4.7% water content. Results showed that even with the varying dry densities, there only existed a 92 kPa (13.4 psi) difference in matric suction. It appears that the range of suction varying decreases with increasing as-compacted water content. Specimens tested at 11.7% ranged in matric suction by a very negligible value of 3 kPa (0.4 psi).

4.6 Collapse Potential

4.6.1 Introduction

Double Oedometer tests were used to determine collapse potential of as-compacted

material prepared to dry densities ranging from 1.53 Mg/m^3 to 1.90 Mg/cm^3 and as-compacted water contents ranging from 4.7% to 22%. The test procedure (explained in detail in previous sections) involved loading both an as-compacted sample and a sample that had been inundated using the following desired series of overburden pressures (5kPa, 25 kPa, 50 kPa, 100 kPa, 200 kPa, 400 kPa, 800 kPa). The following sections provide the results obtained from collapse potential testing.

4.6.2 As-Compacted Specimens

The following set of figures (Figure 4.6.1 through Figure 4.6.6) show the volumetric strain versus overburden pressure for specimens compacted with varying as-compacted water contents (4.7% - 22%) and as-compacted dry densities (1.53 Mg/cm^3 – 1.90 Mg/m^3). The series of figures are displayed in a specific arrangement in an attempt to provide the reader with a chronological order in which specimens were tested. The figures are placed in sets of three, with the first three figures always showing the volumetric strain versus overburden pressure for as-compacted specimens. The second set of three curves show the volumetric strain versus overburden pressure for inundated specimens (varying as-compacted water contents) and the final figures showing the volumetric strain difference (collapse potential) between the as-compacted and inundated specimens. Additionally, the symbols used to describe the specimens tested follow a specific order and pattern. Triangles are used to represent specimens tested with the lowest compactive effort for a given as-compacted water content followed by a square and diamond for the middle and high (Standard Proctor) compactive efforts respectively.

Figure 4.6.1 shows the volumetric strain versus overburden pressure for specimens compacted at an as-compacted water content of 4.7%. It should be noted that

the volumetric strain at 800 kPa for the low density (LD) specimens was not reported due to a break in the porous stone that resulted in data that was not representative of the material behavior. Three separate as-compacted dry densities were selected for comparison. It can be seen that the volumetric strain decreases with increasing as-compacted dry density, as the specimen compacted at the lowest dry density exhibited the largest magnitude of strain followed by the medium density (MD) sample, followed by the high density (HD) specimen.

Figure 4.6.2 shows the volumetric strain versus overburden pressure for material compacted at an as-compacted water content of 11.7%. The data follows the similar trend as specimens compacted at 4.7% as-compacted water content with the highest as-compacted dry density specimen exhibiting the least amount of collapse, and the magnitude of volumetric strain following an inverse relationship with the dry density. Due to erratic data, the low density (1.60 Mg/m^3) sample was retested in both the as-compacted (unsoaked) and inundated conditions. The final figure (Figure 4.6.3) located in this section represents the volumetric strain versus overburden pressure for as-compacted water contents of 16.9% and 22%. It can be seen from the curve that the material compacted at a lower as-compacted water content (16.9%) exhibited a larger magnitude of volumetric strain for a given overburden pressure.

4.6.3 Inundated Material

A second "identical" specimen (same compactive effort, as-compacted dry density, as-compacted water content) was inundated under a 5 kPa seating pressure and allowed to come to equilibrium over a 24-hour period. After the equilibrium period, the

inundated specimen was loaded in the same incremental fashion as the as-compacted (unsoaked) specimen.

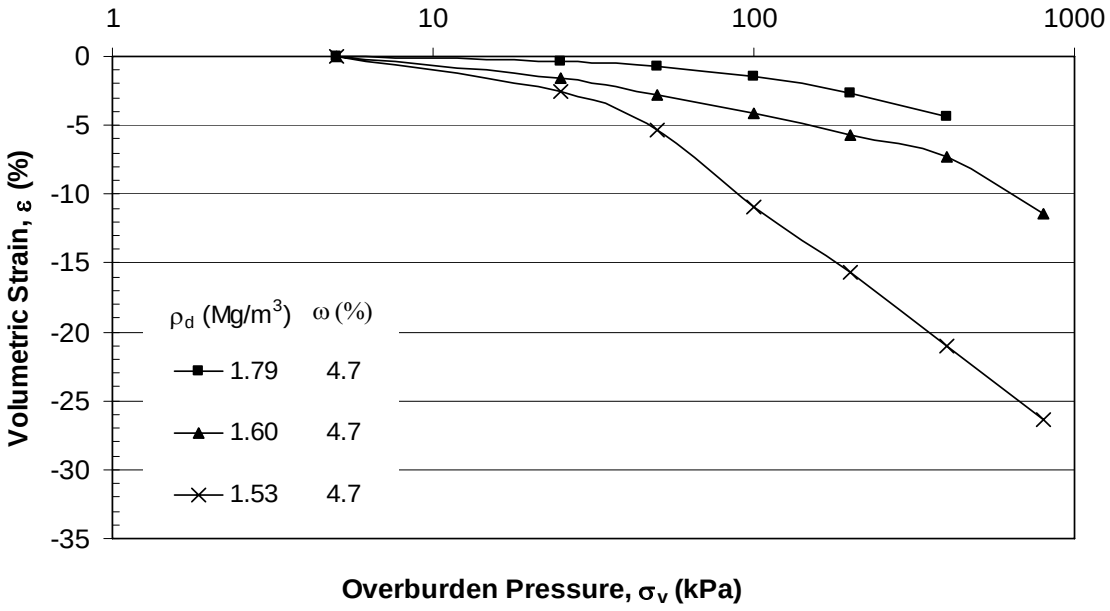

Figure 4.6.1: Double Oedometer Unsoaked (as compacted ω = 4.7%)

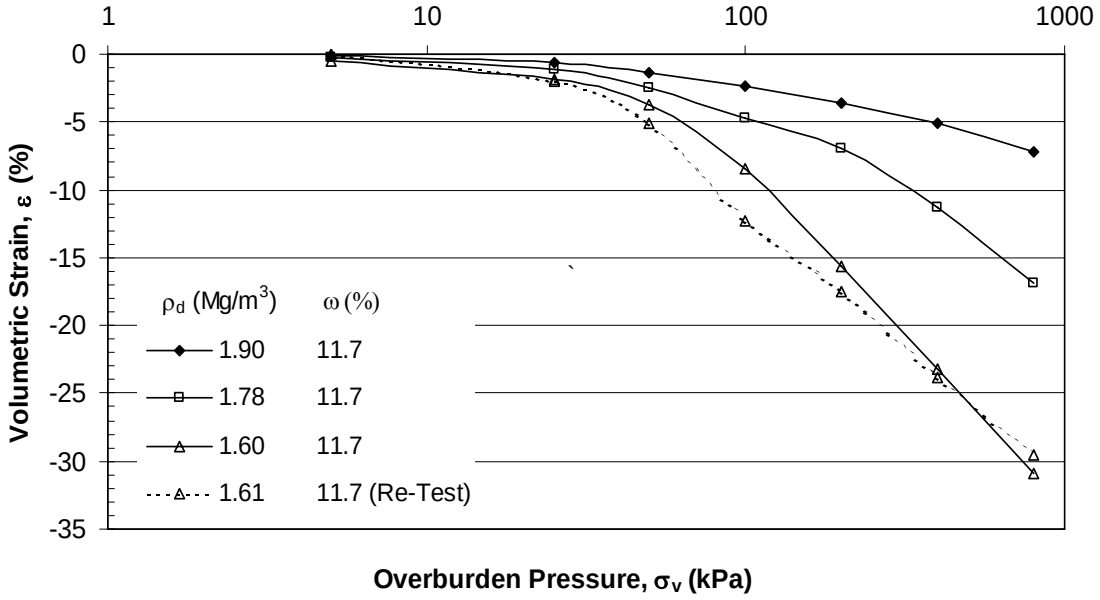

Figure 4.6.2: Double Oedometer Unsoaked (as-compacted ω = 11.7%)

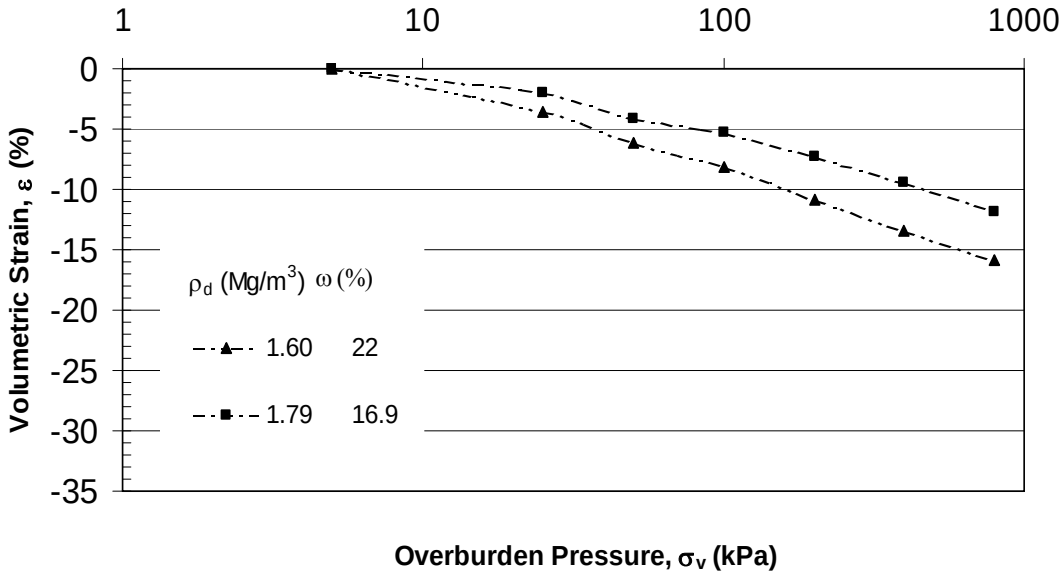

Figure 4.6.3: Double Oedometer Unsoaked (as compacted w =16.9% & 22%)

Similar to the trend displayed in the as-compacted specimens, Figure 4.6.4 through Figure 4.6.6 display a trend of material compacted at lower as-compacted dry densities exhibiting larger magnitudes of volumetric strain for a given overburden pressure than material compacted at higher dry densities. Due to erratic data, a second low density (LD) specimen was tested and the curve has been included for the both the as-compacted and inundated conditions (Figure 4.6.2and Figure 4.6.5).

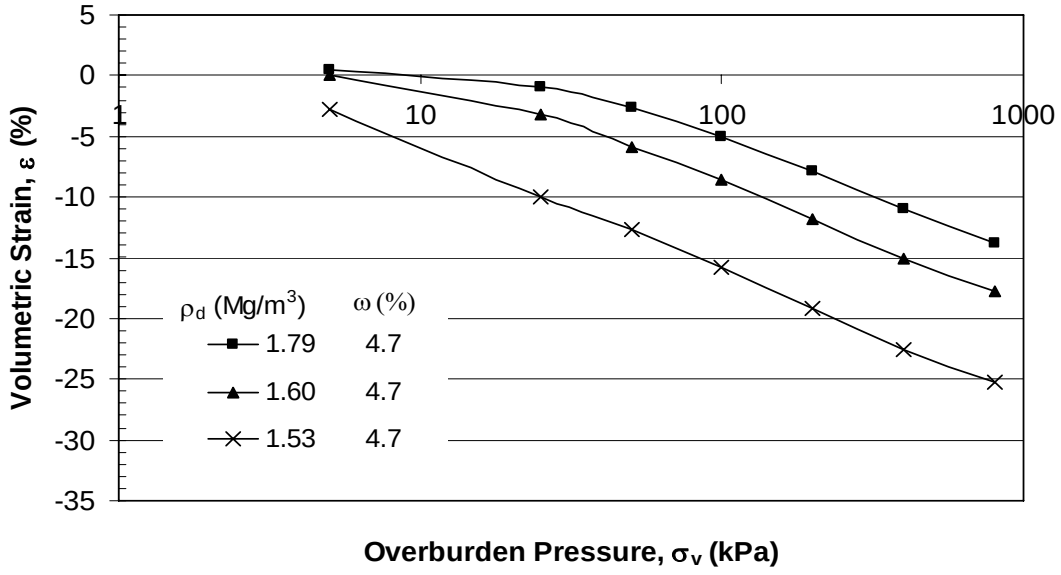

Figure 4.6.4: Double Oedometer Soaked (as compacted ω=4.7%)

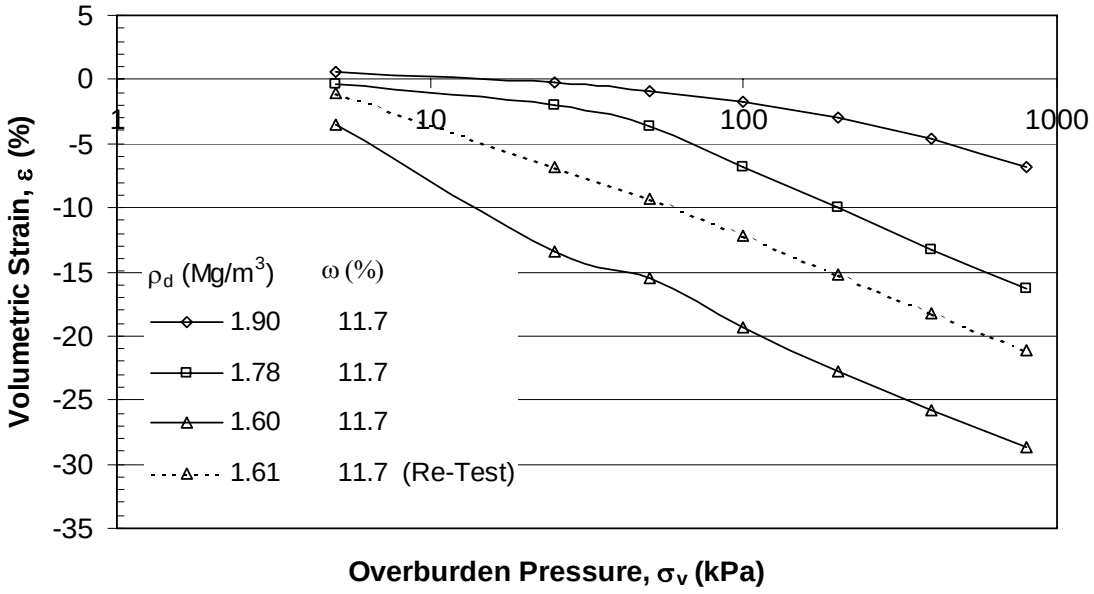

Figure 4.6.5: Double Oedometer Soaked (as compacted ω = 11.7%)

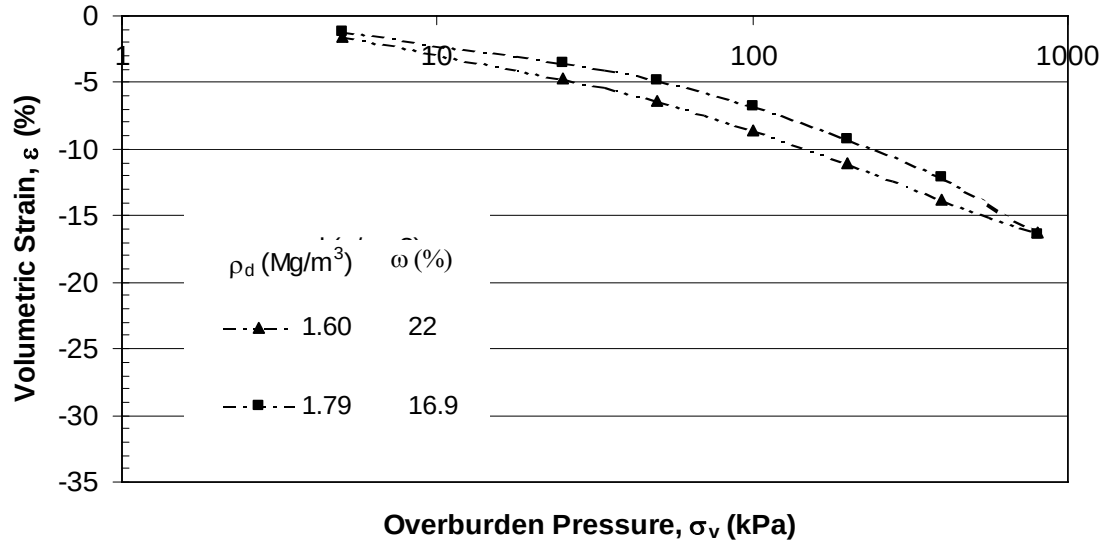

Figure 4.6.6: Double Oedometer Soaked (as compacted ω =16.9% & 22%)

4.7 Falling Head Permeability

4.7.1 Introduction

Falling Head Permeability tests were conducted four (4) separate specimens, compacted at varying dry densities and as-compacted water content. Three of the specimens tested were a low density (1.53 Mg/m^3), medium density (1.60 Mg/m^3), and a high density (1.78 Mg/m^3) specimen. These three specimens used were all compacted at an as-compacted water content of 4.7%. Additionally, one high-density specimen (1.90 Mg/m^3) compacted at 11.7% as-compacted water content was tested.

Three separate overburden pressures were applied to the specimens in an attempt to determine the influence of the change in void ratio on the permeability. Overburden pressures of 5, 50, and 100 kPa were the overburden pressures that were examined.

4.7.2 Permeability Results

The following tables (Table 4.7.1 through Table 4.7.4) and figure summarize the permeability results obtained. The tables show the permeability for each specimen tested, the water content at which it was tested, and the magnitude of overburden pressures applied.

Table 4.7.1: Permeability Results (σ_v = 5 kPa)

ρ_d (Mg/m^3)	ω (%)	k (cm/sec)
1.53	4.7	3.03×10^{-4}
1.60	4.7	7.75×10^{-5}

Table 4.7.2: Permeability Results (σ_v = 50 kPa)

ρ_d (Mg/m^3)	ω (%)	k (cm/sec)
1.53	4.7	1.59×10^{-5}
1.60	4.7	5.25×10^{-5}

Table 4.7.3: Permeability Results (σ_v = 100 kPa)

ρ_d (Mg/m^3)	ω (%)	k (cm/sec)
1.53	4.7	5.705×10^{-5}
1.60	4.7	1.38×10^{-4}

Table 4.7.4: Permeability Results (σ_v= 5 kPa)

ρ_d (Mg/m^3)	ω (%)	k (cm/sec)
1.90	11.7	9.12×10^{-8}

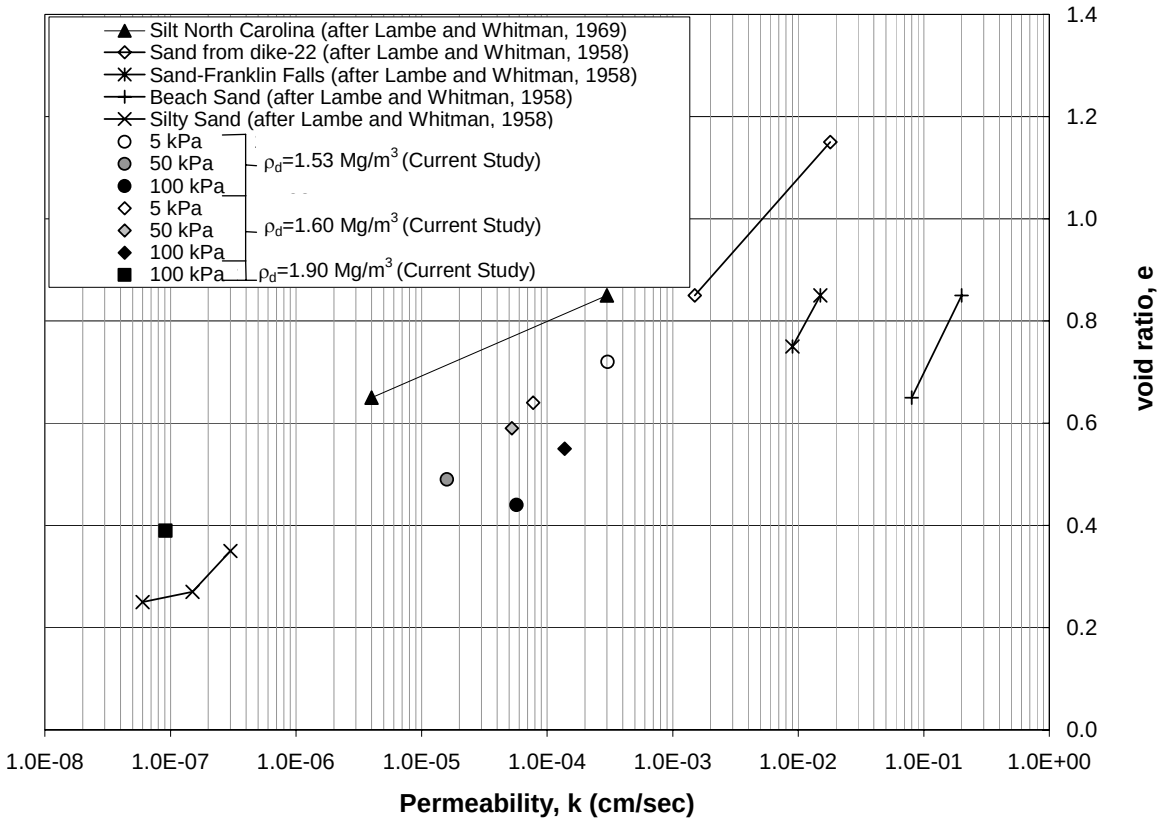

Figure 4.7.1: Permeability vs. Void Ratio (after Lambe and Whitman, 1969)

The data presented in the tables was plotted with respected to published permeability data (Lambe and Whitman, 1969). Figure 4.7.1 shows how the data generated from the current study compares to that within the literature. The figure shows the permeability versus void ratio. The void ratio used for the current study is the void ratio at which the material existed during testing, and not the as-compacted void ratio. This allows the reader to examine the effects of void ratio on permeability.

The majority of the data falls within the 10^{-4} and 10^{-5} range, indicating that the specimens compacted at that specific water content (4.7%) and dry density (1.53 Mg/m^3 and 1.60 Mg/m^3) classified in between having good and poor drainage properties (Holtz and Kovacs, 1981). One specimen, compacted at 11.7% water content and 1.90 Mg/m^3,

had a permeability ($k = 9.12 \times 10^{-8}$ cm/sec) that was significantly lower in magnitude than the other specimens tested. This decrease in magnitude was attributed to both the increase in dry density due to the higher compactive effort, and also the effects of the higher water content on the soil structure. According to the literature, permeabilities within this range classify as "practically impervious" and would be acceptable for usage in impervious sections of earth dams and dikes (Holtz and Kovacs, 1981).

4.7.3 Results Summary

This section has provided the results of pressure plate and filter paper tests for determining the matric suction, collapse potential tests, and falling head permeability tests. Experimental soil water characteristic curves were generated for as-compacted specimens and specimens that had been consolidated to an overburden pressure of 100 kPa. Results showed that the air-entry value increased with increasing as-compacted water content and overburden pressure.

Filter paper test results indicated that the matric suction for the compacted specimens was dependant on the as-compacted water content and not the dry density. Collapse potential tests results showed that the collapse potential increases with decreasing as-compacted water content. The results of falling head permeability tests showed that the permeability did appear to affected by the overburden pressure. While no strong relationship between the two was exhibited for this study, a general relationship did exist nonetheless.

5 DATA SYNTHESIS

5.1 Pressure Plate

The following section presents a synthesis of the data generated during pressure plate testing. It is used to recognize and discuss the trends exhibited through out the duration of the experimental program. Relationships between the air entry value and parameters such as the as-compacted water content, as-compacted dry density, chamber dry density (dry density of the test specimens after consolidation), and compactive effort will be examined. Concurrently, inferences regarding the soil structure and its affect on the soil water characteristic behavior will be made.

5.2 Shape of the Soil Water Characteristic Curve

The discussion regarding the shape of the soil water characteristic curve has been separated into two parts: The first part deals solely with specimens that had not been exposed to overburden pressure, and the second part is for specimens that had been consolidated to 100 kPa and tested with overburden pressures. All curves discussed within this subsection can be found in section 4.3.2.

The shape of the soil water characteristic curves followed a specific trend. Curves for specimens compacted dry of optimum showed lower air-entry values than did those for the optimum and wet of optimum specimens due to the more aggregated structures (Vanapalli et al., 1999). This produced curves that were shifted to the left of the curves generated for the optimum and wet of optimum specimens. Additionally, the slope of the curves past the air-entry value was steeper for specimens compacted dry of optimum. Stated differently, the soil water characteristic curve shifts to the right with increasing as-compacted water content, and

the slope past the air entry value became flatter with increasing as-compacted water.

The second part of this discussion regarding the shape of the soil water characteristic curve involves the effects of the overburden pressure. The air-entry value increased as a result of the overburden pressure. Since only one value of overburden pressure (100 kPa) was applied during this study, it cannot be confirmed that the air-entry value increased with increasing overburden pressure for the material, however it did indeed increase from 0 kPa to 100 kPa. The overburden pressure resulted in a remolded soil structure with smaller voids that contained a higher resistance to water flow that resulted in a curve with a higher air entry value and flatter slope past the air entry value than specimens with no overburden pressure.

5.3 Air-Entry Value

Table 5.3.1 shows the air entry values obtained from each test. Air entry values ranged from 15 to 89 kPa, and followed the trend of increasing with increasing as-compacted water content. Several interrelated factors are responsible for the occurrence of this trend. The factors include the affects of the as-compacted water content and soil structure.

To help the reader distinguish between as-compacted conditions and test conditions, specimens will be referred to as “as-compacted” and “chamber” specimens, for specimens compacted that were tested in its as-compacted state and specimens that have undergone consolidation, respectively. he affects of consolidation.

The SOILVISON software was used to determine the air-entry values for each specimen tested. Since values along the wetting curve became negative, a vertical translation of each curve was required in order to obtain a data set with all positive values that could be used in the analysis. Each curve was vertically translated by the magnitude needed to bring the most negative data point to zero. Once the translation had been made, the necessary data points (gravimetric water content and matric suction) was used in the program to obtain the curve fitting parameters a, n, m, and the air-entry suction value.

The Fredlund and Xing 1994 model was fit to the soil water characteristic curve based on the gravimetric water to determine the air-entry value for each specimen. The gravimetric curve is the default curve with the SOILVISION software, therefore was used to determine the air-entry value for each specimen. A complete list of soil water characteristic curves with the Fredlund and Xing fit are shown in the appendix.

To help the reader distinguish between as-compacted conditions and test conditions, specimens will be referred to as “as-compacted” and “chamber” specimens, for specimens compacted that were tested in its as-compacted state and specimens that have undergone consolidation, respectively.

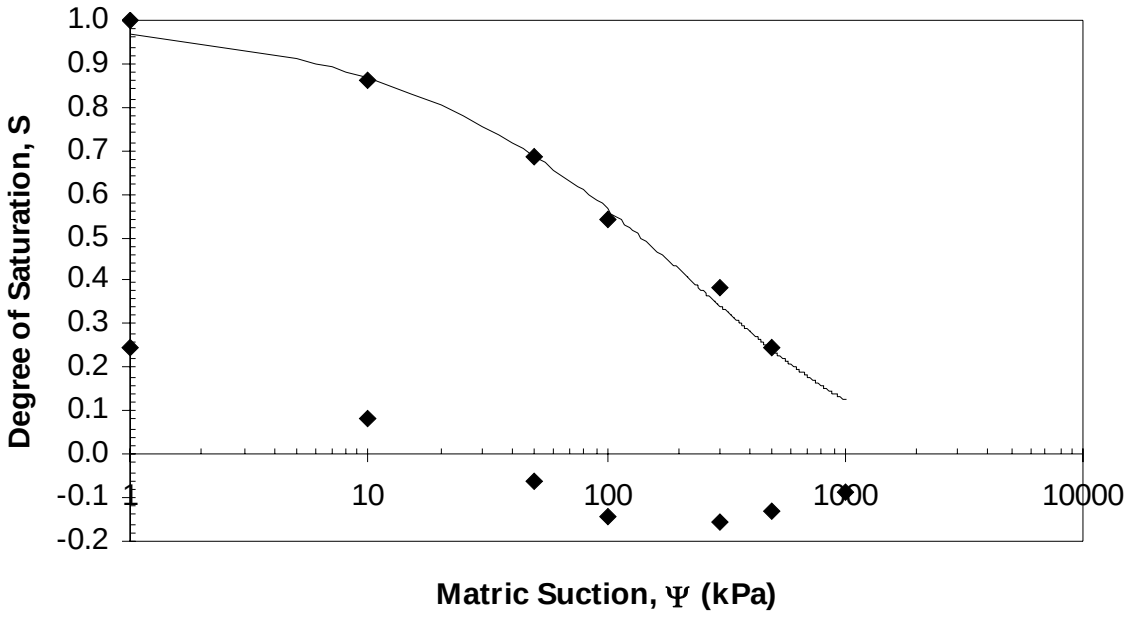

Figure 5.3.1: SWCC fit with Fredlund and Xing, 1994

Table 5.3.1: Air-Entry values for specimens tested

ρ_d (Mg/m^3) as-compacted	ρ_d (Mg/m^3) chamber	e as-compacted	e chamber	ω (%)	Ψa (kPa)
1.60	1.60	0.65	0.65	4.8	20
1.60	1.81	0.65	0.46	4.8	89
1.79	1.79	0.47	0.47	4.8	25
1.78	1.86	0.49	0.42	4.8	88
1.78	1.78	0.48	0.48	11.6	49
1.78	1.85	0.50	0.43	11.6	62

5.3.1 Influence of as-compacted water content on air-entry value

The as-compacted water content has been determined to be the most influential parameter affecting the soil water characteristic behavior of the material used throughout this study. The as-compacted water content dictates the structure (macro and micro) of the material that in turn controls the soil water characteristic behavior. Figure 5.4.1 shows the air-entry value versus chamber void ratio. This initial discussion will be limited to the affects of the as-compacted water content; therefore the open symbols will be compared as they represent specimens tested in their as-compacted state.

From the figures, it can be seen that regardless of the as-compacted dry density, the air-entry values for the three specimens fall within a generally narrow range (20, 25kPa), with one exception (49 kPa). The relationship between the air-entry value and the as-compacted water content follow the expected trend of increasing with increasing as-compacted water content (Tinjum et al., 1995; Tinjum et al., 1997; Vanapalli et al., 1999). From Figure 5.4.1 it can be seen that the air-entry values were nearly identical (20 and 25 kPa) for both specimens compacted at 4.8% as-compacted water content, and increased to 49 kPa for the specimen compacted at 11.6%. This trend is consistent with trends displayed within the literature (Tinjum et al., 1995; Tinjum et al., 1997) and can be seen within this document (Figure 2.6.1).

5.3.2 Influence of overburden pressure on air -entry value

It can be seen from Figure 5.4.1 that the air-entry value increased with increasing chamber void ratio and/or dry density (Note that the lines do not represent any functional relationship between data points. The data set has been presented with a line to remain consist with published data (Figure 2.4.11)). The influence of the overburden pressure

resulted in a change in structure of the compacted specimen from a more open aggregated structure to a more remolded structure (Tinjum et al., 1995). The effects of the overburden pressure are more prevalent for specimens compacted dry of optimum. It has been well documented within the literature that material compacted dry of optimum contain more open flocculated structures (Lambe and Whitman 1969, Holtz and Kovacs 1981) that exhibit lower resistances to water flow than their optimum and wet of optimum counterparts. The overburden pressure resulted in a change in material structure that directly influenced the soil water characteristic behavior. From both figures it can be clearly seen that as the void ratio decreases (dry density increases), the air-entry value increases. This indicates that for specimens that have been exposed to a significant overburden pressure are more resistant to water release due to the smaller void spaces that result from the change in structure.

5.4 Collapse Potential Data Reduction

5.4.1 Influence of Relative Compaction

The two most important parameters affecting the collapse potential of the specimens tested were the as-compacted water content and dry density. The as-compacted water content is the primary parameter that must be controlled when dealing with material compacted less than 100% relative compaction. The difference in soil structure has a great affect on the collapse behavior for material compacted at less than 100% relative compaction. At 100% relative compaction, the collapse potential is essentially mitigated due to the dense

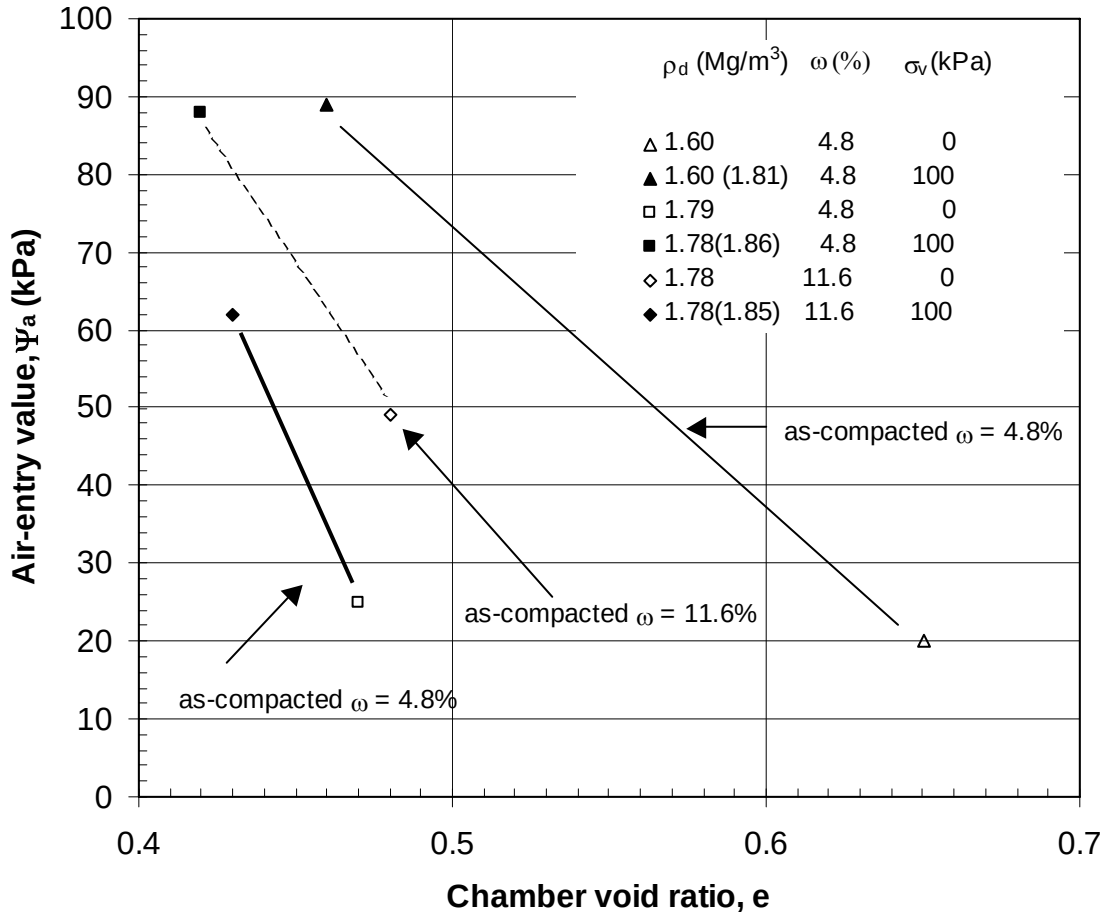

Figure 5.4.1: Air-entry value vs. Chamber void ratio

particle arrangement that results from the high degree of relative compaction (Lawton et al., 1989). Specimens compacted dry of optimum tend to display higher magnitudes of collapse due to their more open structures and gain their structurally stability from the affects of the matric suction and not from the dense particle arrangement (Barden et al., 1979). Conversely, specimens compacted wetter gain their structural stability more from a denser particle orientation and are less dependent on the matric suction (Barden et al., 1979). Investigation of Figure 5.4.2 through Figure 5.4.4 show a distinct trend of

maximum collapse increasing with decreasing as-compacted dry density (decreasing relative compaction).

It can be seen from Figure 5.4.2 that the collapse potential (volumetric strain difference between an as-compacted and inundated specimen) decreases with increasing as-compacted dry density for an as-compacted water content of 4.7%. Specimens with higher

dry densities (compacted with higher degrees of relative compaction) for a given as-compacted water content contain a denser particle arrangement with less inter-aggregate void space. The reduced quantity of void space limits the amount of particle rearrangement when overburden pressure is applied. It can be seen for specimens compacted at relative compactions of 94% and 84% and with an as-compacted water content of 4.7% that the maximum collapse occurs at an overburden pressure of 400 kPa and shows swell behavior past this critical value. Maximum collapse occurs in between 25 and 50 kPa for specimens at 81% relative compaction, and exhibits constant swell behavior past that value.

A similar trend is displayed upon examination of Figure 5.4.3 that shows specimens compacted at optimum conditions. From the figure it can be seen that the magnitude of maximum collapse decreases with increasing relative compaction.

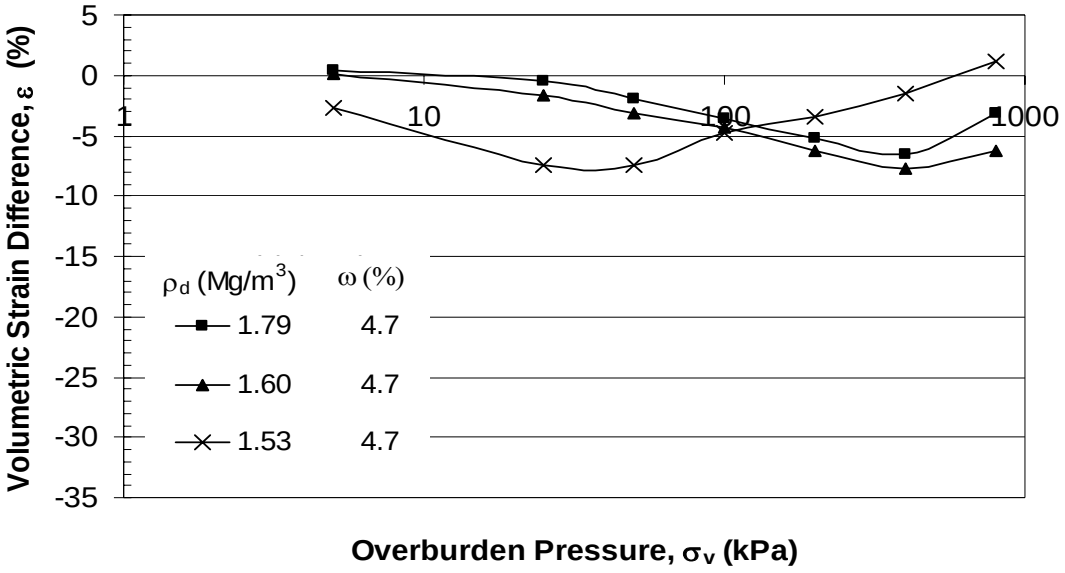

Figure 5.4.2: Collapse Potential vs. Overburden Pressure (as compacted ω = 4.7%)

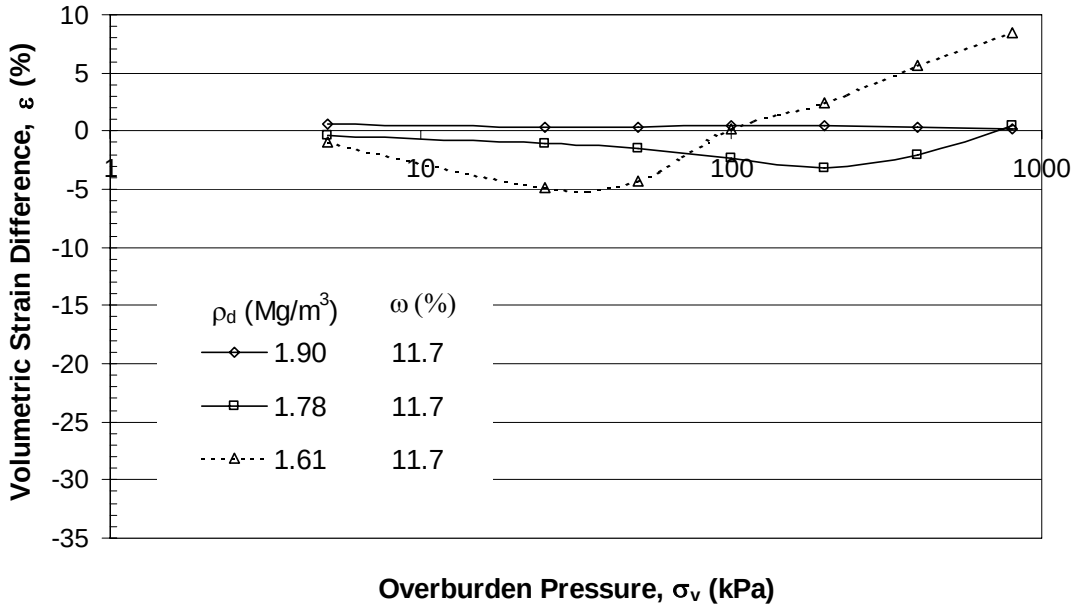

Figure 5.4.3: Collapse Potential vs. Overburden Pressure (as compacted ω = 11.7%)

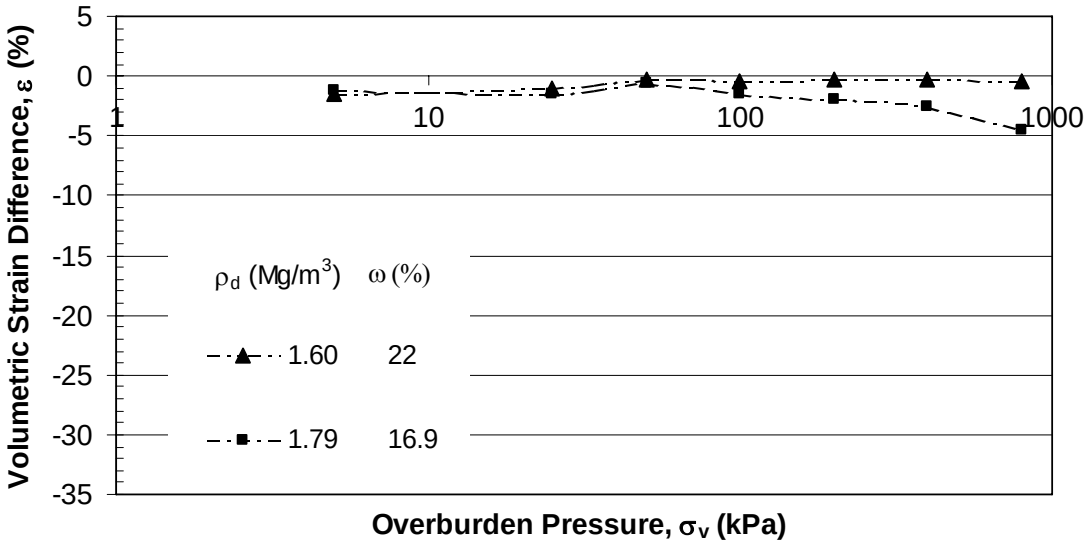

Figure 5.4.4: Collapse Potential vs. Overburden (as-compacted ω =16.9% & 22%)

A maximum collapse of approximately 5% occurs at an overburden pressure of approximately 25 kPa for the specimen compacted at 84% relative compaction. The magnitude of collapse is reduced by nearly 50% for the specimen compacted at 94%, and the overburden pressure required to achieve maximum collapse increased from 25 kPa to 200 kPa. It can be seen at 100% relative compaction (ρ_d = 1.90 Mg/m^3) collapse potential does not exist, as volume change behavior is limited to less than ± 1%. This finding is consistent with literature that states that collapse potential decreases to a negligible value at 100% relative compaction (Lawton et al., 1989; Lawton et al., 1992; Rao and Revanasiddappa, 2000).

The final figure in this section shows the collapse potential of specimens compacted wet of optimum. Generally there existed minimal changes in volume, with a maximum of 5% at 800 kPa overburden pressure, for both specimens tested due to the soil structure that resulted from compacting the specimens at wet of optimum conditions.

Additionally, the higher as-compacted water content lessened the affects of that the matric suction could have on the specimen's structurally stability (Barden et al., 1979).

5.4.2 Collapse Potential vs. As-Compacted Water Content

Figure 5.4.5 shows the influence of the as-compacted water content on the collapse potential of specimens compacted with the same dry density. The figure shows a trend of increasing collapse potential with decreasing as-compacted water content, as the specimen with the lowest as-compacted water content of 4.7% exhibited the largest magnitudes of collapse followed by the 11.7% (Re-test) and 22%, respectively.

This trend is displayed due the as-compacted water content's affects on the structure of compacted fine-grained material. Specimens compacted at lower as-compacted water contents contain more open and aggregated structures with large pore spaces. Upon loading, the particles rearrange and large magnitudes of volume change occur (Barden et al., 1973). The structure becomes less aggregated as the water content increases, that in turn reduces the open structure (primary component needed for collapse) and lessens the chance for soil structure remolding during loading.

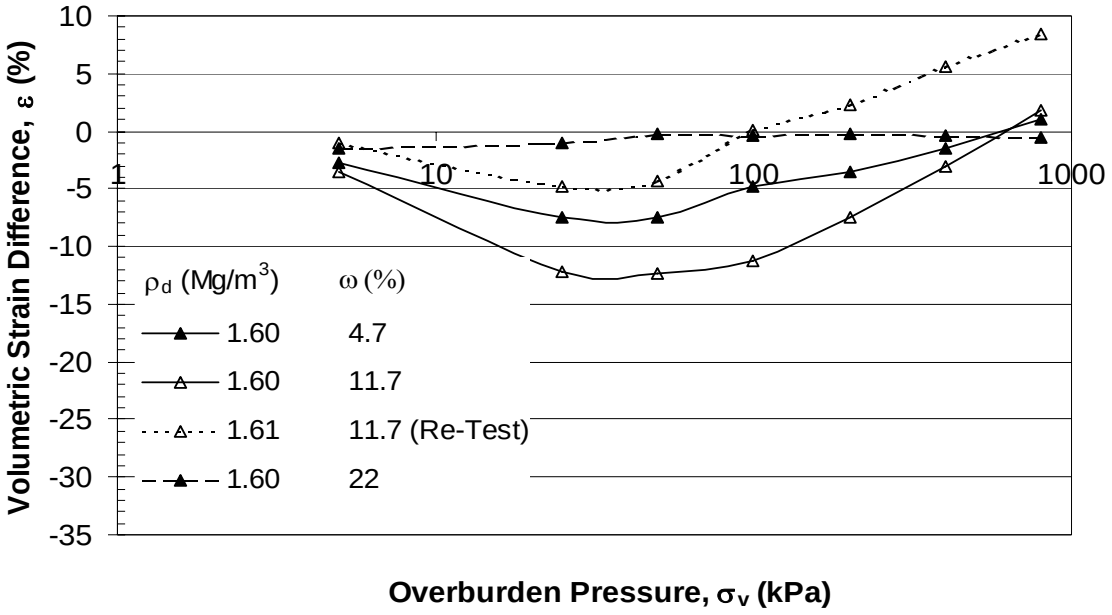

Figure 5.4.5: Influence of As-Compacted Water Content (ρ_d = 1.60 Mg/m^3)

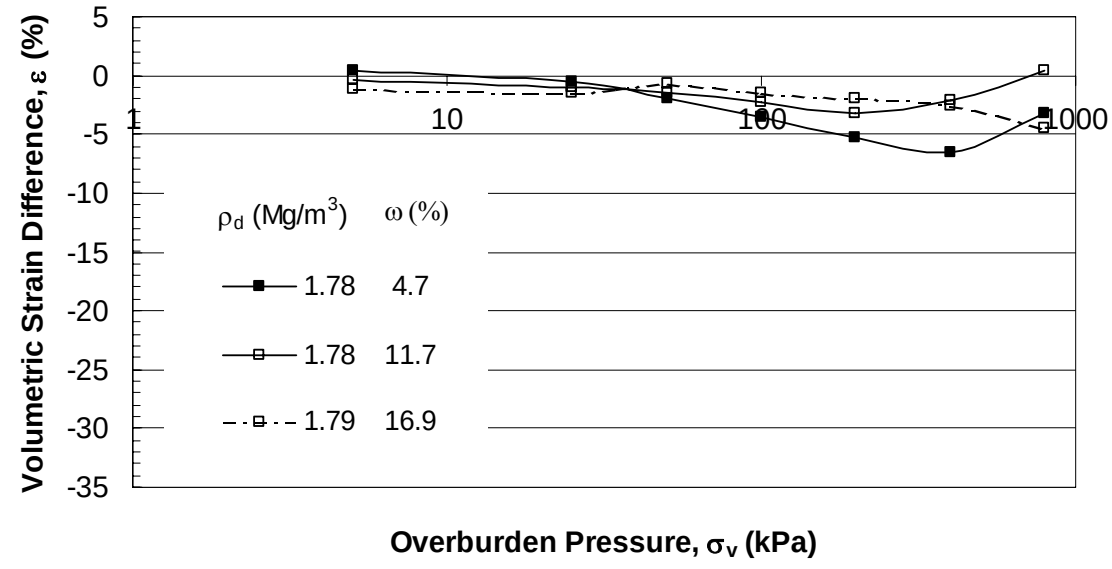

Figure 5.4.6: Influence of As-Compacted Water Content (ρ_d = 1.78 Mg/m^3)

It can be clearly seen from the figure that magnitude of collapse decreases with increasing as-compacted water content. The figure shows specimens compacted at 4.7% water content exhibiting the highest magnitude of collapse, followed by the 11.7% and 22% specimens. A similar trend is experienced for specimens compacted to dry densities of 1.78 Mg/m^3. Figure 5.4.6 shows that the collapse potential increases with decreasing as-compacted water content. It should be noted that there was a porous stone break at 800 kPa for the specimen compacted at an as-compacted water content of 4.7%, therefore the data point shown and circled is not believed to be representative of material behavior.

5.4.3 Collapse Potential and Matric Suction

Another relationship of interest is that between the collapse potential and the matric

suction. Researchers (Rao and Revanasiddappa, 2000) have shown that the collapse potential of compacted fine-grained material increases with decreasing as-compacted water content. Data was taken from the collapse potential section of this body of work and plotted in Figure 5.4.7. The maximum magnitude of collapse experienced by each specimen was plotted against the matric suction obtained by the filter paper tests. It can be seen from Figure 5.4.7 that the collapse potential increases with increasing matric suction, and for this study it generally increased with decreasing relative compaction. For a relative compaction of 84%, there existed a nearly linear relationship between the matric suction and collapse potential. A similar relationship existed for specimens compacted at a relative compaction of 94%.

The expected trend is that the matric suction decreases with increasing relative compaction (Rao and Revanasiddappa, 2000). The trend is displayed in the figure when

comparing as-compacted water contents of 4.7% and 11.7%. From the figure it can be seen that the specimens compacted at lower degrees of relative compaction (84%) exhibited collapse potentials greater than the specimens compacted at the same as-compacted water contents but with a relative compaction of 94%. This finding is expected as the soil becomes more structurally intact and exhibits a denser particle arrangement with increasing relative compaction. The denser particle arrangement resulted in the compacted specimen gaining its structural stability from the dense particle arrangement and not as a result of the matric suction acting as a binding agent between silt particles (Barden et al., 1979).

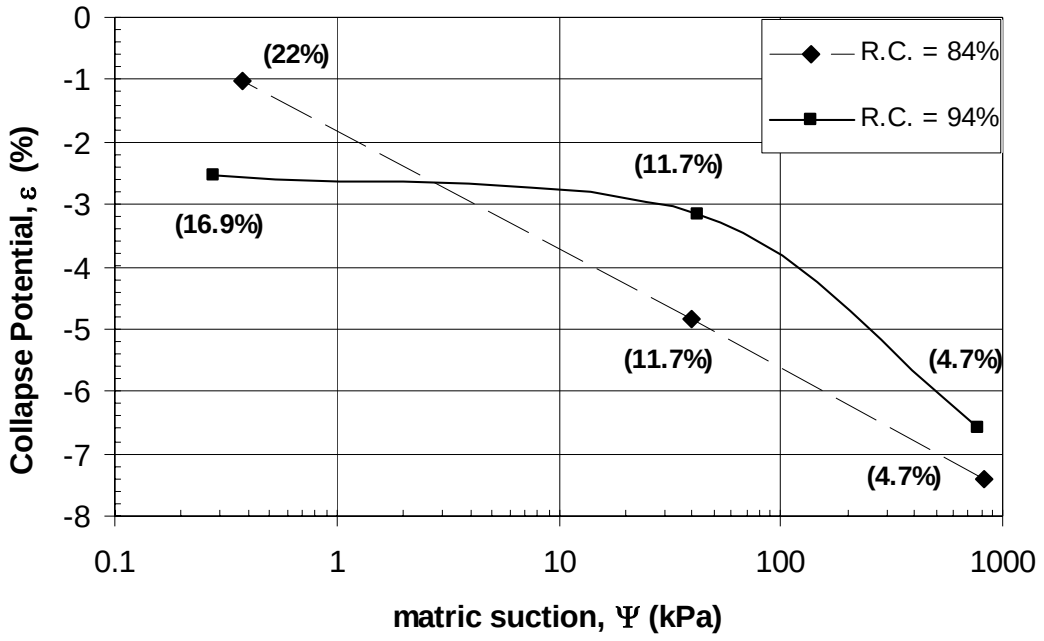

Figure 5.4.7: Collapse Potential vs. Matric Suction

The increased relative compaction results in specimens with less open structures and in denser particle arrangements and configurations. The denser particle arrangements and configurations reduce the possibility of the soil gaining its strength from the matric

suction, as with specimens compacted at lower relative compactions, and instead it gains its strength from its density and tight particle arrangement. This trend and finding is consistent with data presented in the literature (Figure 2.5.4)

Figure 5.4.8 presents the gravimetric water content versus the matric suction for compacted clay specimens tested and reported throughout the literature. Results from the current study were plotted in conjunction with the data obtained from the literature in order to visually depict if the results generated fell within the range of published data. The effects of the as-compacted water content on the matric suction can clearly be examined for all soils

and soil types shown. From the figure it can be seen that small changes in water content can cause significant changes in the matric suction of a specimen. The effects are quite pronounced for nearly each and every specimen plotted. This finding implies that careful consideration of the as-compacted water content should be exercised, as small changes in the as-compacted water content results in large changes in suction that in turn affect the engineering behavior (soil water characteristic curve, permeability, and collapse potential) of the specimens.

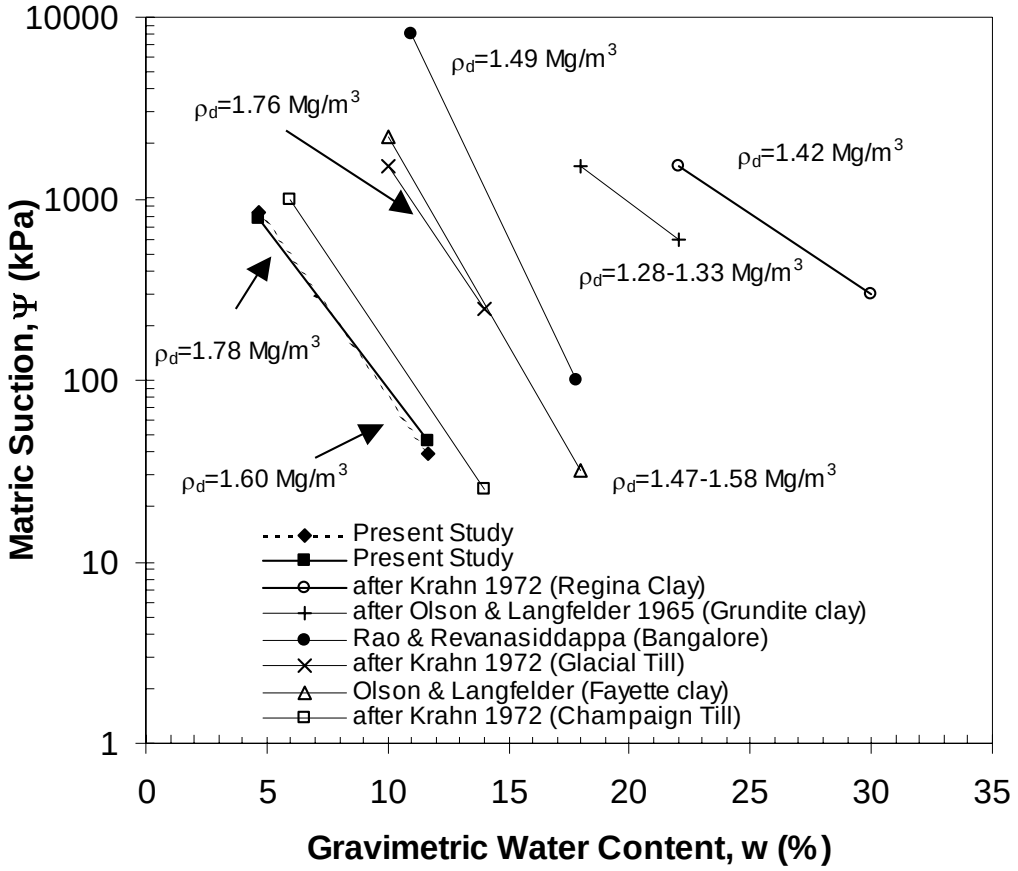

Figure 5.4.8: Matric suction versus gravimetric water content (after Rao and Revanasiddappa, 2000)

6 SUMMARY AND CONCLUSIONS

The body of work presented to the reader has presented an experimental program including the results of pressure plate, collapse potential, and filter paper tests in an attempt to gain a fundamental understanding of the unsaturated behavior of the compacted fine-grained material used for this study. Data within this study was compared to results generated by prior researchers in the area of unsaturated soil mechanics (Vanapalli et al., 1999; Tinjum et al., 1995; Rao and Revanasiddappa, 2000)

in an attempt to validate similar trends and relationships previously experienced for the soil used.

The experimental program involved testing six (6) compacted specimens in volumetric pressure plate extractors designed by previous researchers (Wang and Benson, 2004) in an attempt to generate the soil water characteristic curve (drying and wetting). Two chambers were equipped with overburden pistons that allowed for the application of an overburden pressure of 100 kPa to be applied to the specimens. Additionally, Filter Paper Tests (ASTM D 5298-03) were performed to determine the matric suction of twelve (12) specimens prepared at as-compacted dry densities ranging from 1.53 Mg/m^3 to 1.90 Mg/m^3 and as-compacted water contents ranging from 4.7% to 22%. Collapse potential tests were also conducted in an attempt to determine the volume change behavior of compacted specimens ranging in as-compacted water content from 4.7% to 22% and as-compacted dry densities from 1.53 Mg/m^3 to 1.90 Mg/m^3. Based on the results obtained from the experimental program, some general conclusions can be made:

i. Results from pressure plate tests indicated that the air-entry value of a specimen is directly influenced by the as-compacted water content. The as-compacted water content controls the soil structure of the compacted specimen that in turn dictates the soil water characteristic behavior. Specimens compacted dry of optimum had lower air-entry values than specimens tested at optimum conditions. This finding is consistent with those obtained from Tinjum et al., 1995 and Vanapalli et al., 1999. Additionally, it was determined that the air-entry value increased with as-compacted water content for specimens tested with no overburden pressure. Air- entry values of 8 kPa, 8.5 kPa, 12 kPa were determined for specimens tested under zero overburden pressure and compacted at 1.60 Mg/m^3 (ω = 4.8%), 1.79 Mg/m^3 (ω = 4.8%), and 1.78 Mg/m^3 (ω = 11.6%).

ii. Results showed that there was a significant increase in air-entry values from specimens tested with zero overburden pressure to specimens with 100 kPa overburden pressure. Air-entry values determined were 30 kPa, 35 kPa, and 36 kPa for specimens compacted at 1.60 Mg/m^3 (ω = 4.8%), 1.78 Mg/m^3 (ω = 4.8%), 1.78 Mg/m^3 (ω = 11.6%) and tested at 1.81 Mg/m^3, 1.86 Mg/m^3, and 1.85 Mg/m^3, respectively. However, the same trend of air-entry values increasing with increasing as-compacted water content was exhibited for specimens tested under 100 kPa overburden pressure. This finding is also consistent with those of Vanapalli et al., 1999, as they showed that the air-entry value is greatly influenced by the dry density during testing (generated from overburden pressure) and not the as-compacted dry density.

iii. Filter paper results showed that the matric suction of the compacted specimens appeared to be solely a function of the as-compacted water content, and not the as-compacted dry density. This finding is based on the data falling within a similar suction range for specimens compacted at similar water contents and differing dry densities.

iv. Collapse potential tests exhibited a trend of collapse potential increasing with decreasing as-compacted water content. Specimens compacted at dry of optimum conditions experienced higher magnitudes of collapse that generally occurred at lower magnitudes of overburden pressure. This finding is consistent with findings of previous researchers (Lawton et al., 1989; Lawton et al., 1992; Rao and Revanasiddappa, 2000; Rao and Revanasiddappa, 2002). Additionally, the magnitude of collapse decreased with increasing relative compaction until reaching a negligible value at 100% relative compaction. Again these finding are consistent with findings within the literature (Lawton et al., 1989; Lawton et al., 1992; Rao and Revanasiddappa, 2000; Rao and Revanasiddappa, 2002).

AA general observation and conclusion that can be made from this study deals with the as-compacted water content. The results of each test conducted for this study has indicated that the main parameter to consider when understanding the engineering behavior of the compacted specimens tested is the as-compacted water content. The as-compacted water content dictates what type of soil structure will exist after the specimen is compacted. Additionally the structure controls the soil water characteristic, and

volume change (collapse potential) behavior. From the results, it can be seen that the as-compacted water content appears to be the sole parameter to consider when determining the matric suction via filter paper methods. These general conclusions and observations can be further confirmed through the continually study of unsaturated compacted fine-grained material.

7 FUTURE RESEARCH

To further the knowledge base for future research, the author provides the following suggestions for further study:

I. The addition of an air amplifier that can be used to increase the house air supply to magnitudes large enough to cover the suction range of 0 to 1500 kPa. The air amplifier will allow for the use of high precision line regulators that allow for more precise air pressure application. It will also eliminate problems associated with the unexpected loss of the pressure supply.

II. Continued pressure plate tests using varying overburden pressures in an attempt to gain a wider coverage of material behavior under different magnitudes of loading.

III. An investigation into the Fredlund SoilVision ® software as a basis for comparison of air entry values determined from various soil types and test methods.

REFERENCES

Aung, K.K., Rahardjo, H (2001) "Relationship between porosimetry measurement and soil-water characteristic curve for an unsaturated residual soil" *Geotechnical and Geological Engineering,* 19, 401-416

Barden et al. (1973) "The Collapse Mechanism in Partly Saturated Soil" *Engineering Geology*, 7, 49-60.

Coduto, Donald (1999) Geotechnical Engineering: Principles and Practices. Upper Saddle River, NJ: Prentice Hall

Fredlund, D.G., Barbour S.L., Pham H.Q. "Evaluation of hysteresis models for predicting the boundary wetting curve", Civil Engineering Department, University of Saskatchewan

Fredlund, D.G., Xing, Anqing. (1994) "Equations for the soil-water characteristic curve", Civil Engineering Department, University of Saskatchewan. Canadian Geotechnical Journal (31) pp 521-532.

Fredlund, Delwyn. (2006) "Unsaturated Soil Mechanics in Engineering Practice" . Journal of Geotechnical and Geoenvironmental Engineering (132) pp. 286-321.

Fredlund, Murray D., Fredlund D.G., Wilson, G.W. (1997) "Prediction of the Soil-Water Characteristic Curve from Grain Size Distribution and Volume-Mass Properties" 3rd *Brazilian Symposium on Unsaturated Soils,* Rio de Janeiro.

Fredlund, Murray D., Wilson, G. Ward, Fredlund, Delwyn G. (2002) "Use of the grain-size distribution for estimation of the soil-water characteristic curve" Canadian Geotechnical Journal.

Holtz, Robert; William Kovacs (1981) An Introduction to Geotechnical Engineering. Englewood Cliffs, NJ: Prentice Hall

Lambe, William T.; Whitman, Robert V (1969) Soil Mechanics. New York: Wiley

Lawton, Evert C.; Fragaszy, Richard J.; Hardcastle, James H. (1989) Collapse of Compacted Clayey Sand. *Journal of Geotechnical Engineering*, 115 (9), 1252-1267.

Lawton, Evert C.; Fragaszy, Richard J.; Hetherington, Mark D. (1992) Review of Wetting-Induced Collapse in Compacted Soil. *Journal of Geotechnical Engineering*, 118(9), 1376-1393.

Leong, E.C., Rahardjo, H. (1997) "Review of Soil-Water Characteristic Curve Equations", Journal of Geotechnical and Geoenvironmental Engineering (123) pp. 1106-1117.

Leong, E.C., Rahardjo, H. (1997) “Permeability Functions for Unsaturated Soils”, Journal of Geotechnical and Geoenvironmental Engineering.

Li, A.G., Tham, L.G., Yue, Z.Q., Lee, C.F., Law, K.T. (2005) “Comparison of Field and Laboratory Soil-Water Characteristic Curves” Journal of Geotechnical and Geoenvironmental Engineering.

Lim, Yong Yeow; Miller, Gerald A (2004) Wetting-Induced Compression of Compacted Oklahoma Soils. *Journal of Geotechnical and Geoenvironmental Engineering,* 130(10), 1014-1023.

Miller, C.J., Yesiller, N., Yaldo, K., Merayyan, S. (2002) “Impact of Soil Type and Compaction Conditions of Soil Water Characteristic”, Journal of Geotechnical and Geoenvironmental Engineering.

Mitchell, J. K. (1976) Fabric, structure, and property relationships. Fundamentals of Soils Behavior, John Wiley & Sons, New York, N.Y.

Ng, W. W. Charles, Pang, Y.W. (2000) “Influence of Stress State on Soil-Water Characteristics and Slope Stability”, Journal of Geotechnical and Geoenvironmental Engineering.

Rao, Sudhakar M., Revanasiddappa, K. (2003) “Role of Soil Structure and Matric Suction in Collapse of a Compacted Clay Soil” Journal of Geotechnical Testing

Simms, Paul H., Yanful, Ernest K. (2004) “Estimation of Soil-Water Characteristic Curve of Clayey Till Using Measured Pore-Size Distributions” Journal of Environmental Engineering.

Skaggs, Wayne. Theory of Drainage. NCSU Department of Biological and Agricultural Engineering.

Swanson, D.A., Savci, G., Danziger, G., Mohr, R.N., Weiskopf, T. (1999) “Predicting the soil-water characteristics of mine soils”, Tailings and Mine Waste, pp. 345-349.

Tanner C.B., Elrick D.E. (1958). “Volumetric (Porous) Plate Apparatus for Moisture Hysteresis Measurements”,

Timjum, James M., Benson, Craig H., Blotz, Lisa R. (1997) “Soil-Water Characteristic Curves for Compacted Clays”, Journal of Geotechnical and Geoenvironmental Engineering.

Vanapalli, S.K., Fredlund, D.G. Pufahl, D.E. (1999) “The influence of soil structure and stress history on the soil-water characteristics of a compacted till”

Vanapalli, S.K., Pufahl, D.E., Fredlund, D.G. (1999) “Relationship between soil-water characteristic curves and the as-compacted water content versus soil for a clay till” XI Pan-American Conference on Soil Mechanics and Foundation Engineering, Brazil, 1999. August 8-12, 1999, Vol. 2, pp. 991-998.

Van Genucten, M. T. (1980) “A closed-form equation for prediction they hydraulic conductivity of unsaturated soils” Soil Science Society o America Journal, 44: 892-898.

Zhang, Limin, Chen, Que. “Predicting Bimodal Soil-Water Characteristic Curves” (2005) Journal of Geotechnical and Geoenvironmental Engineering (131) pp. 666-670.

APPENDIX A-SWCC-DATA SHEETS

Test Name: Delta 1_HD_SP_DO_4.8%_1

Date: 3/28/2006

Chamber: 1 100 kPa

ω % 4.8

Compactive Effort: ~~.1SP_.3SP~~_SP

Sample Data

M_m	111.97	g
M_{sat}	133.94	g
ω_{sat}	25.4	%
θ_{sat}	45.8	%

Sample Properties

Pre-Consolidation (Initial Conditions)

e	0.49	NA
n	0.33	NA
ρ_d	1.78	g/cm^3
γ_d	17.5	kN/m^3

Post Consolidation (Chamber Conditions)

e	0.44	NA
n	0.31	NA
ρ_d	1.83	g/cm^3
γ_d	18	kN/m^3

Date	Time (hr)	Overburden (lb)	Suction (kPa)	Outflow (cm)	Δ Outflow (cm)	Dial Gauge (in)	Notes
3/28/2006	1:00 PM	NA	NA	0.3	NA	0.0005	Equilibrium
3/29/2006	9:45 AM	NA	NA	2.7	2.4	0.0072	Equilibrium
3/29/2006	10:00 AM	0.3	10	0.9	NA	0.0000	
3/29/2006	10:00 PM	0.3	10	12.7	11.8	0.0000	
3/30/2006	10:00 AM	0.3	9	13.8	1.1	0.0000	
3/30/2006	10:00 PM	0.3	9	13.8	0	0.0000	
3/31/2006	10:00 AM	0.3	9	13.8	0	0.0000	
3/31/2006	10:00 AM	1.1 (1.4)	50	13.8	0	0.0000	
3/31/2006	10:00 PM	1.1 (1.4)	49.5	18.3	4.5	0.0000	

Date	Time (hr)	Overburden (lb)	Suction (kPa)	Outflow (cm)	Δ Outflow (cm)	Dial Gauge (in)	Notes
4/1/2006	10:00 AM	1.1 (1.4)	50	18.65	0.35	0.0000	
4/1/2006	10:00 PM	1.1 (1.4)	50	18.80	0.15	0.0000	
4/2/2006	10:00 AM	1.1 (1.4)	50	18.80	0	0.0000	
4/2/2006	10:00 PM	1.1 (1.4)	50	18.80	0	0.0000	
4/3/2006	10:00 AM	1.1 (1.4)	49	18.80	0	0.0000	
4/3/2006	10:00 PM	1.3 (2.7)	98	34.85	16.05	0.0001	
4/3/2006	10:00 PM	1.3 (2.7)	100	7.95		0.0001	Drained Value
4/4/2006	10:00 AM	1.3 (2.7)	100	12.55	4.6	0.0001	
4/4/2006	10:00 PM	1.3 (2.7)	100	13.2	0.65	0.0001	
4/5/2006	10:00 AM	1.3 (2.7)	100	13.4	0.2	0.0001	
4/5/2006	10:00 PM	1.3 (2.7)	100	13.5	0.1	0.0001	
4/6/2006	10:00 AM	5.8 (8.5)	301	13.4	-0.1	0.0001	
4/6/2006	11:15 AM	5.8 (8.5)	301	13.6	0.2	0.0001	Direct suction from chamber
4/6/2006	5:30 PM	5.8 (8.5)	300	40.85	27.25	0.0001	
4/6/2006	5:30 PM	5.8 (8.5)	300	4.55		0.0001	Drained Value
4/6/2006	10:00 PM	5.8 (8.5)	299	9.2	4.65	0.0001	
4/7/2006	10:00 AM	5.8 (8.5)	299	11.03	1.83	0.0001	
4/7/2006	10:00 PM	5.8 (8.5)	299	12.25	1.22	0.0001	
4/8/2006	10:00 AM	5.8 (8.5)	299	13.29	1.04	0.0001	
4/8/2006	10:00 PM	5.8 (8.5)	299	13.55	0.26	0.0001	
4/9/2006	10:00 AM	5.8 (8.5)	299	13.65	0.1	0.0001	
4/9/2006	10:00 AM	5.8 (8.5)	299	1.25		0.0001	Drained Value (Increased Suction)
4/9/2006	10:15 AM	5.8(14.3)	501	3.8	2.55	0.0001	
4/9/2006	10:00 PM	5.8 (14.3)	501	15	11.2	0.0001	

Date	Time (hr)	Overburden (lb)	Suction (kPa)	Outflow (cm)	Δ Outflow (cm)	Dial Gauge (in)	Notes
4/10/2006	10:00 AM	5.8 (14.3)	501	16.3	1.3	0.0001	
4/10/2006	10:00 PM	5.8 (14.3)	501	17.7	1.4	0.0001	
4/11/2006	10:00 AM	5.8 (14.3)	501	18.9	1.2	0.0001	
4/11/2006	10:00 PM	5.8 (14.3)	501	20.25	1.35	0.0001	
4/12/2006	10:00 AM	5.8 (14.3)	501	21.5	1.25	0.0001	
4/12/2006	10:00 PM	5.8 (14.3)	501	22.75	1.25	0.0001	
4/13/2006	10:00 AM	5.8 (14.3)	501	24.65	1.9	0.0001	
4/13/2006	10:000 PM	5.8 (14.3)	501	25.8	1.15	0.0001	
4/14/2006	10:00 AM	5.8 (14.3)	501	27.25	1.45	0.0001	
4/14/2006	10:00 PM	5.8 (14.3)	501	28.05	0.8	0.0001	
4/14/2006	10:00 PM	14.7 (29)	501	0.65		0.0001	Drained Value
4/14/2006	10:30 PM	14.7 (29)	1000	24.5	23.85	0.0006	
4/15/2006	10:00 AM	14.7 (29)	0	19.45	-5.05	0.0006	Chamber 1 Leak
4/19/2006	2:00 PM	14.7 (29)	0	13.90	-5.55	0.0081	
4/20/2006	10:40 AM	14.7 (29)	0	13.7	-0.2	0.0095	
4/20/2006	11:10 AM	14.7 (29)	500	13.75	0.05	0.0095	Restarted at 500 kPa
4/20/2006	1:30 PM	14.7 (29)	500	14.05	0.3	0.0095	
4/20/2006	10:00 PM	14.7 (29)	500	14.95	0.9	0.0095	
4/21/2006	10:00 AM	14.7 (29)	500	16.45	1.5	0.0095	

4/21/2006	10:00 PM	14.7 (29)	1000	22.55	6.1	0.0095	
4/22/2006	10:00 AM	14.7 (29)	1000	25.75	3.2	0.0096	
4/22/2006	10:00 PM	14.7 (29)	1000	30.05	4.3	0.0096	
4/23/2006	10:00 AM	14.7 (29)	1000	33.6	3.55	0.0096	
4/23/2006	10:00 AM	14.7 (29)	1000	20.7		0.0098	Drained Value Touched overburden piston
4/23/2006	10:00 PM	14.7 (29)	1000	25.65	4.95	0.0098	
4/24/2006	10:00 AM	14.7 (29)	1000	29.55	3.9	0.0098	
4/24/2006	10:00 PM	14.7 (29)	1000	33.35	3.8	0.0098	
4/25/2006	10:00 AM	14.7 (29)	1000	36.9	3.55	0.0098	
4/25/2006	10:00 PM	14.7 (29)	1000	40.7	3.8	0.0098	
4/25/2006	10:00 PM	14.7 (29)	1000	5.8		0.0098	
4/26/2006	10:00 AM	14.7 (29)	1000	10.6	4.8	0.0098	
4/26/2006	10:00 AM	14.7 (29)	1000	18.65		0.0098	
4/26/2006	10:00 PM	14.7 (29)	1000	22.8	4.15	0.0098	
4/27/2006	10:00 AM	14.7 (29)	1000	26.45	3.65	0.0098	
4/27/2006	10:00 PM	14.7 (29)	100	29.95	3.5	0.0098	
4/28/2006	10:00 AM	5.8 (14.3)	500	31.05	1.1	0.0114	Decreased Suction/Filled
4/28/2006	10:00 PM	5.8 (14.3)	500	49.15	18.1	0.0114	
4/28/2006	10:00 PM	5.8 (14.3)	500	50.3	1.15	0.0114	
4/28/2006	10:00 PM	5.8 (14.3)	500	39.15		0.0114	Drained
4/29/2006	10:00 AM	5.8 (14.3)	500	41.2	2.05	0.0114	
4/29/2006	10:00 PM	5.8 (14.3)	500	41.65	0.45	0.0114	
4/30/2006	10:00 AM	5.8 (14.3)	500	42.05	0.4	0.0114	
4/30/2006	10:00 PM	5.8 (14.3)	500	42.65	0.6	0.0114	
5/1/2006	10:00 AM	5.8 (14.3)	500	43.9	1.25	0.0114	
5/1/2006	10:00 PM	5.8 (14.3)	500	45.15	1.25	0.0114	
5/2/2006	10:00 AM	5.8 (14.3)	500	46.7	1.55	0.0114	
5/2/2006	6:00 PM	5.8 (14.3)	500	47.9	1.2	0.0114	
5/2/2006	6:10 PM	5.8 (8.5)	300	15.25		0.0119	Drained (Hit load Arm)

5/2/2006	10:00 PM	5.8 (8.5)	300	16.25	1	0.0119	
5/3/2006	10:00 AM	5.8 (8.5)	300	17	0.75	0.0119	
5/3/2006	10:00 PM	5.8 (8.5)	300	17.9	0.9	0.0119	
5/4/2006	10:00 AM	5.8 (8.5)	300	18.75	0.85	0.0145	Hit Load Arm
5/4/2006	10:00 AM	1.3 (2.7)	100	18.55	-0.2	0.0146	Decreased to 100 kPa
5/4/2006	6:00 PM	1.3 (2.7)	100	19.15	0.6	0.0146	Test Terminated

Test Name: Delta 2_HD_SP_DO_4.8%_2

Date: 3/28/2006

Chamber: 2

***ω* %** 4.8 **Overburden** 0 **kPa**

Compactive Effort: ~~.1SP_.3SP~~_SP **% Dry - Optimum - Wet**

Sample Data

M_m	114	g
M_{sat}	135.37	g
ω_{sat}	24.4	%
θ_{sat}	43.7	%

Sample Properties

Pre-Consolidation (Initial Conditions)

e	0.47	NA
n	0.32	NA
ρ_d	1.79	g/cm^3
γ_d	17.6	kN/m^3

Post Consolidation (Chamber Conditions)

e	NA	NA
n	NA	NA
ρ_d	NA	g/cm^3
γ_d	NA	kN/m^3

Date	Time (hr)	Overburden (lb)	Suction (kPa)	Outflow (cm)	Δ Outflow (cm)	Dial Gauge (in)	Notes
3/28/2006	1:00 PM	NA	NA	0.5	NA	NA	Equilibrium
3/29/2006	9:45 AM	NA	NA	1	2.4	NA	Equilibrium
3/29/2006	10:00 AM	NA	10	1	NA	NA	
3/29/2006	10:00 PM	NA	10	13.65	12.65	NA	
3/30/2006	10:00 AM	NA	9	18.05	4.4	NA	
3/30/2006	10:00 PM	NA	9	18.95	0.9	NA	
3/31/2006	10:00 AM	NA	9	18.95	0	NA	
3/31/2006	10:00 AM	NA	50	19.8	0.85	NA	
3/31/2006	10:00 PM	NA	49.5	39.7	19.9	NA	

Date	Time (hr)	Overburden (lb)	Suction (kPa)	Outflow (cm)	Δ Outflow (cm)	Dial Gauge (in)	Notes
3/31/2006	10:00 PM	NA	49.5	13.6	NA	NA	Drained Value
4/1/2006	10:00 AM	NA	50	23.75	10.15	NA	
4/1/2006	10:00 PM	NA	50	28.75	5	NA	
4/2/2006	10:00 AM	NA	50	30.65	1.9	NA	
4/2/2006	10:00 PM	NA	50	31.75	1.1	NA	
4/3/2006	10:00 AM	NA	49	31.95	0.2	NA	Increased to 100 kPa
4/3/2006	10:00 PM	NA	98	45.55	13.6	NA	
4/3/2006	10:00 PM	NA	100	6.6		NA	Drained Value
4/4/2006	10:00 AM	NA	100	14.4	7.8	NA	
4/4/2006	10:00 PM	NA	100	17.05	2.65	NA	
4/5/2006	10:00 AM	NA	100	18.15	1.1	NA	
4/5/2006	10:00 PM	NA	100	18.55	0.4	NA	
4/6/2006	10:00 AM	NA	301	18.15	-0.4	NA	
4/6/2006	11:15 AM	NA	301	19.5	1.35	NA	Direct suction from chamber
4/6/2006	5:30 PM	NA	300	30.95	11.45	NA	
4/6/2006	5:30 PM	NA	300	6.25		NA	Drained Value
4/6/2006	10:00 PM	NA	299	12.25	6	NA	
4/7/2006	10:00 AM	NA	299	19.35	7.1	NA	
4/7/2006	10:00 PM	NA	299	23.25	3.9	NA	
4/8/2006	10:00 AM	NA	299	25.55	2.3	NA	
4/8/2006	10:00 PM	NA	299	26.75	1.2	NA	
4/9/2006	10:00 AM	NA	299	27.7	0.95	NA	
4/9/2006	10:00 AM	NA	299	0.45		NA	Drained Value
4/9/2006	10:15 AM	NA	501	2	1.55	NA	

Date	Time (hr)	Overburden (lb)	Suction (kPa)	Outflow (cm)	Δ Outflow (cm)	Dial Gauge (in)	Notes
4/9/2006	10:00 PM	NA	501	9.45	7.45	NA	
4/10/2006	10:00 AM	NA	501	12.35	2.9	NA	
4/10/2006	10:00 PM	NA	501	15.25	2.9	NA	
4/11/2006	10:00 AM	NA	501	17.35	2.1	NA	
4/11/2006	10:00 PM	NA	501	19.25	1.9	NA	
4/12/2006	10:00 AM	NA	501	20.8	1.55	NA	
4/12/2006	10:00 PM	NA	501	22.3	1.5	NA	
4/13/2006	10:00 AM	NA	501	24.45	2.15	NA	
4/13/2006	10:00 PM	NA	501	25.9	1.45	NA	
4/14/2006	10:00 AM	NA	501	27.45	1.55	NA	
4/14/2006	10:00 PM	NA	501	28.65	1.2	NA	
4/15/2006	10:00 AM	NA	1000	17.25	-11.4	NA	Chamber 1 Leak
4/19/2006	10:30 AM	NA	0	15.50	-1.75	NA	
4/19/2006	2:00 PM	NA				NA	Filled
4/20/2006	10:40 AM	NA	500	14.75	14.75	NA	Restart
4/20/2006	11:10 AM	NA	500	14.8	0.05	NA	
4/20/2006	1:30 PM	NA	500	15.2	0.4	NA	
4/20/2006	10:00 PM	NA	500	16	0.8	NA	
4/21/2006	10:00 AM	NA	500	17.5	1.5	NA	
4/21/2006	10:00 PM	NA	1000	22.45	4.95	NA	

4/22/2006	10:00 AM	NA	1000	26.45	4	NA	
4/22/2006	10:00 PM	NA	1000	31.35	4.9	NA	
4/23/2006	10:00 AM	NA	1000	35.55	4.2	NA	
4/23/2006	10:00 AM	NA	1000	13.85		NA	Drained Value
4/23/2006	10:00 PM	NA	1000	19.05	5.2	NA	
4/24/2006	10:00 AM	NA	1000	23.35	4.3	NA	
4/24/2006	10:00 PM	NA	1000	26.45	3.1	NA	
4/25/2006	10:00 AM	NA	1000	30.05	3.6	NA	
4/25/2006	10:00 AM	NA	1000	33.8	3.75	NA	
4/25/2006	10:00 PM	NA	1000	5.5		NA	
4/26/2006	10:00 AM	NA	1000	9.95	4.45	NA	
4/26/2006	10:00 AM	NA	1000	10.01		NA	
4/26/2006	10:00 PM	NA	1000	14.25	4.24	NA	
4/27/2006	10:00 AM	NA	1000	18.15	3.9	NA	

Test Name: Delta 3_MD_.3SP_DO_11.6%_0 kPa_3

Date: 3/28/2006

Chamber: 3 **Overburden** 100 kPa

ω % 11.6 % **Dry - Optimum - Wet**

Compactive Effort: .~~1SP~~_.3SP_~~SP~~

Sample Data

M_m	119.42	g
M_{sat}	128.56	g
ω_{sat}	20.1	%
θ_{sat}	36	%

Sample Properties

Pre-Consolidation (Initial Conditions)

e	0.48	NA
n	0.32	NA
ρ_d	1.78	g/cm^3
γ_d	17.5	kN/m^3

Post Consolidation (Chamber Conditions)

e	NA	NA
n	NA	NA
ρ_d	NA	g/cm^3
γ_d	NA	kN/m^3

Date	Time (hr)	Overburden (lb)	Suction (kPa)	Outflow (cm)	Δ Outflow (cm)	Dial Gauge (in)	Notes
5/11/2006	4:00 PM	NA	NA	3.45	NA	NA	Equilibrium
5/12/2006	10:00 AM	NA	NA	13.25	9.80	NA	Equilibrium
5/12/2006	10:00 AM	NA	10	13.65	0.40	NA	Increased to 10 kPa
5/12/2006	10:00 PM	NA	10	15.35	1.70	NA	
5/13/2006	10:00 AM	NA	10	16.65	1.30	NA	
5/13/2006	10:00 PM	NA	10	17.45	0.80	NA	
5/14/2006	10:00 AM	NA	10	17.50	0.05	NA	
5/14/2006	10:00 PM	NA	10	17.80	0.30	NA	
5/15/2006	10:00 AM	NA	10	18.00	0.20	NA	Increased to 50 kPa

Date	Time (hr)	Overburden (lb)	Suction (kPa)	Outflow (cm)	Δ Outflow (cm)	Dial Gauge (in)	Notes
4/1/2006	10:00 AM	1.1 (1.4)	50	23.2	0.3	0.0232	
4/1/2006	10:00 PM	1.1 (1.4)	50	23.5	0.3	0.0235	
4/2/2006	10:00 AM	1.1 (1.4)	50	23.65	0.15	0.0235	
4/2/2006	10:00 PM	1.1 (1.4)	50	23.65	0	0.0236	
4/3/2006	10:00 AM	1.1 (1.4)	49	23.65	0	0.0236	Increased to 100 kPa
4/3/2006	10:00 PM	1.3 (2.7)	98	34.45	10.8	0.0243	
4/3/2006	10:00 PM	1.3 (2.7)	100	6.25		0.0243	Drained Value
4/4/2006	10:00 AM	1.3 (2.7)	100	8.25	2	0.0243	
4/4/2006	10:00 PM	1.3 (2.7)	100	8.8	0.55	0.0243	
4/5/2006	10:00 AM	1.3 (2.7)	100	8.95	0.15	0.0243	
4/5/2006	10:00 PM	1.3 (2.7)	100	9.05	0.1	0.0243	Increased to 300 kPa
4/6/2006	10:00 AM	5.8 (8.5)	301	8.9	-0.15	0.0243	Outflow decrease
4/6/2006	11:15 AM	5.8 (8.5)	301	9.3	0.4	0.0235	Direct suction from tank Hit load arm with tube
4/6/2006	5:30 PM	5.8 (8.5)	300	34.15	24.85	0.0235	
4/6/2006	5:30 PM	5.8 (8.5)	300	5.85		0.0235	Drained Value
4/6/2006	10:00 PM	5.8 (8.5)	299	8.15	2.3	0.0235	
4/7/2006	10:00 AM	5.8 (8.5)	299	10.35	2.2	0.0235	
4/7/2006	10:00 PM	5.8 (8.5)	299	11.4	1.05	0.0235	
4/8/2006	10:00 AM	5.8 (8.5)	299	12.05	0.65	0.0235	
4/8/2006	10:00 PM	5.8 (8.5)	299	12.6	0.55	0.0235	
4/9/2006	10:00 AM	5.8 (8.5)	299	13.15	0.55	0.0235	
4/9/2006	10:00 AM	5.8 (8.5)	299	0.1		0.0235	Drained Value
4/9/2006	10:15 AM	5.8 (14.3)	501	2.6	2.5	0.0222	Repositioned Weights
4/9/2006	10:00 PM	5.8 (14.3)	501	13.55	10.95	0.0222	

Date	Time (hr)	Overburden (lb)	Suction (kPa)	Outflow (cm)	Δ Outflow (cm)	Dial Gauge (in)	Notes
4/10/2006	10:00 AM	5.8 (14.3)	501	14.8	1.25	0.0222	
4/10/2006	10:00 PM	5.8 (14.3)	501	16.35	1.55	0.0222	
4/11/2006	10:00 AM	5.8 (14.3)	501	17.35	1	0.0222	
4/11/2006	10:00 PM	5.8 (14.3)	501	18.85	1.5	0.0235	Repositioned Weights
4/12/2006	10:00 AM	5.8 (14.3)	501	20.2	1.35	0.0235	
4/12/2006	10:00 PM	5.8 (14.3)	501	21.45	1.25	0.0235	
4/13/2006	10:00 AM	5.8 (14.3)	501	23.15	1.7	0.0235	
4/13/2006	5:00 PM	5.8 (14.3)	501	24.15	1	0.0235	
4/13/2006	5:00 PM	5.8 (14.3)	501	22.5		0.0230	Flushed Air From Line Adjusted dial gauge
4/13/2006	10:00 PM	5.8 (14.3)	501	23.25	0.75	0.0230	
4/14/2006	10:00 AM	5.8 (14.3)	501	24.25	1	0.0235	
4/14/2006	10:00 PM	5.8 (14.3)	501	24.75	0.5	0.0235	
4/15/2006	10:00 AM	5.8 (14.3)	501	16.75	-8	0.0235	
4/19/2006	10:30 AM	5.8 (14.3)	501	2.2	-14.55	0.0235	

Test Name: Epsilon 1_MD_.3SP_DO_4.8%_100 kPa_1

Date: 5/11/2006

Chamber: 1 **Overburden** 100 **kPa**

ω % 4.8 % **Dry - ~~Optimum - Wet~~**

Compactive Effort: ~~.1SP_.3SP~~_SP

Sample Data

M_m	100.67	g
M_{sat}	114.75	g
ω_{sat}	19.5	%
θ_{sat}	45	%

Sample Properties

Pre-Consolidation (Initial Conditions)

e	0.65	NA
n	0.39	NA
ρ_d	1.6	g/cm^3
γ_d	15.7	kN/m^3

Post Consolidation (Chamber Conditions)

e	0.46	NA
n	0.32	NA
ρ_d	1.81	g/cm^3
γ_d	17.8	kN/m^3

Date	Time (hr)	Overburden (lb)	Suction (kPa)	Outflow (cm)	Δ Outflow (cm)	Dial Gauge (in)	Notes
5/11/2006	4:00 PM	NA	NA	6.6	NA	0.0000	Equilibrium
5/12/2006	10:00 AM	NA	NA	10.6	4.00	0.0098	Equilibrium
5/12/2006	10:00 AM	0.3	10	10.7	0.10	0.0127	Increased to 10 kPa
5/12/2006	10:00 PM	0.3	10	23.7	13.00	0.0151	
5/13/2006	10:00 AM	0.3	10	23.8	0.10	0.0169	
5/13/2006	10:00 PM	0.3	10	23.8	0.00	0.0169	
5/14/2006	10:00 AM	0.3	10	23.8	0.00	0.0169	
5/14/2006	10:00 PM	0.3	10	23.8	0.00	0.0184	
5/15/2006	10:00 AM	0.3	10	23.8	0.00	0.0184	Increased to 50 kPa

Date	Time (hr)	Overburden (lb)	Suction (kPa)	Outflow (cm)	Δ Outflow (cm)	Dial Gauge (in)	Notes
5/15/2006	10:00 AM	1.1 (1.4)	50	23.8	0.00	0.0184	
5/15/2006	3:00 PM	1.1 (1.4)	50	26.50	2.70	0.0184	Drained Tube
5/15/2006	3:00 PM	1.1 (1.4)	50	3.85		0.0184	
5/15/2006	10:00 PM	1.1 (1.4)	50	5.95	2.10	0.0184	Tank = 176 Bar
5/16/2006	10:00 AM	1.1 (1.4)	50	6.25	0.30	0.0184	
5/16/2006	10:00 PM	1.1 (1.4)	50	6.35	0.10	0.0184	
5/17/2006	10:00 AM	1.1 (1.4)	50	6.35	0.00	0.0197	
5/17/2006	10:00 PM	1.1 (1.4)	50	6.35	0.00	0.0213	
5/18/2006	10:00 AM	1.1 (1.4)	50	6.35	0.00	0.0213	Increased to 100 kpa
5/18/2006	10:00 AM	1.3 (2.7)	100	6.35	0.00	0.0213	Switched to HP Regulator
5/18/2006	10:00 AM	1.3 (2.7)	100	6.65	0.30	0.0213	
5/18/2006	4:00 PM	1.3 (2.7)	100	22.65	16.00	0.0213	
5/18/2006	4:00 PM	1.3 (2.7)	100	5.55		0.0213	
5/18/2006	10:00 PM	1.3 (2.7)	100	12.5	6.95	0.0213	
5/19/2006	10:00 AM	1.3 (2.7)	100	15.4	2.90	0.0214	
5/19/2006	10:00 PM	1.3 (2.7)	100	15.95	0.55	0.0214	
5/20/2006	10:00 AM	1.3 (2.7)	100	16.2	0.25	0.0214	
5/20/2006	10:00 PM	1.3 (2.7)	100	16.35	0.15	0.0214	
5/21/2006	10:00 AM	1.3 (2.7)	100	16.55	0.20	0.0214	
5/21/2006	10:00 PM	1.3 (2.7)	100	16.75	0.20	0.0233	
5/22/2006	10:00 AM	1.3 (2.7)	100	16.80	0.05	0.0233	Increased to 300 kPa
5/22/2006	10:00 AM	5.8 (8.5)	300	17.20	0.40	0.0253	
5/22/2006	4:30 PM	5.8 (8.5)	300	40.25	23.05	0.0253	Drained Tube
5/22/2006	4:30 PM	5.8 (8.5)	300	4.95		0.0253	

5/31/2006	10:00 AM	5.8 (14.3)	500	40.3	1.4	.0323(.0331)	Air Flushed Hit load frame during flush
5/31/2006	10:00 PM	5.8 (14.3)	500	41.5	1.2	0.0345	
6/1/2006	10:00 AM	5.8 (14.3)	500	42.2	0.7	0.0345	Drained Tube
6/1/2006	10:10 AM	5.8 (14.3)	500	2.5		0.0345	Increased to 1000 kPa
6/1/2006	10:10 AM	14.7 (29)	1000	3.75	1.25	0.0356	Tank = 173 Bar
6/1/2006	10:00 PM	14.7 (29)	1000	17.3	13.55	0.0356	
6/2/2006	10:00 AM	14.7 (29)	1000	21.2	3.90	0.0356	
6/2/2006	10:00 PM	14.7 (29)	1000	24.75	3.55	0.0356	
6/3/2006	10:00 AM	14.7 (29)	1000	28.2	3.45	0.0356	Tank = 173 Bar
6/3/2006	10:00 PM	14.7 (29)	1000	31.35	3.15	0.0356	Air Flushed
6/3/2006	10:00 PM	14.7 (29)	1000	34.8		0.0356	
6/4/2006	10:00 AM	14.7 (29)	1000	37.9	3.10	0.0356	
6/4/2006	10:00 PM	14.7 (29)	1000	40.5	2.60	0.0356	
6/5/2006	10:00 AM	14.7 (29)	1000	43.8	3.3	0.0356	
6/5/2006	4:00 PM	14.7 (29)	1000	45.45	1.65	0.0356	Drained Tube
6/5/2006	4:00 PM	14.7 (29)	1000	7.2	NA	0.0356	
6/5/2006	10:00 PM	14.7 (29)	1000	10.75	3.55	0.0356	
6/6/2006	10:00 AM	14.7 (29)	1000	13.75	3	0.0356	
6/6/2006	9:30 PM	14.7 (29)	1000	16.4	2.65	0.0356	Air Flushed
6/6/2006	9:30 PM	14.7 (29)	1000	19		0.0356	
6/7/2006	10:00 AM	14.7 (29)	1000	22.1	3.1	0.0356	
6/7/2006	10:00 PM	14.7 (29)	1000	25.7	3.6	0.0356	
6/8/2006	10:00 AM	14.7 (29)	1000	28.75	3.05	0.0374	Hit Arm
6/8/2006	10:00 PM	14.7 (29)	1000	31.9	3.15	0.0374	
6/9/2006	10:00 AM	14.7 (29)	1000	35.1	3.2	0.0375	Decreased to 500 kPa
6/9/2006	10:00 AM	5.8 (14.3)	500	36.6	1.5	0.0375	

6/9/2006	10:00 AM	5.8 (14.3)	500	36.55	-0.05		
6/9/2006	8:00 PM	5.8 (14.3)	500	36.45	-0.1	.0405 (Hit Arm Unloading)	
6/10/2006	8:00 AM	5.8 (14.3)	500	37.7	1.25	0.0405	
6/10/2006	8:00 PM	5.8 (14.3)	500	39.45		0.0405	
6/10/2006	8:00 PM	5.8 (14.3)	500	41.35	1.9	0.0405	
6/11/2006	8:00 AM	5.8 (14.3)	500	42.5	1.15	0.0405	
6/11/2006	8:00 AM	5.8 (14.3)	500	44.05	1.55	0.0405	
6/11/2006	8:00 PM	5.8 (14.3)	500	45.25	1.2	0.0405	
6/12/2006	8:00 AM	5.8 (14.3)	500	46.6	1.35	0.0405	
6/12/2006	8:00 PM	5.8 (14.3)	500	47.5	0.9	0.0405	
6/13/2006	8:00 AM	5.8 (14.3)	500	47.5	0	0.0405	
6/13/2006	8:00 AM	5.8 (14.3)	500	47.7	0.2	.0422 (Hit arm Unloading)	Decreased to 300 kPa
6/13/2006	8:00 PM	5.8 (8.5)	300	47.65	-0.05		
6/14/2006	8:00 AM	5.8 (8.5)	300	48.3	0.65		
6/14/2006	8:00 AM	5.8 (8.5)	300	7.9	-40.4		
6/14/2006	6:00 PM	5.8 (8.5)	300	10.9	3		
6/15/2006	10:00 AM	5.8 (8.5)	300	12.2	1.3		
6/15/2006	10:00 AM	1.3 (2.7)	100	33.9	21.7		
6/15/2006	6:00 PM	1.3 (2.7)	100	34.2	0.3		
6/16/2006	10:00 AM	1.3 (2.7)	100	34.6	0.4		
6/16/2006	6:00 PM	1.3 (2.7)	100	34.8	0.2		
6/17/2006	10:30 AM	1.3 (2.7)	100	35.3	0.5		
6/17/2006	10:30 AM	1.1 (1.4)	50	29.8	-5.5		
6/17/2006	6:00 PM	1.1 (1.4)	50	24.2	-5.6		
6/18/2006	10:00 AM	1.1 (1.4)	50	12.5	-11.7		

6/18/2006	6:00 PM	1.1 (1.4)	50	41.1	28.6		
6/19/2006	11:00 AM	1.1 (1.4)	50	40.55	-0.55		
6/19/2006	6:00 PM	1.1 (1.4)	50	40.05	-0.5		
6/20/2006	10:00 AM	1.1 (1.4)	50	40	-0.05		
6/20/2006	10:00 AM	0.3	10	40	0		
6/20/2006	6:00 PM	0.3	10	39.95	-0.05		
6/21/2006	10:00 AM	0.3	10	28.65	-11.3		
6/21/2006	6:00 PM	0.3	10	22.35	-6.3		
6/22/2006	10:30 AM	0.3	10	17.95	-4.4		
6/22/2006	6:30 PM	0.3	10	17.8	-0.15		
6/23/2006	10:00 AM	0.3	10	14.9	-2.9		
6/23/2006	6:00 PM	0.3	10	17.1	2.2		
6/24/2006	10:00 AM	0.3	10	19.50	2.4		
6/24/2006	6:00 PM	0.3	10	12.20	-7.3		Re-applied 10 kPa
6/25/2006	10:00 AM	0.3	10	13.40	1.2		
6/25/2006	6:00 PM	0.3	10	15.50	2.1		
6/25/2006	6:00 PM	0.3	10	15.50	0		Decreased to 0 kPa
6/25/2006	6:00 PM	0.3	10	15.50	0		
6/26/2006	10:00 AM	0	0	14.25	-1.25		Filled
6/26/2006	6:00 PM	0	0	24.45			
6/27/2006	10:00 AM	0	0	20.75	-3.7		

6/27/2006	6:00 PM	0	0	20.10	-0.65		
6/28/2006	10:00 AM	0	0	19.25	-0.85		
6/28/2006	6:00 PM	0	0	18.75	-1.35		
6/29/2006	10:00 AM	0	0	16.50	-2.25		
6/29/2006	6:00 PM	0	0	14.70	-1.8		
6/30/2006	10:00 AM	0	0	14.45	-0.25		
6/30/2006	6:00 PM	0	0	12.60	-1.85		
7/1/2006	10:00 AM	0	0	9.90	-2.7		
7/2/2006	6:00 PM	0	0	7.40	-2.5		
7/3/2006	10:00 AM	0	0	5.70	-1.7		
7/4/2006	6:00 PM	0	0	34.50			Filled
7/5/2006	10:00 AM	0	0	32.55	-1.95		
7/5/2006	6:00 PM	0	0	32.40	-0.15		
7/6/2006	10:00 AM	0	0	28.40	-4		

Test Name: Epsilon 2_MD_.3SP_DO_4.8%_0 kPa_2

Date: 5/11/2006

Chamber: 2

ω % 4.8 **Overburden** 0 **kPa**

Compactive Effort: .1SP_~~.3SP~~_SP **% Dry - Optimum - Wet**

Sample Data

M_m	100.66	g
M_{sat}	120.19	g
ω_{sat}	25.1	%
θ_{sat}	40	%

Sample Properties

Pre-Consolidation (Initial Conditions)

e	0.65	NA
n	0.39	NA
ρ_d	1.60	g/cm^3
γ_d	15.7	kN/m^3

Post Consolidation (Chamber Conditions)

e	NA	NA
n	NA	NA
ρ_d	NA	g/cm^3
γ_d	NA	kN/m^3

Date	Time (hr)	Overburden (lb)	Suction (kPa)	Outflow (cm)	Δ Outflow (cm)	Dial Gauge (in)	Notes
5/11/2006	4:00 PM	NA	NA	2.20	NA	NA	Equilibrium
5/12/2006	10:00 AM	NA	NA	6.95	4.75	NA	Equilibrium
5/12/2006	10:00 AM	NA	10	7.20	0.25	NA	
5/12/2006	10:00 PM	NA	10	28.25	21.05	NA	
5/13/2006	10:00 AM	NA	10	31.85	3.60	NA	
5/13/2006	10:00 PM	NA	10	33.35	1.50	NA	
5/14/2006	10:00 AM	NA	10	33.60	0.25	NA	
5/14/2006	10:00 PM	NA	10	33.60	0.00	NA	
5/15/2006	10:00 AM	NA	10	33.60	0.00	NA	Increased to 50 kPa

Date	Time (hr)	Overburden (lb)	Suction (kPa)	Outflow (cm)	Δ Outflow (cm)	Dial Gauge (in)	Notes
5/15/2006	10:00 AM	NA	50	33.60	0	NA	
5/15/2006	3:00 PM	NA	50	45.20	11.6	NA	Drained Tube
5/15/2006	3:00 PM	NA	50	8.25		NA	
5/15/2006	10:00 PM	NA	50	17.00	8.75	NA	Tank 176 Bar
5/16/2006	10:00 AM	NA	50	24.95	7.95	NA	
5/16/2006	10:00 PM	NA	50	28.60	3.65	NA	
5/17/2006	10:00 AM	NA	50	30.10	1.50	NA	
5/17/2006	10:00 PM	NA	50	30.70	0.60	NA	
5/18/2006	10:00 AM	NA	50	31.15	0.45	NA	Increased to 100 kPa
5/18/2006	10:00 AM	NA	100	31.65	0.50	NA	
5/18/2006	4:00 PM	NA	100	45.60	13.95	NA	
5/18/2006	4:00 PM	NA	100	6.15		NA	
5/18/2006	10:00 PM	NA	100	14.30	8.15	NA	
5/19/2006	10:00 AM	NA	100	19.25	4.95	NA	
5/19/2006	10:00 PM	NA	100	20.55	1.30	NA	
5/20/2006	10:00 AM	NA	100	20.85	0.30	NA	
5/20/2006	10:00 PM	NA	100	20.95	0.10	NA	
5/21/2006	10:00 AM	NA	100	21.05	0.10	NA	
5/21/2006	10:00 PM	NA	100	21.20	0.15	NA	
5/22/2006	10:00 AM	NA	100	21.20	0.00	NA	Increased to 300 kPa
5/22/2006	10:00 AM	NA	300	21.50	0.30	NA	
5/22/2006	4:30 PM	NA	300	37.15	15.65	NA	Drained Tube
5/22/2006	4:30 PM	NA	300	1.50		NA	
5/22/2006	10:00 PM	NA	300	6.85	5.35	NA	

Date	Time (hr)	Overburden (lb)	Suction (kPa)	Outflow (cm)	Δ Outflow (cm)	Dial Gauge (in)	Notes
5/23/2006	10:00 AM	NA	300	10.05	3.20	NA	
5/23/2006	10:00 PM	NA	300	11.25	1.20	NA	
5/24/2006	10:00 AM	NA	300	12.05	0.80	NA	
5/24/2006	10:00 PM	NA	300	12.85	0.80	NA	
5/25/2006	10:00 AM	NA	300	13.55	0.70	NA	
5/25/2006	10:00 PM	NA	300	14.45	0.90	NA	
5/26/2006	10:00 AM	NA	300	15.35	0.90	NA	Increased to 500 kPa
5/26/2006	10:00 AM	NA	500	15.60	0.25	NA	
5/26/2006	10:00 PM	NA	500	23.20	7.60	NA	
5/27/2006	10:00 AM	NA	500	26.10	2.90	NA	
5/27/2006	10:00 PM	NA	500	27.90	1.80	NA	
5/28/2006	10:00 AM	NA	500	29.30	1.40	NA	
5/28/2006	10:00 PM	NA	500	31.00	1.70	NA	
5/29/2006	10:00 AM	NA	500	32.45	1.45	NA	Air, Flushed Tube
5/29/2006	10:00 AM	NA	500	34.95	NA	NA	
5/29/2006	10:15 AM	NA	500	34.20	NA	NA	
5/29/2006	10:00 PM	NA	500	36.15	1.95	NA	
5/30/2006	10:00 AM	NA	500	38.20	2.05	NA	
5/30/2006	10:00 PM	NA	500	39.70	1.50	NA	
5/31/2006	10:00 AM	NA	500	41.20	1.50	NA	
5/31/2006	10:00 PM	NA	500	42.70	1.50	NA	
6/1/2006	10:00 AM	NA	500	44.45	1.75	NA	
6/1/2006	10:10 AM	NA	500	3.10		NA	

6/1/2006	10:10 AM	NA	1000	3.85	0.75	NA	
6/1/2006	10:00 PM	NA	1000	14.45	10.60	NA	
6/2/2006	10:00 AM	NA	1000	20.25	5.80	NA	
6/2/2006	10:00 PM	NA	1000	24.90	4.65	NA	
6/3/2006	10:00 AM	NA	1000	29.10	4.20	NA	
6/3/2006	10:00 PM	NA	1000	32.90	3.80	NA	Air, Flushed Tube
6/3/2006	10:00 PM	NA	1000	35.20		NA	
6/4/2006	10:00 AM	NA	1000	39.40	4.20	NA	
6/4/2006	10:00 PM	NA	1000	42.95	3.55	NA	
6/5/2006	10:00 AM	NA	1000	46.75	3.80	NA	
6/5/2006	4:00 PM	NA	1000	48.60	1.85	NA	Drained Tube
6/5/2006	4:00 PM	NA	1000	2.70		NA	
6/5/2006	10:00 PM	NA	1000	6.50	3.80	NA	
6/6/2006	10:00 AM	NA	1000	9.85	3.35	NA	
6/6/2006	9:30 PM	NA	1000	12.90	3.05	NA	Air, Flushed Tube
6/6/2006	9:30 PM	NA	1000	16.25	NA	NA	
6/7/2006	10:00 AM	NA	1000	20.00	3.75	NA	
6/7/2006	10:00 PM	NA	1000	24.10	4.10	NA	
6/8/2006	10:00 AM	NA	1000	28.10	4.00	NA	
6/8/2006	10:00 PM	NA	1000	32.25	4.15	NA	
6/9/2006	10:00 AM	NA	1000	35.90	3.65	NA	
6/9/2006	10:00 AM	NA	1000	37.30	1.40	NA	
6/9/2006	10:00 AM	NA	500	37.15	-0.15	NA	
6/9/2006	8:00 PM	NA	500	38.30	1.15	NA	
6/10/2006	8:00 AM	NA	500	39.75	1.45	NA	
6/10/2006	8:00 PM	NA	500	41.25	1.50	NA	
6/11/2006	8:00 AM	NA	500	43.20	1.95	NA	

6/11/2006	8:00 PM	NA	500	44.20	1.00	NA	
6/12/2006	8:00 AM	NA	500	45.05	0.85	NA	
6/12/2006	8:00 PM	NA	500	45.70	0.65	NA	
6/13/2006	8:00 AM	NA	500	49.20	3.50	NA	Decreased to 300 kPa
6/13/2006	8:00 AM	NA	300	49.20	0.00	NA	
6/13/2006	8:00 PM	NA	300	49.10	-0.10	NA	
6/14/2006	8:00 AM	NA	300	50.50	1.40	NA	Drained Tube
6/14/2006	8:00 AM	NA	300	8.30		NA	
6/14/2006	6:00 PM	NA	300	10.60	2.30	NA	
6/15/2006	10:00 AM	NA	300	11.80	1.20	NA	
6/15/2006	10:00 AM	NA	300	31.30	19.50	NA	Decreased to 100 kPa
6/15/2006	6:00 PM	NA	100	31.70	0.40	NA	
6/16/2006	10:00 AM	NA	100	31.80	0.10	NA	
6/16/2006	6:00 PM	NA	100	32.20		NA	
6/17/2006	10:30 AM	NA	100	32.40	0.20	NA	
6/17/2006	10:30 AM	NA	50	32.70		NA	
6/17/2006	6:00 PM	NA	100	29.90	-2.80	NA	
6/18/2006	10:00 AM	NA	50	20.60	-9.30	NA	Filled
6/18/2006	10:00 AM	NA	50	42.40		NA	
6/18/2006	6:00 PM	NA	50	40.00	-2.40	NA	
6/19/2006	11:00 AM	NA	50	37.77	-2.23	NA	
6/19/2006	6:00 PM	NA	50	36.95	-0.82	NA	
6/20/2006	10:00 AM	NA	50	35.70	-1.25	NA	
6/20/2006	10:00 AM	NA	50	35.70	0.00	NA	
6/20/2006	6:00 PM	NA	50	35.50	-0.20	NA	Decreased to 10 kPa
6/21/2006	10:00 AM	NA	10	24.35	-11.15	NA	
6/21/2006	6:00 PM	NA	10	17.65	-6.70	NA	

6/22/2006	10:30 AM	NA	10	11.40	-6.25	NA	
6/22/2006	6:00 PM	NA	10	10.90	-0.50	NA	
6/23/2006	10:00 AM	NA	10	10.00	-0.90	NA	
6/23/2006	6:00 PM	NA	10	9.50	-0.50	NA	
6/24/2006	10:00 AM	NA	10	9.00	-0.50	NA	
6/24/2006	6:00 PM	NA	10	9.00	0.00	NA	
6/25/2006	10:00 AM	NA	10	8.30	-0.70	NA	
6/25/2006	6:00 PM	NA	10	6.90	-1.40	NA	
6/25/2006	6:00 PM	NA	0	6.90	0.00	NA	Decreased to 0 kPa
6/25/2006	6:00 PM	NA	0	6.80	-0.10	NA	
6/26/2006	10:00 AM	NA	0	6.25	-0.55	NA	
6/26/2006	6:00 PM	NA	0	20.40		NA	Filled
6/27/2006	10:00 AM	NA	0	14.80	-5.60	NA	Filled
6/27/2006	6:00 PM	NA	0	13.8	-1.00	NA	
6/28/2006	10:00 AM	NA	0	11.56	-2.24	NA	
6/28/2006	6:00 PM	NA	0	8.15	-3.41	NA	
6/29/2006	10:00 AM	NA	0	4.85	-3.30	NA	
6/29/2006	6:00 PM	NA	0	4.7	-0.15	NA	
6/30/2006	10:00 AM	NA	0	1.9	-2.80	NA	
6/30/2006	6:00 PM	NA	0	11.25		NA	Filled
7/1/2006	10:00 AM	NA	0	7.25	-4.00	NA	
7/2/2006	6:00 PM	NA	0	3.50	-3.75	NA	
7/3/2006	10:00 AM	NA	0	0.00	-3.50	NA	Filled
7/4/2006	6:00 PM	NA	0	33.25		NA	
7/5/2006	10:00 AM	NA	0	29.55	-3.70	NA	
7/5/2006	6:00 PM	NA	0	29.15	-0.40	NA	
7/6/2006	10:00 AM	NA	0	22.25	-6.90	NA	

Test Name: Epsilon 3_MD_.3SP_DO_11.6%_0 kPa_3

Date: 3/28/2006

Chamber: 3 **Overburden** 100 kPa

ω % 11.6 % **Dry - Optimum - Wet**

Compactive Effort: .~~1SP~~_.3SP_~~SP~~

Sample Data

M_m	119.42	g
M_{sat}	128.56	g
ω_{sat}	20.1	%
θ_{sat}	36	%

Sample Properties

Pre-Consolidation (Initial Conditions)

e	0.48	NA
n	0.32	NA
ρ_d	1.78	g/cm^3
γ_d	17.5	kN/m^3

Post Consolidation (Chamber Conditions)

e	NA	NA
n	NA	NA
ρ_d	NA	g/cm^3
γ_d	NA	kN/m^3

Date	Time (hr)	Overburden (lb)	Suction (kPa)	Outflow (cm)	Δ Outflow (cm)	Dial Gauge (in)	Notes
5/11/2006	4:00 PM	NA	NA	3.45	NA	NA	Equilibrium
5/12/2006	10:00 AM	NA	NA	13.25	9.80	NA	Equilibrium
5/12/2006	10:00 AM	NA	10	13.65	0.40	NA	Increased to 10 kPa
5/12/2006	10:00 PM	NA	10	15.35	1.70	NA	
5/13/2006	10:00 AM	NA	10	16.65	1.30	NA	
5/13/2006	10:00 PM	NA	10	17.45	0.80	NA	
5/14/2006	10:00 AM	NA	10	17.50	0.05	NA	
5/14/2006	10:00 PM	NA	10	17.80	0.30	NA	
5/15/2006	10:00 AM	NA	10	18.00	0.20	NA	Increased to 50 kPa

Date	Time (hr)	Overburden (lb)	Suction (kPa)	Outflow (cm)	Δ Outflow (cm)	Dial Gauge (in)	Notes
5/15/2006	10:00 AM	NA	50	19.15	1.15	NA	
5/15/2006	3:00 PM	NA	50	32.00	12.85	NA	Drained Tube
5/15/2006	3:00 PM	NA	50	4.95		NA	
5/15/2006	10:00 PM	NA	50	12.20	7.25	NA	Tank=176 Bar
5/16/2006	10:00 AM	NA	50	16.90	4.70	NA	
5/16/2006	10:00 PM	NA	50	18.55	1.65	NA	
5/17/2006	10:00 AM	NA	50	19.45	0.90	NA	
5/17/2006	10:00 PM	NA	50	20.25	0.80	NA	
5/18/2006	10:00 AM	NA	50	20.25	0.00	NA	Increased to 100 kPa
5/18/2006	10:00 AM	NA	100	21.20	0.95	NA	
5/18/2006	4:00 PM	NA	100	24.30	3.10	NA	Drained Tube
5/18/2006	4:00 PM	NA	100	5.75		NA	
5/18/2006	10:00 PM	NA	100	7.75	2.00	NA	
5/19/2006	10:00 AM	NA	100	11.10	3.35	NA	
5/19/2006	10:00 PM	NA	100	13.25	2.15	NA	
5/20/2006	10:00 AM	NA	100	14.60	1.35	NA	
5/20/2006	10:00 PM	NA	100	15.45	0.85	NA	
5/21/2006	10:00 AM	NA	100	16.40	0.95	NA	
5/21/2006	10:00 PM	NA	100	16.95	0.55	NA	
5/22/2006	10:00 AM	NA	100	17.45	0.50	NA	Increased to 300 kPa
5/22/2006	10:00 AM	NA	300	18.20	0.75	NA	
5/22/2006	4:30 PM	NA	300	21.35	3.15	NA	Drained Tube
5/22/2006	4:30 PM	NA	300	7.10		NA	
5/22/2006	10:00 PM	NA	300	9.15	2.05	NA	

Date	Time (hr)	Overburden (lb)	Suction (kPa)	Outflow (cm)	Δ Outflow (cm)	Dial Gauge (in)	Notes
5/23/2006	10:00 AM	NA	300	12.80	3.65	NA	
5/23/2006	10:00 PM	NA	300	15.45	2.65	NA	
5/24/2006	10:00 AM	NA	300	17.65	2.20	NA	
5/24/2006	10:00 PM	NA	300	19.25	1.60	NA	
5/25/2006	10:00 AM	NA	300	20.60	1.35	NA	
5/25/2006	10:00 PM	NA	300	21.85	1.25	NA	
5/26/2006	10:00 AM	NA	300	22.35	0.50	NA	
5/26/2006	10:00 AM	NA	500	22.60	0.25	NA	
5/26/2006	10:00 PM	NA	500	25.60	3.00	NA	
5/27/2006	10:00 AM	NA	500	28.30	2.70	NA	
5/27/2006	10:00 PM	NA	500	30.20	1.90	NA	
5/28/2006	10:00 AM	NA	500	32.75	2.55	NA	
5/28/2006	10:00 PM	NA	500	34.70	1.95	NA	
5/29/2006	10:00 AM	NA	500	36.55	1.85	NA	
5/29/2006	10:00 PM	NA	500	38.30	1.75	NA	
5/30/2006	10:00 AM	NA	500	39.90	1.60	NA	
5/30/2006	10:00 PM	NA	500	41.60	1.70	NA	
5/31/2006	10:00 AM	NA	500	42.95	1.35	NA	
5/31/2006	10:15 AM	NA	500	25.90	NA	NA	
5/31/2006	10:00 PM	NA	500	27.05	1.15	NA	
6/1/2006	10:00 AM	NA	500	27.85	0.80	NA	
6/1/2006	10:10 AM	NA	500	2.45	NA	NA	
6/1/2006	10:10 AM	NA	1000	2.80	0.35	NA	

6/1/2006	12:00 PM	NA	1000	5.40	2.60	NA	
6/2/2006	10:00 PM	NA	1000	8.90	3.50	NA	
6/2/2006	10:00 AM	NA	1000	13.00	4.10	NA	
6/2/2006	10:00 PM	NA	1000	17.60	4.60	NA	
6/3/2006	10:00 AM	NA	1000	21.90	4.30	NA	
6/3/2006	10:00 PM	NA	1000	25.90	4.00	NA	Chamber Flushed
6/3/2006	10:00 PM	NA	1000	28.65		NA	
6/4/2006	10:00 AM	NA	1000	32.65	4.00	NA	
6/4/2006	10:00 PM	NA	1000	36.00	3.35	NA	
6/5/2006	10:00 AM	NA	1000	39.75	3.75	NA	
6/5/2006	4:00 PM	NA	1000	41.65	1.90	NA	
6/5/2006	4:00 PM	NA	1000	3.30		NA	
6/5/2006	10:00 PM	NA	1000	5.90	2.60	NA	
6/6/2006	10:00 AM	NA	1000	9.10	3.20	NA	
6/6/2006	9:30 PM	NA	1000	12.00	2.90	NA	
6/6/2006	9:30 PM	NA	1000	16.80	NA	NA	Chamber Flushed
6/7/2006	10:00 AM	NA	1000	19.65	2.85	NA	
6/7/2006	10:00 PM	NA	1000	23.10	3.45	NA	
6/8/2006	10:00 AM	NA	1000	25.50	2.40	NA	
6/8/2006	10:00 PM	NA	1000	29.60	4.10	NA	
6/9/2006	10:00 AM	NA	1000	32.90	3.30	NA	
6/9/2006	10:00 AM	NA	1000	36.45	3.55	NA	
6/9/2006	10:00 AM	NA	500	36.40	-0.05	NA	
6/9/2006	8:00 PM	NA	500	37.30	0.90	NA	
6/10/2006	8:00 AM	NA	500	38.50	1.20	NA	
6/10/2006	8:00 PM	NA	500	40.25	1.75	NA	
6/11/2006	8:00 AM	NA	500	41.30	1.05	NA	

6/11/2006	8:00 PM	NA	500	42.15	0.85	NA	
6/12/2006	8:00 AM	NA	500	44.05	1.90	NA	
6/12/2006	8:00 PM	NA	500	45.00	0.95	NA	
6/13/2006	8:00 AM	NA	500	46.60	1.60	NA	Decreased to 300 kPa
6/13/2006	8:00 AM	NA	300	46.60	0.00	NA	
6/13/2006	8:00 PM	NA	300	46.90	0.30	NA	
6/14/2006	8:00 AM	NA	300	47.15	0.25	NA	Drained Tube
6/14/2006	8:00 AM	NA	300	3.40		NA	
6/14/2006	6:00 PM	NA	300	4.20	0.80	NA	
6/15/2006	10:00 AM	NA	300	5.00	0.80	NA	
6/15/2006	10:00 AM	NA	300	32.60		NA	Decreased to 100 kPa,filled
6/15/2006	6:00 PM	NA	100	31.40	-1.20	NA	
6/16/2006	10:00 AM	NA	100	30.60	-0.80	NA	
6/16/2006	6:00 PM	NA	100	30.80	0.20	NA	
6/17/2006	10:30 AM	NA	100	24.50	-6.30	NA	
6/17/2006	10:30 AM	NA	50	23.70	-0.80	NA	
6/17/2006	6:00 PM	NA	50	20.10	-3.60	NA	
6/18/2006	10:00 AM	NA	50	41.50	21.40	NA	Filled
6/18/2006	10:00 AM	NA	50	40.40	-1.10	NA	
6/18/2006	6:00 PM	NA	50	38.30	-2.10	NA	
6/19/2006	11:00 AM	NA	50	37.25	-1.05	NA	
6/19/2006	6:00 PM	NA	50	35.50	-1.75	NA	
6/20/2006	10:00 AM	NA	50	35.60	0.10	NA	
6/20/2006	10:00 AM	NA	50	35.50	-0.10	NA	
6/20/2006	6:00 PM	NA	50	27.65	-7.85	NA	Decreased to 10 kPa
6/21/2006	10:00 AM	NA	10	22.3	-5.35	NA	
6/21/2006	6:00 PM	NA	10	15.60	-6.70	NA	

6/22/2006	10:30 AM	NA	10	14.90	-0.70	NA	
6/22/2006	6:00 PM	NA	10	13.70	-1.20	NA	
6/23/2006	10:00 AM	NA	10	13.00	-0.70	NA	
6/23/2006	6:00 PM	NA	10	8.50	-4.50	NA	
6/24/2006	10:00 AM	NA	10	5.00	-3.50	NA	Re-applied 10 kPa
6/24/2006	6:00 PM	NA	10	7.45	2.45	NA	
6/25/2006	10:00 AM	NA	10	8.35	0.90	NA	
6/25/2006	6:00 PM	NA	10	9.65	1.30	NA	
6/25/2006	6:00 PM	NA	0	9.45	-0.20	NA	Decreased to 0 kPa
6/25/2006	6:00 PM	NA	0	7.95	-1.50	NA	
6/26/2006	10:00 AM	NA	0	26.10	18.15	NA	Filled
6/26/2006	6:00 PM	NA	0	20.20	-5.90	NA	
6/27/2006	10:00 AM	NA	0	19.00	-1.20	NA	Filled
6/27/2006	6:00 PM	NA	0	17.25	-1.75	NA	
6/28/2006	10:00 AM	NA	0	15.25	-3.75	NA	
6/28/2006	6:00 PM	NA	0	12.45	-2.80	NA	
6/29/2006	10:00 AM	NA	0	8.75	-3.70	NA	
6/29/2006	6:00 PM	NA	0	8.60	-0.15	NA	
6/30/2006	10:00 AM	NA	0	8.00	-0.60	NA	
6/30/2006	6:00 PM	NA	0	1.70	-6.30	NA	
7/1/2006	10:00 AM	NA	0	0.50	-1.20	NA	
7/2/2006	6:00 PM	NA	0	0.00	-0.50	NA	
7/3/2006	10:00 AM	NA	0	40.60	40.60	NA	Filled
7/4/2006	6:00 PM	NA	0	38.25	-2.35	NA	
7/5/2006	10:00 AM	NA	0	37.45	-0.80	NA	
7/5/2006	6:00 PM	NA	0	37.10	-0.35	NA	
7/6/2006	10:00 AM	NA	0	31.15	-5.95	NA	

Chamber ID	1	
Volume	58.26	cm^3
Diameter	0.39	cm
S	1	
ω_{sat}	0.169	
θ_{sat}	0.31434	
ρ_d	1.86	g/cm^3

ψ (kPa)	Cap. Reading (cm)	Outflow (cm^3)	θ	ω	S
0.1	0	0	0.314	0.169	1
10	6.12	0.73	0.302	0.162	0.960
50	5	0.60	0.292	0.157	0.927
100	21.6	2.58	0.247	0.133	0.787
300	35.55	4.25	0.174	0.094	0.555
500	26.8	3.20	0.119	0.064	0.380
1000	44.35	5.30	0.028	0.015	0.091

HD_SP_DO_4.8% (Delta 1)

Chamber ID	2	
Volume	60.14	cm^3
Diameter	0.39	cm
S	1	
ω_{sat}	0.24	
θ_{sat}	0.4296	
ρ_d	1.79	g/cm^3

ψ (kPa)	Cap. Reading (cm)	Outflow (cm^3)	θ	ω	S
0.01	0	0	0.430	0.24	1
10	17.95	2.14	0.394	0.220	0.917
50	39.10	4.67	0.316	0.177	0.736
100	25.55	3.05	0.266	0.148	0.618
300	33.85	4.04	0.198	0.111	0.462
500	31.10	3.72	0.137	0.076	0.318
1000	53.89	6.44	0.029	0.016	0.069

HD_SP_DO_4.8% (Delta 2)

Chamber ID	3	
Volume	57.92	cm^3
Diameter	0.39	cm
S	1	
ω_{sat}	0.25	
θ_{sat}	0.458	
ρ_d	1.83	g/cm^3

ψ (kPa)	Cap. Reading (cm)	Outflow (cm^3)	θ	ω	S
0.01	0	0	0.458	0.25	1
10	13.27	1.59	0.431	0.235	0.940
50	6.25	0.75	0.418	0.228	0.912
100	13.6	1.62	0.390	0.213	0.851
300	32.4	3.87	0.323	0.176	0.705
500	23.8	2.84	0.274	0.150	0.598

HD_SP_DO_11.6% (Delta 3)

Chamber ID	1	
Volume	53.11	cm^3
Diameter	0.39	cm
S	1	
ω_{sat}	0.193	
θ_{sat}	0.35	
ρ_d	1.81	g/cm^3

ψ (kPa)	Cap. Reading (cm)	Outflow (cm^3)	θ	ω	S
1	0	0	0.350	0.193	1
10	6.6	0.79	0.335	0.185	0.958
50	5.2	0.62	0.323	0.179	0.924
100	27.3	3.26	0.262	0.145	0.749
300	34.00	4.06	0.186	0.103	0.530
500	25.20	3.01	0.129	0.071	0.368
1000	64.80	7.74	-0.017	-0.009	-0.048
500	10.85	1.30	-0.041	-0.023	-0.118
300	4.9	0.59	-0.052	-0.029	-0.149
100	1.4	0.17	-0.055	-0.031	-0.158
50	-23.9	-2.86	-0.002	-0.001	-0.005
10	-24.5	-2.93	0.053	0.030	0.153
1	-26.1	-3.12	0.112	0.062	0.320

MD_.3SP_DO_4.8%_100 kPa (Epsilon 1)

Chamber ID	2	
Volume	60.14	cm^3
Diameter	0.39	cm
S	1	
ω_{sat}	0.244	
θ_{sat}	0.39	
ρ_d	1.6	g/cm^3

ψ (kPa)	Cap. Reading (cm)	Outflow (cm^3)	θ	ω	S
1	0	0	0.390	0.244	1
10	26.65	3.18	0.337	0.211	0.864
50	34.50	4.12	0.269	0.168	0.689
100	29.50	3.52	0.210	0.131	0.538
300	29.80	3.56	0.151	0.094	0.387
500	27.35	3.27	0.096	0.060	0.247
1000	65.25	7.79	-0.033	-0.021	-0.085
500	8.55	1.02	-0.050	-0.031	-0.129
300	4.80	0.57	-0.060	-0.037	-0.153
100	-2.10	-0.25	-0.056	-0.035	-0.142
50	-16.20	-1.94	-0.023	-0.015	-0.060
10	-28.6	-3.42	0.033	0.021	0.086
1	-32.05	-3.83	0.097	0.061	0.249

MD_.3SP_DO_4.8% (Epsilon 2)

Chamber ID	3	
Volume	60.14	cm^3
Diameter	0.39	cm
S	1	
ω_{sat}	0.180	
θ_{sat}	0.32	
ρ_d	1.78	g/cm^3

ψ (kPa)	Cap. Reading (cm)	Outflow (cm^3)	θ	ω	S
1	0	0	0.32	0.180	1
10	4.75	0.57	0.311	0.174	0.971
50	29.29	3.50	0.252	0.142	0.789
100	15.75	1.88	0.221	0.124	0.691
300	19.15	2.29	0.183	0.103	0.572
500	22.55	2.69	0.138	0.078	0.432
1000	61.25	7.32	0.017	0.009	0.052
500	9.3	1.11	-0.002	-0.001	-0.006
300	2.15	0.26	-0.006	-0.003	-0.019
100	-8.1	-0.97	0.010	0.006	0.031
50	-17.45	-2.08	0.045	0.025	0.139
10	-18	-2.15	0.080	0.045	0.251
1	-37.25	-4.45	0.154	0.087	0.482

MD_.3SP_DO_11.6%_0 kPa (Epsilon 3)

APPENDIX B-SWCC – Fit to Fredlund and Xing

Appendix B1-Volumetric Water Content

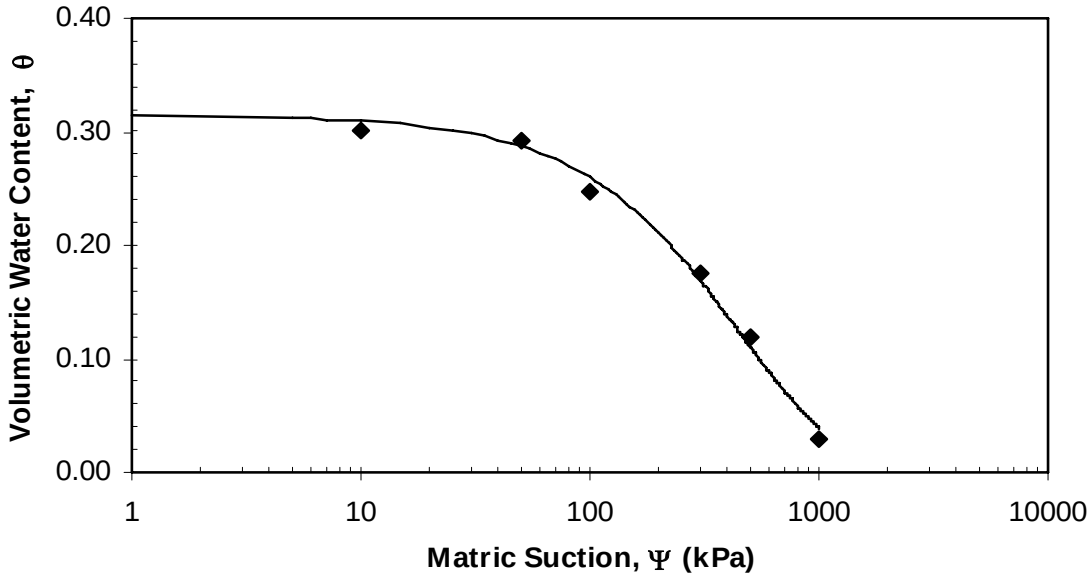

HD_SP_DO_4.8% (Delta 1)

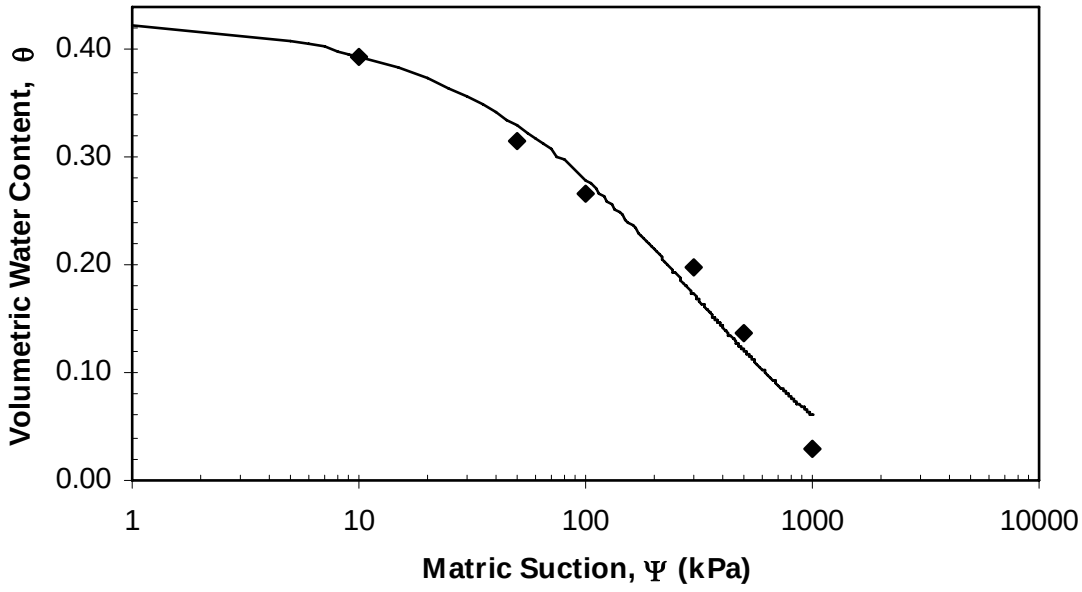

HD_SP_DO_4.8% (Delta 2)

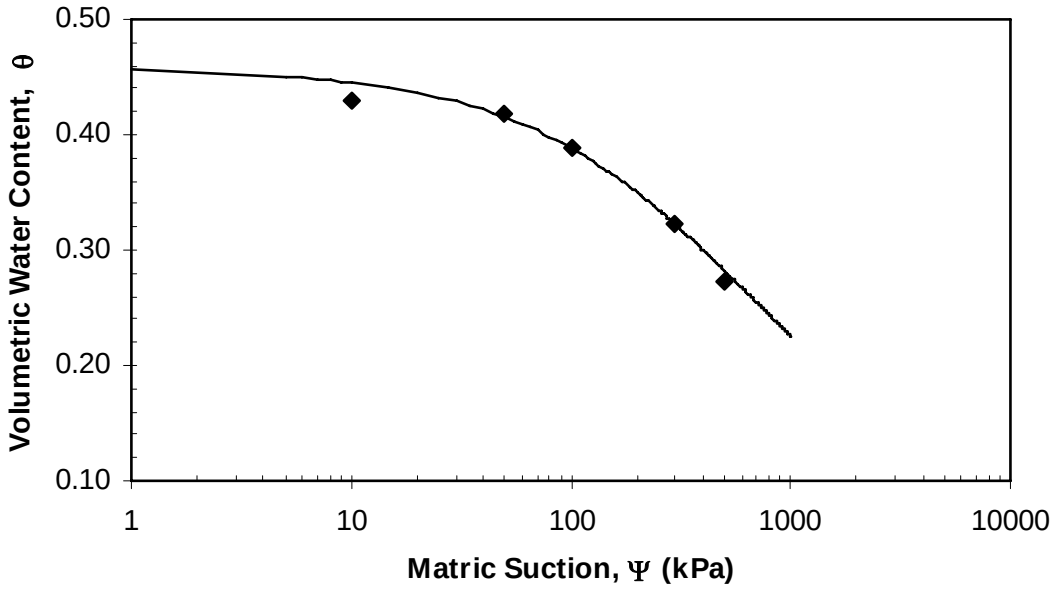

HD_SP_DO_11.6% (Delta 3)

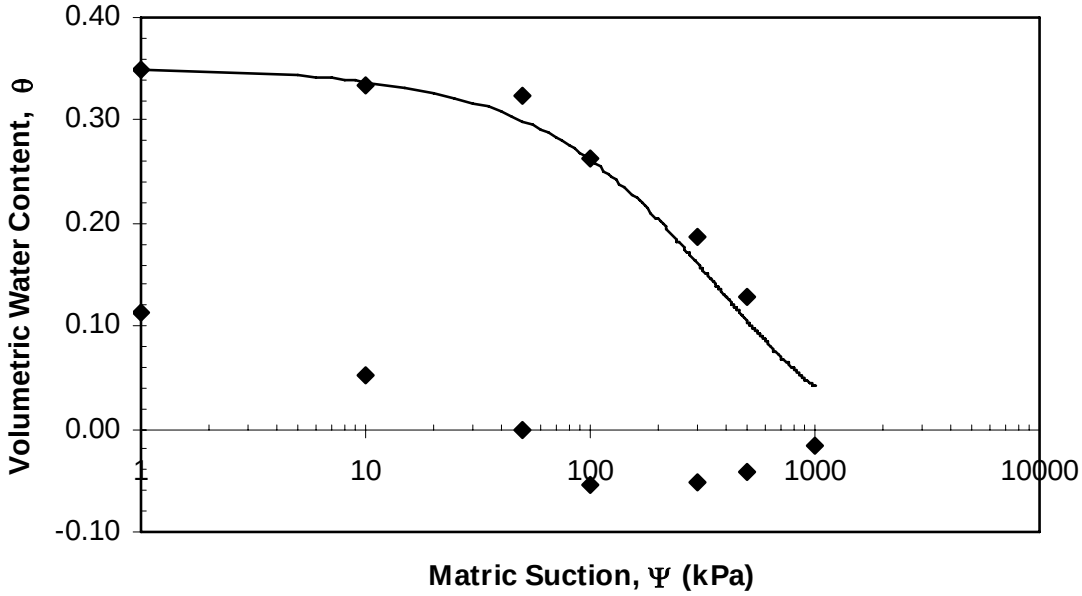

MD_.3SP_DO_4.8%_100 kPa (Epsilon 1)

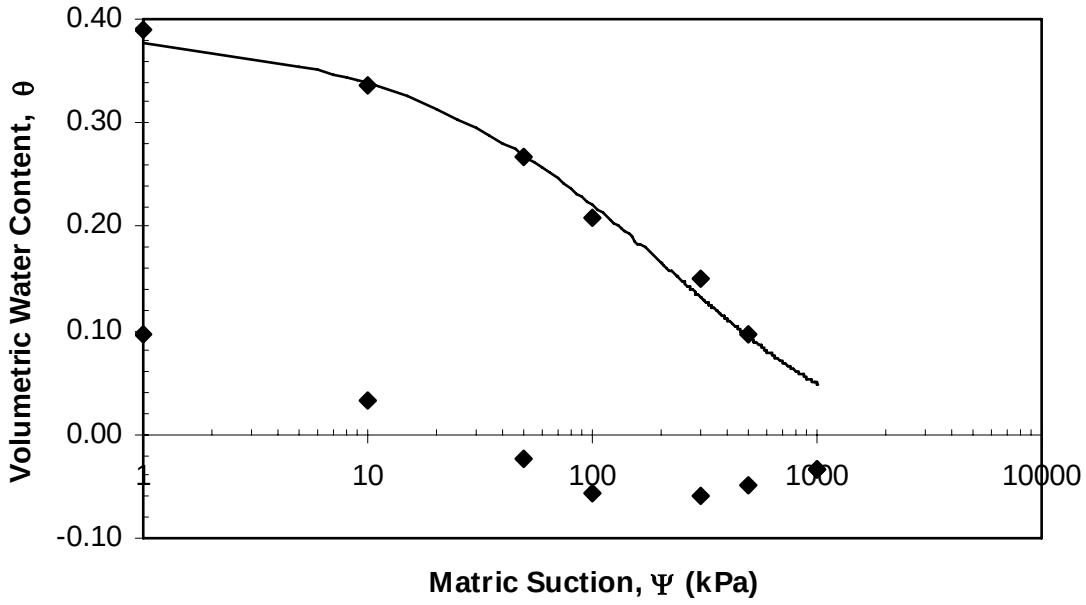

MD_.3SP_DO_4.8% (Epsilon 2)

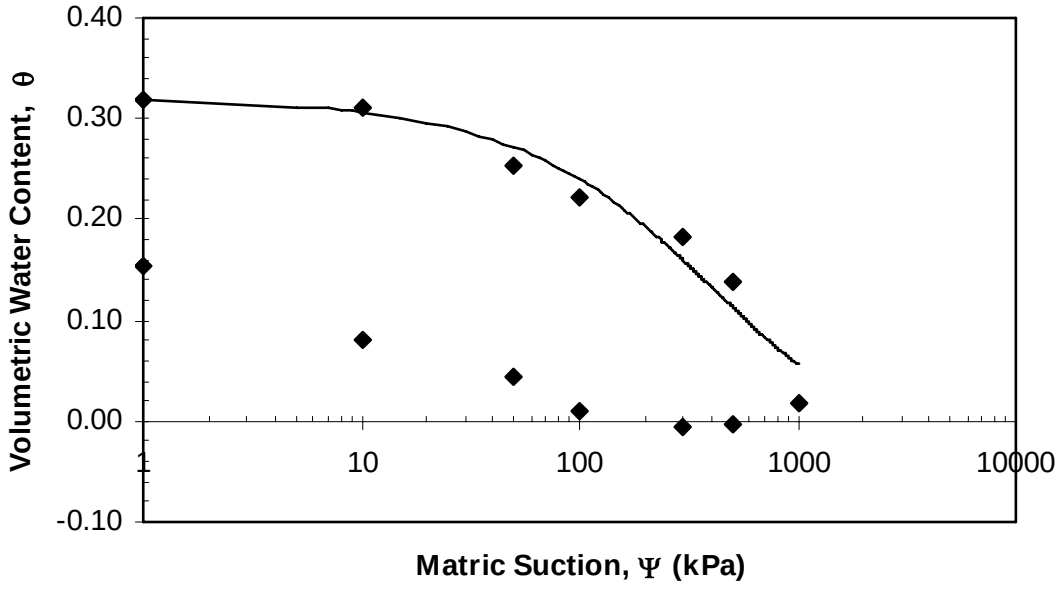

MD_.3SP_DO_11.6%_0 kPa (Epsilon 3)

Appendix B2-SWCC Gravimetric Water Content

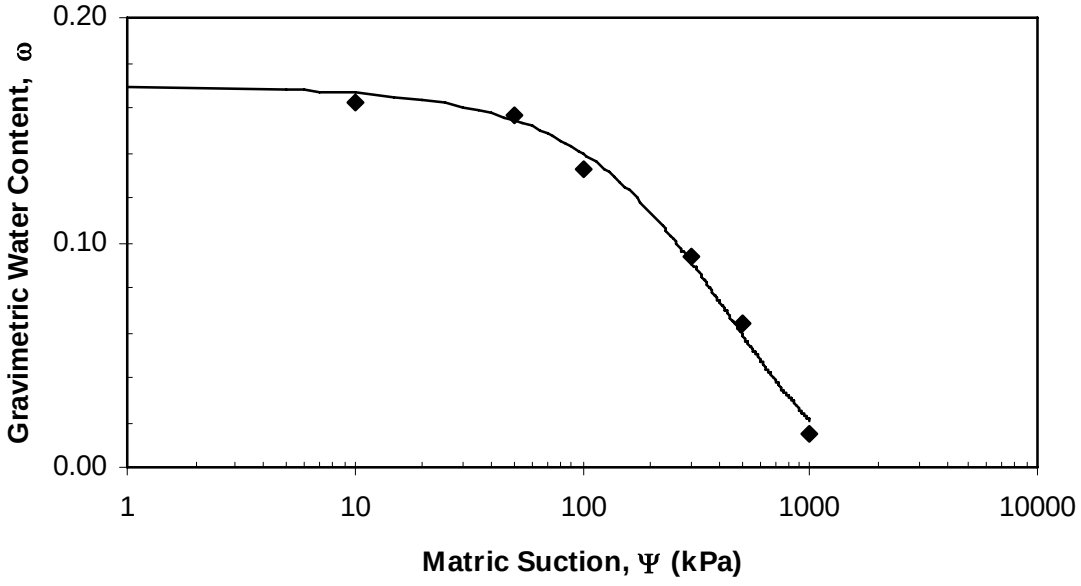

HD_SP_DO_4.8% (Delta 1)

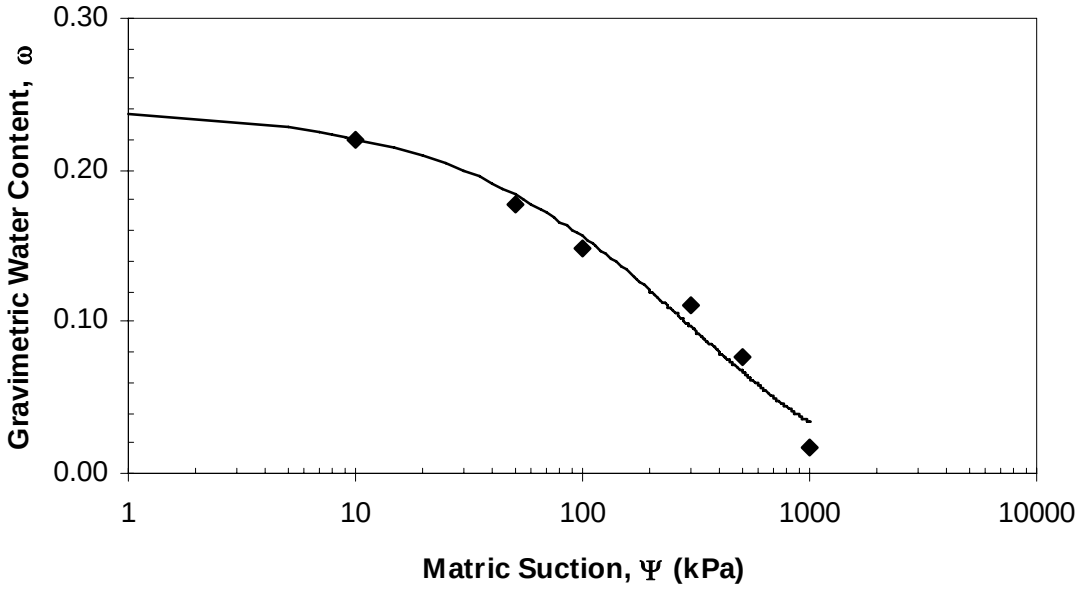

HD_SP_DO_4.8% (Delta 2)

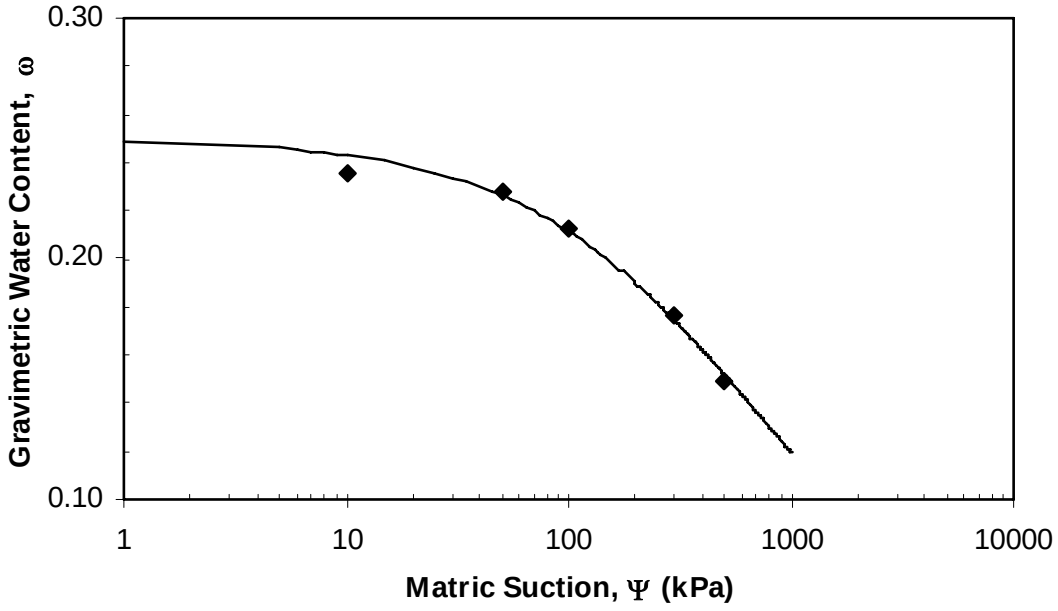

HD_SP_DO_11.6% (Delta 3)

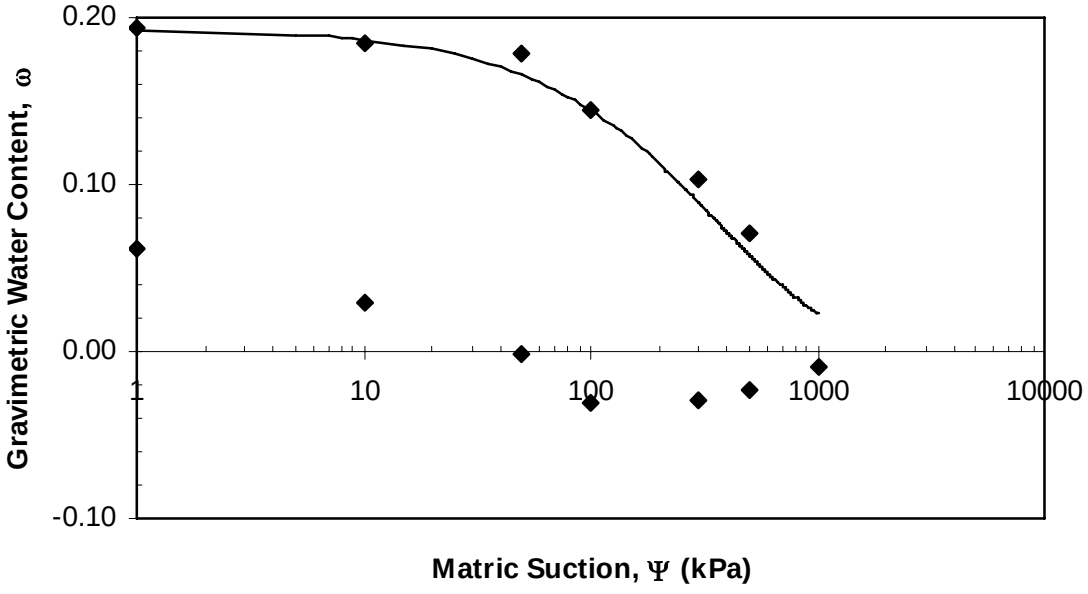

MD_.3SP_DO_4.8%_100 kPa (Epsilon 1)

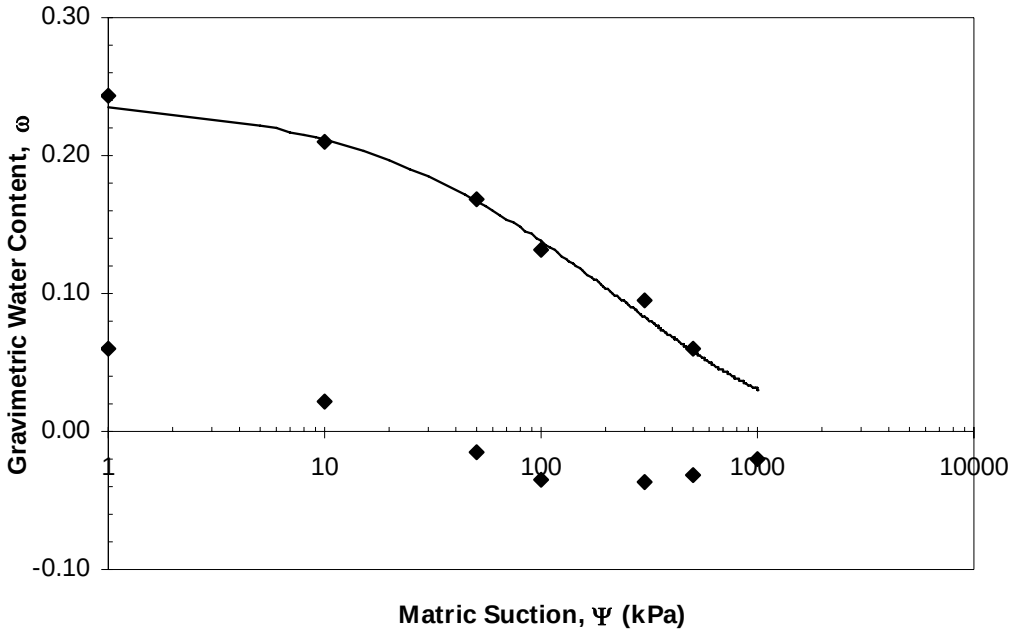

MD_.3SP_DO_4.8% (Epsilon 2)

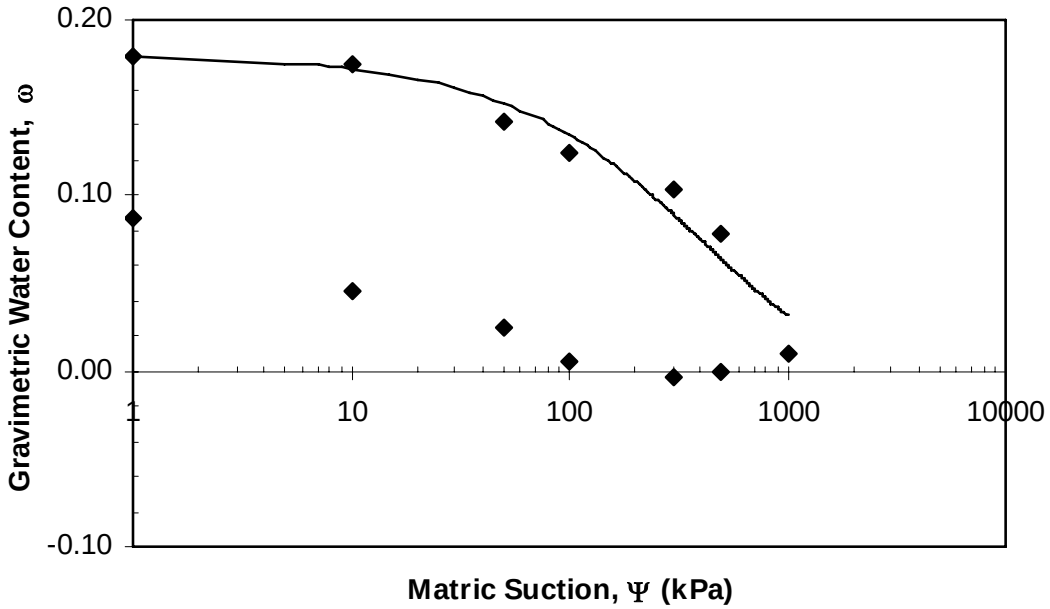

MD_.3SP_DO_11.6%_0 kPa (Epsilon 3)

Appendix B3-SWCC-Degree of Saturation

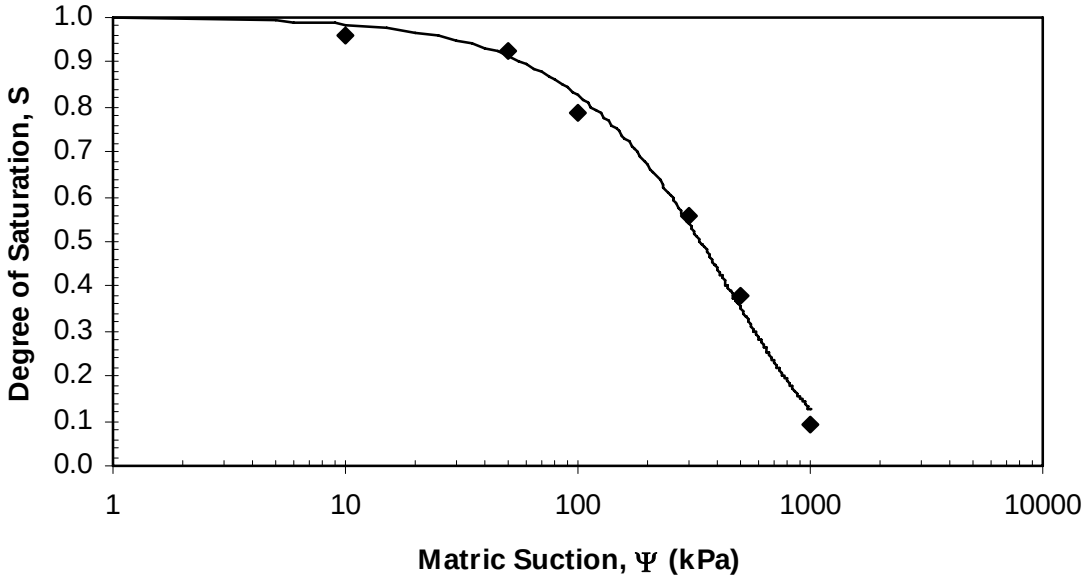

HD_SP_DO_4.8% (Delta 1)

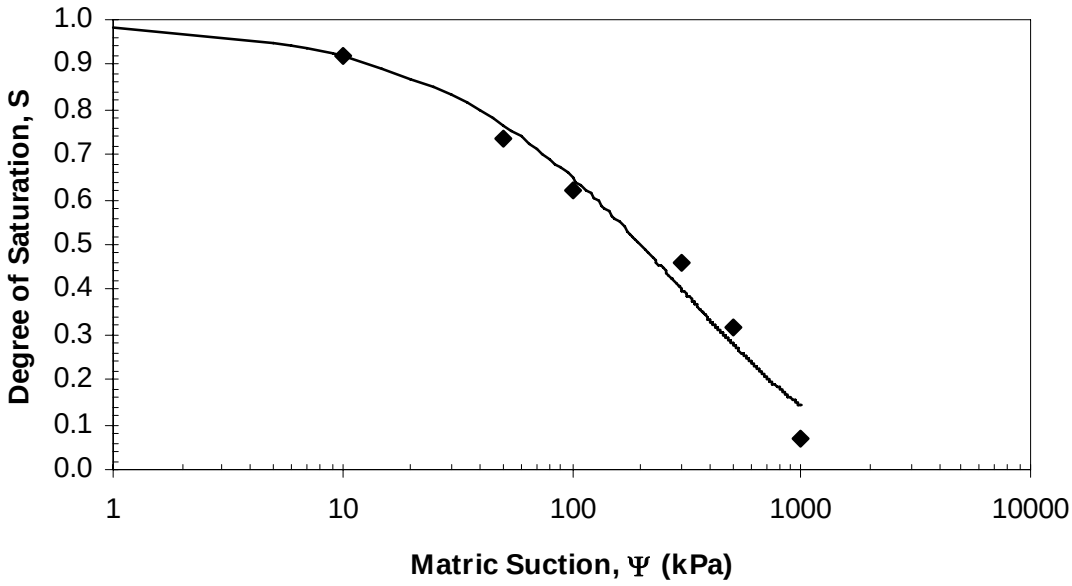

HD_SP_DO_4.8% (Delta 2)

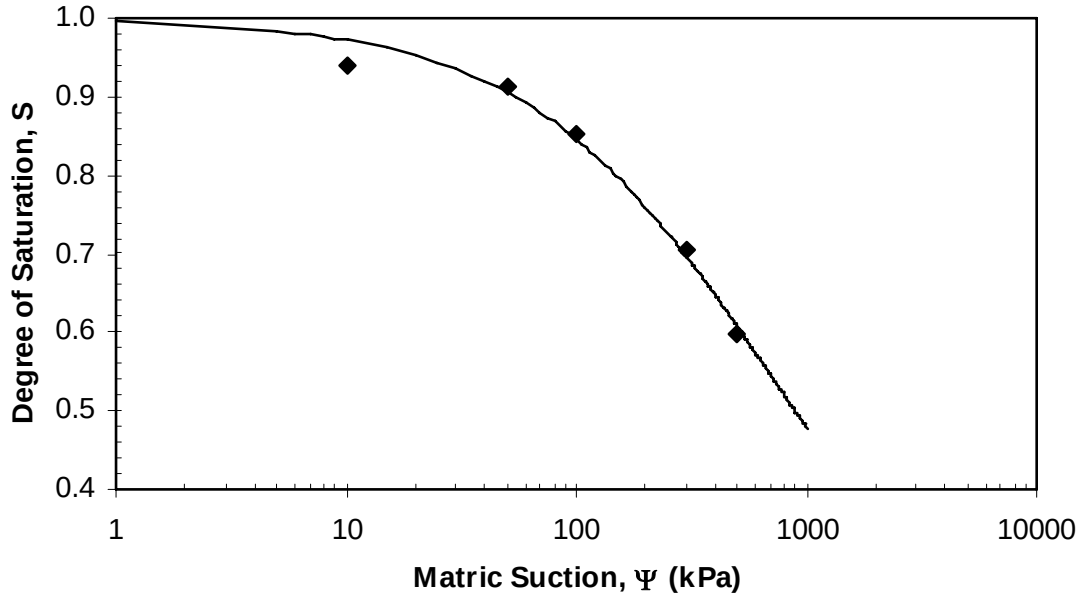

HD_SP_DO_11.6% (Delta 3)

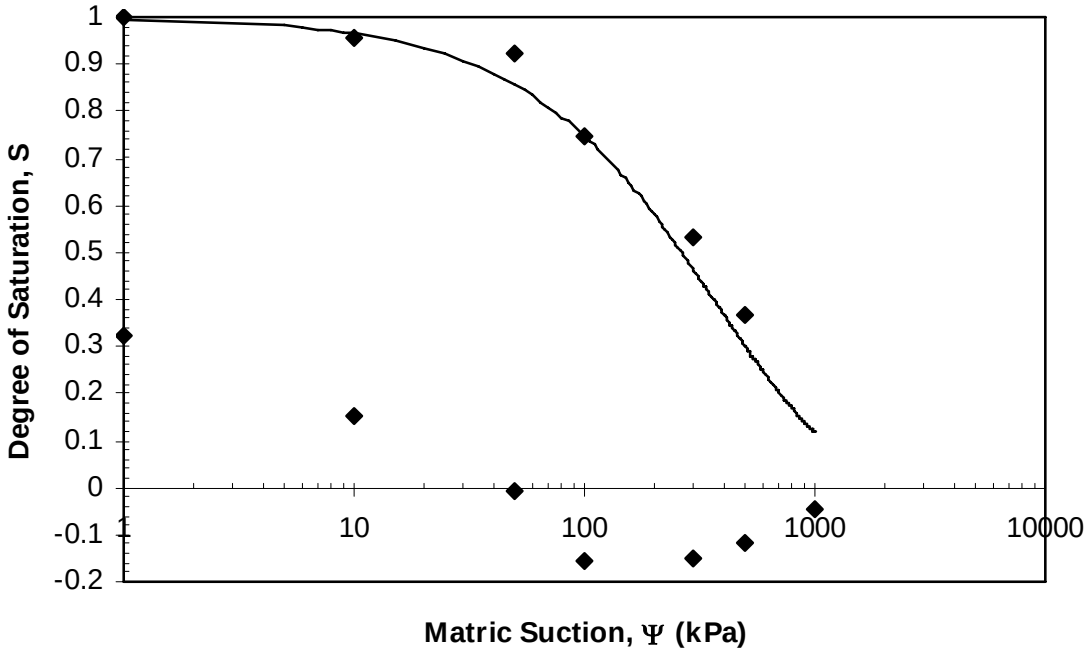

MD_.3SP_DO_4.8%_100 kPa (Epsilon 1)

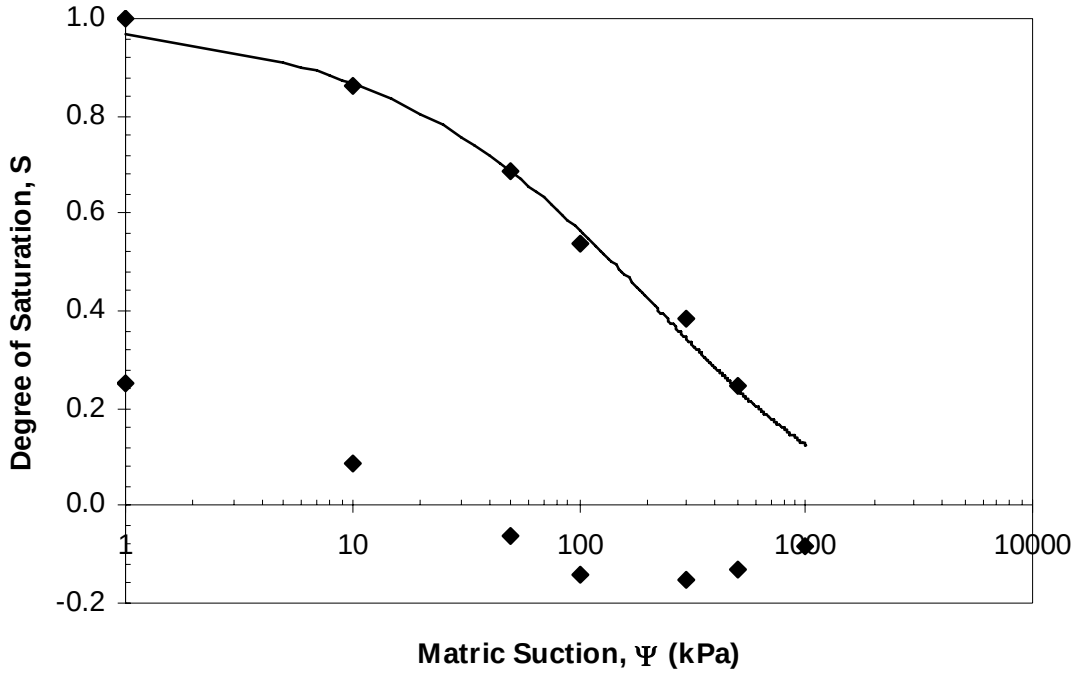

MD_.3SP_DO_4.8% (Epsilon 2)

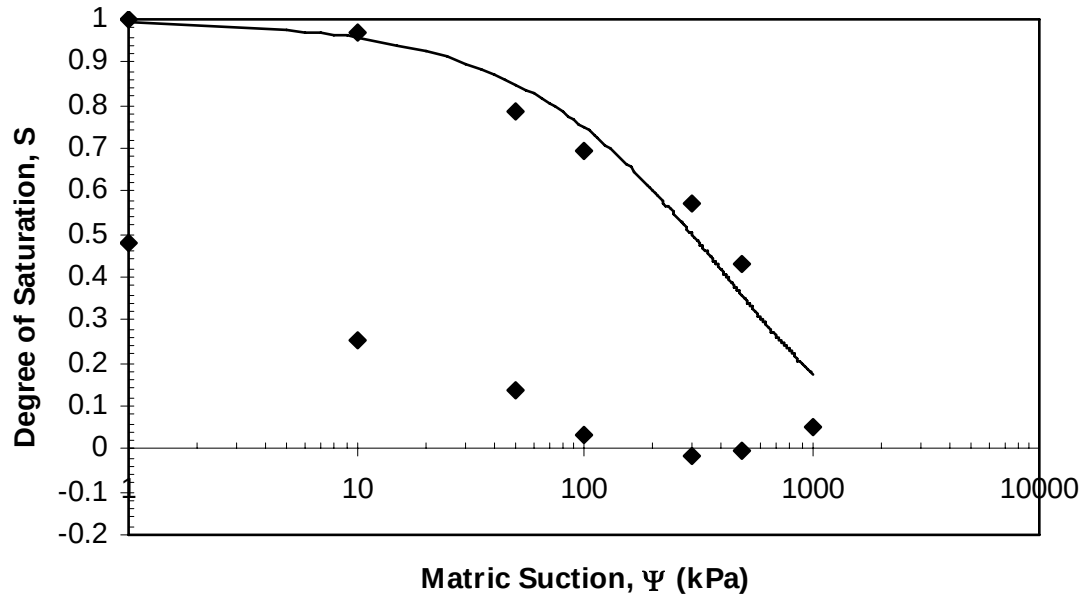

MD_.3SP_DO_11.6%_0 kPa (Epsilon 3)

APPENDIX C-Collapse Potential

Appendix C1- HD_SP_DO_11.7%

Test Name: **HD_SP_DO_11.7%_Unsoaked**

Date: **4/15/2006**

Time: **11:00** AM ~~PM~~

Compactive Effort ~~10% SP~~ ~~(3" x 10 x 3)~~
~~30% SP~~ ~~(6" x 15 x 3)~~
Standard (12" x 25 x 3)

Mass

Ring (ID: A) **76.87** g	Ring (ID:)	g
Ceramic (saturated)	**NA**	g
Soil (moist) + ring(s) + ~~ceramic~~	**204.51**	g
Soil (sat.) + ring(s) + ceramic	**NA**	g
Soil (Moist)	**127.64**	g
Soil (dry)	**114.27**	g
Soil (sat.)	**NA**	g
Top Filter Paper (dry)	**NA**	g
Top Filter Paper (sat.)	**NA**	g
Water (Top Filter Paper)	**NA**	g
Bottom Filter Paper (dry)	**NA**	g
Bottom Filter Paper (sat.)	**NA**	g
Water (Bottom Filter Paper)	**NA**	g

Density (Mold)

Mold + Base + Ring(s)	**4438**	g
Mold + Base + Soil + Ring(s)	**6457**	g
Soil mass (wet)	**2019**	g
ρ_m (moist density)	**2.14**	g/cm^3
ρ_d (dry density)	**1.91**	g/cm^3
γ_d (dry unit weight)	**18.8**	kN/m^3

Notes:

Water Content Determination

CAN ID	**003**	
Can Mass	**11.30**	g
Can + Soil (wet)	**31.45**	g
Can + Soil (dry)	**29.34**	g
ω	**11.7**	%

Density (Ring)

Ring Mass	**76.87**	g
Ring + Soil (moist)	**204.51**	g
Ring Volume	**60.14**	cm^3
ρ_m (moist density)	**2.12**	g/cm^3
ρ_d (dry density)	**1.90**	g/cm^3
γ_d (dry unit weight)	**18.6**	kN/m^3

Test Name: **HD_SP_D0_11.7%_Unsoaked**

Date: **4/15/2006**

Time: **12:40** AM ~~PM~~

ω **11.7** %

ρ_d **1.9** g/cm^3

Load (kPa)	Elasped Time (min)	Deformation (in)
Seating Pressure 5 kPa	0	0.0000
	0.25	0.0006
	0.5	0.0007
	1	0.0008
	2	0.0009
	3	0.0009
	4	0.0009
	5	0.0010
	10	0.0010
	15	0.0010
	20	0.0011

Load (kPa)	Elasped Time (min)	Deformation (in)	Load (kPa)	Elasped Time (min)	Deformation (in)
25 kPa	0	0.0000	**50 kPa**	0	0.0039
	0.25	0.0024		0.25	0.0077
	0.5	0.0025		0.5	0.0079
	1	0.0029		1	0.0080
	2	0.0031		2	0.0082
	3	0.0032		3	0.0084
	4	0.0032		4	0.0084
	5	0.0033		5	0.0085
	10	0.0035		10	0.0087
	20	0.0037		20	0.0088
	30	0.0038		30	0.0089
	40	0.0039		40	0.0089
	50	0.0039		50	0.0090
	60	0.0039		60	0.0090

Load (kPa)	Elasped Time (min)	Deformation (in)	Load (kPa)	Elasped Time (min)	Deformation (in)
100 kPa	0	0.009	**200 kPa**	0	0.0166
	0.25	0.0151		0.25	0.0239
	0.5	0.0152		0.5	0.0241
	1	0.0155		1	0.0245
	2	0.0158		2	0.0247
	3	0.0159		3	0.0248
	4	0.0159		4	0.0249
	5	0.0160		5	0.0250
	10	0.0162		10	0.0253
	20	0.0163		20	0.0254
	30	0.0164		30	0.0255
	40	0.0165		40	0.0256
	50	0.0165		50	0.0256
	60	0.0166		60	0.0256

Load (kPa)	Elasped Time (min)	Deformation (in)	Load (kPa)	Elasped Time (min)	Deformation (in)
400 kPa	0	0.0256	**800 kPa**	0	0.0369
	0.25	0.0350		0.25	0.0501
	0.5	0.0353		0.5	0.0504
	1	0.0356		1	0.0508
	2	0.0359		2	0.0512
	3	0.0361		3	0.0515
	4	0.0361		4	0.0517
	5	0.0362		5	0.0518
	10	0.0365		10	0.0521
	20	0.0367		20	0.0524
	30	0.0368		30	0.0525
	40	0.0368		40	0.0526
	50	0.0369		50	0.0526
	60	0.0369		60	0.0527

Test Name: **HD_SP_DO_11.7%_Soaked**

Date: **4/19/2006**

Time: **11:00** AM ~~PM~~

ω **11.7** %

ρ_d **1.9** g/cm^3

Loading **5** kPa

Elasped Time (min)	Square Root Time	Deformation (in)
0	0.0	0.0000
0.25	0.5	0.0002
0.5	0.7	0.0000
1	1.0	-0.0001
2	1.4	-0.0003
4	2.0	-0.0004
8	2.8	-0.0011
15	3.9	-0.0019
30	5.5	-0.0035
60	7.7	-0.0042
120	11.0	-0.0044
240	15.5	-0.0045
360	19.0	-0.0046
1440	37.9	-0.0048

Test Name: **HD_SP_DO_11.7%_Soaked**

Date: **4/19/2006**

Time: **11:00** AM ~~PM~~

ω **11.7** %

ρ_d **1.9** g/cm^3

Load (kPa)	Elasped Time (min)	Sq. Rt. Time	Deformation (in)
25 kPa	0	0.0	-0.0048
	0.25	0.5	-0.0004
	0.5	0.7	-0.0001
	1	1.0	0.0001
	2	1.4	0.0003
	3	1.7	0.0005
	4	2.0	0.0005
	5	2.2	0.0006
	10	3.2	0.0008
	20	4.5	0.0010
	30	5.5	0.0011
	45	6.7	0.0012
	60	7.7	0.0013
	180	13.4	0.0014
	1440	37.9	
Load (kPa)	Elasped Time (min)	Sq. Rt. Time	Deformation (in)
50 kPa	0	0.0	0.0014
	0.25	0.5	0.0047
	0.5	0.7	0.0050
	1	1.0	0.0053
	2	1.4	0.0055
	3	1.7	0.0056
	4	2.0	0.0057
	5	2.2	0.0058
	10	3.2	0.0060
	20	4.5	0.0061
	30	5.5	0.0062
	45	6.7	0.0064
	60	7.7	0.0065
	480	21.9	
	1440	37.9	
Load (kPa)	Elasped Time (min)	Sq. Rt. Time	Deformation (in)
100 kPa	0	0.0	0.0065
	0.25	0.5	0.0118
	0.5	0.7	0.0120
	1	1.0	0.0122
	2	1.4	0.0124
	3	1.7	0.0125
	4	2.0	0.0126
	5	2.2	0.0127
	10	3.2	0.0129
	20	4.5	0.0131
	30	5.5	0.0132
	45	6.7	0.0133
	60	7.7	
	480	21.9	
	1440	37.9	

Load (kPa)	Elasped Time (min)	Sq. Rt. Time	Deformation (in)
200 kPa	0	0.0	0.0133
	0.25	0.5	0.0202
	0.5	0.7	0.0205
	1	1.0	0.0207
	2	1.4	0.0210
	3	1.7	0.0212
	4	2.0	0.0213
	5	2.2	0.0213
	10	3.2	0.0216
	20	4.5	0.0218
	30	5.5	0.0219
	45	6.7	0.0220
	60	7.7	0.0220
	480	21.9	
	1440	37.9	
Load (kPa)	Elasped Time (min)	Sq. Rt. Time	Deformation (in)
400 kPa	0	0.0	0.0220
	0.25	0.5	0.0320
	0.5	0.7	0.0324
	1	1.0	0.0327
	2	1.4	0.0330
	3	1.7	0.0332
	4	2.0	0.0333
	5	2.2	0.0334
	10	3.2	0.0337
	20	4.5	0.0340
	30	5.5	0.0341
	45	6.7	0.0341
	60	7.7	0.0342
	480	21.9	
	1440	37.9	
Load (kPa)	Elasped Time (min)	Sq. Rt. Time	Deformation (in)
800 kPa	0	0.0	0.0342
	0.25	0.5	0.0482
	0.5	0.7	0.0486
	1	1.0	0.0491
	2	1.4	0.0496
	3	1.7	0.0499
	4	2.0	0.0501
	5	2.2	0.0502
	10	3.2	0.0508
	20	4.5	0.0510
	30	5.5	0.0512
	45	6.7	0.0513
	60	7.7	0.0514
	480	21.9	
	1440	37.9	

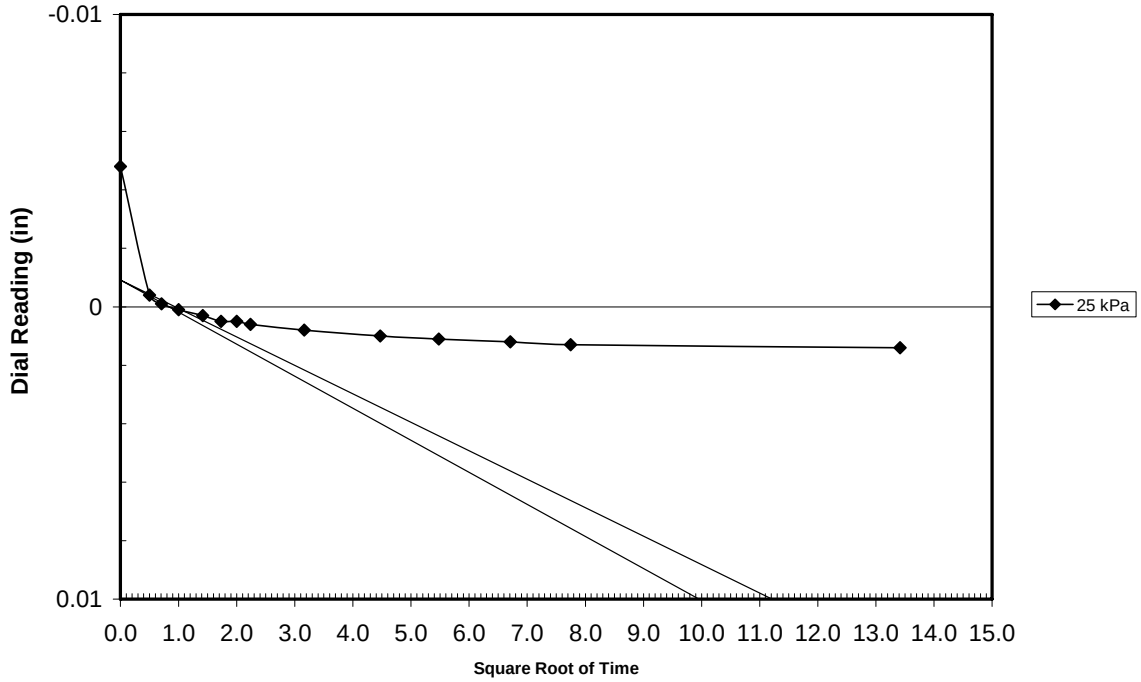

Taylor Curve (25 kPa)

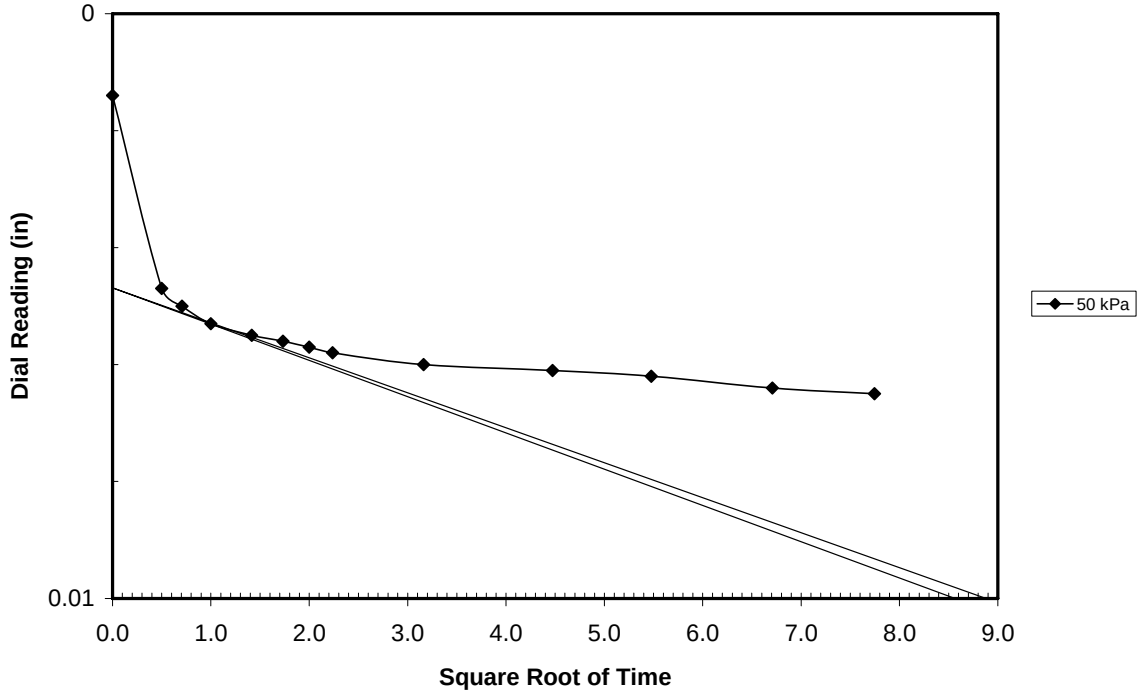

Taylor Curve (50 kPa)

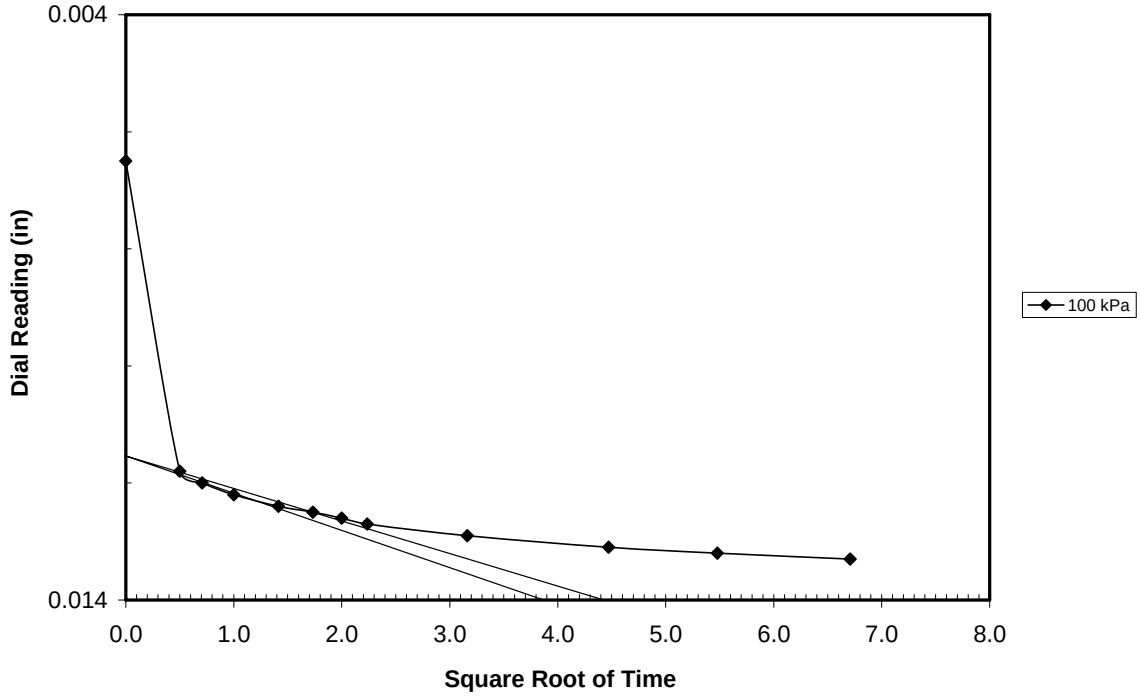

Taylor Curve (100 kPa)

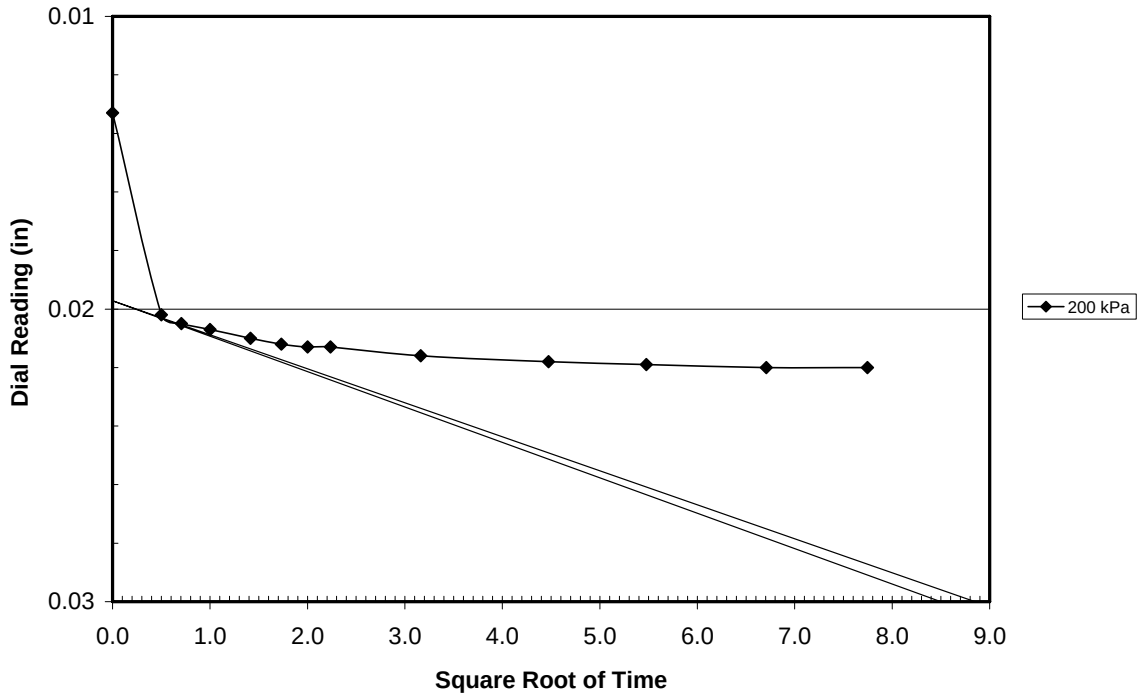

Taylor Curve (200 kPa)

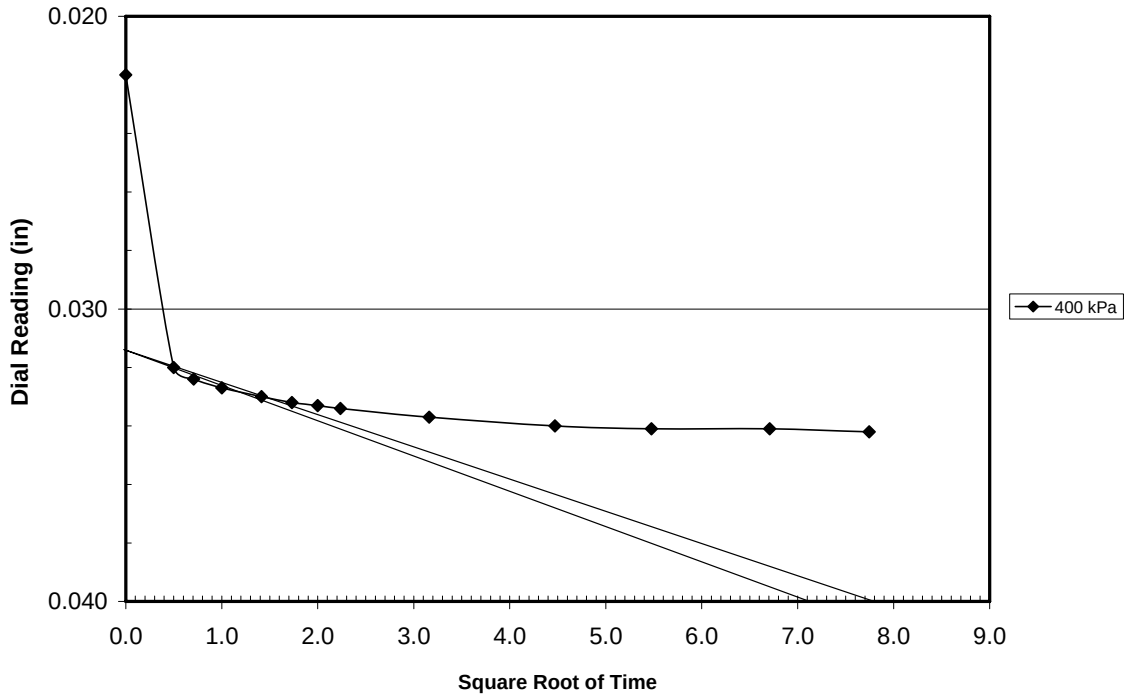

Taylor Curve (400 kPa)

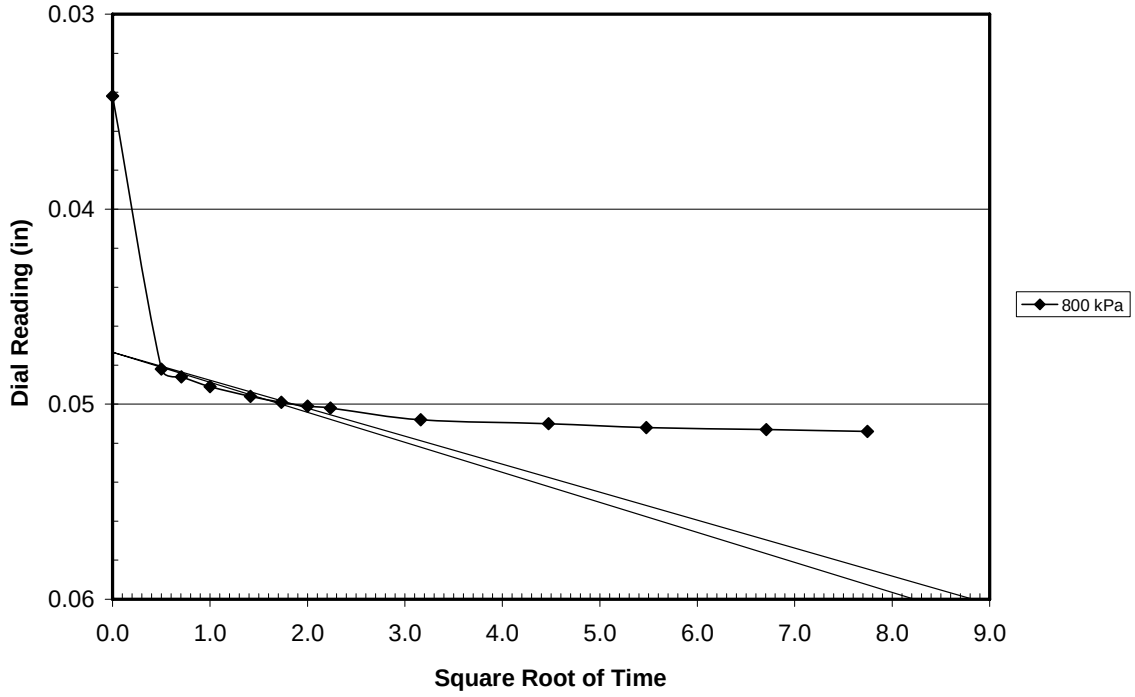

Taylor Curve (800 kPa)

Appendix C2-MD_.3SP_DO_11.7%

Test Name: **MD_.3SP_DO_11.7%_Unsoaked**

Date: **4/15/2006**

Time: **11:00** AM ~~PM~~

Compactive Effort ~~10% SP~~ ~~(3" x 10 x 3)~~
30% SP (6" x 15 x 3)
~~Standard~~ ~~(12" x 25 x 3)~~

Mass

Ring (ID: B)	**76.59** g	Ring (ID:)	g
Ceramic (saturated)	**NA**		g
Soil (moist) + ring(s) + ~~ceramic~~	**196.16**		g
Soil (sat.) + ring(s) + ceramic	**NA**		g
Soil (Moist)	**119.57**		g
Soil (dry)	**107.05**		g
Soil (sat.)	**NA**		g
Top Filter Paper (dry)	**NA**		g
Top Filter Paper (sat.)	**NA**		g
Water (Top Filter Paper)	**NA**		g
Bottom Filter Paper (dry)	**NA**		g
Bottom Filter Paper (sat.)	**NA**		g
Water (Bottom Filter Paper)	**NA**		g

Density (Mold)

Mold + Base + Ring(s)	**4438**	g
Mold + Base + Soil + Ring(s)	**6238**	g
Soil mass (wet)	**1800**	g
ρ_m (moist density)	**1.91**	g/cm^3
ρ_d (dry density)	**1.71**	g/cm^3
γ_d (dry unit weight)	**16.7**	kN/m^3

Notes:

Water Content Determination

CAN ID	**003**	
Can Mass	**11.30**	g
Can + Soil (wet)	**31.45**	g
Can + Soil (dry)	**29.34**	g
ω	**11.7**	%

Density (Ring)

Ring Mass	**76.59**	g
Ring + Soil (moist)	**196.16**	g
Ring Volume	**60.14**	cm^3
ρ_m (moist density)	**1.99**	g/cm^3
ρ_d (dry density)	**1.78**	g/cm^3
γ_d (dry unit weight)	**17.5**	kN/m^3

Test Name: **MD_.3SP_D0_11.7%_Unsoaked**

Date: **4/15/2006**

Time: **12:40** AM ~~PM~~

ω **11.7** %

ρ_d **1.9** g/cm^3

Load (kPa)	Elasped Time (min)	Deformation (in)
Seating Pressure 5 kPa	0	0.0000
	0.25	0.0011
	0.5	0.0012
	1	0.0012
	2	0.0012
	3	0.0013
	4	0.0013
	5	0.0013
	10	0.0013
	15	0.0013
	20	0.0014

Load (kPa)	Elasped Time (min)	Deformation (in)	Load (kPa)	Elasped Time (min)	Deformation (in)
25 kPa	0	0.0014	**50 kPa**	0	0.0085
	0.25	0.0072		0.25	0.0139
	0.5	0.0073		0.5	0.0142
	1	0.0074		1	0.0145
	2	0.0074		2	0.0150
	3	0.0076		3	0.0153
	4	0.0076		4	0.0155
	5	0.0077		5	0.0157
	10	0.0078		10	0.0162
	20	0.0081		20	0.0170
	30	0.0082		30	0.0175
	40	0.0083		40	0.0179
	50	0.0084		50	0.0182
	60	0.0085		60	0.0184

Load (kPa)	Elasped Time (min)	Deformation (in)	Load (kPa)	Elasped Time (min)	Deformation (in)
100 kPa	0	0.0184	**200 kPa**	0	0.0555
	0.25	0.0298		0.25	0.0691
	0.5	0.0304		0.5	0.0697
	1	0.0311		1	0.0702
	2	0.0324		2	0.0707
	3	0.0351		3	0.0710
	4	0.0542		4	0.0712
	5	0.0545		5	0.0713
	10	0.0550		10	0.0718
	20	0.0552		20	0.0721
	30	0.0554		30	0.0723
	40	0.0554		40	0.0725
	50	0.0555		50	0.0725
	60	0.0555		60	0.0727

Load (kPa)	Elasped Time (min)	Deformation (in)	Load (kPa)	Elasped Time (min)	Deformation (in)
400 kPa	0	0.0729	**800 kPa**	0	0.1056
	0.25	0.1001		0.25	0.1421
	0.5	0.1012		0.5	0.1428
	1	0.1020		1	0.1439
	2	0.1028		2	0.1448
	3	0.1033		3	0.1452
	4	0.1036		4	0.1451
	5	0.1037		5	0.1456
	10	0.1044		10	0.1463
	20	0.1049		20	0.1468
	30	0.1052		30	0.1471
	40	0.1053		40	0.1472
	50	0.1055		50	0.1474
	60	0.1056		60	0.1475

Test Name: **MD_.3SP_DO_11.7%_Soaked**

Date: **4/19/2006**

Time: **11:00** AM ~~PM~~

ω **11.7** %

ρ_d **1.78** g/cm^3

Loading **5** kPa

Elasped Time (min)	Square Root Time	Deformation (in)
0	0.0	0.0000
0.25	0.5	0.0031
0.5	0.7	0.0032
1	1.0	0.0032
2	1.4	0.0032
4	2.0	0.0032
8	2.8	0.0030
15	3.9	0.0027
30	5.5	0.0025
60	7.7	0.0024
120	11.0	0.0024
240	15.5	0.0024
360	19.0	0.0024
1440	37.9	0.0023

Test Name: **MD_.3SP_DO_11.7%_Soaked**

Date: **4/19/2006**

Time: **11:00** AM ~~PM~~

ω **11.7** %

ρ_d **1.78** g/cm^3

Load (kPa)	Elasped Time (min)	Sq. Rt. Time	Deformation (in)
25 kPa	0	0.0	0.0028
	0.25	0.5	0.0123
	0.5	0.7	0.0128
	1	1.0	0.0133
	2	1.4	0.0139
	3	1.7	0.0141
	4	2.0	0.0143
	5	2.2	0.0144
	10	3.2	0.0147
	20	4.5	0.0150
	30	5.5	0.0151
	45	6.7	0.0152
	60	7.7	0.0154
	180	13.4	0.0154
	1440	37.9	
Load (kPa)	Elasped Time (min)	Sq. Rt. Time	Deformation (in)
50 kPa	0	0.0	0.0154
	0.25	0.5	0.0239
	0.5	0.7	0.0250
	1	1.0	0.0256
	2	1.4	0.0263
	3	1.7	0.0267
	4	2.0	0.0270
	5	2.2	0.0271
	10	3.2	0.0276
	20	4.5	0.0279
	30	5.5	0.0281
	45	6.7	0.0282
	60	7.7	0.0283
	480	21.9	
	1440	37.9	
Load (kPa)	Elasped Time (min)	Sq. Rt. Time	Deformation (in)
100 kPa	0	0.0	0.0283
	0.25	0.5	0.0468
	0.5	0.7	0.0479
	1	1.0	0.0482
	2	1.4	0.0494
	3	1.7	0.0498
	4	2.0	0.0502
	5	2.2	0.0504
	10	3.2	0.0510
	20	4.5	0.0515
	30	5.5	0.0517
	45	6.7	0.0518
	60	7.7	
	480	21.9	
	1440	37.9	

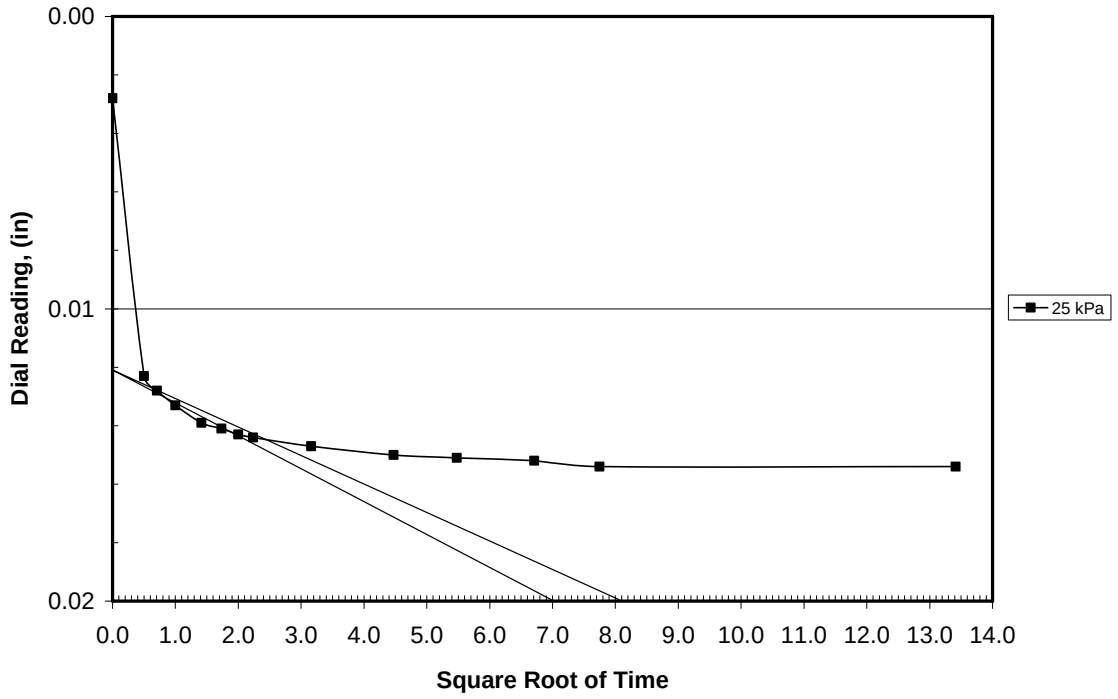

Taylor Curve (25 kPa)

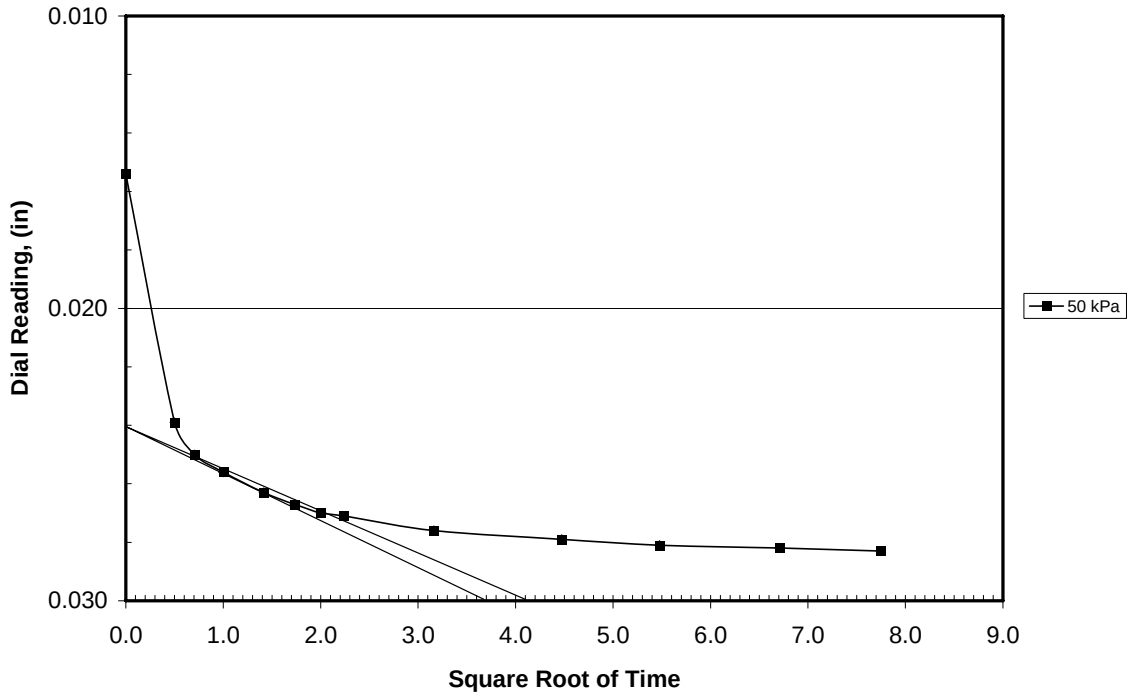

Taylor Curve (50 kPa)

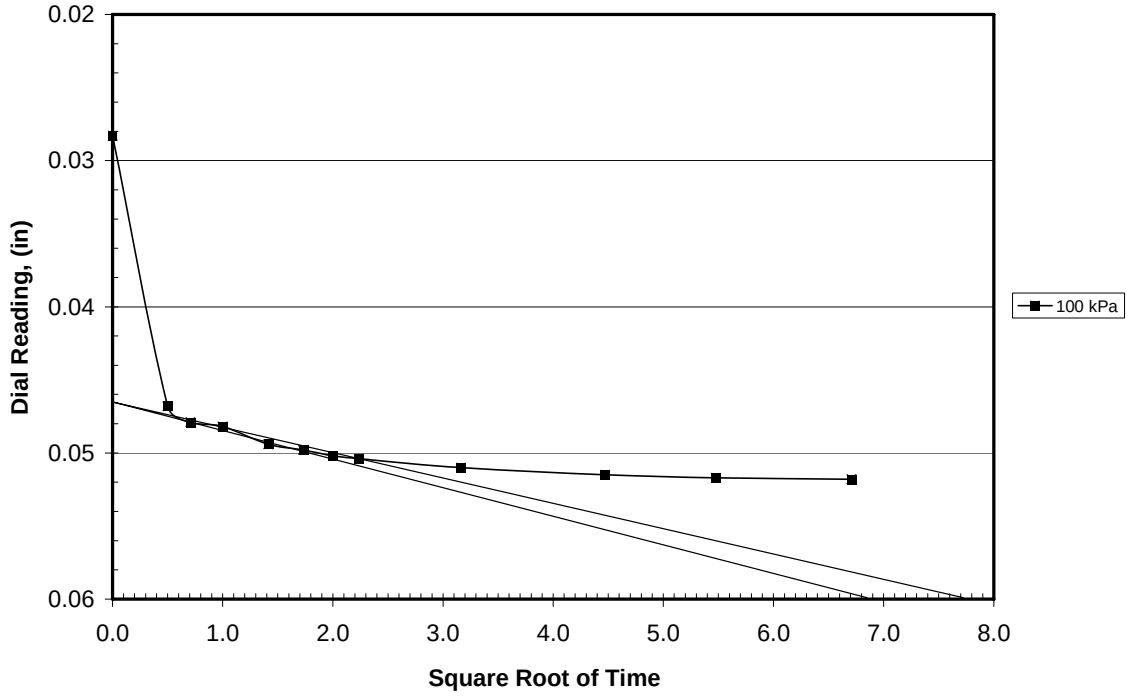

Taylor Curve (100 kPa)

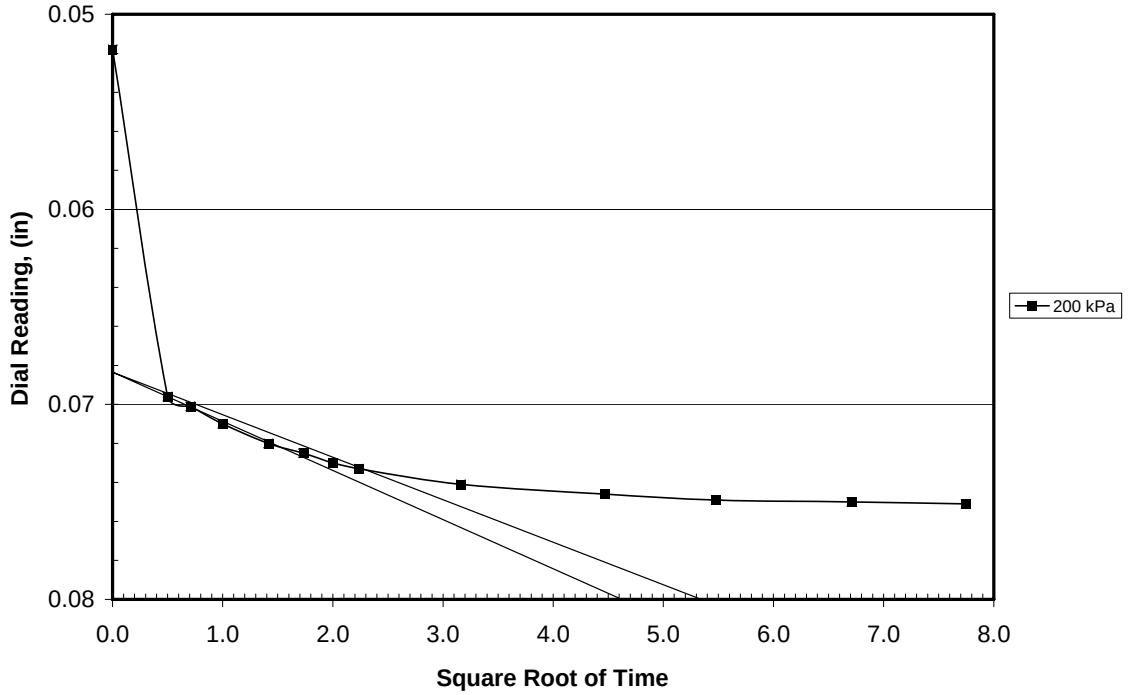

Taylor Curve (200 kPa)

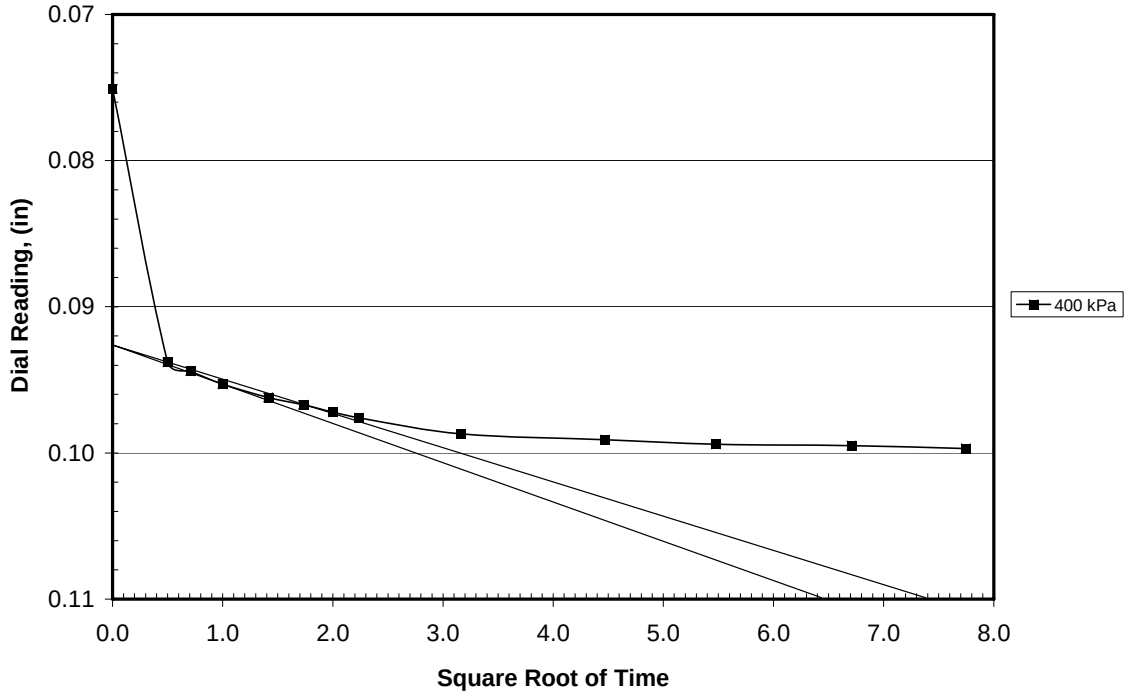

Taylor Curve (400 kPa)

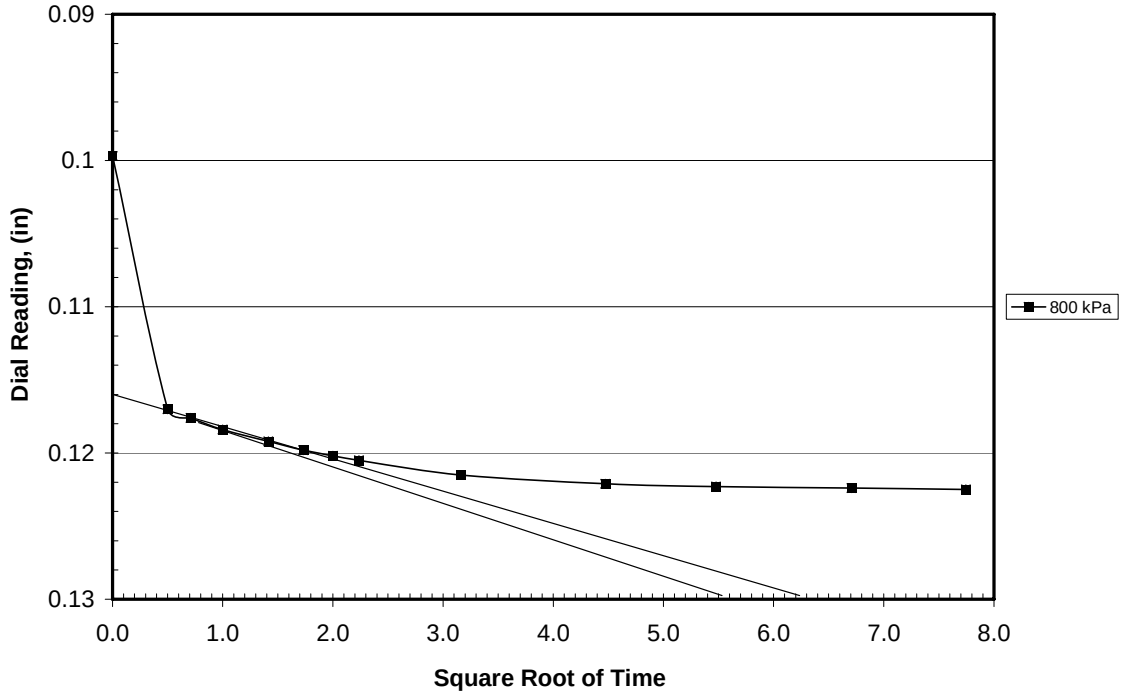

Taylor Curve (800 kPa)

Appendix C3-LD_.3SP_DO_11.7%

Test Name: **LD_.1SP_DO_11.7%_Unsoaked**

Date: **4/15/2006**

Time: **11:00** AM ~~PM~~

Compactive Effort: 10% SP (3" x 10 x 3); ~~30% SP (6" x 15 x 3)~~; ~~Standard (12" x 25 x 3)~~

Mass

Ring (ID: C)	**76.34**	g	Ring (ID:) _____ g
Ceramic (saturated)	**NA**	g	
Soil (moist) + ring(s) + ~~ceramic~~	**183.82**	g	
Soil (sat.) + ring(s) + ceramic	**NA**	g	
Soil (Moist)	**107.48**	g	
Soil (dry)	**96.22**	g	
Soil (sat.)	**NA**	g	
Top Filter Paper (dry)	**NA**	g	
Top Filter Paper (sat.)	**NA**	g	
Water (Top Filter Paper)	**NA**	g	
Bottom Filter Paper (dry)	**NA**	g	
Bottom Filter Paper (sat.)	**NA**	g	
Water (Bottom Filter Paper)	**NA**	g	

Density (Mold)

Mold + Base + Ring(s)	**4437**	g
Mold + Base + Soil + Ring(s)	**6037**	g
Soil mass (wet)	**1600**	g
ρ_m (moist density)	**1.69**	g/cm^3
ρ_d (dry density)	**1.52**	g/cm^3
γ_d (dry unit weight)	**14.9**	kN/m^3

Notes:

Water Content Determination

CAN ID	**003**	
Can Mass	**11.30**	g
Can + Soil (wet)	**31.45**	g
Can + Soil (dry)	**29.34**	g
ω	**11.7**	%

Density (Ring)

Ring Mass	**76.34**	g
Ring + Soil (moist)	**183.82**	g
Ring Volume	**60.14**	cm^3
ρ_m (moist density)	**1.79**	g/cm^3
ρ_d (dry density)	**1.60**	g/cm^3
γ_d (dry unit weight)	**15.7**	kN/m^3

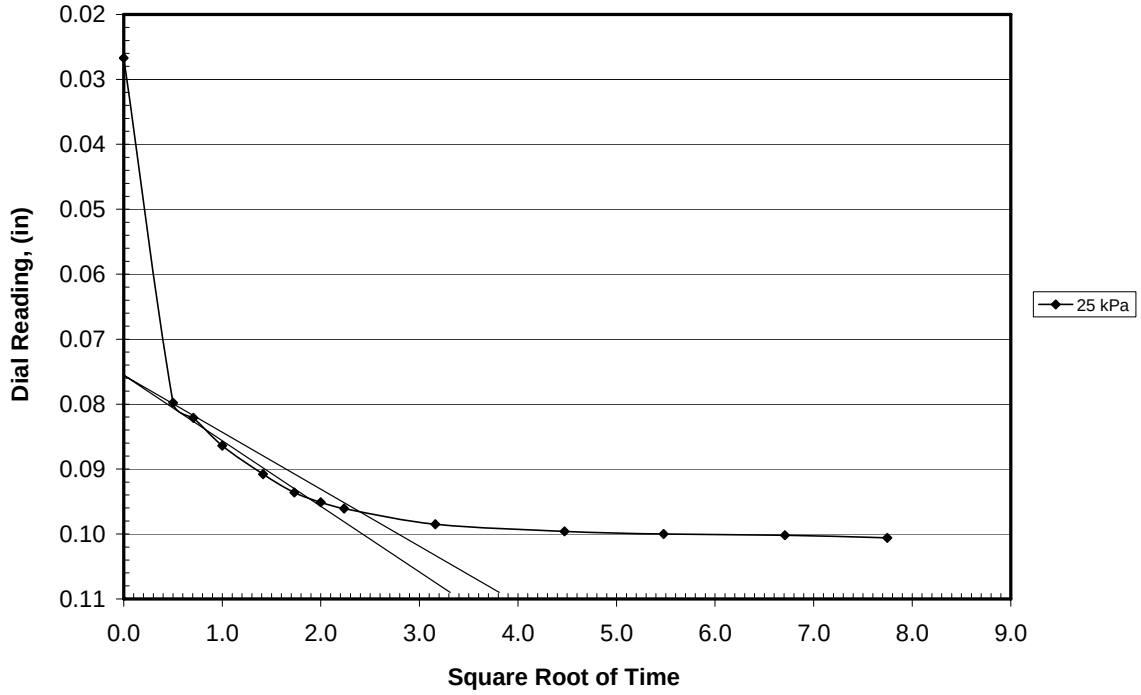

Taylor Curve (25 kPa)

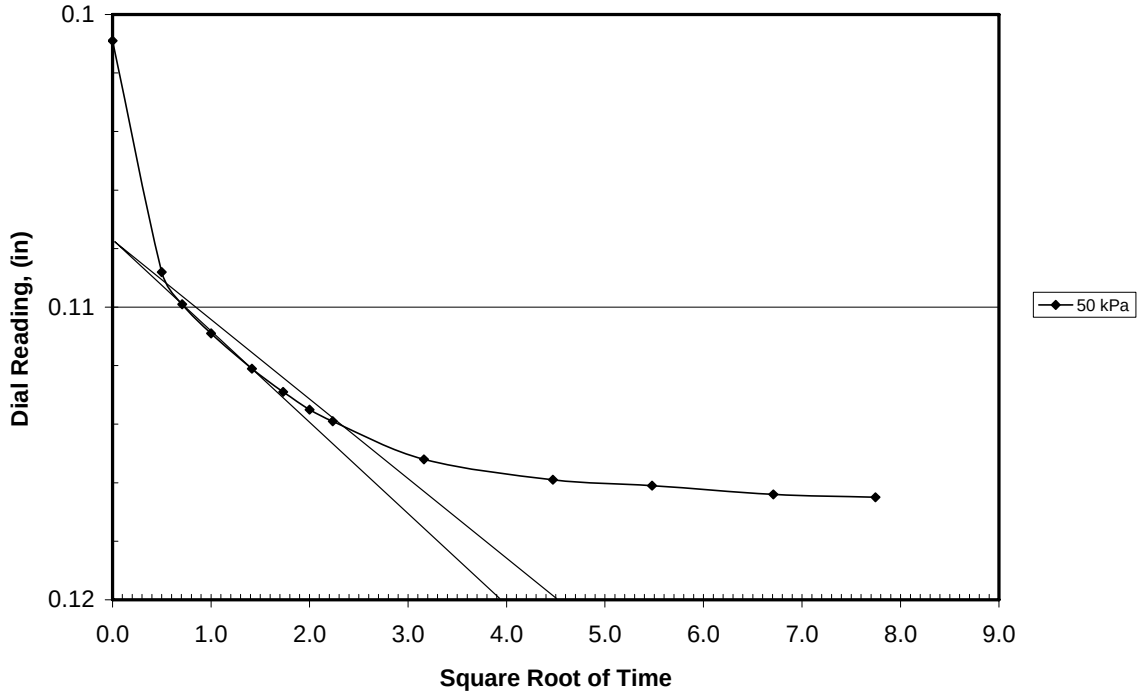

Taylor Curve (50 kPa)

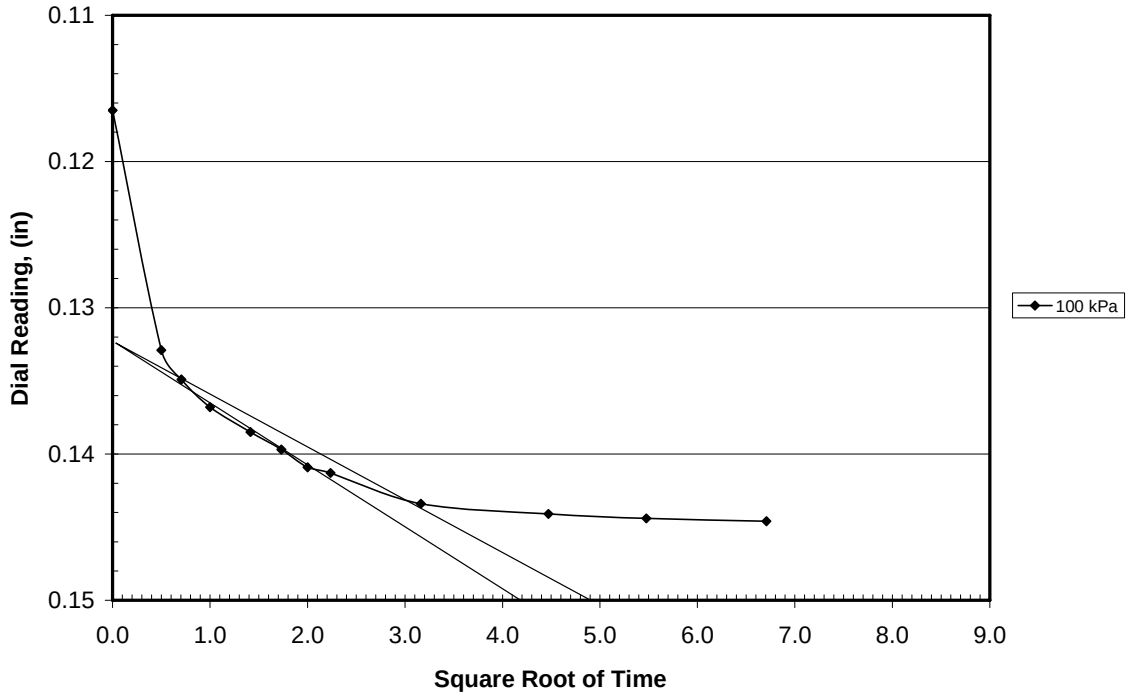

Taylor Curve (100 kPa)

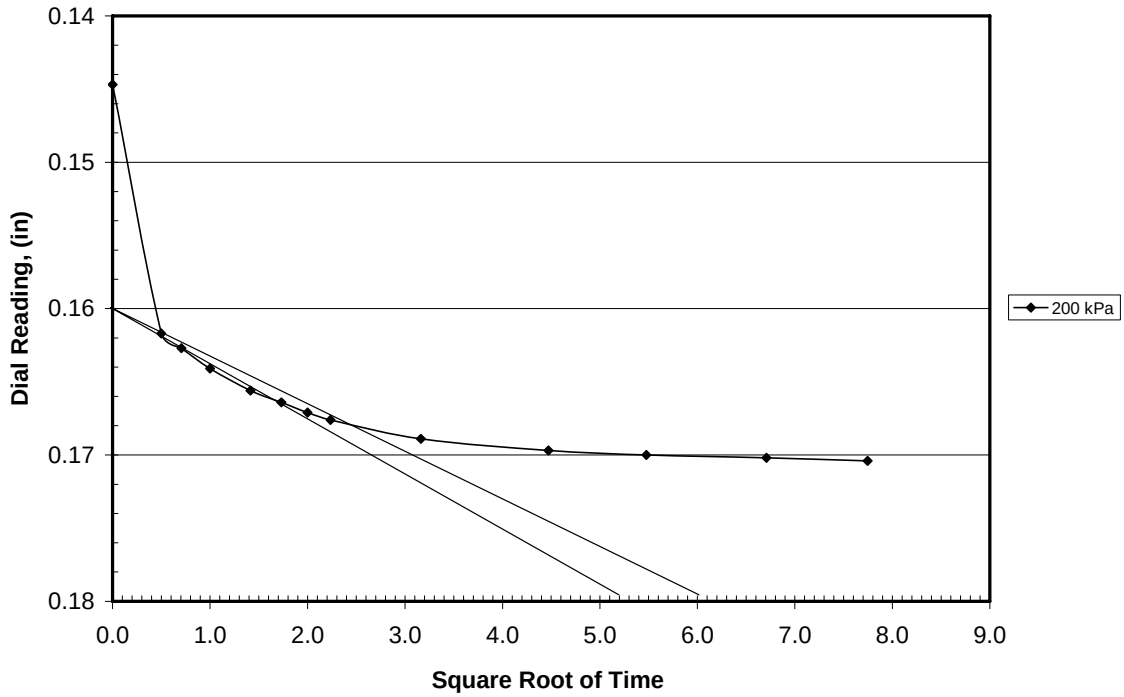

Taylor Curve (200 kPa)

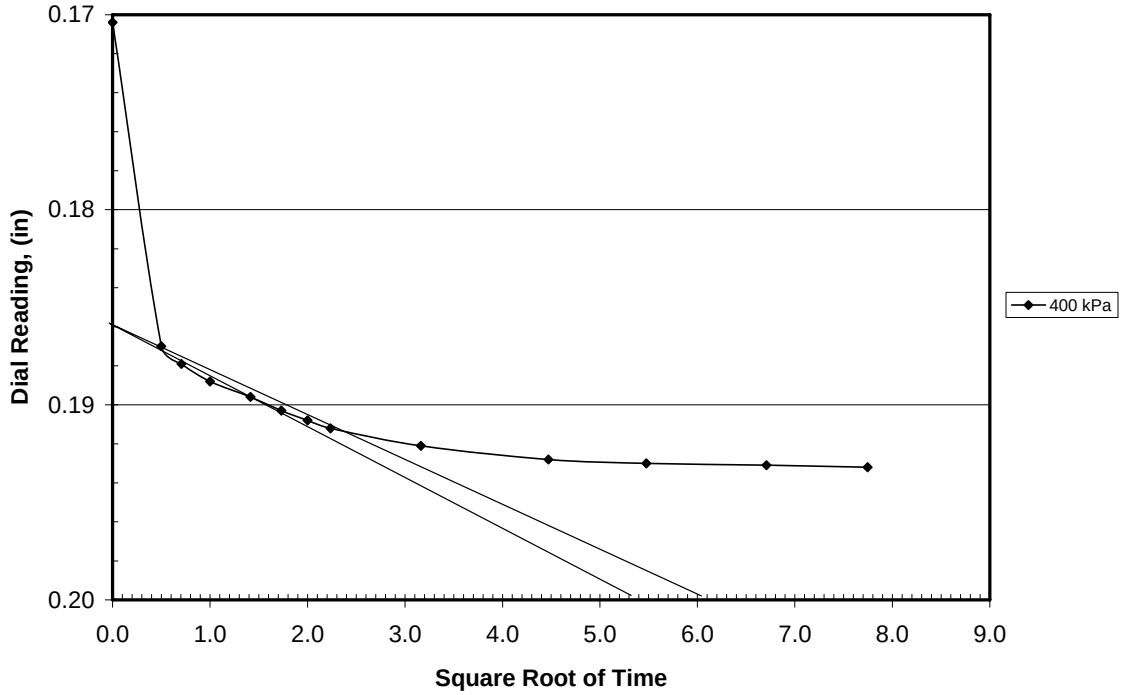

Taylor Curve (400 kPa)

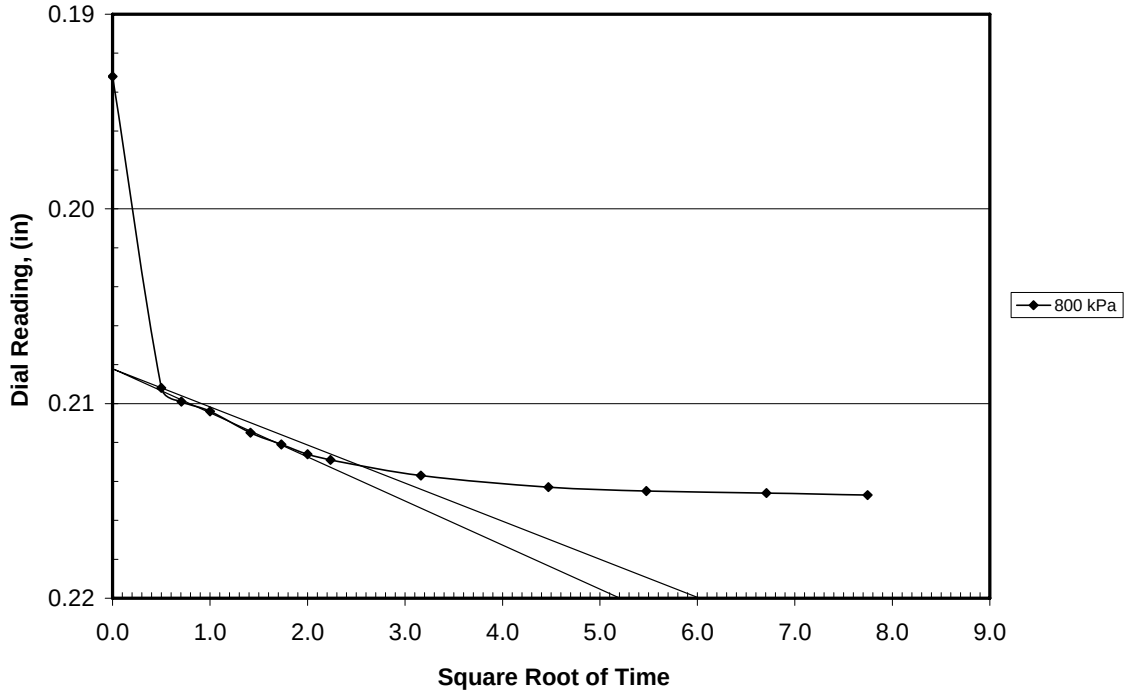

Taylor Curve (800 kPa)

AppendixC4-HD_SP_DO_4.7%

Test Name: **HD_SP_DO_4.7%_Unsoaked**

Date: **4/13/2006**

Time: **4:45** ~~AM~~ PM

Compactive Effort ~~10% SP~~ ~~(3" x 10 x 3)~~
~~30% SP~~ ~~(6" x 15 x 3)~~
Standard (12" x 25 x 3)

Mass

Ring (ID: A)	**76.87** g	Ring (ID:)	g
Ceramic (saturated)	**NA**		g
Soil (moist) + ring(s) + ~~ceramic~~	**189.34**		g
Soil (sat.) + ring(s) + ceramic	**NA**		g
Soil (Moist)	**112.47**		g
Soil (dry)	**107.42**		g
Soil (sat.)	**NA**		g
Top Filter Paper (dry)	**NA**		g
Top Filter Paper (sat.)	**NA**		g
Water (Top Filter Paper)	**NA**		g
Bottom Filter Paper (dry)	**NA**		g
Bottom Filter Paper (sat.)	**NA**		g
Water (Bottom Filter Paper)	**NA**		g

Density (Mold)

Mold + Base + Ring(s)	**4438**	g
Mold + Base + Soil + Ring(s)	**6243**	g
Soil mass (wet)	**1805**	g
ρ_m (moist density)	**1.91**	g/cm^3
ρ_d (dry density)	**1.83**	g/cm^3
γ_d (dry unit weight)	**17.9**	kN/m^3

Notes:

Water Content Determination

CAN ID	**003**	
Can Mass	**11.30**	g
Can + Soil (wet)	**31.50**	g
Can + Soil (dry)	**30.59**	g
ω	**4.7**	%

Density (Ring)

Ring Mass	**76.87**	g
Ring + Soil (moist)	**189.34**	g
Ring Volume	**60.14**	cm^3
ρ_m (moist density)	**1.87**	g/cm^3
ρ_d (dry density)	**1.79**	g/cm^3
γ_d (dry unit weight)	**17.5**	kN/m^3

Test Name: **HD_SP_D0_4.7%_Unsoaked**

Date: **4/12/2006**

Time: **1:45** AM ~~PM~~

ω **4.7** %

ρ_d **1.79** g/cm^3

Load (kPa)	Elasped Time (min)	Deformation (in)
Seating Pressure 5 kPa	0	0.0001
	0.25	0.0001
	0.5	0.0001
	1	0.0001
	2	0.0001
	3	0.0001
	4	0.0001
	5	0.0001
	10	0.0001
	15	0.0001
	20	0.0002

Load (kPa)	Elasped Time (min)	Deformation (in)	Load (kPa)	Elasped Time (min)	Deformation (in)
25 kPa	0	0.0002	**50 kPa**	0	0.0028
	0.25	0.0022		0.25	0.0040
	0.5	0.0023		0.5	0.0045
	1	0.0023		1	0.0047
	2	0.0024		2	0.0047
	3	0.0024		3	0.0048
	4	0.0024		4	0.0048
	5	0.0025		5	0.0048
	10	0.0025		10	0.0050
	20	0.0026		20	0.0051
	30	0.0027		30	0.0052
	40	0.0027		40	0.0053
	50	0.0027		50	0.0053
	60	0.0028		60	0.0054

Load (kPa)	Elasped Time (min)	Deformation (in)	Load (kPa)	Elasped Time (min)	Deformation (in)
100 kPa	0	0.0054	**200 kPa**	0	0.0113
	0.25	0.0100		0.25	0.0188
	0.5	0.0102		0.5	0.0190
	1	0.0103		1	0.0192
	2	0.0104		2	0.0194
	3	0.0106		3	0.0196
	4	0.0107		4	0.0197
	5	0.0107		5	0.0199
	10	0.0110		10	0.0201
	20	0.0111		20	0.0202
	30	0.0111		30	0.0203
	40	0.0111		40	0.0204
	50	0.0112		50	0.0204
	60	0.0113		60	0.0204

Load (kPa)	Elasped Time (min)	Deformation (in)	Load (kPa)	Elasped Time (min)	Deformation (in)
400 kPa	0	0.0204	**800 kPa**	0	0.0328
	0.25	0.0308		0.25	0.0780
	0.5	0.0311		0.5	0.0782
	1	0.0313		1	0.0783
	2	0.0316		2	0.0788
	3	0.0317		3	0.0789
	4	0.0318		4	0.0790
	5	0.0319		5	0.0791
	10	0.0323		10	0.0794
	20	0.0325		20	0.0796
	30	0.0326		30	0.0798
	40	0.0327		40	0.0798
	50	0.0327		50	0.0799
	60	0.0328		60	0.0799

Test Name: **HD_SP_DO_4.7%_Soaked**

Date: **4/13/2006**

Time: **6:00** AM PM

ω **4.7** %

ρ_d **1.79** g/cm^3

Loading **5** kPa

Elasped Time (min)	Square Root Time	Deformation (in)
0	0.0	0.0000
0.25	0.5	0.0005
0.5	0.7	0.0004
1	1.0	0.0003
2	1.4	0.0002
4	2.0	-0.0004
8	2.8	-0.0020
15	3.9	-0.0026
30	5.5	-0.0029
60	7.7	-0.0030
120	11.0	-0.0030
240	15.5	-0.0031
360	19.0	-0.0031
1440	37.9	-0.0031

Test Name: **HD_SP_DO_4.7%_Soaked**

Date: **4/14/2006**

Time: **11:30** AM ~~PM~~

ω **4.7** %

ρ_d **1.79** g/cm^3

Load (kPa)	Elasped Time (min)	Sq. Rt. Time	Deformation (in)
25 kPa	0	0.0	-0.0031
	0.25	0.5	0.0036
	0.5	0.7	0.0042
	1	1.0	0.0048
	2	1.4	0.0053
	3	1.7	0.0056
	4	2.0	0.0057
	5	2.2	0.0058
	10	3.2	0.0061
	20	4.5	0.0063
	30	5.5	0.0065
	45	6.7	0.0066
	60	7.7	0.0066
	480	21.9	NA
	1440	37.9	NA
Load (kPa)	Elasped Time (min)	Sq. Rt. Time	Deformation (in)
50 kPa	0	0.0	0.0066
	0.25	0.5	0.0149
	0.5	0.7	0.0161
	1	1.0	0.0170
	2	1.4	0.0177
	3	1.7	0.0179
	4	2.0	0.0182
	5	2.2	0.0183
	10	3.2	0.0186
	20	4.5	0.0190
	30	5.5	0.0192
	45	6.7	0.0193
	60	7.7	0.0194
	480	21.9	
	1440	37.9	
Load (kPa)	Elasped Time (min)	Sq. Rt. Time	Deformation (in)
100 kPa	0	0.0	0.0194
	0.25	0.5	0.0325
	0.5	0.7	0.0336
	1	1.0	0.0347
	2	1.4	0.0356
	3	1.7	0.0361
	4	2.0	0.0362
	5	2.2	0.0365
	10	3.2	0.0369
	20	4.5	0.0372
	30	5.5	0.0374
	45	6.7	0.0375
	60	7.7	
	480	21.9	
	1440	37.9	

Load (kPa)	Elasped Time (min)	Sq. Rt. Time	Deformation (in)
200 kPa	0	0.0	0.0375
	0.25	0.5	0.0537
	0.5	0.7	0.0549
	1	1.0	0.0561
	2	1.4	0.0572
	3	1.7	0.0578
	4	2.0	0.0582
	5	2.2	0.0584
	10	3.2	0.0588
	20	4.5	0.0592
	30	5.5	0.0593
	45	6.7	0.0594
	60	7.7	
	480	21.9	
	1440	37.9	
Load (kPa)	Elasped Time (min)	Sq. Rt. Time	Deformation (in)
400 kPa	0	0.0	0.0594
	0.25	0.5	0.0766
	0.5	0.7	0.0775
	1	1.0	0.0786
	2	1.4	0.0795
	3	1.7	0.0802
	4	2.0	0.0805
	5	2.2	0.0808
	10	3.2	0.0813
	20	4.5	0.0817
	30	5.5	0.0818
	45	6.7	0.0819
	60	7.7	
	480	21.9	
	1440	37.9	
Load (kPa)	Elasped Time (min)	Sq. Rt. Time	Deformation (in)
800 kPa	0	0.0	0.0819
	0.25	0.5	0.0989
	0.5	0.7	0.0995
	1	1.0	0.1005
	2	1.4	0.1012
	3	1.7	0.1018
	4	2.0	0.1020
	5	2.2	0.1023
	10	3.2	0.1029
	20	4.5	0.1034
	30	5.5	0.1035
	45	6.7	0.1036
	60	7.7	
	480	21.9	
	1440	37.9	

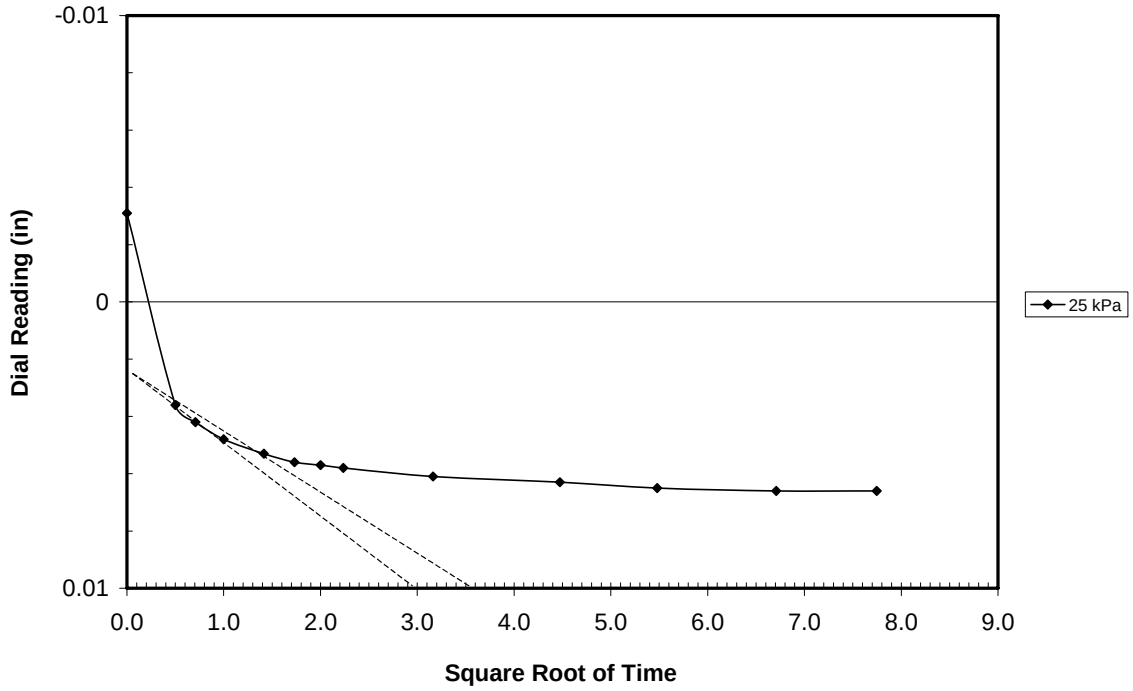

Taylor Curve (25 kPa)

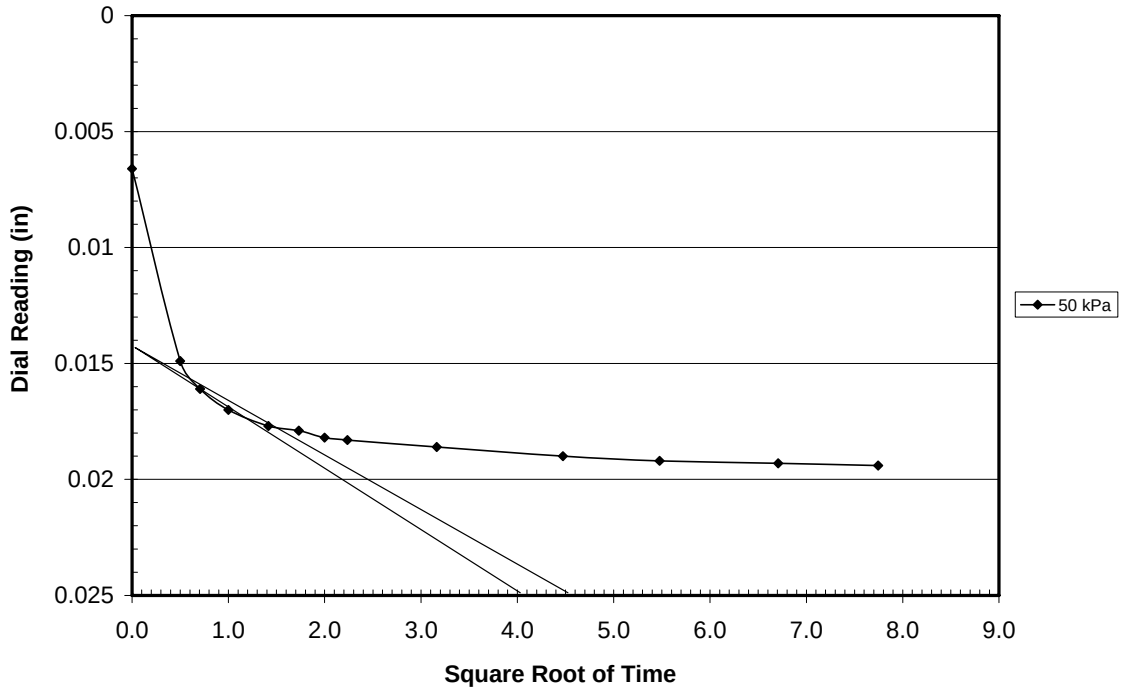

Taylor Curve (50 kPa)

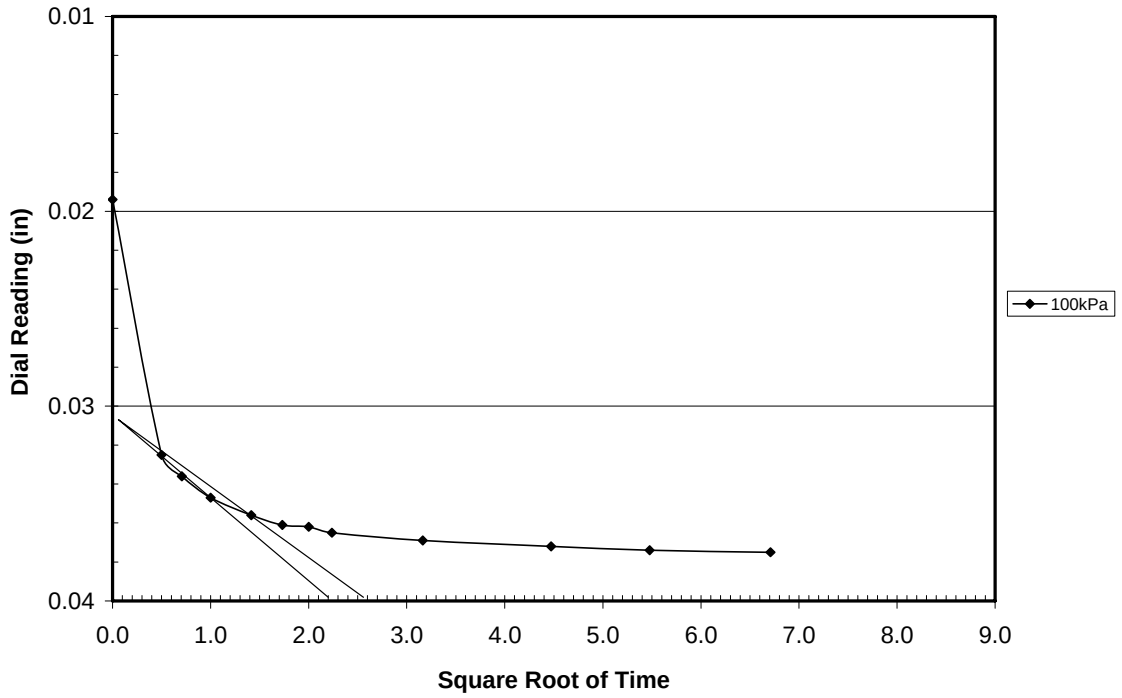

Taylor Curve (100 kPa)

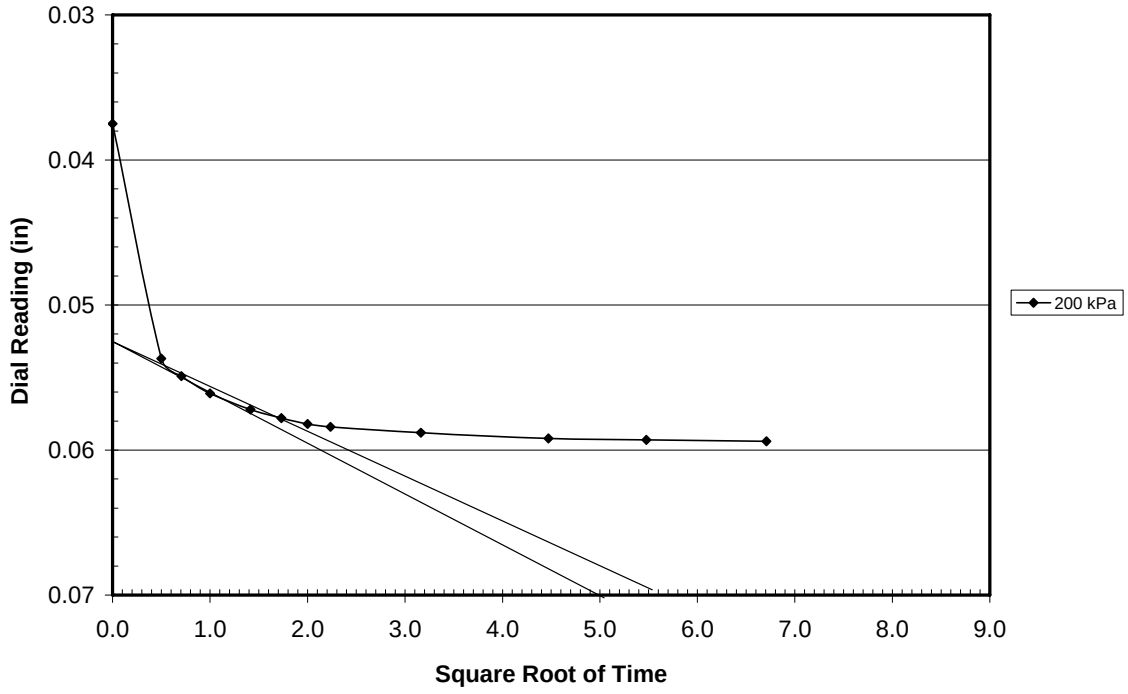

Taylor Curve (200 kPa)

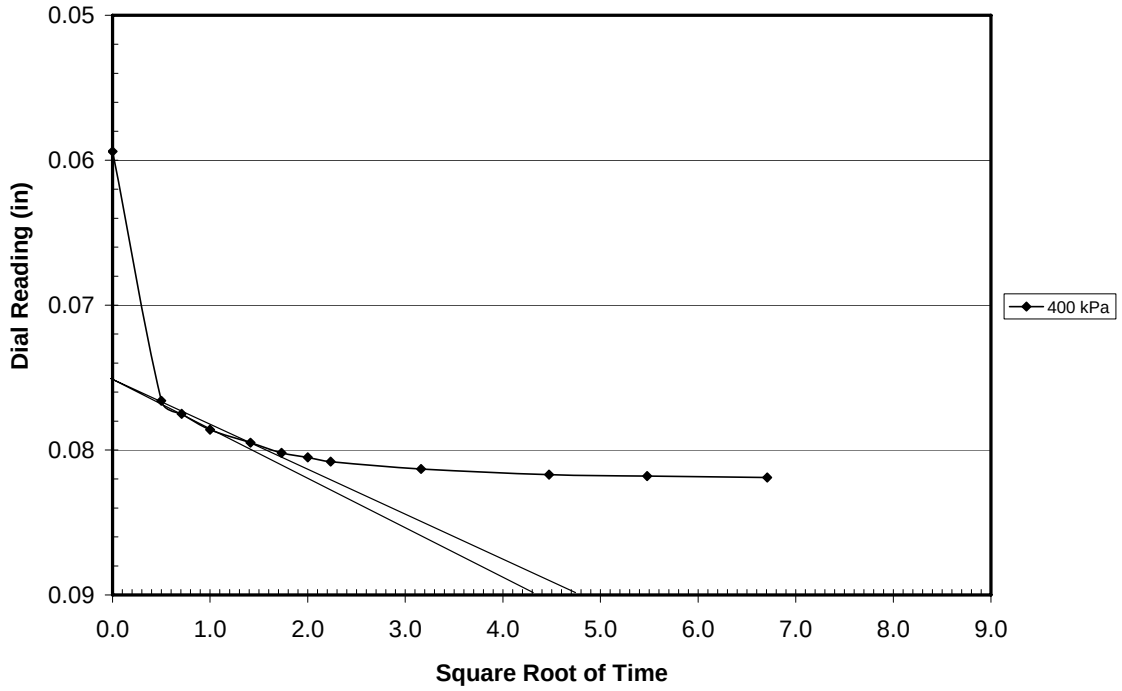

Taylor Curve (400 kPa)

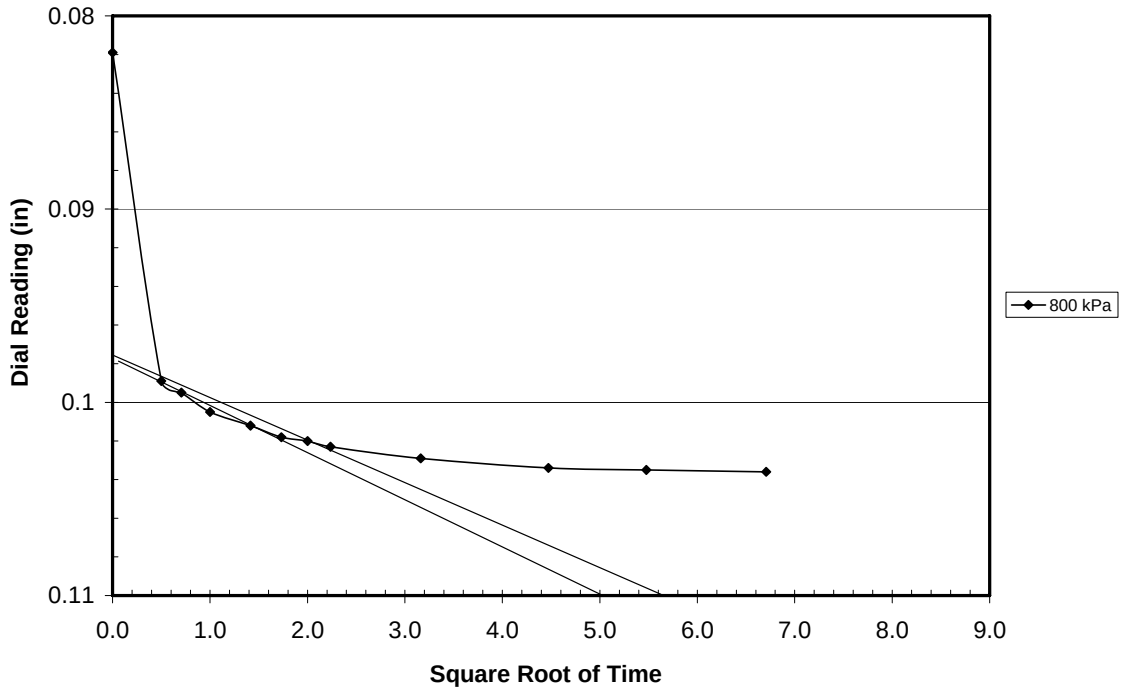

Taylor Curve (800 kPa)

Appendix C5- MD_.3SP_DO_4.7%

Test Name: **MD_.3SP_DO_4.7%_Unsoaked**

Date: **4/13/2006**

Time: **4:45** ~~AM~~ PM

Compactive Effort ~~10% SP~~ ~~(3" x 10 x 3)~~
30% SP (6" x 15 x 3)
~~Standard~~ ~~(12" x 25 x 3)~~

Mass

Ring (ID: B)	**76.59** g	Ring (ID:)	g
Ceramic (saturated)	**NA**		g
Soil (moist) + ring(s) + ~~ceramic~~	**177.43**		g
Soil (sat.) + ring(s) + ceramic	**NA**		g
Soil (Moist)	**100.84**		g
Soil (dry)	**96.31**		g
Soil (sat.)	**NA**		g
Top Filter Paper (dry)	**NA**		g
Top Filter Paper (sat.)	**NA**		g
Water (Top Filter Paper)	**NA**		g
Bottom Filter Paper (dry)	**NA**		g
Bottom Filter Paper (sat.)	**NA**		g
Water (Bottom Filter Paper)	**NA**		g

Density (Mold)

Mold + Base + Ring(s)	**4438**	g
Mold + Base + Soil + Ring(s)	**6115**	g
Soil mass (wet)	**1677**	g
ρ_m (moist density)	**1.78**	g/cm^3
ρ_d (dry density)	**1.70**	g/cm^3
γ_d (dry unit weight)	**16.6**	kN/m^3

Notes:

Water Content Determination

CAN ID	**003**	
Can Mass	**11.30**	g
Can + Soil (wet)	**31.50**	g
Can + Soil (dry)	**30.59**	g
ω	**4.7**	%

Density (Ring)

Ring Mass	**76.59**	g
Ring + Soil (moist)	**177.43**	g
Ring Volume	**60.14**	cm^3
ρ_m (moist density)	**1.68**	g/cm^3
ρ_d (dry density)	**1.60**	g/cm^3
γ_d (dry unit weight)	**15.7**	kN/m^3

Test Name: **MD_SP_DO_4.7%_Unsoaked**

Date: **4/12/2006**

Time: **11:30** AM ~~PM~~

ω **4.7** %

ρ_d **1.79** g/cm^3

Load (kPa)	Elasped Time (min)	Deformation (in)
Seating Pressure 5 kPa	0	0.0000
	0.25	0.0004
	0.5	0.0004
	1	0.0004
	2	0.0006
	3	0.0006
	4	0.0007
	5	0.0007
	10	0.0008
	15	0.0008
	20	0.0009

Load (kPa)	Elasped Time (min)	Deformation (in)	Load (kPa)	Elasped Time (min)	Deformation (in)
25 kPa	0	0.0009	**50 kPa**	0	0.0123
	0.25	0.0106		0.25	0.0183
	0.5	0.0108		0.5	0.0197
	1	0.0111		1	0.0200
	2	0.0113		2	0.0203
	3	0.0114		3	0.0203
	4	0.0115		4	0.0206
	5	0.0116		5	0.0206
	10	0.0117		10	0.0210
	20	0.0119		20	0.0212
	30	0.0120		30	0.0213
	40	0.0121		40	0.0214
	50	0.0122		50	0.0215
	60	0.0123		60	0.0215

Load (kPa)	Elasped Time (min)	Deformation (in)	Load (kPa)	Elasped Time (min)	Deformation (in)
100 kPa	0	0.0215	**200 kPa**	0	0.0319
	0.25	0.0301		0.25	0.0352
	0.5	0.0303		0.5	0.0354
	1	0.0305		1	0.0356
	2	0.0308		2	0.0359
	3	0.0309		3	0.0361
	4	0.0310		4	0.0362
	5	0.0311		5	0.0363
	10	0.0315		10	0.0366
	20	0.0316		20	0.0368
	30	0.0317		30	0.0370
	40	0.0317		40	0.0371
	50	0.0318		50	0.0371
	60	0.0319		60	0.0372

Load (kPa)	Elasped Time (min)	Deformation (in)	Load (kPa)	Elasped Time (min)	Deformation (in)
400 kPa	0	0.0372	**800 kPa**	0	0.0496
	0.25	0.0466		0.25	0.0768
	0.5	0.0471		0.5	0.0773
	1	0.0475		1	0.078
	2	0.0479		2	0.0785
	3	0.0482		3	0.0789
	4	0.0484		4	0.0791
	5	0.0485		5	0.0793
	10	0.0491		10	0.0799
	20	0.0492		20	0.0802
	30	0.0494		30	0.0804
	40	0.0495		40	0.0805
	50	0.0496		50	0.0806
	60	0.0496		60	0.0807

Test Name: **MD_.3SP_DO_4.7%_Soaked**

Date: **4/13/2006**

Time: **6:00** AM PM

ω **4.7** %

ρ_d **1.6** g/cm^3

Loading **5** kPa

Elasped Time (min)	Square Root Time	Deformation (in)
0	0.0	0.0000
0.25	0.5	0.0006
0.5	0.7	0.0005
1	1.0	0.0004
2	1.4	0.0003
4	2.0	0.0001
8	2.8	-0.0002
15	3.9	-0.0003
30	5.5	-0.0003
60	7.7	-0.0004
120	11.0	-0.0004
240	15.5	-0.0004
360	19.0	-0.0004
1440	37.9	-0.0004

Test Name: **MD_.3SP_DO_4.7%_Soaked**

Date: **4/14/2006**

Time: **11:30** AM ~~PM~~

ω **4.7** %

ρ_d **1.6** g/cm^3

Load (kPa)	Elasped Time (min)	Sq. Rt. Time	Deformation (in)
25 kPa	0	0.0	-0.0004
	0.25	0.5	0.0178
	0.5	0.7	0.0190
	1	1.0	0.0207
	2	1.4	0.0219
	3	1.7	0.0224
	4	2.0	0.0227
	5	2.2	0.0229
	10	3.2	0.0233
	20	4.5	0.0237
	30	5.5	0.0238
	45	6.7	0.0240
	60	7.7	0.0241
	480	21.9	NA
	1440	37.9	NA
Load (kPa)	Elasped Time (min)	Sq. Rt. Time	Deformation (in)
50 kPa	0	0.0	0.0241
	0.25	0.5	0.0369
	0.5	0.7	0.0387
	1	1.0	0.0405
	2	1.4	0.0419
	3	1.7	0.0424
	4	2.0	0.0427
	5	2.2	0.0429
	10	3.2	0.0433
	20	4.5	0.0437
	30	5.5	0.0438
	45	6.7	0.0439
	60	7.7	0.0440
	480	21.9	
	1440	37.9	
Load (kPa)	Elasped Time (min)	Sq. Rt. Time	Deformation (in)
100 kPa	0	0.0	0.0444
	0.25	0.5	0.0582
	0.5	0.7	0.0596
	1	1.0	0.0609
	2	1.4	0.0620
	3	1.7	0.0629
	4	2.0	0.0631
	5	2.2	0.0633
	10	3.2	0.0638
	20	4.5	0.0641
	30	5.5	0.0642
	45	6.7	0.0644
	60	7.7	
	480	21.9	
	1440	37.9	

Load (kPa)	Elasped Time (min)	Sq. Rt. Time	Deformation (in)
200 kPa	0	0.0	0.0644
	0.25	0.5	0.0825
	0.5	0.7	0.0839
	1	1.0	0.0855
	2	1.4	0.0869
	3	1.7	0.0875
	4	2.0	0.0878
	5	2.2	0.0881
	10	3.2	0.0886
	20	4.5	0.0891
	30	5.5	0.0893
	45	6.7	0.0894
	60	7.7	
	480	21.9	
	1440	37.9	
Load (kPa)	Elasped Time (min)	Sq. Rt. Time	Deformation (in)
400 kPa	0	0.0	0.0894
	0.25	0.5	0.1079
	0.5	0.7	0.1087
	1	1.0	0.1099
	2	1.4	0.1111
	3	1.7	0.1117
	4	2.0	0.1120
	5	2.2	0.1123
	10	3.2	0.1128
	20	4.5	0.1131
	30	5.5	0.1133
	45	6.7	0.1134
	60	7.7	
	480	21.9	
	1440	37.9	
Load (kPa)	Elasped Time (min)	Sq. Rt. Time	Deformation (in)
800 kPa	0	0.0	0.1134
	0.25	0.5	0.1294
	0.5	0.7	0.1300
	1	1.0	0.1307
	2	1.4	0.1317
	3	1.7	0.1321
	4	2.0	0.1324
	5	2.2	0.1326
	10	3.2	0.1332
	20	4.5	0.1336
	30	5.5	0.1337
	45	6.7	0.1338
	60	7.7	
	480	21.9	
	1440	37.9	

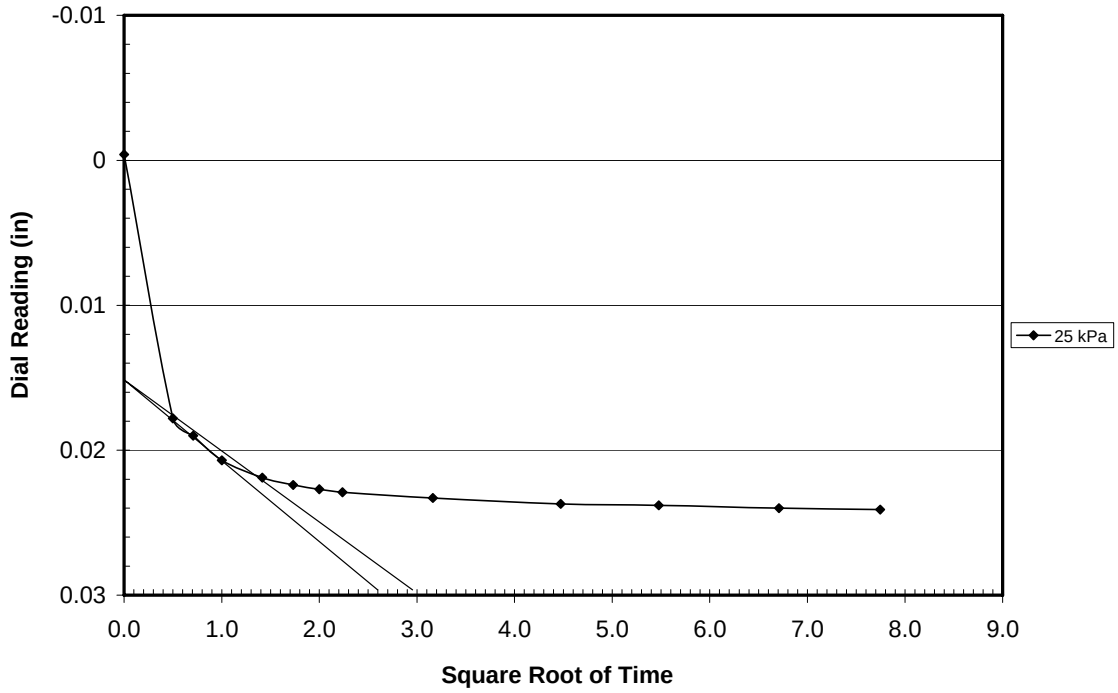

Taylor Curve (25 kPa)

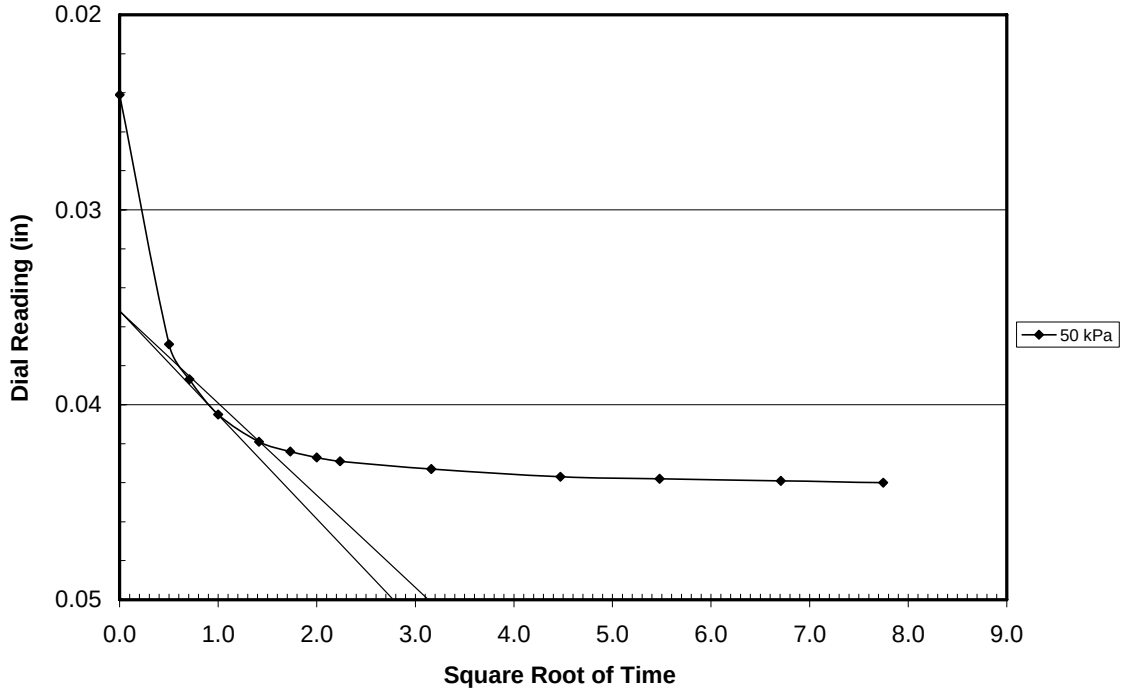

Taylor Curve (50 kPa)

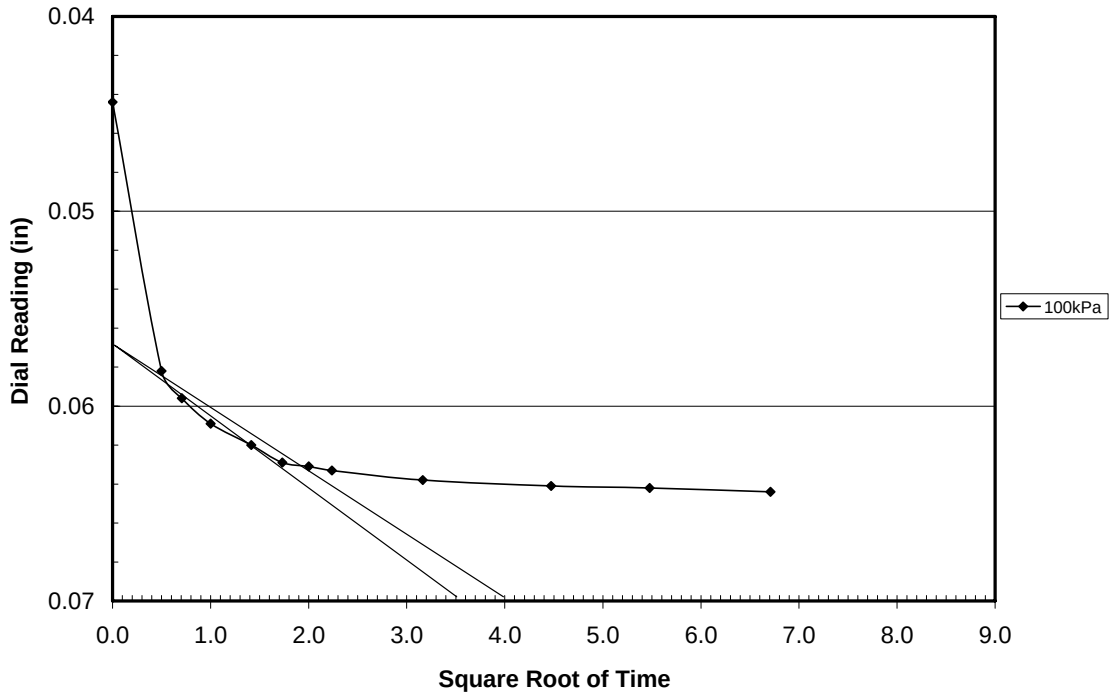

Taylor Curve (100 kPa)

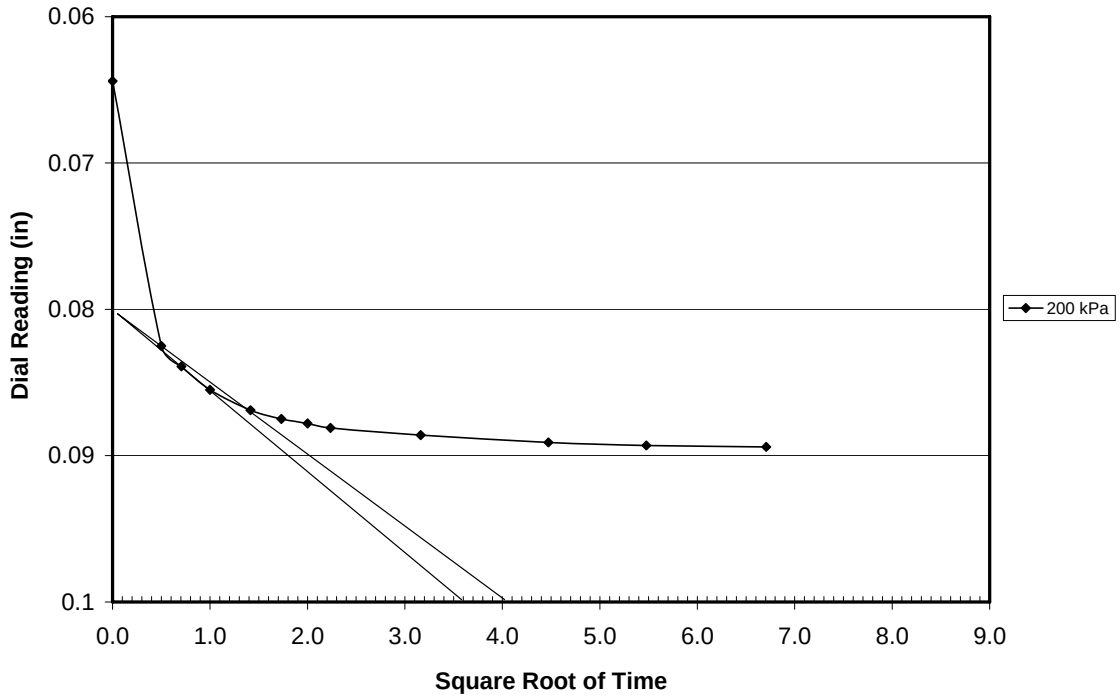

Taylor Curve (200 kPa)

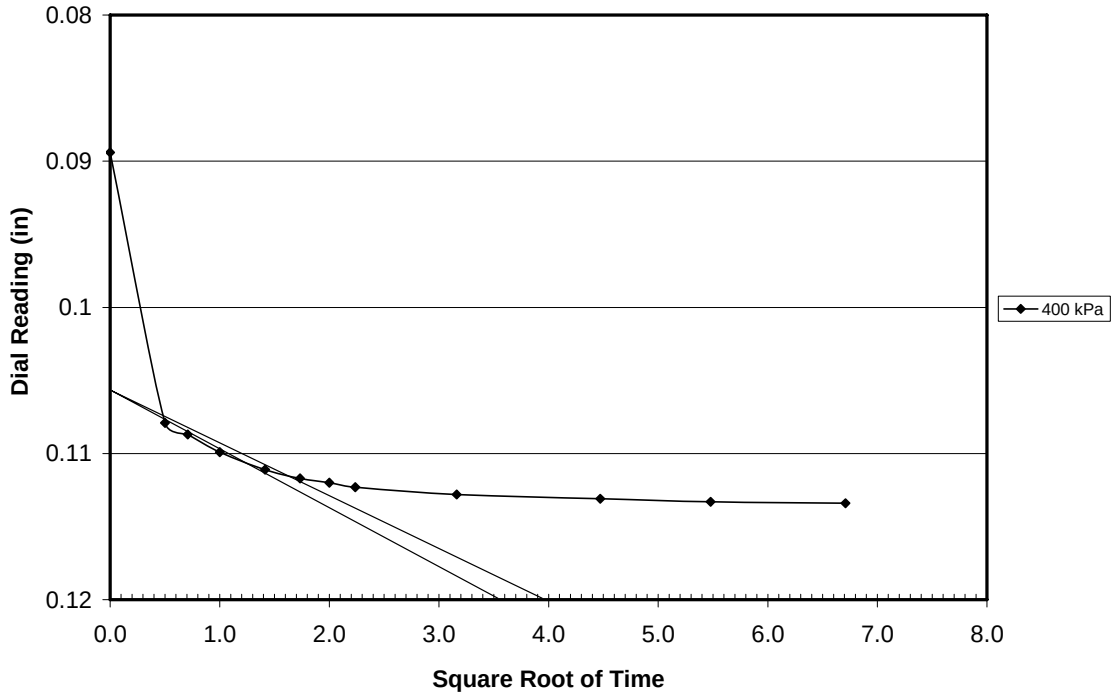

Taylor Curve (400 kPa)

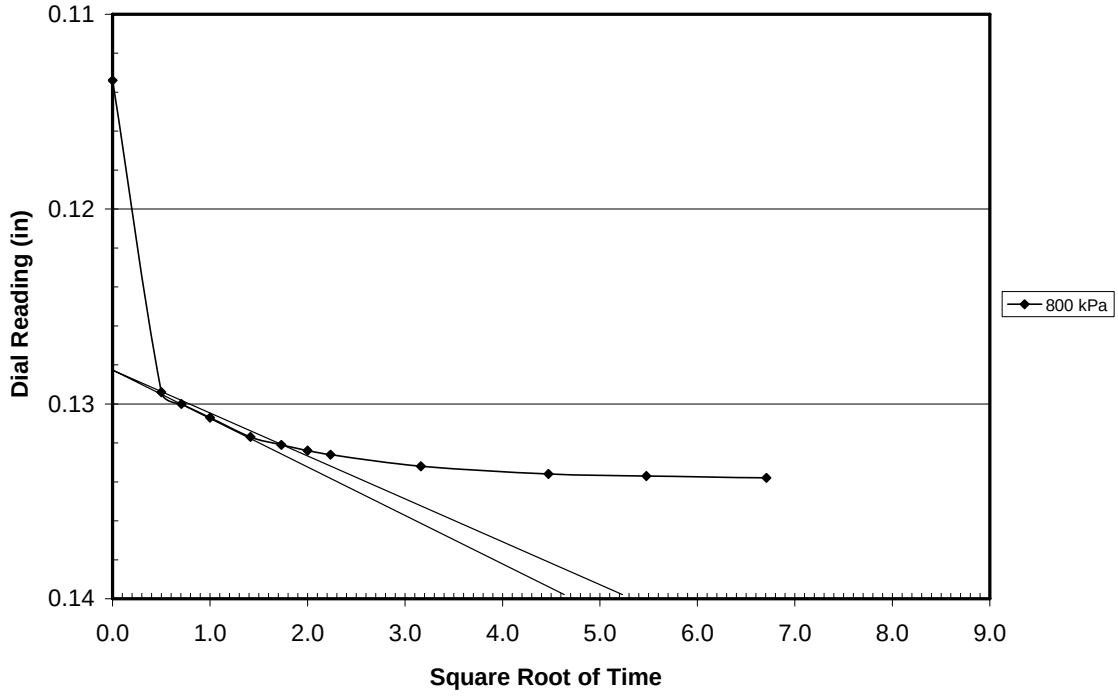

Taylor Curve (800 kPa)

Appendix C6-LD_.1SP_DO_4.7%

Test Name: **LD_.1SP_DO_4.7%_Unsoaked**

Date: **4/12/2006**

Time: **12:00** ~~AM~~ PM

Compactive Effort: 10% SP (3" x 10 x 3); ~~30% SP (6" x 15 x 3)~~; ~~Standard (12" x 25 x 3)~~

Mass

Ring (ID: C)	**76.34**	g	Ring (ID:) _____ g
Ceramic (saturated)	**NA**	g	
Soil (moist) + ring(s) + ~~ceramic~~	**172.62**	g	
Soil (sat.) + ring(s) + ceramic	**NA**	g	
Soil (Moist)	**96.28**	g	
Soil (dry)	**91.96**	g	
Soil (sat.)	**NA**	g	
Top Filter Paper (dry)	**NA**	g	
Top Filter Paper (sat.)	**NA**	g	
Water (Top Filter Paper)	**NA**	g	
Bottom Filter Paper (dry)	**NA**	g	
Bottom Filter Paper (sat.)	**NA**	g	
Water (Bottom Filter Paper)	**NA**	g	

Density (Mold)

Mold + Base + Ring(s)	**4438**	g
Mold + Base + Soil + Ring(s)	**5960**	g
Soil mass (wet)	**1522**	g
ρ_m (moist density)	**1.61**	g/cm^3
ρ_d (dry density)	**1.54**	g/cm^3
γ_d (dry unit weight)	**15.1**	kN/m^3

Notes:

Water Content Determination

CAN ID	**003**	
Can Mass	**11.30**	g
Can + Soil (wet)	**31.50**	g
Can + Soil (dry)	**30.59**	g
ω	**4.7**	%

Density (Ring)

Ring Mass	**76.34**	g
Ring + Soil (moist)	**172.62**	g
Ring Volume	**60.14**	cm^3
ρ_m (moist density)	**1.60**	g/cm^3
ρ_d (dry density)	**1.53**	g/cm^3
γ_d (dry unit weight)	**15.0**	kN/m^3

Test Name: **LD_.1SP_D0_4.7%_Unsoaked**

Date: **4/12/2006**

Time: **1:45** AM ~~PM~~

ω **4.7** %

ρ_d **1.53** g/cm^3

Load (kPa)	Elasped Time (min)	Deformation (in)
Seating Pressure 5 kPa	0	0.0000
	0.25	0.0023
	0.5	0.0027
	1	0.0027
	2	0.0027
	3	0.0027
	4	0.0027
	5	0.0027
	10	0.0028
	15	0.0028
	20	0.0029

Load (kPa)	Elasped Time (min)	Deformation (in)	Load (kPa)	Elasped Time (min)	Deformation (in)
25 kPa	0	0.0029	**50 kPa**	0	0.0220
	0.25	0.0194		0.25	0.0246
	0.5	0.0199		0.5	0.0396
	1	0.0202		1	0.0400
	2	0.0206		2	0.0407
	3	0.0209		3	0.0409
	4	0.0209		4	0.0411
	5	0.0211		5	0.0413
	10	0.0215		10	0.0417
	20	0.0215		20	0.0422
	30	0.0216		30	0.0424
	40	0.0218		40	0.0425
	50	0.0219		50	0.0426
	60	0.0220		60	0.0427

Load (kPa)	Elasped Time (min)	Deformation (in)	Load (kPa)	Elasped Time (min)	Deformation (in)
100 kPa	0	0.0427	**200 kPa**	0	0.0852
	0.25	0.0667		0.25	0.1167
	0.5	0.0675		0.5	0.1175
	1	0.0681		1	0.1181
	2	0.0688		2	0.1187
	3	0.0691		3	0.1191
	4	0.0695		4	0.1192
	5	0.0696		5	0.1194
	10	0.0834		10	0.1199
	20	0.0843		20	0.1203
	30	0.0847		30	0.1205
	40	0.0849		40	0.1207
	50	0.0851		50	0.1208
	60	0.0852		60	0.1208

Load (kPa)	Elasped Time (min)	Deformation (in)	Load (kPa)	Elasped Time (min)	Deformation (in)
400 kPa	0	0.1208	**800 kPa**	0	0.1607
	0.25	0.1563		0.25	0.1962
	0.5	0.1571		0.5	0.1971
	1	0.1578		1	0.1976
	2	0.1584		2	0.1981
	3	0.1588		3	0.1984
	4	0.1591		4	0.1987
	5	0.1592		5	0.1988
	10	0.1599		10	0.1993
	20	0.1602		20	0.1998
	30	0.1603		30	0.2000
	40	0.1605		40	0.2001
	50	0.1606		50	0.2002
	60	0.1607		60	0.2003

Test Name: **LD_.1SP_SO_4.7%_Soaked**

Date: **4/14/2006**

Time: **11:30** AM ~~PM~~

ω **4.7** %

ρ_d **1.53** g/cm^3

Load (kPa)	Elasped Time (min)	Sq. Rt. Time	Deformation (in)
25 kPa	0	0.0	0.0205
	0.25	0.5	0.0583
	0.5	0.7	0.0623
	1	1.0	0.0669
	2	1.4	0.0703
	3	1.7	0.0716
	4	2.0	0.0723
	5	2.2	0.0727
	10	3.2	0.0735
	20	4.5	0.0739
	30	5.5	0.0741
	45	6.7	0.0744
	60	7.7	0.0745
	480	21.9	NA
	1440	37.9	NA
Load (kPa)	Elasped Time (min)	Sq. Rt. Time	Deformation (in)
50 kPa	0	0.0	0.0745
	0.25	0.5	0.0853
	0.5	0.7	0.0874
	1	1.0	0.0898
	2	1.4	0.0917
	3	1.7	0.0928
	4	2.0	0.0933
	5	2.2	0.0936
	10	3.2	0.0944
	20	4.5	0.0948
	30	5.5	0.0950
	45	6.7	0.0953
	60	7.7	0.0953
	480	21.9	NA
	1440	37.9	NA
Load (kPa)	Elasped Time (min)	Sq. Rt. Time	Deformation (in)
100 kPa	0	0.0	0.0953
	0.25	0.5	0.1108
	0.5	0.7	0.1117
	1	1.0	0.1137
	2	1.4	0.1157
	3	1.7	0.1162
	4	2.0	0.1167
	5	2.2	0.1170
	10	3.2	0.1177
	20	4.5	0.1181
	30	5.5	0.1183
	45	6.7	0.1185
	60	7.7	NA
	480	21.9	NA
	1440	37.9	NA

Load (kPa)	Elasped Time (min)	Sq. Rt. Time	Deformation (in)
200 kPa	0	0.0	0.1185
	0.25	0.5	0.1372
	0.5	0.7	0.1389
	1	1.0	0.1401
	2	1.4	0.1417
	3	1.7	0.1425
	4	2.0	0.1429
	5	2.2	0.1433
	10	3.2	0.1439
	20	4.5	0.1442
	30	5.5	0.1445
	45	6.7	0.1446
	60	7.7	NA
	480	21.9	NA
	1440	37.9	NA
Load (kPa)	Elasped Time (min)	Sq. Rt. Time	Deformation (in)
400 kPa	0	0.0	0.1446
	0.25	0.5	0.1624
	0.5	0.7	0.1633
	1	1.0	0.1649
	2	1.4	0.1665
	3	1.7	0.1672
	4	2.0	0.1676
	5	2.2	0.1681
	10	3.2	0.1686
	20	4.5	0.1690
	30	5.5	0.1692
	45	6.7	0.1694
	60	7.7	NA
	480	21.9	NA
	1440	37.9	NA
Load (kPa)	Elasped Time (min)	Sq. Rt. Time	Deformation (in)
800 kPa	0	0.0	0.1694
	0.25	0.5	0.1849
	0.5	0.7	0.1857
	1	1.0	0.1865
	2	1.4	0.1874
	3	1.7	0.1880
	4	2.0	0.1882
	5	2.2	0.1885
	10	3.2	0.1890
	20	4.5	0.1894
	30	5.5	0.1896
	45	6.7	0.1897
	60	7.7	NA
	480	21.9	NA
	1440	37.9	NA

Test Name: **LD_.1SP_DO_4.7%_Soaked**

Date: **4/13/2006**

Time: **6:00** ~~AM~~ PM

ω **4.7** %

ρ_d **1.53** g/cm^3

Loading **5** kPa

Elasped Time (min)	Square Root Time	Deformation (in)
0	0.0	0.0000
0.25	0.5	0.0128
0.5	0.7	0.0143
1	1.0	0.0156
2	1.4	0.0173
4	2.0	0.0190
8	2.8	0.0194
15	3.9	0.0196
30	5.5	0.0198
60	7.7	0.0198
120	11.0	0.0201
240	15.5	0.0203
360	19.0	0.0205
1440	37.9	0.0205

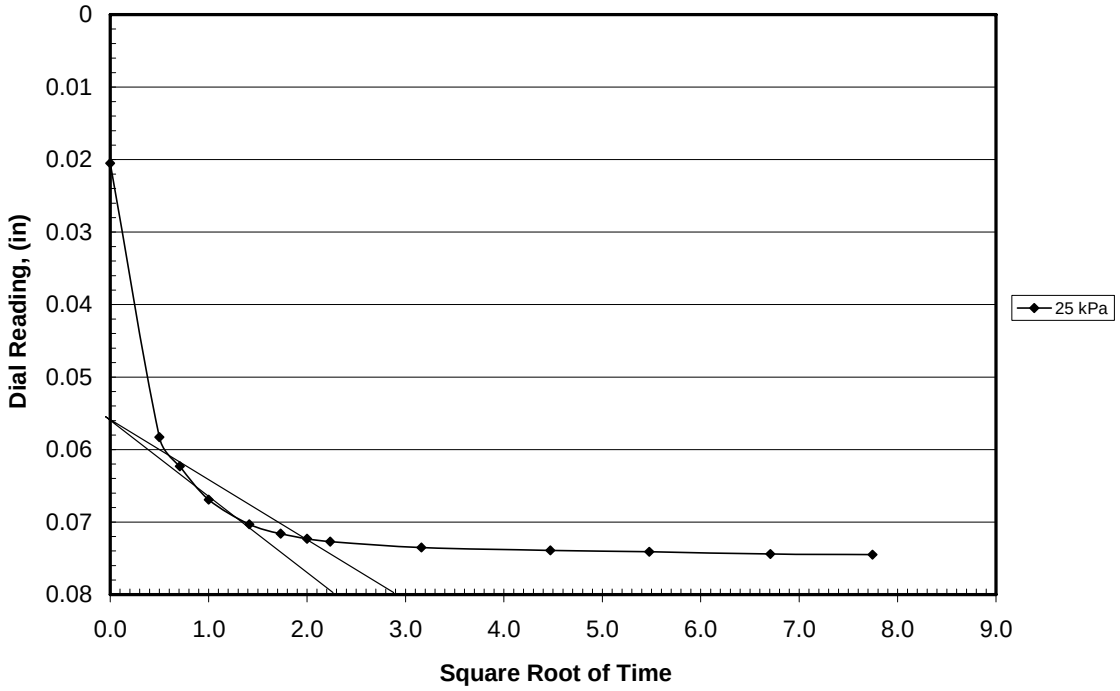

Taylor Curve (25 kPa)

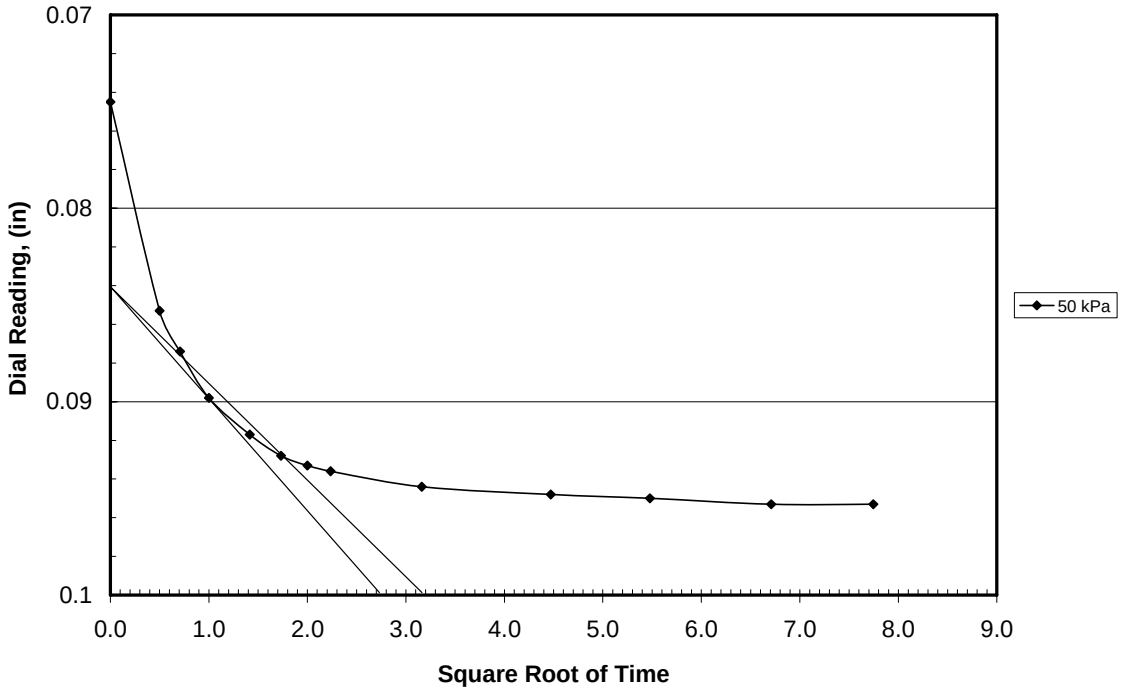

Taylor Curve (50 kPa)

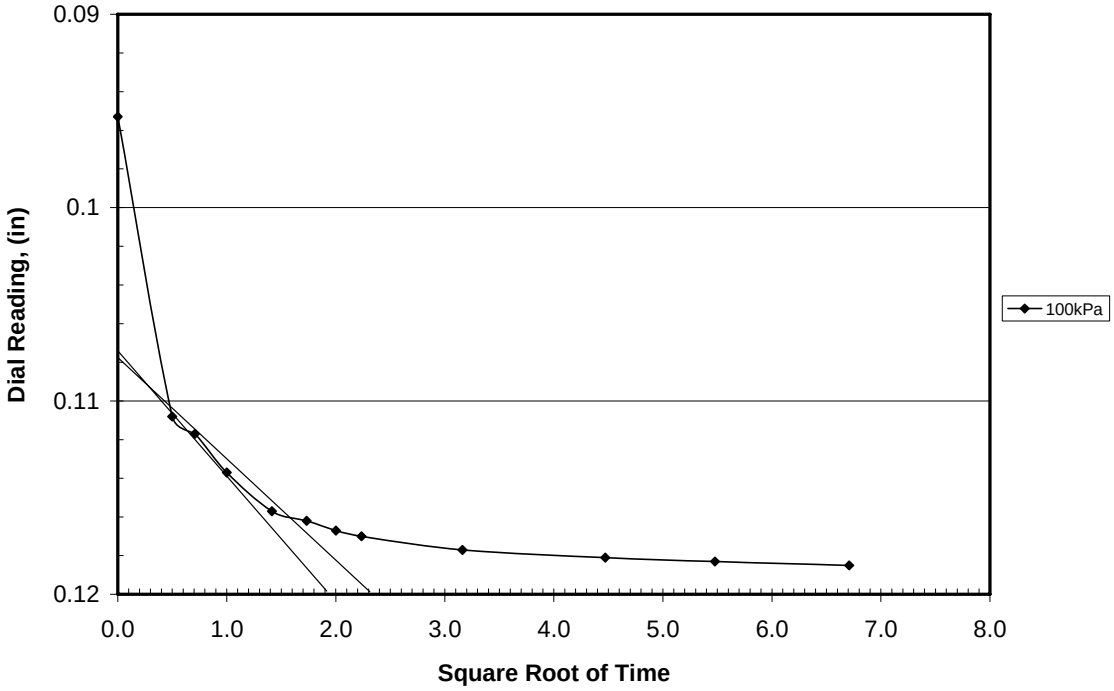

Taylor Curve (100 kPa)

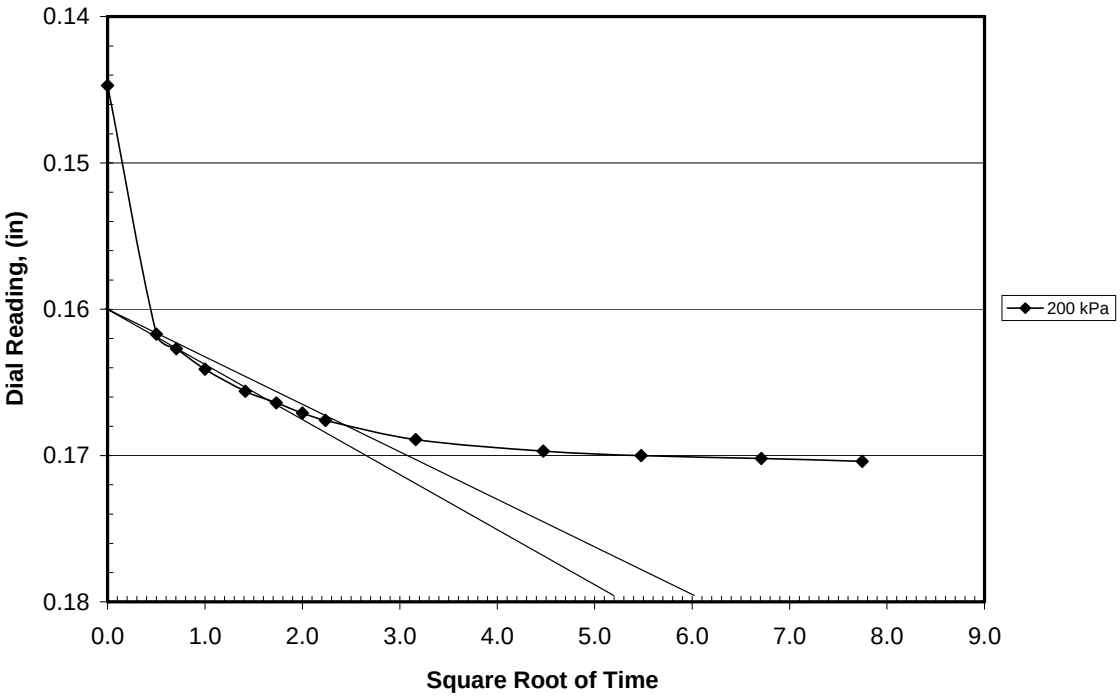

Taylor Curve (200 kPa)

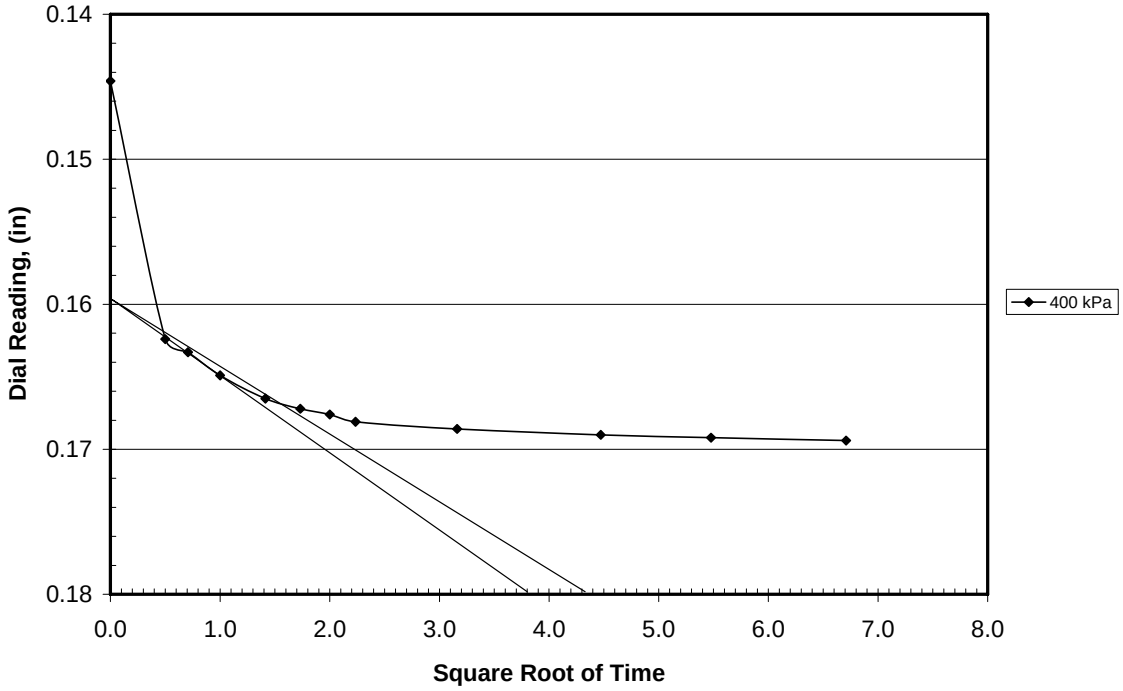

Taylor Curve (400 kPa)

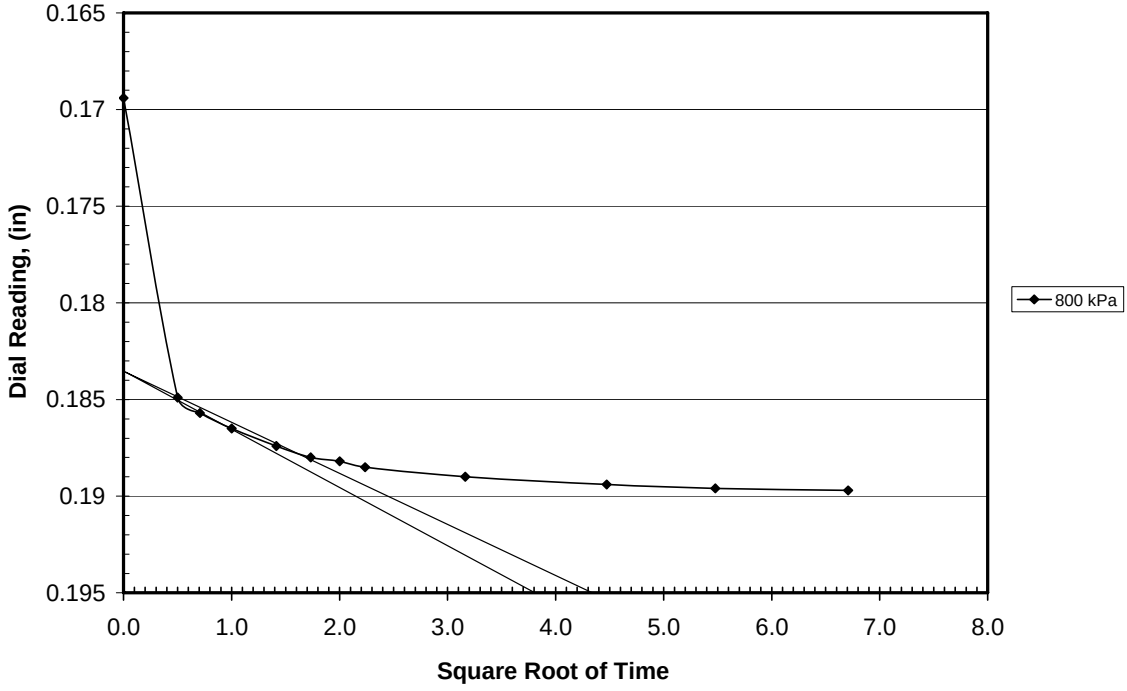

Taylor Curve (800 kPa)